GAS-PHASE BIOFILTRATION FOR LIVESTOCK BUILDING AMMONIA EMISSION MITIGATION

BY

LIANGCHENG YANG

DISSERTATION

Submitted in partial fulfillment of the requirements
for the degree of Doctor of Philosophy in Agricultural and Biological Engineering
in the Graduate College of the
University of Illinois at Urbana-Champaign, 2013

Urbana, Illinois

Doctoral Committee:

Associate Professor Xinlei Wang, Chair
Extension Specialist Ted L. Funk, Co-director of research
Professor Richard S. Gates
Associate Professor Angela D. Kent
Professor Yuanhui Zhang

ABSTRACT

Biofiltration is recognized as an effective technology to mitigate certain livestock building ammonia emissions. Biofilters are bio-reactors that can absorb ammonia and then oxidize it into nitrite and nitrate using microorganisms. Woodchips and composts are often used as packing materials thus making it an affordable method. It was originally developed in Germany to treat odors in the 1950s and later became popular in both the United States and the Europe. Most previous studies worked on maximizing biofilter ammonia removal ability; however, recent reports about generation of nitrous oxide from biofilters have spurred researchers to consider the consequences of greenhouse gas emissions. This study aims to improve the basic biofilter engineering designs (media selection, airflow resistance measurement), ammonia removal efficiency, and also to examine the effect of moisture on nitrous oxide generation. Besides that, a moisture sensor was developed to control the moisture content in biofilter media in order to achieve high ammonia removal efficiency and low nitrous oxide generation.

Biofilter media selection and pressure drop management affect the affordability of biofilters. In this study, physical, chemical properties and airflow resistances of eleven commonly used biofilter media, including ten organic and one inorganic materials, were characterized. The density, porosity, particle size distribution, pH, total C, total N, and organic matter content of each material were analyzed using standard methods. The airflow resistance property was tested on a large chamber (L ×W ×H: 1.0m ×0.6m ×0.6m) with cross-section airflow rate of 0-0.15 $m^3.m^{-2}.s^{-1}$. Airflow resistance driving factors, including moisture content, particle size distribution, bed thickness and compaction, were experimentally evaluated. The testing results were fitted into *Hukill and Ives* (1955) equation, and then two equation constants, *a* and *b*, were calculated for comparison and also used as an initial database for future biofilter designs. Based on the observations of moisture, bed thickness and compaction effects on air flow resistance, an empirical modification implementing derating factors was suggested to improve the *Hukill and Ives* equation.

In order to evaluate the function of biofilters, a baseline test was carried out to examine ammonia removal efficiency and nitrification kinetics at extreme conditions where a high ammonia loading without pre-humidifying was introduced and a high pH value was maintained in the biofilter media. Two bench-scale biofilters were built for this study and the test was composed of an N-enriching step, an N-depleting step, and a second N-enriching step. The

results showed that 90-94% ammonia removal efficiencies were observed for about ten days and then decreased in the first N-enriching step. An N-depleting step, a process that reduced the concentration of nitrogen containing compounds in the biofilter media, was applied between the two N-enriching steps. The results obtained in the second N-enriching step showed that the N-depleting step partially recovered ammonia removal efficiency, but did not last long. It was found that NH_4^+-N, NO_2^--N and NO_3^--N accumulated in media accounted for 50-100% of the total N captured from the inlet gas. To study the nitrification kinetics, a model that considers nitrification process as two continuous first-order reactions was applied and two nitrification transformation constants, k_1 and k_2, were calculated. The results show that both constants were decreased in the N enriching steps, indicating the reactions were inhibited when nitrogen compounds, especially the free ammonia (FA), were accumulated in the biofilter media. The results suggested that nitrogen compounds management is critical in achieving stable and high ammonia removal efficiency.

Moisture is believed to be the most important factor in determining biofilter performance. It affects both ammonia mitigation and nitrous oxide generation. Most likely, generation of nitrous oxide is caused by the incomplete denitrification inside of biofilters where anaerobic zones are created due to high moisture contents or compaction. To examine the role of moisture content in biofilter application, a four-month test was conducted on four bench-scale biofilters. The moisture contents in the treatment biofilters were manipulated from 35% to 55%, then to 63%, with a final step of 55%; while the moisture content in control biofilters were managed at 35% and then kept constantly at 55%. It was found that ammonia removal efficiency was improved when media moisture content was increased from 35% to 55%; but further increasing moisture content to 63% did not enhance ammonia mitigation much. In contrast, little increase of nitrous oxide (0.10−0.15 ppm) was observed when moisture content was increased from 35% to 55%, but further increasing moisture content to 63% caused a peak of nitrous oxide generation. Work on microbial communities showed that the ammonia oxidizer communities were resistant to the "moisture disturbance -disturbance relief" process based on the T-RFLP test results. This observation supports the relative flat of the ammonia removal efficiency in the treatment biofilters when moisture content was changed from 55% to 63% and then back to 55%. However, the bacterial communities and *nosZ* gene communities displayed a functional redundancy to the moisture changes. Interestingly, the real-time qPCR results showed that the quantity of *nosZ*

gene copy was reduced significantly at 63% moisture content. This observation can explain the increasing of nitrous oxide concentrations in this step.

Based on the previous study results of moisture effects on biofilter performance, it becomes necessary to manage the moisture content in the biofilter media. To achieve this goal, a moisture sensor based on media impedance measurement was developed. The sensor is composed of a sensing unit and a circuit that returns dc voltages. In a validation test, the sensor was used to measure moisture contents in two woodchips and one compost with moisture contents of 5-65%. The results fitted theoretical predictions quite well, showing that impedance can be a reliable indicator of moisture content. Besides that, temperature and compaction effects on impedance measurement were explored. It was found that increasing temperature from 22℃ to 27℃ and further to 32℃ did not change impedance of media (which is closely related to sensor reading) while compaction for eight days did. Applying the sensors in two bench-scale ammonia mitigation biofilters for one month showed that the sensors were sensitive to moisture changes. Incorporated with a water pump control strategy, the media moisture contents were successfully managed within a desired range of 44-47% according to the sensor readings. Water balance calculation based on daily water addition and water loss rates supported the sensor measured results, while moisture measurement using oven drying method at 105℃ showed slightly higher moisture contents than the sensors measured results. At the controlled moisture condition, the two biofilters reached high ammonia removal efficiencies (82-92%) and low produced nitrous oxide concentrations (0-0.32 ppm).

ACKNOWLEDGEMENTS

I would like to extend my sincerest thanks and appreciation to those helped me accomplish this study. I would like first to thank my two advisors, Dr. Xinlei Wang and Dr. Ted L. Funk, for the support, guidance and opportunities you gave to me during graduate school. I am deeply grateful for the faith and confidence you placed on me. Appreciation is extended to Mrs. Wang and Mrs. Funk for providing encouragement and joyful memories. I would also like to greatly thank other committee members- Dr. Richard S. Gates, Dr. Angela D. Kent and Dr. Yuanhui Zhang- for serving as my mentor and role model through constant display of professionalism and enthusiasm to research. Your suggestions, guidance and assistance are invaluable. I want to say thank you from the bottom of my heart.

A big appreciation goes to Dr. Dave B. Funk for guiding me through impedance study. I would also like to thank Dr. Tony E. Grift for helping me on the sensor development and Dr. Anthony Yannarell for supporting me on microbiology study.

This work would not have been possible without the help of many at the University of Illinois and the University of Kentucky. I greatly appreciate Steven E. Ford and Jinwei Su for the continued assistance on the labs. Life has been much easier with your help. I also wish to acknowledge Duane R. Kimme, Yigang Sun, Matt Robert, Guilherme Maia and Li Xu for your technical supports. Thanks are also extended to Shijie Si, Yixiong Liu, Hogyun Cheong and Alex Gui for your contributions to this project. Appreciation also goes to Dr. George B. Day at the University of Kentucky for the suggestions and the help on airflow resistance test.

I take this opportunity to thank my colleagues and friends Xufei Yang, Hai Wu, Nan Jiang, Dongfang Li, Guo Yu, Haibo Huang, Doug Barker, Phil Johnson, Chris Cirone, Lei Zhang and Qing Ye. The past years have been very wonderful in so many ways and I can always count on you for support in science related matters and others.

Last but definitely not least, I thank my family and friends away from graduate school. I want to thank Desa Phetchareun for opening an exciting window in interpersonal communication. I wish to thank the members of McKinley Toastmaster Club for helping me on public speaking and the member of Lion's Club for sharing a great experience of being volunteers. Finally, I would like to thank my parents, my sisters and their families, and my wife Yi Lou- words alone cannot express what I owe you for your endless love and support that enabled me to complete this dissertation. Thank you for always being there for me.

TABLE OF CONTENTS

LIST OF TABLES

LIST OF FIGURES

LIST OF SYMBOLS

A	Area, m^2
C	Capacitor/capacitance, pF
D	Diode, or distance, m
L	Biofilter bed thickness, m
ΔP	Pressure drop, Pa
Q	Airflow rate, m^3/sec
R	Resistor, resistance, or test statistic
V	Volume, m^3
W	Weight, kg
X	Reactance, ohms
Z	Impedance, ohm
c	Concentration
n	Total number of samples, or day number
r_B	the average of rank similarities between groups
r_W	the average of all rank similarities within groups
a	Constant
b	Constant
j	Imaginary unit
k	Nitrification rate constants, day^{-1}
p	Significance level
ϵ_a	Dielectric permittivity of air
ϵ_i	Dielectric permittivity of ice
ϵ_{om}	Dielectric permittivity of organic matter
ϵ_t	Total dielectric permittivity
ϵ_w	Dielectric permittivity of water
θ	Volume fraction
λ	BoxCox best fit parameter
ω	Angular frequency, radians/second

LIST OF ABBREVIATIONS

AFO	Animal Feeding Operation
ANCOVA	Analysis of Covariance
ANOSIM	Analysis of Similarity
ANOVA	Analysis of Variance
AOA	Ammonia-Oxidizing Archaea
AOB	Ammonia-Oxidizing Bacteria
AOAC	Association of Analytical Communities
ARISA	Automated Ribosomal Intergenic Spacer Analysis
ASABE	American Society of Agricultural and Biological Engineers
CTAB	Cetyltrimethylammonium Bromide
DAQ	Data Acquisition
DGGE	Denaturing Gradient Gel Electrophoresis
DMPP	3,4-Dimethylpyrazole Phosphate
EBRT	Empty Bed Retention Time
FA	Free Ammonia
FAM	Carboxyfluorescein
FNA	Free Nitrous Acid
GHG	Greenhouse Gas
IPCC	Intergovernmental Panel on Climate Change
LSD	Least Significant Difference
NOB	Nitrite-Oxidizing Bacteria
MDS	Multidimensional Scaling
NRCS	Natural Resources Conservation Service
OP-AMP	Operational Amplifier
OTUs	Operation Taxanomic Units
OU	Odor Unit
PCR	Polymerase Chain Reaction
PerMANOVA	Permutational Multivariate Analysis of Variance
PM	Particulate Matter
PSD	Particle Size Distribution
PVA	Polyvinyl Alcohol
RH	Relative Humidity
ROX	Rhodamine X-labeled
RPM	Revolutions Per Minute
SPICE	Simulation Program with Integrated Circuit Emphasis
TDR	Time-Domain-Reflectometry
TMECC	Test Methods for Evaluation of Compost and Composting
T-RFLP	Terminal Restriction Fragment Length Polymorphism
VOCs	Volatile Organic Compounds
UV	Ultra Violet

Chapter 1: INTRODUCTION

1.1 Background

Animal feeding operations (AFO) generate airborne emissions such as ammonia, odors, particular matters, and greenhouse gases. These emissions may affect surrounding environment (de Vries and de Boer, 2010; Havlikova et al., 2008; Seedorf, 2004). To control livestock emissions, in the US, EPA announced a voluntary Air Quality Compliance Agreement with animal feeding operations on January 21, 2005 (USEPA, 2005). AFOs that signed the Agreement were required to pay a civil penalty if their emissions exceeded the thresholds. This agreement established a framework for farmers to participate in a monitoring study in which over 2,600 agreements were signed, representing approximately 14,000 swine, dairy, egg-laying, and broiler chicken (meat-bird) farms (an AFO can include more than one farm). Compulsory regulations have been debated for a long time. In Europe, the *Gothenburg protocol* was signed in 2007, and the livestock industry is challenged to comply with emission standards of airborne sulphur, NO_x, VOC_s, and ammonia. The "Reference Document on Best Available Technologies for Intensive Rearing of Poultry and Pig" covers more than 40,000 places for poultry, or 2000 places for production pigs over 30 kg, or 750 places for sows in Europe (EC, 2003; Melse et al., 2009).

Livestock production has been identified as a major source of ammonia emission. As shown in Table 1-1, the total ammonia emission was estimated to be 2,418,595 ton/yr in 2002 in the US (USEPA, 2004a). Emission factors of most AFO are higher than 10 kg NH_3 $head^{-1}yr^{-1}$(Faulkner and Shaw, 2008). Ammonia emission rates of commercial broiler chicken houses range from 0.47 to 1.18 g/bird-day in the US, and is much lower (0.09-0.48 g/bird-day) in the Europe (Gates, 2008). In a typical confinement livestock building, ammonia concentration ranges from 0.1ppm to 30ppm depending on the type of building system and the ventilation rate, and can exceed 200 ppm in some extreme cases (Arogo et al., 2003; Demmers et al., 2003; Manuzon et al., 2007; Wheeler et al., 2006). The ammonia concentration in livestock buildings is usually higher in the cold weather than in the warm weather during to lower ventilation rate (Wheeler et al., 2006). The major source of ammonia in the livestock and poultry production is the biological conversion of urea and uric acid to NH_4^+/NH_3, respectively (Arogo et al., 2001; Dewes, 1999).

Table 1-1 Summary of ammonia emissions from U.S. animal husbandry operations.

Group	Dairy	Beef	Poultry	Swine	Sheep	Goats	Horse	Total
NH_3, ton/yr	558,094	656,648	664,238	429,468	24,835	14,028	71,285	2,418,595

Source: (USEPA, 2004b).

Most malodorous compounds from livestock buildings and manure storage sources are byproducts of incomplete anaerobic decomposition of organic matters, especially proteins and carbohydrates (Rappert and Muller, 2005; Sunesson et al., 2001; Zhu, 2000). Typical odor emission rates of 0.20-19.2 $OU.s^{-1}.m^{-2}$ were reported in Minnesota and the Netherlands (Gay et al., 2003). Concerns about odor from swine operations have become a limiting factor for state and local governments to permit expanding and new livestock facilities (Pan et al., 2007; Radon et al., 2004).

The fate and transport of ammonia and odors are correlated and are complicated (Baxevanou et al., 2008; Hartung, 1995). A strong correlation exists between a presence of odors and aerosol particles from livestock buildings (Burnett, 1969). Moreover, gaseous ammonia and odors can be adsorbed onto dust particles and transported to a long distance (Lee and Zhang, 2008). Reactive nitrogen facilitates particulate matter (PM) formation in the atmosphere and contributes to the formation of haze. In the United States, ammonia emitted from livestock operations contributes to 5-11% of the total $PM_{2.5.}$ In the north central region, this number can reach 20% (Hristov, 2011). Deposition of atmospheric ammonia may degrade ecosystem and may cause eutrophication of natural soil and water (Hao et al., 2005).

Controlling air borne pollutants from livestock buildings is a technical challenge, since it is usually composed of low concentration but mixed pollutants, including ammonia, hydrogen sulfide, odorous and potentially hazardous gases, greenhouse gases, particular matters and microbes, with a large volume (Devinny et al., 1999). These pollutants come from multiple sources and emitted as a mixture (Chen and Hoff, 2009; Lee and Zhang, 2008; Mackie et al., 1998). Traditional air pollution control technologies such as chemical absorption and physical adsorption might not be able to function very well in this case. Chemical absorption is generally effective to remove ammonia, hydrogen sulfide and particles, but is expensive, inefficient for odor mitigation, and has significant challenges in by-product treatment (Melse and Ogink, 2005). Physical adsorption is widely used for removal of trace air pollutants, but its disadvantages are also obvious: water and particles can easily destroy the adsorption ability (Ivanova et al., 1984) and is energy intensive to regenerate the adsorbents (Liu et al., 2004). Therefore, interested

parties in industrial and academic fields are seeking alternative effective and affordable solutions (Hassan and Sorial, 2009; Jiang et al., 2009b).

Biofiltration can be used to mitigate livestock air emissions (Chen et al., 2005; Melse and Ogink, 2005). In general, biofiltration technologies include gas phase biofilters, biotrickling filters and bioscrubbers. Biofilters often incorporate water addition to control moisture content but are not saturated. For biotrickling filters, microbes are usually fixed to inorganic packing materials and suspended in the water phase. For bioscrubbers, air contaminants are removed in a spray tower by water absorption. This work only focuses on biofilters for gas-phase ammonia mitigation. Gas phase biofilters are a type of bio-reactor that absorbs ammonia (or other gases, and odors) and then the ammonia is oxidized into nitrite and nitrate by microorganism oxidation. Often, it uses soil, woodchips, or composts, as the packing material and nutrient carrier.

The original biofilters were designed to treat odors in the 1950s in both the United States and West Germany (Ergas and Gonzalez, 2004; Leson and Winer, 1991). In 1966, a biofilter was applied for livestock emission mitigation (Zeisig and Munchen, 1987). Biofilters built in 1960's and 1970's were open top and used support media of bark, polystyrene, etc. to reduce channeling and compaction. In the 1980's, biofilter studies attracted much interest in both Germany and Netherlands (Ergas and Gonzalez, 2004); and in the 1990's, biofilters become more prevalent in the United States (Nicolai and Janni, 1997). Computed-operated, enclosed systems were designed and inorganic media were extensively tested (Graham, 1996; Liu et al., 1994; Medina et al., 1995). After decades of development, biofilter is now listed by the Illinois State Office of the Natural Resource Conservation Service as a candidate technology for livestock air pollution control.

Biofilters can be categorized as vertical or horizontal by airflow direction or open or closed by configuration. There are multiple advantages in the use of biofilters, such as (1) low construction and operation costs, as the media are locally available and not expensive (Menig et al., 1997); (2) capable of dealing with mixed pollutants, for example, both organic and inorganic pollutants can be absorbed or adsorbed and then degraded in biofilters; and (3) reliable for a long term operation. Biofilter media can last for years without replacing.

Besides the advantages, biofilters may also have at least the following concerns: (1) microorganism growth needs water, carbon source, nutrients, and living space. To keep biofilter active, management of microbes is a key to success; (2) high airflow pressure drop, which is

critical for building ventilation and fan selection since most livestock building fans are not designed to have very high pressure head; (3) generation of nitrous oxide. Nitrous oxide is a greenhouse gas that has 310 times the ability to trap heat in the atmosphere compared to carbon dioxide (Ciarlo et al., 2007; IPCC, 2007); (4) biomass growth causing biofilter clogging and PM loading. The clogging will increase biofilter pressure drop and even lead to failures; (5) leachate causing groundwater and/or surface water pollution; and (6) cost. Although the construction and operation costs of biofilters are lower than wet scrubbers, it is still a constraint.

1.2 Objectives

The present study aims to improve the design and management of gas phase ammonia mitigation biofilters, and also to understand the fundamental science of biofiltration. The objectives include:

a. To evaluate commonly used biofilter media by characterizing their physical, chemical properties and airflow resistance (Chapter 3). We aim to initiate a database of the media properties to facilitate future biofilter design.
b. To study the baseline performance of biofilters and to research the transformation and fate of nitrogen-containing compounds in biofilters by studying the transformation kinetics during the processes that converting ammonium to nitrite and then to nitrate (Chapter 4). We want to explore the dynamics of the nitrogen-containing compounds within biofilter media.
c. To test the moisture effects on biofilter ammonia removal efficiency and nitrous oxide generation rate, and to link the function of a biofilter to microbial communities in the media (Chapter 5). We seek for microbial evidences to support the observations of biofilter performance.
d. To develop a moisture sensor (Chapter 6) and use it for biofilter applications (Chapter 7). Given the importance of moisture control, it is necessary to have a reliable moisture sensor. We intend to design a large-format moisture sensor based on impedance measurement.

Chapter 2: LITERATURE REVIEW

The following paragraphs review the past and current studies of the gas-phase ammonia mitigation biofilter from different aspects.

2.1 Biofilter media

A large number of materials (both organic and inorganic) have been used as biofilter media, including peat, compost, sludge, woodchip, rock wool, ceramics, polyurethane foam, lava stone and so on (Colon et al., 2009; Kastner et al., 2004b; Kim et al., 2000; Ramirez et al., 2009; Sakuma et al., 2008; Yin and Xu, 2009). Their physical and chemical properties, including porosity, particle size distribution, surface area, pore volume, water holding capacity, pressure drop, pH condition, surface functional groups, carbon/nitrogen content, organic matter content, and trace element content are important for biofilter operations. Organic media may be preferred (Kim et al., 2000), and mixtures of several media were often used (Nicolai and Janni, 2001a). A summary of some selected biofilter media with their reported ammonia removal efficiencies (RE) are listed in Table 2-1. The removal efficiency depends on the type of selected materials and many other factors as well. The cost and availability of the media also affect selection of biofilter media. In general, woodchips and compost are two most commonly used media in agricultural biofilters.

Table 2-1 Selected biofilter media and their ammonia removal efficiency (RE).

Media	RE, %	Source
Peat	75-100 [a]	(Kim et al., 2000)
Rock wool	40-100 [a]	
Fuyolite	55-100 [a]	
Ceramics	50-100 [a]	
Compost	97	(Shah et al., 2003)
Yard waste compost	25-95	(Kastner et al., 2004a)
Coconut fiber	55-100	(Baquerizo et al., 2005)
Compost	95.9	(Pagans et al., 2005)
50:50 mixture of yard waste compost and wood chip	80.4	(Nicolai et al., 2005)
Wastewater sludge	85-100	(Kim et al., 2007)
A mixture of compost, sludge and hard plastics	97.9	(Taghipour et al., 2008)
UP20 [b]	93	(Dumont et al., 2008)
Activated carbon	80	(Ro et al., 2008)
Woodchip	58%	(Hoff et al., 2009)
Cork	45-100	(Park et al., 2009a)

Continue.

Compost Sludge	97-99 [c] 95-99 [c]	(Jiang et al., 2009b)
Woodchip	90	(Colon et al., 2009)
Compost Sludge	97-99 95-99	(Yin and Xu, 2009)
Sewage sludge and yard waste compost	94	(Hort et al., 2009)
Wood chip	99.4-99.8	(Chen et al., 2009)
Wood chip	41-92	(Colon et al., 2009)
Polyurethane foam	~100	(Ramirez et al., 2009)
Polyurethane bed	97-99	(Ryu et al., 2011)
Lava rock	56	(Akdeniz et al., 2011)
Woodchip	45.8	(Lim et al., 2012)
Compost	~100	(Maia et al., 2012a)
Kaldnes K1 [d]	99	(De Clippeleir et al., 2012)

[a] based on the author's interpretation of figures in the original paper.
[b] contains CH_4NO_2, H_3PO_4, $CaCO_3$ (C/N/P molar ratio: 100/5/1) and an organic binder (20% in mass).
[c] the media was inoculated.
[d] commercial available from AnoxKaldnes, Lund, Sweden.

2.2 Airflow resistance

Airflow resistance, or pressure drop, is a constraint for installing biofilters on livestock buildings. Most livestock building ventilation fans do not have much extra pressure head. Replacing ventilation fans is expensive, and is resisted by livestock owners. Therefore, it challenges biofilter designers to minimize biofilter pressure drop to avoid replacing fans.

Airflow resistance is related to porosity and airflow rate (Schmidt et al., 2004a); but other factors matter as well (Kevin et al., 2009). For example, media compaction leads to airflow resistance increase with time. A fresh biofilter with initial pressure drop of 500-1000 Pa might end its media change-out cycle with 2500 Pa pressure drop due to biomass accumulation, settling and mineralization (Yang and Allen, 1994). Moisture, temperature, biomass accumulation, particular matter (PM) loading, media degradation and mixing also can lead to changes in airflow resistance.

2.3 Moisture content management

Water availability to microbes in biofilters is a major factor of pollutant degradation rates. Too much liquid phase water fills biofilter media pores and slows the transport of air contaminates, O_2 and CO_2 across the water film coating the microbes; while too little moisture slows microbial activities. Numerous studies in literatures have discussed how moisture affects biofilter

performances (Bohn and Bohn, 1999; Kapfenberger et al., 2003; Klapkova et al., 2006a, b; Lu et al., 2002; Marek et al., 1999; Nicolai et al., 2006b; Sun et al., 2002). A typical observation is "Increasing moisture content from 40% to 50% w.b. (wet basis, usage continued in the following paragraphs) increased removal efficiency (RE) from an average of 76.7% to 82.3%. Further increasing moisture content to 60% did not significantly change RE" (Nicolai et al., 2006a). Based on available literature, it appears that most ammonia removal biofilters are operated with moisture content of 35-65% w.b.

In most cases, moisture contents were measured by finding the weight loss in a 105 ℃ oven drying for either 12 or 24 hours. This method takes time. In a biofilter using organic media, such as wood chip and compost, the moisture distribution is less likely to be even. Thus, the moisture contents of the samples may not truly represent the moisture content of media as a whole. It was also very challenging to measure the moisture contents in real time using current moisture sensing technologies.

To solve this moisture management problem, many alternatives have been proposed. Biofilter drying rate can be related to media moisture content (Maia et al., 2012b) and many novel moisture sensing technologies have been developed and tested, including X-radiation sensor (Nordell and Vikterloef, 2000), Time-Domain-Reflectometry (TDR) sensor (D'Amico et al., 2010), capacitance sensor (Funk et al., 2007; Matthew et al., 2005; Nelson et al., 1992; Nystrom and Dahlquist, 2004), thermal conductance sensor (Melo, 2011) and impedance sensor (Tiitta and Olkkonen, 2002; Zelinka et al., 2008). The X-ray sensor can measure moisture content accurately, but is expensive; the capacitance and TDR sensor are reliable for measuring low moisture content range. For biofilter applications, a sensor capable of measuring moisture over a large area is preferred.

2.4 Management of pH condition

The pH condition in media influences biofilter performance. The optimum pH value required to effectively remove ammonia is about 7.5 or near neutral (Chung and Huang, 1998; Swanson and Loehr, 1997). Due to the release of H^+ during a nitrification process, biofilter media can be acidified in a long-term operation (Rodriguez et al., 2008).

How pH condition affects nitrous oxide generation is still not clear. Increasing of N_2O/N_2 ratio with decreasing pH within the range of 5 to 8 in a long-term soil experiment was observed (Liu et al., 2010); while, another study showed that "the $N_2O/(N_2O+N_2)$ ratio increased with

decreasing pH, while no change in N_2O production" (Cuhel et al., 2010). The effects become more pronounced with even lower pH values, as the major denitrification gaseous products will be N_2O and NO at pH 4.9 (Wijler and Delwiche, 1954) and eighty percent of N_2O will be from denitrification at pH 4.5 (Baggs et al., 2010). To maximize ammonia removal and minimize nitrous oxide generation, further studies about pH effects are needed.

2.5 Generation of greenhouse gases

There are conflicting findings about greenhouse gas (nitrous oxide, and methane) generation in biofilter operations. Yasuda *et al.* found that NH_3 can be treated without causing an extra increase in two greenhouse gases, N_2O and CH_4, in a full-scale biofilter using rockwool mixture as packing material (Yasuda et al., 2009). However, Ro and his co-workers observed that a PVA coated activated carbon biofilter produced significantly more N_2O than introduced in the inlet gas (Ro et al., 2008). Clemens *et al*. also noticed that approximately 26% of the NH_3-N that was removed in an industrial biofilter was transformed into N_2O when NH_3 was the only nitrogen source (Clemens and Cuhls, 2003). Maia *et al*. reported that 0.6-2.0 ppm nitrous oxide was produced in a start-up biofilter with about 60% moisture content (Maia et al., 2012a; Maia et al., 2012b). Adsorption of nitrous oxide to media surfaces can complicate the observations as several studies reported mitigation of nitrous oxide through biofilters (Akdeniz and Janni, 2012; Akdeniz et al., 2011). However, water competes with nitrous oxide for adsorption spots, especially when the media is decorated with hydrophilic functional groups such as -OH or –COOH (Bradley, 2011). A lot of research on soil emission confirmed the generation of nitrous oxide and further concluded that the generation rate depends on the soil moisture, pH, aeration and nitrate availability (Akiyama and Tsuruta, 2003; McLain and Martens, 2006; Morkved et al., 2007; Petersen et al., 2004; Rosenkranz et al., 2006; Venterea et al., 2003).

The possible nitrous oxide generation pathways include both nitrification and denitrification. Tallec and his colleagues worked on a wastewater treatment biofilter to remove nitrogen. They showed that during nitrification, N_2O emissions are positively related to oxygenation (R^2= 0.99) (Tallec et al., 2006). Nitrous oxide generation during denitrification can be due to an incomplete denitrification, and is therefore affected by aeration conditions.

2.6 Biofilter microbiology

The microbial communities, especially the functional groups involved in nitrification and denitrification processes, play an important role in determining biofilter performance.

Inoculation of a biofilter can improve overall removal performance (Gadal-Mawart et al., 2012). In a biofilter treating air emissions from a livestock facility, *Actinobacteria* (Microbacterium, Gordonia, Dietzia, Rhodococcus, Propionibacterium, and Janibacter) was found to be the predominant bacterial phylum along with several (ammonia-oxidizing) *Betaproteobacteria* (Kristiansen et al., 2011a); while N. eutropha/Nc. mobilis-lineage and Nitrosospira cluster 3 were found as the main ammonia oxidizers (Kristiansen et al., 2011b; Yasuda et al., 2010). In another study, however, the phylum of *Proteobacteria* was found to be predominant, followed by *Actinobacteria*, *Bacteroidetes*, and *Firmicutes*, in a descending order (Chung, 2007). In a long term biofilter operation, the diversity of microbes appeared to decrease but the diversity of ammonia monooxygenase genes did not decrease. The monooxygenase genes community composition was changed and a new gene was discovered (Sakano and Kerkhof, 1998).

Linking the function of biofilters to microbial community dynamics has been attracting a lot of research attentions. The concept of resistance, resilience and redundancy was adopted to describe the relationships (Allison and Martiny, 2008). A stable function was sustained in a biofilter treating ammonia and VOCs emissions for a long term, although the microbial communities were highly dynamic (Cabrol et al., 2012b). Redundancy under temperature change was also observed in a biotrickling filter treating volatile organic compounds under thermophilic conditions (Kong et al., 2001; Park et al., 2009b). Meanwhile in another study carried out by Gentile et al. demonstrated resilience of microbial communities to environmental disturbances in a denitrifying reactor (Gentile et al., 2006); and studies in soil science showed that the resilience depends on both soil structure and soil microbial community composition (Braker and Conrad, 2011; Griffiths et al., 2008).

2.7 Nitrification inhibitors

Studies show that some chemical compounds can inhibit nitrification. Agrawal et al. observed inhibitory effect of potassium chloride on nitrification of ammonium sulfate and urea in acid, neutral and calcareous soils (Agrawal et al., 1985). Souri et al. also had a similar observation when they compared the inhibitory effects of potassium chloride to 3,4-dimethylpyrazole phosphate (DMPP), which is a standard nitrification inhibitor (Souri, 2010). Oslislo et al. compared the inhibition constants of four organic compounds, including methanol, acetone, formalin and glucose. All, but glucose, demonstrated inhibitory effects on nitrification (Oslislo and Lewandowski, 1985). Choi and Hu evaluated the toxicity of several metallic/oxide

nanoparticles (TiO_2, CuO, ZnO and Ag) on nitrification and noticed that inhibition effects increased in the order of TiO_2 < CuO < ZnO < Ag. TiO_2 nanoparticles were not toxic under ambient conditions, but can be activated with UV light (Choi and Hu, 2009).

Besides the chemicals mentioned above, the inhibitory effects of nitrogen-containing compounds are critical. Anthonisen and his colleagues showed that free ammonia (FA) and free nitrous acid (FNA) can inhibit nitrification process (Anthonisen et al., 1976). It was observed that 10-150 mg/L of FA can start inhibiting *Nitrosomonas*, 0.1-1.0 mg/L FA can begin to inhibit *Nitrobacter*, and 0.22-2.8 mg/L FNA was able to inhibit nitrifying organisms. Later studies demonstrated that nitrite-oxidizing bacteria (NOB) are likely to be more sensitive than ammonium-oxidizing bacteria (AOB) to these inhibitors (Hanaki et al., 1990; Park et al., 2010). One reason for the inhibition may be the limitation of dissolved oxygen (Bernet et al., 2001). In the biofilter performance modeling practices, the inhibitory effects of FA and FNA have been considered as an important factor (Baquerizo et al., 2005).

2.8 Costs and marketplace

The major costs of a biofilter (Chen and Hoff, 2009) include the cost of construction and the cost of operation and maintenance. The construction cost of a biofilter using 50:50 by weight mixture of yard waste compost and woodchip was estimated to be about $0.062 per CFM (cubic feet per minute) treated, and the operation and maintenance costs were about $275 per year for rodent control and $125 per year for watering system (Nicolai and Janni, 1998). Another study carried out by Schmidt et al. estimated the annual operation cost of a biofilter to be $5- $15 per 1000-CFM treated (Schmidt et al., 2004b). Both investment costs and operating costs of biofilters are much cheaper than absorption technologies (such as wet scrubbers) and catalytic oxidation technologies (Menig et al., 1997).

The application of biofiltration technology has increased rapidly due to the demands of mitigating ammonia and odors. A study estimated the U.S. market was $100 million in 2000 (Yudelson, 1996), and involved industries including media surface coating, municipal composting, and site remediation (Kosteltz et al., 1996).

Chapter 3: MEDIA CHARACTERIZATION AND AIRFLOW RESISTANCE

3.1 Introduction

Media selection is the first step in biofilter design. Here are some concerns about it.

First of all, pressure drop across biofilter is very critical for agricultural building ventilation fan operation. Most livestock ventilation fans do not develop much pressure head, and adding booster fans is expensive in both construction and operation. Selection of feasible media is considered a key step to controlling pressure drop. Several studies have measured the airflow resistance of biofilter media. Kristensen and Kofman examined the pressure drop of several types of woodchip/chunk with diameter ranging from 28mm to 200mm (Kristensen and Kofman, 2000). Nicolai and Janni tested pressure drop of compost and wood chip media mixtures ranging from 30:70 to 50:50 percent by weight and estimated the relationship of unit pressure drop to unit flow and media voids (Nicolai and Janni, 2001b). Sadaka et al. measured pressure drop of wood aggregate and compost mixtures (Sadaka et al., 2002). They found that pressure drop was linearly correlated with bed depth, and pressure drop in the horizontal direction was about 0.65 times that of the pressure drop in the vertical direction. Janni et al. evaluated pressure drop of six media including wood mulch, lava rock, cedar chips, pine bark nuggets, western pine bark and wood shred (Janni et al., 2009). Maia et al. observed that the airflow resistance of organic materials ranged from 98 Pa/m to 6350 Pa/m (Maia et al., 2012).These results provide a guide for general media selection regarding airflow resistance.

Secondly, microorganism growth needs water, carbon source, nutrients, oxygen, living space, and so on. For that reason, media has to have good water holding capacity, large surface area and be the carbon source as well. Combined with pressure drop, these constraints are conflicting. For example, in general, media with small particle size provide large surface area; however, small particles usually lead to high pressure drop compared with large particles of same treating volume (Kristensen and Kofman, 2000).

So far, a large number of materials have been used and reported as biofilter media, including peat, compost, sludge, wood chip, rock wool, ceramics, polyurethane foam, activated carbon and lava rock (Colon et al., 2009; Kastner et al., 2004b; Kim et al., 2000; Ramirez et al., 2009;

Sakuma et al., 2008; Yin and Xu, 2009). It is known that their physical and chemical properties, including porosity, particle size distribution, surface area, pore volume, airflow resistance, water holding capacity, pH, surface functional groups, carbon/nitrogen content, organic matter content, and trace element contents are important factors for biofilter operation.

The objective of this study was:

(i) to systematically characterize these media, provide a starting database of the physical and chemical properties of biofilter media,

(ii) and to improve the pressure drop prediction model.

To achieve the goals, eleven media were selected. These media have been used quite often in livestock biofilters and are usually quite low cost and easily available. In a series of tests, density, porosity, particle size distribution, pH, total carbon, total nitrogen, organic matter content and unit pressure drop ($\Delta P/L$) were measured. The *Hukill and Ives* (1955) equation was applied to model airflow resistance and an empirical modification was developed (ASAE, 2007).

3.2 Materials and Methods

3.2.1Material selection

In this test, eleven media including ten organic media and one inorganic media were selected (Fig. 3.1). The inorganic media is activated carbon received from Bisco Enterprise, Inc. (Addison, IL, $200 per 200 lb.). This activated carbon is designed as air filter media. The ten organic media are two shredded hardwood mulch ("fine" and "medium", based on the relative particle sizes), two chipped hardwood mulch ("fresh' and "aged"), one softwood mulch, two composts ("manure" and "leaf"), topsoil (the above eight media were received from landscape recycling center in Urbana, Illinois); sludge (obtained from Champaign sanitary district in Champaign, IL.); and peat (purchased from Premier Horticultural Inc., Quakertown, PA). The organic media were purchased with very low costs ($5-30 per cubic yard). A preliminary test conducted in our group by using N_2 adsorption method (data not shown here) demonstrated that there is little, if any, micro-pore (pore diameter less than 20 micrometers) and micro surface area in the organic media; therefore, in some cases, activated carbon is added to the organic media to provide micro-pores and large surface area. These materials combined with the media tested by the other groups provide a pool for biofilter media selection.

Figure 3.1 Eleven selected materials.

The shredded media was composed of brush and log material with a percentage of mixed green leaf materials. This mixture was composted and aged for several months at the landscape recycling center before finally shredding with a tub grinder into shredded hardwood mulch. The chipped hardwood mulch were made of fresh cut wood, ground in a tub grinder, the wood being a by-product of utility, public and private tree maintenance work. The softwood mulch was basically tub-ground pine species mixed with pine needles. The manure compost was produced

from horse manure and shredded hardwood bark medium. The leaf compost was obtained by composting leaf windrows in the fall of the year. The topsoil was a mixture of 2/3 local pulverized topsoil (upper, outermost layer of soil, usually the top 5-20cm) and 1/3 compost; the combined soil product was then screened through a 12 mm trammel screen. Soil aeration and water retention capacity and microorganism abundance of topsoil are improved by adding compost, which make it a better media for biofilter. The sludge was collected from a municipal wastewater treatment plant's activated sludge bed. The fresh liquid sludge was dehydrated into solid phase before being applied in this test. The peat was commercial peat moss.

3.2.2Media characterization

The density of each media was determined by measuring the mass of a 1000 ml sample. Media were dried in an oven at 105^{o}C for 24-hr to completely remove moisture; the dry weight was then measured. Porosity was recorded as a ratio of the volume of void space to the bulk volume of the sample. 1000 ml dried sample was put into a beaker and then water was added until the media was totally covered. The beaker was shaken for 30 minutes to push air out and fill the pores on the media with water. More water was added after shaking to cover the media. The volume of added water equals the void space of media. Both the density and porosity tests were repeated three times. The pH, total carbon, total nitrogen, C/N and organic matter contents were analyzed by Midwest Laboratories, Inc., Omaha, Nebraska. Total nitrogen was analyzed using AOAC 993.13 method; total carbon was analyzed using TMECC 04.01method; and the organic matter was determined using TMECC 03.02 method.

Particle size distribution (PSD) analysis was conducted using a Penn State Forage Particle Separator (NASCO, product #: C24682N, Fig. 3.2). The sieve apparatus is composed of four trays that stack on top of each other; the top three trays have unique hole sizes (1.9cm, 0.8cm and 0.2cm, respectively) designed to separate samples into four distinct particle size ranges. A total amount of 2 kg raw sample was separated by sieving, and the weights of samples remaining in the four trays were measured and normalized. Three replicates were conducted for each media.

Figure 3.2 Penn State Forage Particle Separator.

3.2.3Pressure drop test

An experimental setup was developed to test airflow resistance (Fig. 3.3, and Fig. 3.4). A centrifugal fan (Motor: Dayton Model 3N852BA; Blower: Grainger Model 2C820) with speed controller (ACS200, ABB) provided 0-510 m^3/hr. air. The airflow rate was measured by a standard nozzle with throat tap (ASHRAE 51-07). A porous aeration floor beneath the media was used to improve air distribution. The size of the testing chamber was 1.0m×0.6m×0.6m (L×W×H), about 0.36 m^3 in volume. The large size testing chamber was selected in this study in order to reduce the edge effect and thus was seen as a useful tool to generate reliable data for pilot and full scale biofilter design in the future. Both a digital manometer (Model 477, Dwyer Instruments Inc., Michigan City, IN) and a fluid filled manometer (Model 424, Dwyer Instruments Inc.) were used to record the static pressure in eight monitoring ports located on the wall of the testing chamber.

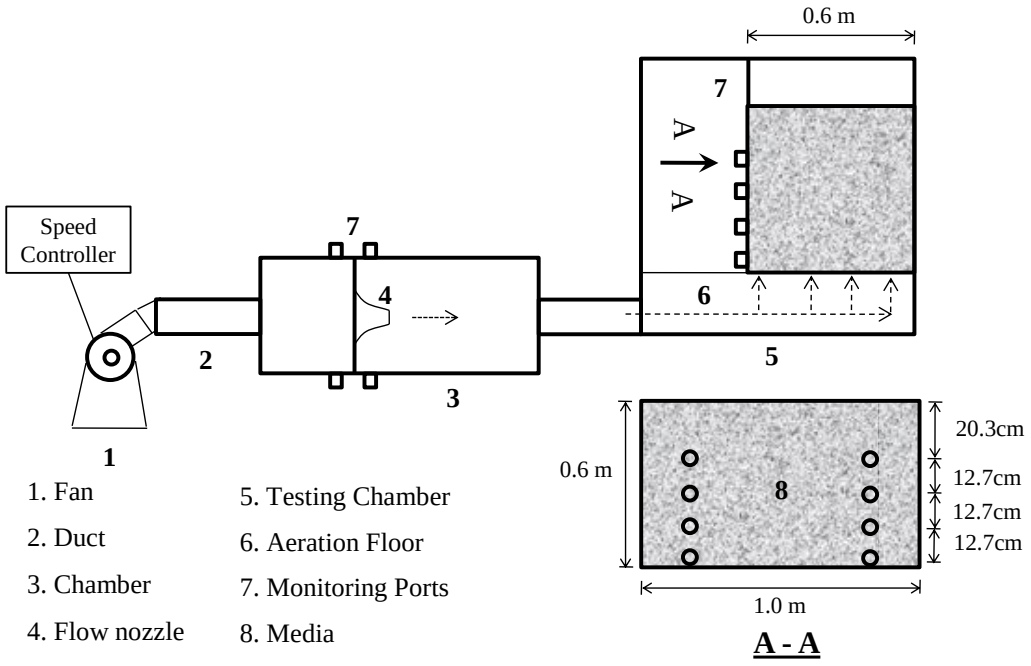

Figure 3.3 Schematic of pressure drop experimental setup.

Figure 3.4 Pressure drop test experimental setup.

3.2.4Media compaction and wetting

Biofilter media will be compacted due to gravity during operation, thus increasing its pressure drop (Devinny et al., 1999). In previous research, media was subjected to mechanical motion to be compacted in order to simulate the gravity settling (Sadaka et al., 2002). Similarly, in this

study, an impact drill was used to shake the wall of the testing chamber to compact the media. The original media bed thickness was 0.6m; after the shaking, the media was settled down by about 3 cm. Extra media was added to bring the thickness back to 0.6m.

In order to obtain media with desired moisture content, media with low moisture was wetted in a 0.57 m^3 container by adding water incrementally. The media was mixed to improve water distribution. Five replicates were sampled to obtain the final moisture content.

3.2.5Model fitting

There are several models that have been used to predict airflow resistance (unit pressure drop vs. airflow rate), including *Shedd* equation, *Hukill and Ives* (1955) equation and *Ergun* equation (1952). The *Hukill and Ives* (1955) equation was selected as an ASAE standard (ASAE, 2007) for pressure drop prediction in grain and other agricultural materials. Therefore, in this test, the airflow resistance results were fitted into the *Hukill and Ives* (1955) equation as shown in the following equation 3-1.

$$\frac{\Delta P}{L} = \frac{aQ^2}{\ln(1+bQ)} \tag{3-1}$$

Where

ΔP = pressure drop, Pa

L = bed thickness, m

Q = cross section airflow rate (m^3/ m^2-sec), also known as superficial velocity (m/sec).

a, *b* =constants for particular material, obtained from curve fitting (Pa-s^2/m^3 and m^2-s/m^3, respectively).

3.3 Results and Discussion

3.3.1Properties of media

The physical and chemical properties, including density, porosity, pH, total carbon content, total nitrogen and organic matters contents of the eleven media are shown in Table 3-1. The dry matter density of wood mulch (167-257 g/L) and peat (158 g/L) are much lower than the others (407-983 g/L). The porosities of all eleven materials are higher than 60%. Except the peat, the pH values of all the other ten media are among typical biofilter operation conditions which generally are recommended from 6 to 9 depending on the targeted pollutants (Acuna et al., 1999; Chen et al., 2005; Chou and Wang, 2007; Liu et al., 2009; Pagans et al., 2005). The nitrogen

contents (0.4-1.5%) in the eleven media are slightly lower than reported values which are 2.2%, 2.4% from Chen's study and 1.10-1.71 from Colon's study (Chen et al., 2005; Colon et al., 2009). In general, low nitrogen content benefits the operation of ammonia degradation biofilter in the long term by retarding the over accumulation of nitrite and nitrate in the media. Organic matter content of organic media, except topsoil, is higher than 15% w.b.; organic matter enables these media to be excellent food sources for biofilm microorganisms.

Table 3-1 Density, porosity, pH, total carbon, total nitrogen and organic matter contents.

Media		Density (g/L)	Porosity (%)	pH[1]	Total C %[1]	Total N %[1]	C/N[1]	Org. matt. %[1]
chipped hardwood mulch	fresh	257.4±2.5	67.7±1.6	6.9±0.1	23.6±1.2	0.4±0.0	64:1	46.2±2.3
	aged	242.4±3.7	68. 7±2.1	8.2±0.2	21.2±0.8	0.4±0.0	59:1	41.3±1.4
shredded hardwood mulch	medium	167.9±2.3	76.1±2.1	8.4±0.2	19.4±0.7	0.5±0.0	39:1	37.2±1.7
	fine	232.6±1.9	61.5±0.7	8.8±0.1	21.7±1.1	0.6±0.0	37:1	39.3±1.7
softwood mulch		170.3±1.6	73.2±0.7	7.0±0.2	21.9±1.3	0.6±0.0	37:1	40.8±1.2
compost	manure	407.5±2.5	62.2±0.2	8.5±0.1	15.5±1.0	1.1±0.0	15:1	28.5±1.3
	leaf	689.5±0.8	62.7±0.2	8.2±0.3	10.0±1.1	0.6±0.0	16:1	17.6±0.9
topsoil		983.2±0.6	61.8±0.1	8.0±0.1	6.8±0.8	0.4±0.0	17:1	6.9±0.3
sludge		467.2±1.2	73.2±1.1	8.5±0.1	9.3±0.9	1.5±0.2	6:1	17.1±0.5
peat		158.7±5.6	66.8±0.1	4.3±0.1	28.0±2.1	0.5±0.0	55:1	49.9±0.9
activated carbon		681.7±11.3	66.6±1.1	8.2±0.2	63. 6±1.6	0.5±0.0	132:1	-

Average ±SD, three replicates.
[1]Data were provided by Midwest Laboratories, Inc.

Particle size distribution (PSD) of media is considered to be an important factor for contaminant removal efficiency according to a previous research (Sales et al., 2008). PSD mainly describes the surface area of media which have very little micro-pores. Smaller particles offer higher surface area; at the same time, however, small particles may cause dead zones and reduce available surface area within a biofilter (Sales et al., 2008). PSD also matters much to media airflow resistance. The results are shown in Table 3-2. The size of activated carbon particles is between 0.2 and 0.8 cm. Peat particles are very small, 36.8% of particles are smaller than 0.2 cm and only about 9.4% particles are larger than 0.8 cm. The large particles basically are clusters caused by the moisture. Sludge has 24.7% particles larger than 1.9 cm, mainly because they are wet and agglomerated. Also, the fresh chipped hardwood mulch and medium shredded hardwood mulch have 32.6% and 21.5% particles larger than 1.9cm, respectively. Middle size particles (0.2cm-1.9cm) quite dominate aged chipped hardwood mulch, fine shredded hardwood mulch and softwood much, the weight percent of which is 85.3%, 75.2% and 77.3%, respectively. Note that different media can be mixed to adjust particle size distribution and porosity.

Table 3-2 Particle size distribution (weight percent).

Media		Particle size (cm)			
		>1.9	0.8-1.9	0.2-0.8	<0.2
chipped hardwood mulch	fresh	32.6±0.2	42.4±3.0	20.7±2.6	4.4±0.6
	aged	4.8±0.5	39.5±4.1	45.8±3.1	9.9±0.7
shredded hardwood mulch	medium	21.5±2.9	33.3±4.4	35.8±2.9	9.4±2.0
	fine	6.0±0.9	32.1±1.3	43.1±0.8	18.8±0.7
softwood mulch		11.7±1.2	33.5±3.6	43.8±2.0	6.0±1.3
compost	manure	1.3±1.1	12.7±0.7	79.1±2.9	7.0±1.4
	leaf	4.5±2.8	28.6±4.4	55.0±5.2	11. 8±2.9
topsoil		7.5±2.9	25.6±1.4	56.8±3.1	10. 2±0.5
sludge		24.7±0.2	51.0±0.5	24.1±0.6	0.1±0.1
peat		0.0	9.4±0.3	53.8±0.6	36.8±0.7
activated carbon		0.0	0.0	100.0	0.0

Results are shown in the form of average ± SD. Three replicates were conducted.

3.3.2Airflow resistance

Fresh chipped hardwood mulch was first used to test the pressure drop variation in the horizontal direction. Airflow rate was $0.112 m^3/m^2$-sec. A manometer tube was inserted into the media at both left and right monitoring ports (Fig. 3.2) with length of 7.6cm, 30.5cm and 53.3 cm to measure the static pressure drop. It was found that the static pressure drop in the horizontal direction (perpendicular to airflow) was nearly constant (Fig. 3.5) which indicated that the edge effect was negligible in this test. The manometer tube was inserted into the media at both ports with length of 7.6cm in the following tests.

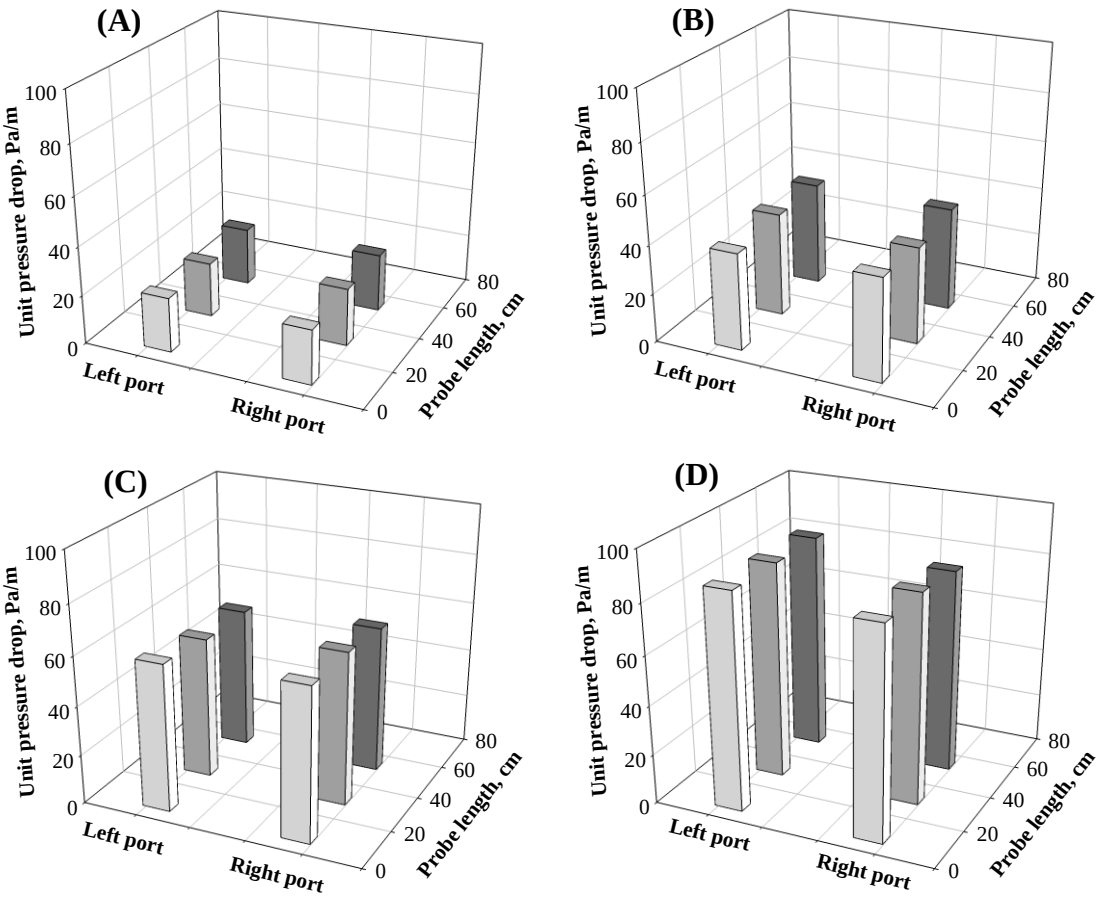

Figure 3.5 Unit pressure drop distribution. A: bed thickness of 20.3cm, B: bed thickness of 33.0 cm, C: bed thickness of 45.7 cm, and D: bed thickness of 58.4 cm.

The general airflow resistance results of the eleven media are shown in Fig. 3.6. The moisture contents of media were 50-55%wb, except for activated carbon (20.2%wb) and sludge (75.7%wb). The bed thickness was 58.4 cm, except for activated sludge and topsoil (45.7cm), and activated carbon (25.4cm). The airflow rate was from 0.07m^3/m^2-sec to 0.130m^3/m^2-sec, which is in line with the other studies (Nicolai and Janni, 2001; Sadaka et al. 2002 and Janni et al. 2009). The lowest EBRT (Empty Bed Retention Time) was 4.5 sec. The dashed lines in the Fig. 3.2, and in the following figures, are model fitting results based on the *Hukill and Ives* (1955) equation. The dots represent the averaged values of unit pressure drop (Pa/m) obtained from the left and right ports. Results (R^2 >0.99) shown in Fig. 3.5 were obtained from as tested un-compacted media. The figure shows that wood mulch had the lowest airflow resistance. It is reasonable because the mulch particles are relatively larger in size which allows air to pass through easily. Although the activated sludge had large particles size and high porosity, its unit pressure drop was slightly higher than the wood mulch. This might be due to the fact that sludge

is softer and prone to be compacted in the testing chamber, besides having a more regular shape compared to the mulch. The airflow resistance of manure compost was 50-100% higher than the leaf compost, even though they were close in porosity. Most likely, it is because the manure compost particles were smaller compared to the leaf compost particles. The topsoil and activated carbon also showed about 1-3 times higher pressure drops compared to the wood mulch. The peat media displayed the highest airflow resistance compared to all other media types, which is not surprising because its particle size was much smaller than all the others (Table 3-2). Fig. 3.6 shows a rough indication of unit pressure drop of the eleven media, and may be useful for biofilter designers in choosing a category of media, especially when the fan pressure head is limited.

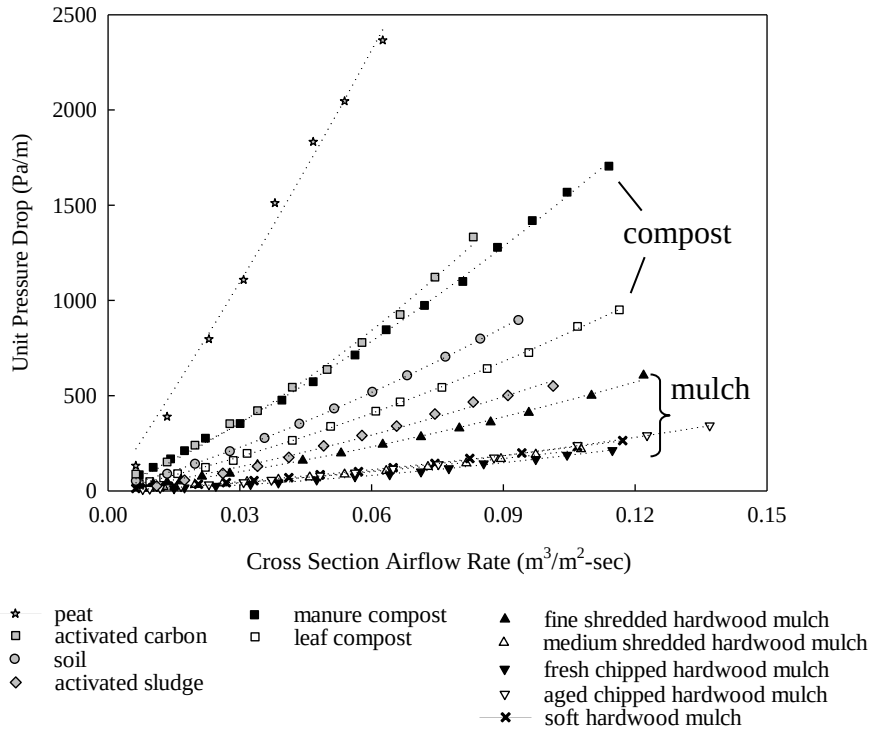

Figure 3.6 Airflow resistance of eleven candidate media tested.

The effects of moisture content, compaction and particle size distribution on airflow resistance were investigated in the study. Only the results of medium shredded hardwood mulch are shown here (Fig. 3.7) as an example. The other testing data are available in the appendix A1.

Moisture contents of 39.5%wb and 52.1%wb were selected because most biofilters are operated with 35-65%wb moisture (Juneson et al., 2001). The results showed that the un-

compacted 52.1%wb media had slightly higher (5-8%) airflow resistance than the 39.5%wb media. Similar observations were obtained from the other media as well. In all, within this moisture range of interest, about 5-15% increase of unit pressure drop was resulted from 10-15%wb of moisture increase.

One important expectation in biofilter operation is that media would experience compaction and increased pressure drop over time. This phenomenon is believed to be worthy of study. Based on the medium shredded hardwood mulch, about 20% increase of unit pressure drop was observed. Even higher unit pressure drop increases were found in the fine shredded hardwood mulch (30-35%) and leaf compost (40-50%) following compaction (Table 3-4). Obviously, the mechanical compaction of media can lead to a significant increase in airflow resistance. Therefore, the settling of media during the biofilter operation cannot be ignored. This test provided an evidence of the increase of pressure drop due to compaction; however, more work still needs to be done to make a reliable comparison of the effect of mechanical compaction vs. gravity settling.

The third observation is the huge unit pressure drop difference between the fine shredded hardwood mulch and medium shredded hardwood mulch (Fig. 3.7). These two media were derived from the same materials, and were the same except for their particle size distribution. The medium shredded mulch had a generally larger particle size than the fine shredded mulch (Table 3-2). The moisture contents of medium and fine shredded hardwood mulch were 52.1%wb and 54.4%wb, respectively. The moisture difference was not significant in this case. As Fig. 3.7 indicates, the particle size distribution affected airflow resistance significantly. The pressure drop of fine shredded hardwood mulch was approximately three times that of the medium shredded hardwood mulch. It was most likely because the small particles in the fine shredded hardwood mulch reduced its porosity (Table 3-1) and caused higher airflow resistance. It is well known that an animal house is a PM source; thus during the biofilter operation, more and more PM can be accumulated in biofilters (Swanson and Loehr, 1997). Furthermore, biomass will accumulate in biofilters as well, and most likely the media would be degraded as time goes by. These three effects combined together are expected to gradually change the particle size distribution toward more and finer particles. Fig. 3.7 indicates the potential increase of airflow resistance of biofilters due to these effects based on the tests of three laboratory created conditions.

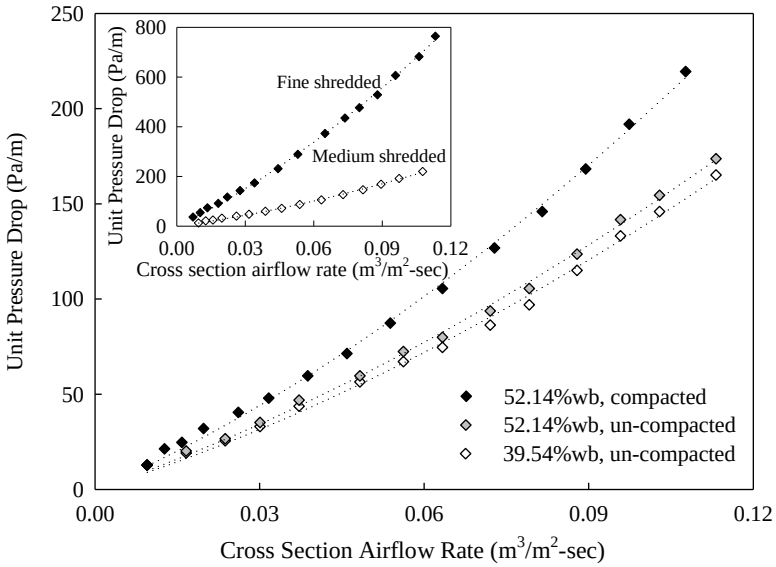

Figure 3.7 The effect of moisture, compaction and particle size distribution on airflow resistance in medium shredded hardwood mulch.

The above observations were combined together to examine the interaction between porosity and pressure drop. Table 3-1 shows the porosity of fine and medium hardwood mulch is 76.1% and 61.5%, respectively. If we roughly assume water density is 1g/cm^3 and moisture changes the porosity but does not change the bulk volume of media, we computed approximate wetted-media porosities of: fine: 33.8% (54.4%wb MC) and medium: 57.8% (52.1%wb MC), and 65.1% (39.5%wb) in this testing condition. The pressure drop increased 5-8% when porosity of medium shredded hardwood mulch reduced from 65.1% to 57.8%. However, the pressure drop was tripled when porosity reduced from 57.8% (medium shredded hardwood mulch) to 33.8% (fine shredded hardwood mulch). Another example was the fresh chipped hardwood mulch, when increasing moisture from 41.7%wb to 59.2%wb, which reduced porosity from 49.3% to 30.4%, the airflow resistance increased by 30-40%. Even though the fine shredded mulch (33.8%) had slightly higher porosity than the 59.2%wb wetted fresh chipped mulch (30.4%), it had about two times higher unit pressure drop. This phenomenon suggests: (1) porosity alone cannot fully characterize airflow resistance and (2) for wood mulch/chips media, which are usually coarse in size and porous in structure, particle size distribution plays a more important role than moisture content in determining airflow resistance. It probably is because water is absorbed by woody materials and fills macro/meso pores. As a result, moisture content increases in the coarser

materials may not reduce air resistance dramatically. However, the other materials, like activated sludge the shape of which highly depends on the moisture, the results might be much different.

In most large-scale biofilters, media are usually mixtures of different materials in order to provide enough food sources, trace elements, surface area, and water holding capacity and so on. Therefore, it is of practical interest to test the airflow resistance of the mixtures. Two examples are shown in Fig. 3.8. The mixture was made based on 1:1 volume ratio of leaf compost and medium shredded hardwood mulch. From this figure, the unit pressure drop of the mixture was slightly (5-10%) higher than the average of the two un-mixed media. Similar result was also obtained from the mixture of manure compost and medium shredded hardwood mulch. It indicates that particle size distribution plays an important role in air flow resistance.

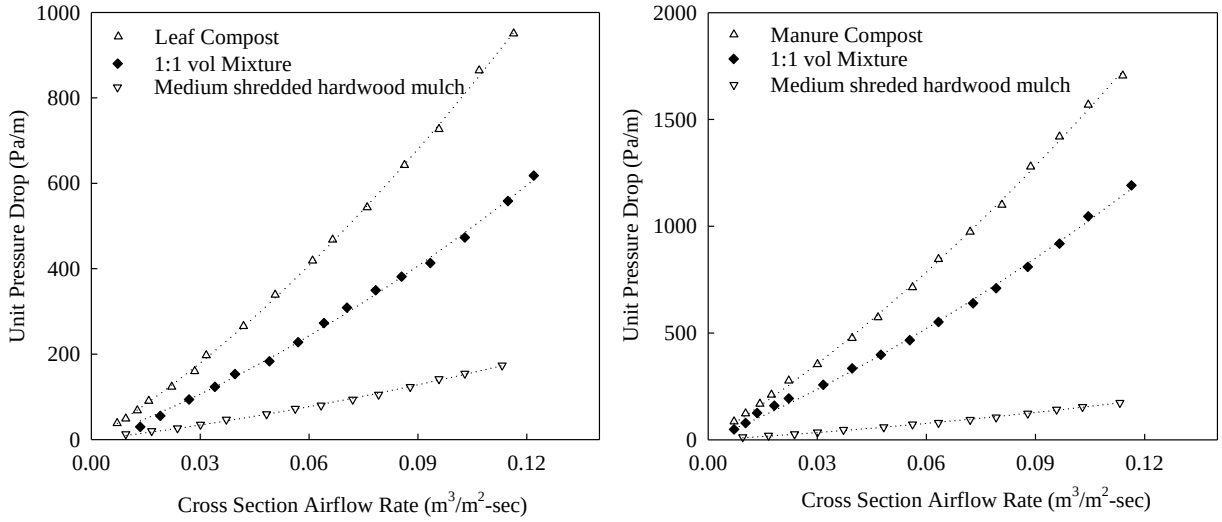

Figure 3.8 Airflow resistance of mixture.

The last test conducted in this research was the effect of bed thickness on airflow resistance. As shown in Fig. 3.3, the unit pressure drop was measured with bed thickness of 20.3 cm, 33.0 cm, 45.7 cm and 58.7 cm with airflow rate up to about 0.12 m^3/m^2-sec. Only the results obtained with the highest airflow are shown in the following Table 3-3, the results with the other airflow rates can be calculated from Table 3-4. In this table, the unit pressure drop of media with bed thickness of 20.3 cm was set as the starting value (1.00), while the unit pressure drop with the other bed thicknesses were normalized according to this starting value. The results show that the airflow resistances increased with bed thickness, indicating the media in the lower layers of biofilters became more compacted by gravity as media was added to increase the thickness of

biofilters. From the table, the ratio of ΔP/L evaluated with deep thickness vs. shallow can be as high as 1.53 and 1.64 in softwood mulch and manure compost, respectively, indicating the big change in airflow resistance in the vertical direction.

Table 3-3 Unit airflow resistance of four kinds of media as a function of bed thickness.

Media	Bed thickness, cm			
	20.3	33.0	45.7	58.4
Fresh chipped hardwood mulch	1.00	1.09	1.18	1.26
Fine shredded hardwood mulch	1.00	1.21	1.24	1.30
Softwood mulch	1.00	1.19	1.43	1.53
Manure compost	1.00	1.07	1.25	1.64

Cross section airflow rate: ~0.12m^3/m^2-sec., MC: ~52.5%wb.

3.3.3Model fitting and empirical improvement

All the airflow resistance results were fitted into *Hukill and Ives* (1955) equation. The parameters (*a*, *b*) are summarized in Table 3-4. Parameter *a* is in a scale of 10E+4. R^2 values are higher than 0.99 in all cases which indicate that *Hukill and Ives* (1955) equation is a powerful tool to predict airflow resistance. 91 sets of data are listed in Table 3-4 to provide a starting database for future biofilter design, especially for media and fan selection. All the measured airflow resistance data was listed in the Appendix A2.

Table 3-4 provides the airflow resistance in the limited operation conditions. Practically, biofilters are designed to be operated in the more general conditions with different moisture, PSD, compaction, and bed thickness. In order to apply the results obtained from this work to broader applications, the following several derating factors are inserted into the *Hukill and Ives* (1955) equation. The constants are empirical data which were derived from this work.

$$\frac{\Delta P}{L} = \frac{aQ^2}{\ln(1+bQ)}[1+c(MC-52.5)]\times[1+d(L-0.2)]\times(1+tT) \qquad (3\text{-}2)$$

Where,

MC = moisture content during operation, wet weight percent.

T = expected operation time between changes of media, year

c, d, t = empirical constants

Most biofilters are operated with moisture of 35-65%wb, and a lot of media moisture content tested in this work is from 50 to 55%wb; the average, 52.5%wb, was set as the base point, and the derating factor will affect the final result if the average expected moisture content is much greater. Also, 0.2m is selected as the baseline of bed thickness to account for compaction when

designing with greater bed depths. The constants can be varied. In this test, about 5-15% increase of unit pressure drop caused by every 10%wb of moisture increase (Fig. 3.7) was typical. Therefore, we recommend c = 0.005~0.015. Based on our experiences, the value for constant c is likely to be a low value for media with less macro/meso pores such as wood mulch.

The unit pressure drop increased with bed thickness (Table 3-3). As we can see, with surface velocity of about 0.12m^3/m^2-sec, the unit pressure drop increased about 26% for fresh chipped hardwood mulch and 64% for manure compost when comparing the 58.4 cm bed thickness to the 20.3 cm bed thickness. The effect of bed thickness on airflow resistance might highly depend on the particle size and the physical properties of media. These two media are recognized as the two extreme conditions, therefore we can suggest d = 0.65~1.70. The value of for constant d depends on the physical properties of the media. Soft media such as peat and compost will likely have a high value.

The effect of compaction might be more complicated since it might be caused by gravity settling, PM loading and biomass accumulation. Yang and Allen (Yang and Allen, 1994) predicted that a fresh biofilter with pressure drop of 500-1000 Pa might end its media change-out cycle with 2500 Pa pressure drop due to biomass accumulation, settling and mineralization. Sadaka et al. (Sadaka et al., 2002) put biofilter media in a trailer and pull the trailer at a velocity of 40 km/h for 10 km to compact the media. However, very little increase of pressure drop was found in their research. It seems difficult to simulate, i.e. in an accelerated test, how compaction would affect media pressure drop and to predict how long it takes to completely settle biofilter media. In this research, the media compaction led to 20-50% increase in pressure drop. If we conservatively assume that same amount of compaction would happen within two years via gravity settling alone, the constant t would be 0.10~0.25. The constant t depends on the media's physiochemical characteristics. Low values for constant t are appropriate for wood mulch and activated carbon since both are less likely to be changed by gravity.

Other factors, including mixing of media, temperature, biomass accumulation, PM loading and media degradation, may have important influences on the airflow resistance as well. These factors are not included in the suggested model modification and more work is needed.

Table 3-4 Summary of airflow resistance tests of eleven media and mixtures with varied bed thickness.

Media	Bed thickness							
	58.4 cm		45.7 cm		33.0 cm		20.3 cm	
	$a \times 10^4$	b	$a \times 10^4$	b	$a \times 10^4$	b	$a \times 10^4$	b
fresh chipped hardwood mulch, 41.7%wb moisture, same below	2.3	55.5	2.0	52.2	1.8	54.2	1.4	36.1
fresh chipped hardwood mulch, 55.0%wb	1.4	15.8	1.0	10.7	0.6	6.3		
fresh chipped hardwood mulch, 59.2 %wb	3.0	44.5	2.6	38.0	2.2	32.2	1.9	29.5
aged chipped hardwood mulch, 40.1%wb	2.3	22.8	2.0	21.1	1.6	18.0	1.1	13.5
aged chipped hardwood mulch, 53.4%wb	2.9	28.1	2.7	27.2	2.3	25.9	1.9	25.0
softwood mulch, 40.2%wb	1.4	11.4	1.3	11.4	0.6	5.6		
softwood mulch, 55.1%wb	1.7	12.1	1.5	11.0	1.1	8.8	0.5	4.0
medium shredded hardwood mulch, 39.5%wb, un-compacted	1.2	12.9	1.1	11.4	1.1	12.6	0.8	9.5
medium shredded hardwood mulch, 52.1%wb, un-compacted	1.1	11.4	1.1	11.2	1.0	10.6	0.8	7.4
medium shredded hardwood mulch, 52.1%wb, compacted	1.7	13.9	1.6	13.6	1.6	12.6	1.2	8.5
fine shredded hardwood mulch, 42.0%wb, un-compacted	2.5	8.6	3.1	13.3	2.3	8.5		
fine shredded hardwood mulch, 54.4 %wb, un-compacted	3.8	13.5	3.3	12.3	2.7	9.1	1.1	3.5
fine shredded hardwood mulch, 54.4%wb, compacted	4.5	10.2	4.3	9.3	4.2	8.2	3.5	6.1
manure compost, 34.2%wb	8.4	8.6	7.7	8.4	7.6	8.8	6.9	10.1
manure compost, 44.2%wb	9.0	8.5	6.3	7.6	5.1	7.0	4.6	6.8
leaf compost, 51.4%wb, un-compacted	6.2	12.1	6.1	11.9	5.4	11.2	4.5	11.1
leaf compost, 51.4%wb, compacted	9.3	10.5	9.3	9.2	9.1	8.6	9.0	7.9
manure compost and fine shredded hardwood mulch mixture, 54.7%wb	9.4	10.2	8.4	11.3	6.3	10.4	4.9	10.8
manure compost and medium shredded hardwood mulch mix., 50.2%wb	5.9	8.3	3.9	6.3	4.0	7.8	4.1	8.3
leaf compost and medium shredded hardwood mulch mixture, 55.1%wb	3.8	12.8	4.1	17.1	3.9	18.8	3.6	23.3
leaf compost and fine shredded hardwood mulch mixture,53.3%wb	6.3	25.4	4.4	17.3	4.4	15.8	9.4	47.6
peat, 48.7%wb	14.2	4.1	18.7	5.7	14.1	4.1		
activated sludge, 75.7%wb			5.1	14.5	6.6	52.7		
Soil, 50.2%wb			7.5	11.5	7.2	13.8	8.3	19.9
activated carbon, 8.3%wb, bed thickness:25.4cm	5.5	85.2						
activated carbon, 20.2%wb, bed thickness:25.4cm	17.3	18.2						

3.4 Conclusions

Eleven biofilter media were characterized for their physical and chemical properties, including density, porosity, particle size distribution, pH, total carbon, nitrogen and organic matter contents in this study. The airflow resistances of the eleven media and their mixture were measured as well. The moisture content, particle size distribution, compaction and bed thickness were found to be significant in determining airflow resistance. *Hukill and Ives* (1955) equation was used to

model airflow resistance and the constants were calculated as a database for future biofilter designs. Based on these results, an empirical modification implementing derating factors was estimated to improve the *Hukill and Ives* (1955) equation to enable predictions that take in account effects present in an application. This study can benefit agricultural biofilter designers for media and fan selection.

Chapter 4:TRANSPORT AND FATE OF NITROGEN-CONTAINING COMPOUNDS IN GAS-PHASE BIOFILTERS

4.1 Introduction

To date, many inexpensive organic materials have been tested as biofilter media. These materials include wood chips, compost, sludge, coconut fibre, bark, pruning wastes, and peat (Chen et al., 2005; Colon et al., 2009; Kastner et al., 2004b; Kim et al., 2000; Pagans et al., 2007; Poulsen and Moldrup, 2007; Ramirez et al., 2009; Sadaka et al., 2002; Yin and Xu, 2009). These materials have irregular shapes, various specific surface areas, and dissimilar carbon and nitrogen contents. Unlike pure inorganic materials in which physical absorption is thought to dominate, these materials have physical adsorption, chemical absorption, and microbial degradation happening simultaneously (Devinny et al., 1999).

The transport and fate of nitrogen (N) within a gas phase biofilter using agricultural products or byproducts is complicated (Poulsen and Jensen, 2007). There are several models describing the N transport and fate in biofilters. Kastner et al. worked on a pilot scale biofilter and proposed the kinetics of ammonia oxidation to be a first-order reaction (Kastner et al., 2004b). That study analyzed ammonia removal efficiency to validate the removal model. Nicolai and his colleagues proposed a nitrogen cycle in a biofilter (Nicolai et al., 2006b). The cycle was developed from a soil nitrogen cycle (Brady and Weil, 2000) and was described by four major steps: ammonia adsorption, nitrification, immobilization, and mineralization. A first-order reaction model was developed to calculate the N transformation rates. However, the model has not been tested; and in their studies, the total collected N only accounted for 29% of the N removed from the inlet ammonia gas. It would be worthwhile to test this model, since it provides very measurable indicators (nitrification rate constants, k_1 and k_2) of biofilter performance. Baquerizo et al. took the microbial activities into consideration (Baquerizo et al., 2005). The inhibitory effects of free ammonia (FA), free nitrous acid (FNA), and oxygen limitation were included in their model. Accumulation of N in a biofilter may be a concern, since it was reported that 10-150 mg/L FA can inhibit *Nitrosomonas* (a genus that oxidizes ammonia into nitrite), 0.1-1.0 mg/L FA can inhibit *Nitrobacter* (a genus that oxidizes nitrite into nitrate), and 0.22-2.8 mg/L FNA can inhibit nitrifying organisms (Anthonisen et al., 1976). Further studies show that nitrite-oxidizing

bacteria (NOB) are likely to be more sensitive than ammonium-oxidizing bacteria (AOB) to these inhibitors (Hanaki et al., 1990; Park et al., 2010).

In most, if not all, of the biofilter nitrogen fate and transport studies, the nitrogen compounds accumulate constantly. Under real conditions, however, they do not always happen in that way. Many biofilters are open to the atmosphere. As a result, rain, snowmelt, and deliberate over-irrigation can wash nitrogen compounds away from biofilters. The reduction of nitrogen compounds (N-depleting process) can affect the inhibitory effects, the ammonia separation and conversion rates, and will eventually change the nitrogen transport and fate. How the N-depleting process would affect biofilter performance is not clear.

The objective of this work was:

(i) to test the nitrification model (modified from Nicolai's (Nicolai et al., 2006b) first-order reaction model),

(ii) and to study the transport and fate of N during a swing test, which was composed of an N-enriching step, an N-depleting step and a second N-enriching step in two gas phase ammonia mitigation biofilters. The ammonia removal efficiency and the nitrification kinetic rates were studied.

4.2 Experimental Setup and Analytical Methods

4.2.1Experimental setup

The experimental setup is shown in Figure 4.1. Two bench-scale cylindrical biofilters with high aspect ratio (ID=45 cm, H=50 cm) were made of transparent plastics and were operated at regular lab conditions (T=20-25 $^{\circ}$C, room air RH=30-60%). Anhydrous ammonia (99.99%, S.J. Smith Co., Urbana, IL) regulated by a mass flow controller (Model 825, Edwards High Vacuum International, Wilmington, MA) was mixed with ambient air to provide 100 l/min mixture of ammonia and air into each biofilter. Air from the blower supplying the biofilters was 2-3 $^{\circ}$C (Type T thermocouple wire, #5ZPW6, Grainger Industrial Supply) higher than the ambient room temperature; therefore, a cooling coil was used to reduce the air temperature. Inlet gas passed through a gas distributor and a plenum. A layer of organic biofilter media of 25 cm thickness was supported 10 cm above the bottom of the biofilter tank by a perforated floor. The empty bed retention time (EBRT) was 23.8 sec. Water was sprayed at a constant rate periodically; the spraying time was adjusted based on the difference of inlet and outlet humidity and the media moisture content changes. Inlet and outlet ammonia concentrations were measured by an

ammonia analyzer (Model 17C, Thermo Environmental Instruments Inc. Franklin, MA). The ammonia analyzer was calibrated before the start of the experiment and then checked with certified ammonia gases (80 ppm) every two weeks. The analyzer was re-calibrated once during the experiment when the reading was 5% different from the certified gas concentration. From time to time, the relative humidity was measured using a probe (HMP155, Vaisala Inc., Woburn, MA). The media samples were taken out of the biofilters from two sampling ports, which were located 5 cm above the bottom of the media (lower port) and 5 cm beneath the surface of the media (upper port), respectively. The ammonia concentrations and gas temperature were monitored and recorded; the water pump (170DM5, Stenner Pumps & Parts, Indianapolis, IN) and solenoid valves were controlled by a site-built control and data acquisition system (Labview, National Instruments CO., Austin, TX, and Personal Daq/56, Measurement Computing CO., Norton, MA).

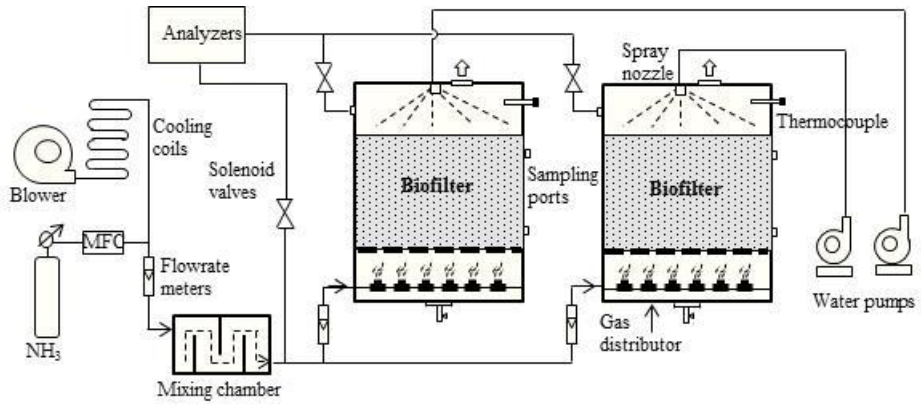

Figure 4.1 Schematic of bench-scale biofilter experimental setup.

Like most large scale site-built biofilters, this experimental setup did not have a pre-humidifying unit to add water to wet the inlet gas. The moisture of the biofilter media was carefully controlled manually, based on regular media sampling and moisture addition via the spray nozzles, in order to not leach chemicals out of the biofilter. The inputs of the system included inlet gas and water, and the only output was the outlet gas. This operational strategy helped in the tracking of nitrogen compounds and also accelerated the accumulation of nitrogen compounds in the biofilter system, compared to a biofilter system where leachate is produced. The experiment was operated for three months (between September and December 2010.)

4.2.2Media selection

Wood chip and compost are widely used in agricultural biofilters to mitigate air emissions from livestock buildings (Jones and Banuelos, 2000). The mixture of wood chip and compost provides nutrients, carbon source and abundant microbial communities. In this test, the mixture of fine shredded hardwood mulch and manure compost at a 1:1 weight ratio was used as the biofilter media. These two materials were described in a previous study (Yang et al., 2011). Their physical and chemical properties are summarized in Table 4-1. The media were dried at a 105℃ oven for 24 hours (final MC: ~ 0% w.b.) before the density and porosity were measured.

Table 4-1 Selected physical and chemical properties of the biofilter media.

Media	Density, g/L	Porosity,%	pH [a]	Total C % [a]	Total N % [a]	C/N [a]	Org. matt. % [a]
Fine shredded hardwood mulch	231.1 ±2.3	61.1 ±0.6	8.4 ±0.1	21.5 ±1.2	0.7 ±0.1	31:1	39.0 ±2.2
Manure compost	406.5 ±1.9	62.0 ±0.2	8.5 ±0.1	15.2 ±1.2	1.0 ±0.1	15:1	28.1 ±1.7

[a] sample analysis performed by Midwest Laboratories, Inc., Omaha, NE. Mean ± standard deviation (n=3).

4.2.3Sampling and analysis

Each of the three gas sources (inlet gas, biofilter 1 and 2 outlet gas) was analyzed eight hours daily in a rotation, using one ammonia analyzer, by means of the control system via the solenoid valves (C2DB1062, and C3LM1075, Parker Hannifin, Cleveland, OH). Media were sampled from both the upper and lower ports every two days. The media pH values were measured at each experiment transition. The media samples were extracted by DI water according to the TMECC 04.11 method (Thompson et al., 2002). The slurry pH value was then measured by a pH meter (PH1100 Series, OAKTON^{TM}, Vernon Hills, IL).

The moisture, nitrite, nitrate and ammonium in the media were measured in 30-g media samples. The samples were returned to the top of the biofilter media after the measurement. A ten gram sample was dried in a 105 ℃ oven for 24 hours to calculate the wet-basis moisture content. Ammonium and nitrate were measured according to slightly modified TMECC 04.02 standards (Thornpson et al., 2002). A ten gram sample of media was extracted by 100 ml DI water. The filtrate was centrifuged (3000 rpm for 30 minutes) and then analyzed in a Hach DR/2010 spectrophotometer (Hach Co., Loveland, CO.) Ammonium was measured using method 8155 and nitrate was measured using method 8039, respectively (Company, 1996-2000). Compared to the regular TMECC standard, a smaller amount of sample was used in this study in order to minimize the sampling disturbance to the biofilters. The nitrogen compound

concentrations in the media reported in this study were calculated as: [measured compound concentration × 100mL]/ [10 gram × (1-moisure content)]. Moisture contents measured via the previously-described method were used in this calculation. The rest of the ten gram sample was put into a sealed container with 100 ml DI water. Since nitrite is unstable and can be oxidized to nitrate easily during handling, the sample was not mechanically stirred to extract chemicals; instead, the extraction was allowed to happen by diffusion over one hour with the sealed container at rest. The filtrate was analyzed immediately using the HACH DR/2010 (method 8507, Hach Company, 1996-2000). The concentration reported in this study was calculated as before: [measured compound concentration × 100mL]/ [10 gram × (1-moisure content)].

The un-ionized ammonia, or free ammonia, (FA) and un-ionized nitrous acid (FNA) was calculated based on the dissociation constant. For FA, $[FA] = [NH_4^+][OH^-]/K_b$, $pK_b = -\log_{10}K_b = 4.75$; and for FNA, $[FNA] = [NO_2^-][H^+]/K_a$, $pK_a = -\log_{10}K_a = 3.398$.

4.2.4Nitrogen enriching and depleting steps

When the inlet ammonia gas concentration was high (>30 ppm), and the N compounds were accumulating in the biofilter media, the process is defined as the N enriching step in this study. In contrast, when inlet ammonia gas concentration was very low (<10 ppm), and N compounds left the biofilter, the process is named N depleting step. In the N depleting step, the inlet gas flowrate was doubled to 200 l/min, while the moisture content in the media was held constant (59-61% w.b.) by adding water, based on regular media sampling and oven testing. Given the high air velocity, low inlet ammonia concentration and high pH condition in the depleting step, some ammonia gas was assumed desorbed from the media. Also, because of the high air velocity and high outlet relative humidity in the depleting step, the water irrigation rate was increased. As a result, free water was presented in the media. The free water can be brought out of the biofilters by the outlet air as small water droplets. Since ammonia, nitrous acid and nitric acid are highly soluble in water (the Henry's Law constants are 59, 49 and 2.1E+5, respectively; the solubility of ammonia is 31% at 25^{o}C, and the nitric acid is completely miscible with water), some nitrogen compounds exited the system via the water droplets, if that mechanism actually occurred. Compared to replacing media, the N depleting step by excess ventilation would not bring new microorganisms or chemicals into the system; and compared to water washing, this method would change the aeration conditions and media structure less intensively.

4.2.5Nitrogen balance

The nitrogen balance was evaluated every two days by measuring the following ratio:

$$\text{Ratio}= \frac{\text{Total amount of N accumulated in the biofilter media}}{\text{Total amount of N separated from the inlet gas}} \quad (4\text{-}1)$$

Where, total amount of N accumulated in the biofilter media was the collected N in the media from day 1 to day n when the ratio was calculated; and total amount of N separated from the inlet gas was the cumulative N difference between inlet gas and outlet gas from day 1 to day n when the ratio was calculated.

In this study, the only accumulated N compounds considered in the biofilter media were NH_4^+-N/ NH_4OH-N, NO_2^-N/HNO_2-N and NO_3-N/HNO_3-N. The concentrations of N compounds obtained from the upper and lower sampling ports were averaged. Organic-N compounds were not measured in this study. N_2, N_2O and other gas-phase N compounds were also not included in the mass balance calculation. There was no leachate observed during the experiment period, therefore, no N was washed away by leachate.

4.2.6Transformation rates

The nitrification process was considered as two consecutive first order reactions. The kinetic model was modified from Nicolai's study (Nicolai et al., 2006b). Since it was a continuous process, the first step of nitrification was expressed as:

$$\frac{dC_{\mathrm{NH_4^+}}}{dt} = -k_1\left[C_{\mathrm{NH_4^+}}\right] + C_{in} \quad (4\text{-}2)$$

Where,

$C_{NH_4^+}$ = NH_4^+-N concentration in the media

t = time, day

k = rate constant, day^{-1}

C_{in} = daily absorbed NH_4^+-N concentration, equal to the daily inlet and outlet NH_3-N difference divided by the total dry mass of biofilter media.

In the second step, the reaction was modeled as:

$$\frac{dC_{\mathrm{NO_3^-}}}{dt} = k_2\left[C_{\mathrm{NO_2^-}}\right] \quad (4\text{-}3)$$

Where,

$C_{NO_3^-}$ = NO_3^--N concentration in the media

$C_{NO_2^-}$ = NO_2^--N concentration in the media.

Solving equations 4-1 and 4-2, we get:

$$C_{\mathrm{NH_4^+}} = \frac{C_{in-}(C_{in}-k_1\mathrm{CH_4^+},0\,)e^{-k_1 t}}{k_1} \quad (4\text{-}4)$$

$$C_{\mathrm{NO_2^-}} = \frac{C_{in}}{k_2}(1-e^{-k_2 t}) + \frac{C_{in}-k_1\mathrm{CH_4^+},0}{k_2-k_1}\,(e^{-k_2 t} - e^{-k_1 t}) \quad (4\text{-}5)$$

$C_{NH_4^+}$, $C_{NO_2^-}$, and $C_{NO_3^-}$ were measured every two days, and the rate constants k_1 and k_2 were calculated by fitting measured data back into equations 4-4 and 4-5. Within any two-day period, day n to day ($n+2$), the rate constants were calculated. The $C_{NH_4^+,\,n}$ was used as the $C_{NH_4^+,0}$ in equations 4-4 and 4-5 to get $k_{1,\,n+2}$ and $k_{2,\,n+2}$.

4.3 Results and Discussion

4.3.1 First N enriching step (day 1- day 28)

The initial inlet ammonia concentration was about 52 ppm and then stabilized at 60-70 ppm. There was no start-up period allowed. Both biofilters started removing ammonia immediately (Fig. 4.2A). The removal efficiencies (REs) reached 94% on day 14 and lasted for ten days. On day 24, the REs started to decline. The two biofilters had similar trends. Temperatures inside biofilters were 1-3^{o}C higher than the surrounding environment (probably due to the air temperature rise supplied by the blower). The initial pH values of the two biofilter media were 8.4±0.1 and 8.5±0.1, respectively (Table 4-1). On day 27, the pH values were 8.5±0.1and 8.4±0.2, respectively.

Concomitant with the change of REs was the accumulation of nitrogen compounds in the media. As shown in the Fig. 4.2B, the concentrations of NH_4^+-N and NO_3^--N were increasing dramatically. By day 28, the sum of NH_4^+-N, NO_2^--N and NO_3^--N, shown as N-sum in the figure, reached 15.2 and 19.2 mg(N)/g(dry media) in biofilter 1 and 2, respectively. The results showed that NO_3^--N was the dominate (60-70%) nitrogen compound in the media. 30-40% of absorbed NH_3 was not oxidized into either nitrite or nitrate, but stayed as NH_4^+-N. This observation was similar to a previous study carried out by Baquerizo et al. (2009), who found that only 50% of NH_3 was oxidized in a biofilter. If we assume that roughly all the NH_4^+-N was dissolved in the biofilm moisture (this assumption might be overestimated, because a very low percent of NH_4^+-N can be adsorbed by the media), the concentration of free ammonia (FA) is calculated as high as 658 and 784 mg/L in the biofilm moisture of biofilter 1 and 2, respectively. The high concentrations of FA can inhibit the nitrification process (Anthonisen et al., 1976) and lead to a decrease of ammonia removal efficiency. As shown in Figure 4.2B, the NO_2^--N concentration

increased slightly in both biofilters, indicating the possible inhibition of *Nitrobacter* by FA. If we apply the same assumption to FNA, on day 28 the concentrations of FNA in the media of biofilter 1 and 2 were 1.55E-3 and 2.11E-3 mg/L, respectively. According to Anthonisen's research, FNA can inhibit nitrification when its concentration reaches 0.22-2.8 mg/L. Based on his conclusions, the low concentration of FNA in our biofilter media might not be an inhibitor in this step.

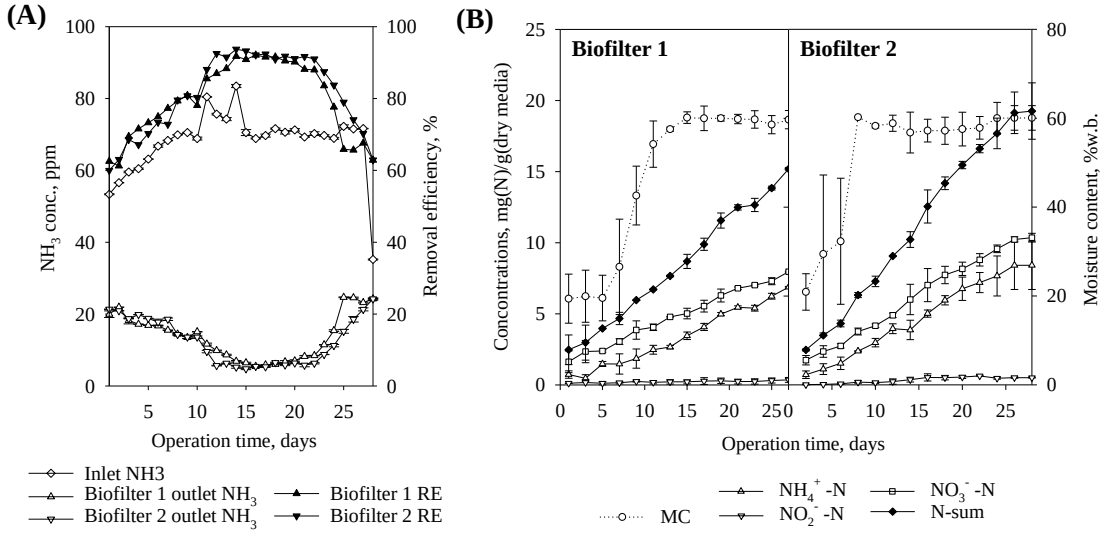

Figure 4.2 Biofilters performance (A) and N-compound concentrations (B) in the first N enriching step.

Note: the measured data is listed in the appendix B1 and B2.

4.3.2Nitrogen depleting step (day 29- day 48)

The N depleting step started on day 29. Nitrogen exited the biofilter media in this step. The inlet ammonia concentrations were decreased gradually to 10 ppm (Fig. 4.3A). The outlet ammonia concentrations were even higher than the inlet ammonia concentration, showing the depleting step compelled some absorbed/adsorbed ammonia gas to leave the system.

In the depleting step, the concentrations of nitrogen compounds in the media were reduced (Fig. 4.3B). However, the reductions of NO_3^-N and NH_4^+-N were quite different. In the first week, the NH_4^+-N concentrations were dropped about a half while the NO_3^--N concentrations were relatively stable, because that nitrification was still processing, which compensated for the loss of NO_3^--N. After the first week, both NO_3^-N and NH_4^+-N were decreased. The depleting step cleaned out 60-80% of NH_4^+-N and 20-30% of NO_3^--N. At the end of that step, the pH values of both biofilter media were 8.2 ±0.1 which were lower than the pH values on day 28 (8.5 and 8.4 in biofilter 1 and 2, respectively). The FA concentrations were also decreased. Using the

assumption mentioned above, FA concentrations on day 48 were calculated as 185 and 235 mg/L for biofilter 1 and 2, respectively. They were 72% and 70% lower than the values on day 28, respectively. However, FA concentrations might still be higher than the inhibition threshold based on Anthonisen's research (Anthonisen et al., 1976).

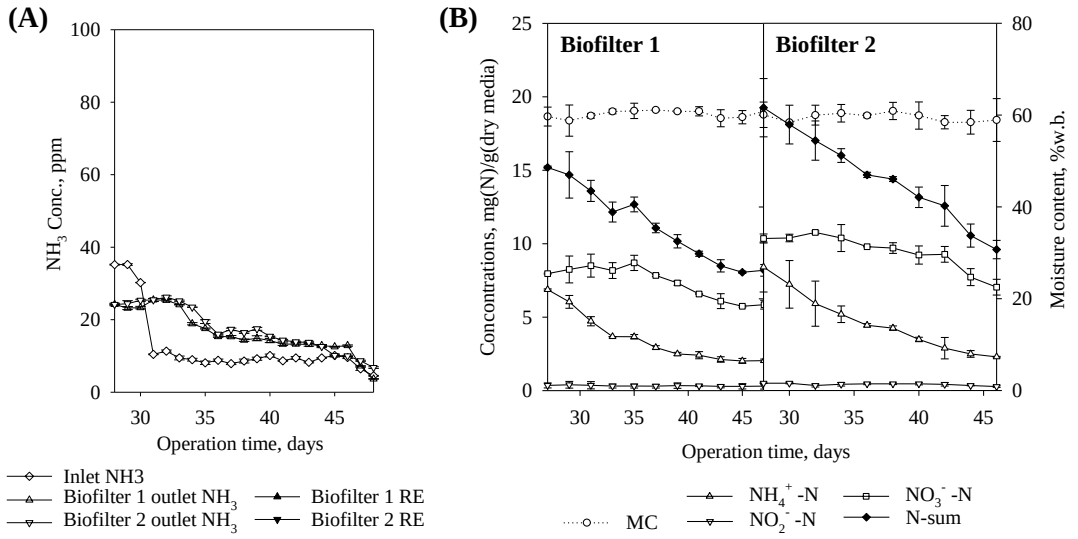

Figure 4.3 Biofilters performance (A) and N-compound concentrations (B) in the N depleting step.

Note: the measured data is listed in the Appendix B1 and B2.

4.3.3Second nitrogen enriching step (day 49- day 83)

Given the high FA concentration in the second N enriching step, the inlet NH_3 concentration was set at 40 ppm which was lower than it was in the first enriching step. The REs of both biofilters were 70-80% in the first ten days, but then decreased gradually (Fig. 4.4A). On day 83, an NH_3 break-through phenomenon was observed. The results showed that the N-depleting step helped a little bit in recovering ammonia removal efficiency, but its capability was limited. The nitrogen compounds continued to accumulate (Fig. 4.4B). NH_4^+-N concentrations increased 60-100% in both biofilters during the first ten days. After day 70, the N-sum concentrations were relatively stable and reached the concentrations observed before the depleting step (day 28). On day 83, the pH values of both biofilter media were 8.3±0.2. The FA concentrations were 446 and 592 mg/L in biofilter 1 and 2, respectively.

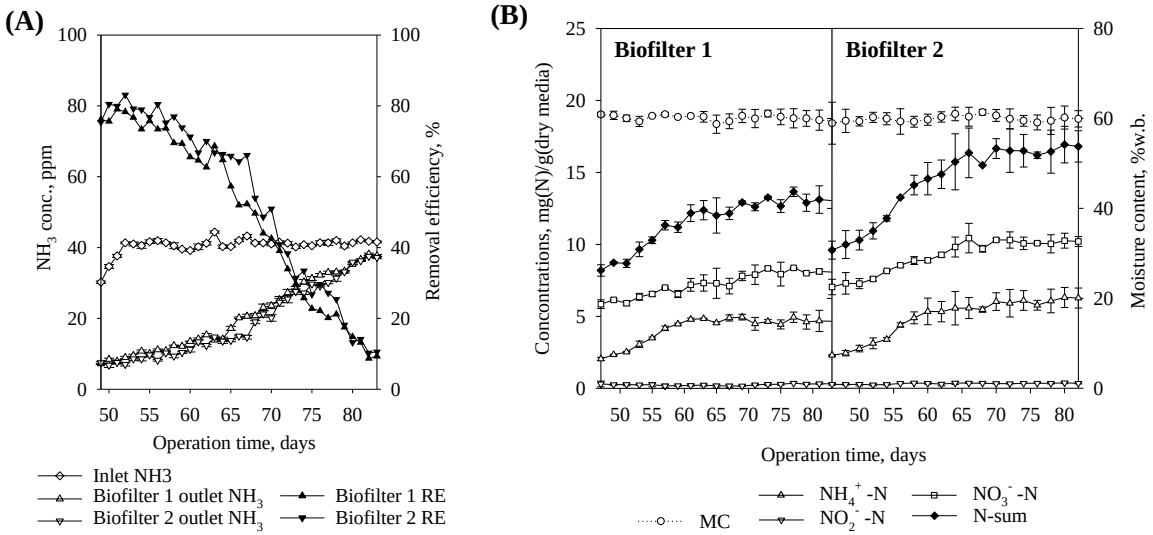

Figure 4.4 Biofilters performance (A) and N-compound concentrations (B) in the second N enriching step.

Note: the measured data is listed in the appendix B1 and B2.

4.3.4Nitrogen balance and fate

The NH_4^+-N, NO_2^--N and NO_3^--N accumulated in the media accounted for 50-100% of N captured from inlet gas (Fig. 4.5). This ratio was higher than the percentages observed in a previous study (Nicolai et al., 2006b). The ratios were increasing in the enriching steps and were decreasing in the depleting step, suggesting that there was an edge effect. The media samples were taken from the near edge of the biofilter (2 inches away from the biofilter wall). The air surface velocity was higher near the edge than it was in the biofilter center. Therefore, in the enriching steps, the near-edge media can absorb more ammonia than the near-center media did. As a result, the calculated nitrogen balance ratios (which assumed N was evenly distributed in the media) would be higher than the real values. In the second enriching step, the inlet ammonia concentration was lower than it was in the first enriching step; therefore, the curves were relatively flat compared to the first enriching step. The results also indicate that less than 50% of N may be transformed into organic-N compounds, N_2O, N_2 or others. More work will be needed to trace these N compounds.

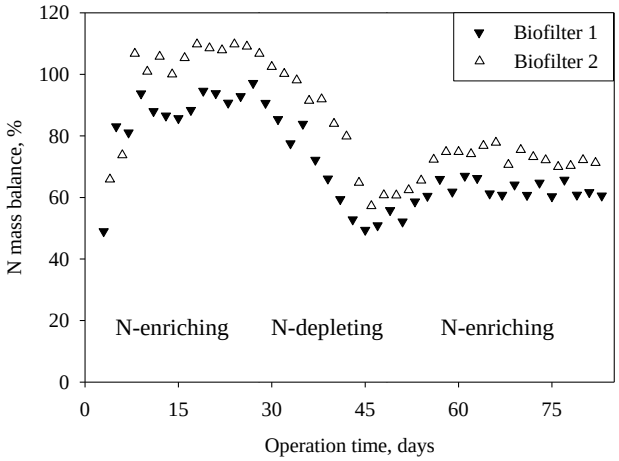

Figure 4.5 Nitrogen balance in two biofilters.

The fate of nitrogen was very different among the enriching and depleting steps as shown in Table 4-2. The amount of inlet NH_3-N is defined as 100 to facilitate comparison. In the first enriching step, more than two thirds (73.5% and 86.6% for biofilter 1 and 2, respectively) of N was transformed into either NH_4^+-N, NO_2^--N or NO_3^--N. In the second enriching step, however, only about one third of N (33.4% and 46.2% for biofilter 1 and 2, respectively) was transformed into either NH_4^+-N, NO_2^--N or NO_3^--N. Another interesting difference is the changing of N composition. The NH_4^+-N/NO_3^--N ratios were close to 1 in the enriching steps in both biofilters, suggesting that half of the absorbed ammonia was converted into nitrate; while in the depleting step, 270.3% and 221.9% equivalent NH_4^+-N was lost from biofilter 1 and 2, respectively, much higher than the loss of NO_3^--N in this step. It greatly changed the distribution of N in the biofilters, and also firmly indicated that in the depleting step, the nitrification inhibition was reduced and NH_4^+-N was converted into NO_3^--N. This nitrification partially made up for the loss of NO_3-N and increased the loss of NH_4^+-N.

Table 4-2 Fate of N.

Step	Biofilter 1					Biofilter 2				
	inlet NH_3-N	Outlet NH_3-N	NH_4^+-N	NO_2^--N	NO_3^--N	inlet NH_3-N	outlet NH_3-N	NH_4^+-N	NO_2^--N	NO_3^--N
First enriching step	100[a]	19.1	35.5	1.4	36.6	100	17.4	39.7	2.5	44.4
Depleting step	100	160.5	-270.3[b]	-3.0	-118.1	100	145.8	-221.9	-8.4	-120.3
Second enriching step	100	52.5	18.1	0.4	14.9	100	47.5	25.9	0.6	19.7

[a] the amount of inlet NH3-N is defined as 100.
[b] the N compound concentration is decreasing.

4.3.5Transformation rate

The time constants k_1 and k_2 decreased dramatically in the two N enriching steps (Figure 4.6). Time constant k_1 changed from 0.5/day to 0.005/day, and k_2 changed from 8/day to 0.15/day, suggesting that the reactions slowed down. These time constant values strongly supported the inhibition of accumulated N compounds, especially FA, on the microbial activities. The results also show that more variables, such as FA concentration, are needed to model the two-step nitrification process. Furthermore, the contribution of denitrification should be considered as well (Saliling et al., 2007). The first step of denitrification is converting nitrate to nitrite, which is opposite of the second step of the nitrification process. Therefore, in the first order reaction model, the first step denitrification and the second step nitrification might be considered as a reversible reaction.

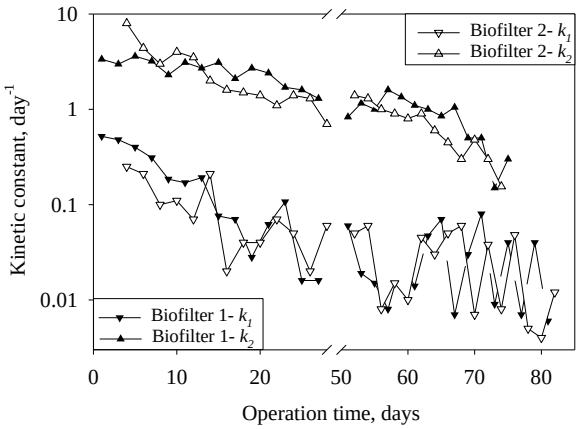

Figure 4.6 Nitrogen transformation rates.

In order to reduce the inhibition effects of N compounds, a lower ammonia loading rate or a lower media pH value might be needed. In either situation, the accumulation of FA and FNA will be slowed down or maintained at a certain range which will not inhibit nitrification. However, running a biofilter at low pH values may increase the production of N_2O - a very strong greenhouse gas (Weslien et al., 2009). Generating N_2O and removing ammonia presents a technical conflict. Therefore, the pH value of biofilter media should be optimized.

4.3.6Limitations

Measurement: in this study, the organic N compounds and most of denitrification products were not measured. The N compounds dissolved in the outlet mist (if any droplets were formed)

were not measured. The edge effects at the physical boundaries of the biofilter containers may affect the measurement.

Modeling: given the complexity of the microbial activities, the two consecutive first-order reactions may not explain the nitrification process perfectly. Denitrification was not included in this study.

4.4 Conclusions

With high ammonia loading concentrations (70 ppm) and high pH values (8.2-8.5), the biofilters reached high ammonia removal efficiency (94%) for 10 days. The biofilter performance fell at the end of the first N-enriching step. The N-depleting step partially cleaned the accumulated N, and recovered ammonia removal efficiency for a short time. The ammonia removal efficiency quickly dropped after ten days in the second N-enriching step.

NH_4^+-N, and NO_3^--N were the two major compounds in the media, and FA concentration is 185-784 mg/L in the media moisture. NH_4^+-N, NO_2^--N and NO_3^--N accumulated in media accounted for 50-100% of N captured from the inlet gas. These accumulated N compounds, especially FA, may have a strong negative feedback to the biofilter performance.

The nitrification transformation rates were determined in the N enriching steps. Time constant k_1 changed from 0.5/day to 0.005/day, and k_2 changed from 8/day to 0.15/day, indicating the reactions were inhibited. One very likely reason for the decrease could be the inhibition of the microbial activities caused by the accumulated FA. A lower ammonia loading rate or a lower media pH value might be needed to reduce the FA accumulation and to improve biofilter performance.

Practical use of the results

The study recommended a feasible model to analyze the performance of biofilters for the agricultural industry. The two nitrification time constants can be easily measured and can be used as biofilter operational indicators. If these two constants are decreasing continuously during operation, it suggests a degradation of biofilter performance. The results were obtained from biofilters with high aspect ratio; therefore these findings can be applied to a variety of large-scale biofilter designs. It is also the first time that a reduction of N compounds in the biofilter was performed for a study and its effects on biofilter performance were evaluated. These results can assist in improving biofilter management.

Chapter 5:MOISTURE EFFECTS ON GAS-PHASE BIOFILTER AMMONIA REMOVAL EFFICIENCY, NITROUS OXIDE GENERATION AND MICROBIAL COMMUNITIES

5.1 Introduction

Most of previous studies focused on the value and importance of improving biofilter ammonia capture ability (Baquerizo et al., 2005; Chen et al., 2005; Nicolai et al., 2005), however, recent reports about the generation of nitrous oxide from biofilters have spurred designers to consider the consequences of greenhouse gas emissions (Amlinger et al., 2008; Maia et al., 2012a; Maia et al., 2012b; Pitcher and Ebi, 2004). Nitrous oxide can be produced by both ammonia oxidizers and denitrifiers within a biofilter (Stein and Yung, 2003). A very small group of ammonia oxidizers are able to directly reduce NO_2^- under microaerophilic conditions through the activities of denitrifying enzymes (Casciotti and Ward, 2001; Colliver and Stephenson, 2000), but the majority of nitrous oxide is believed to come from incomplete denitrification (Devinny et al., 1999; Zumft, 1993). Within a large scale biofilter, given the compaction of media (Maia et al., 2012b; Yang et al., 2011), there exist anaerobic zones which favor denitrification (Sales et al., 2008).

Moisture content is a major determinant of biofilter performance (Bohn and Bohn, 1999). Too little moisture slows absorption of gaseous ammonia and microbial activities (VanLith et al., 1997); while too much water fills biofilter media pores and retards the transport of NH_4^+, O_2, and nutrients across the water film coating microbes. Despite the explicit role of moisture content on determining ammonia removal (Nicolai et al., 2006b), the effects of moisture content on nitrous oxide production were rarely specifically considered or tested. A primary reason for this gap is the unawareness of possible regional oxygen limitation in media that caused by high moisture contents (Maia et al., 2012b), because a biofilter is generally recognized as an aerobic environment since air continuously goes through it. Moreover, the adsorption of nitrous oxide to media surface complicates the observations as several studies reported reduction of nitrous oxide through biofilters (Akdeniz and Janni, 2012; Akdeniz et al., 2011). However, water competes with nitrous oxide for adsorption spots, especially when the media is populated with hydrophilic functional groups such as -OH or –COOH (Bradley, 2011). Therefore, at high moisture content, less nitrous oxide adsorption and higher nitrous oxide generation rates are expected (Avrahami and Bohannan, 2007; Wallenstein et al., 2006). Maia *et al*. reported that 0.6-2.0 ppm nitrous

oxide was produced in a start-up biofilter with about 60% media moisture content (Maia et al., 2012a).

Besides the influences of moisture content, how microorganisms respond to moisture changes is another key issue, given the lack of effective moisture managements in agricultural biofilters. The relationship between community dynamics and functional stability has been debated and different phenomenon were observed from case to case (Cabrol et al., 2012a; Valentin-Vargas et al., 2012; Van Nostrand et al., 2011; Wang et al., 2010; Xia et al., 2010). The concept of resistance, resilience and redundancy was applied to describe the relationships (Allison and Martiny, 2008). A stable function was sustained in a biofilter treating ammonia and VOCs emissions for a long term, although the microbial communities were highly dynamic (Cabrol et al., 2012b). Li, *et al*. also observed functional redundancy when phosphorus was added to nitrate removal bioreactors (Li et al., 2010). In another study carried out by Gentile et al. demonstrated resilience of microbial communities to environmental disturbances in a denitrifying reactor (Gentile et al., 2006); and studies in soil science showed that resilience depends on both soil structure and soil microbial community composition (Braker and Conrad, 2011; Griffiths et al., 2008). Resistance to disturbances was observed in the natural systems (Allison et al., 2010; Baho et al., 2012). Given the arguments, an essential approach is to investigate the relationship in an engineered, well controlled system such as the one we present. To our knowledge, no one has studied the response of microbial communities to disturbances caused by moisture change in ammonia removal biofiltration systems.

Unlike creating contaminant gradients (Cabrol et al., 2012b) or toxic chemical stress (Mertens et al., 2007; Taketani et al., 2010), moisture variation not only influences the microbial communities which eventually determine biofilter performance, but also directly affects absorption of ammonia into biofilter (Sakuma et al., 2008). In other words, moisture may affect biofilter performance in different ways. In this study, moisture was manipulated for a wide range from 35% to 63% wet basis to discover its roles. Particular microbial communities such as ammonia oxidizers and denitrifiers are responsible for the ammonia oxidation and nitrous oxide production, and are closely related with biofilter performance. Thus, their communities were examined in this study.

In this investigation, four bench-scale biofilters were studied. Our objectives were:

(i) To test the influence of moisture on biofilter ammonia removal efficiency and nitrous oxide generation, and to determine the appropriate moisture range;

(ii) To explore the response of bacterial communities, ammonia oxidizers and denitrifiers to moisture content change, including community structure shifting and abundance change; and

(iii) To link the microbial communities to biofilter functional stability.

5.2 Materials and Methodologies

5.2.1Reactor design and operation

The system includes a gas preparation unit, a biofiltration unit, an analysis unit, and a control unit (Fig. 5.1 and Fig. 5.2). Anhydrous ammonia (99.99%, S.J. Smith CO., Urbana, IL) regulated by a mass flow controller (Model 825, Edwards High Vacuum International, Wilmington, MA) was mixed with pre-humidified air to provide 70 liter per minute (LPM), 40 ppm ammonia gas for each biofilter (BF). The loading rate was 5.24 g-NH_3 $hr^{-1}.m^{-3}$. Air from the blower was 2-3^oC higher than normal room conditions. Therefore, a cooling coil was used to cool the gas to nearly room temperature. Four cylindrical biofilters (ID=45cm, H=50cm) were made of transparent plastics. A layer of 25 cm media, 1:1 mixed by compost and woodchip, was supported 10 cm above the bottom of the biofilter tank by a perforated floor. For each biofilter, there are four sampling ports (4 $\times 90^o$) located in both upper (5 cm bellow top surface) and lower (5 cm above bottom) layer. Water was pumped at a constant rate through a coiled soaker hose (OD=0.64 cm) onto the top of media. Inlet gas was treated by biofilters and then the purified gas left via an outlet port. Empty bed retention time (EBRT) was 34 seconds. Temperature and relative humidity (RH) were measured using a probe (HMP155, Vaisala Inc., Woburn, MA). Ammonia and nitrous oxide concentrations were measured by a gas analyzer (INNOVA1412, California Analytical, Inc., Orange, CA, Fig. 5.4). The analyzer was calibrated before the experiment began, and then was checked with certified gases (80 ppm) for every two weeks. A site-built control and data acquisition system (Labview, National Instruments CO., Austin, TX, and Personal Daq/56, Measurement Computing Co., Norton, MA, Fig. 5.3. The details about the control system are shown in the Appendix C6) was used to record data and to control the whole biofilter system. Ammonia and nitrous oxide concentrations, gas temperature and relative humidity were recorded every twenty seconds; the water pump (170DM5, Stenner Pumps & Parts, Indianapolis, IN) and solenoid valves (C2DB1062, and C3LM1075, Parker Hannifin, Cleveland, OH) were controlled

automatically. No extra nutrients or inoculum cultures were added, but a 10-day startup step was allowed.

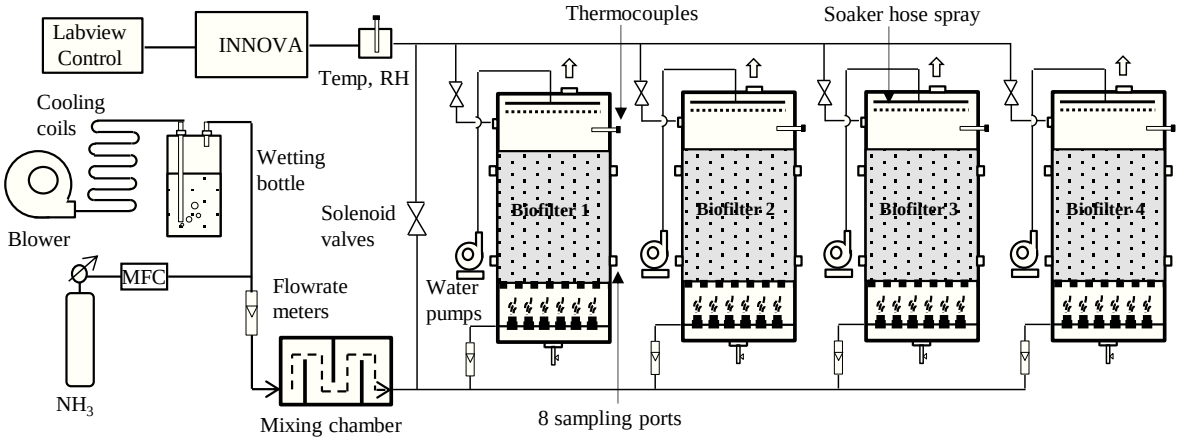

Figure 5.1 Ammonia removal and greenhouse gas generation experimental setup.

Figure 5.2 Experimental setup.

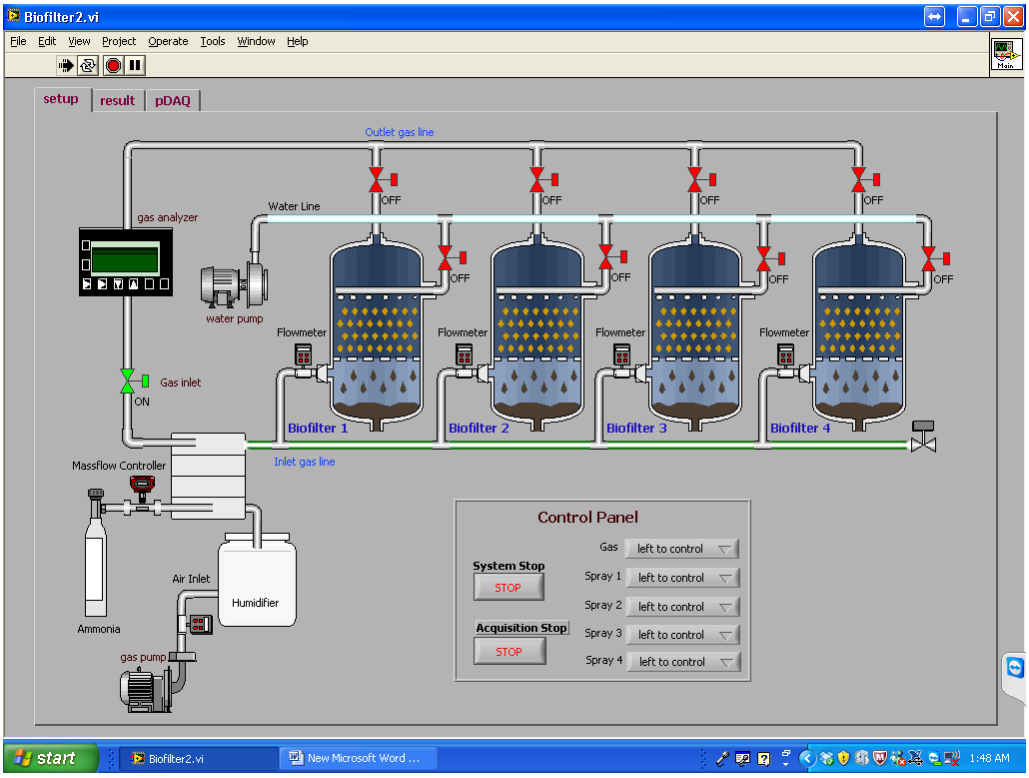

Figure 5.3 Labview control system.

Figure 5.4 INNOVA 1412.

The test was composed of four steps. Designed moisture contents in each biofilter were shown in Table 5-1. BF1 and BF2 were designed as two replicated treatments, while BF3 and BF4 were considered as two controls. Media was received from the Urbana Recycling Center, Urbana, IL, that had an initial moisture content of 33.2%w.b. Moisture content was measured by oven drying

at 105°C for 24 hours, and media size distribution was estimated using a Penn State Forage Particle Separator (NASCO, product #: C24682N).

Table 5-1 Designed moisture contents.

MC, %	BF 1, 2 [a]	BF 3, 4 [b]	Operating Days [c]
Step 1	35	35	23
Step 2	55	55	27
Step 3	63	55	33
Step 4	55	55	25

[a] considered as replicated treatments.
[b] considered as replicated controls.
[c] duration of each step.

5.2.2 Gas and media sampling

Each of the five gas sources (inlet gas, and outlet gases from biofilter 1- 4) was analyzed for 4.8 hours every day in a rotation, using one analyzer, by means of the control system via the solenoid valves. The daily variance is negligible since the temperature and flowrate of inlet gas were stable. Data generated in the first half hour was discarded since a gas transition took 3-5 minutes to completely finish. The INNOVA measured one gas sample for every twenty seconds. 10 g of randomly selected media was sampled into a 15 mL tube from each sampling port in the end of each testing step. Eight original media samples (considered as step 0) were taken as well. The samples were stored in a -80°C freezer before analysis. In total, 136 samples were collected.

5.2.3 DNA extraction and purification

Biofilter media samples were freeze-dried overnight until completely dry (Fig. 5.5). Large pieces of woodchips were physically broken into small ones and then were manually homogenized. DNA was extracted from 0.15 gram dry media using a FastDNA SPIN Kit for Soil (MP Biomedicals, Solon, OH) according to manufacturer's protocol. Extracted DNA was then purified using cetyl trimethyl ammonium bromide (CTAB) extraction to remove humic acids. DNA concentration was adjusted to standard concentrations of 10 ng/µl and 20 ng/µl prior to analyses. The details about DNA extraction and cleaning are shown in the Appendix C3 and C4. The concentrations of DNA after CTAB cleaning are shown in the Appendix C5.

Figure 5.5 Sample freeze-dry.

5.2.4 Microbial community analyses

Bacterial community composition in biofilter media samples was assessed using automated ribosomal intergenic spacer analysis (ARISA) (Fisher and Triplett, 1999). The polymerase chain reaction (PCR) was carried out in an Eppendorf MasterCycler Gradient (Eppendorf AG, Hamburg, Germany) and the reagents included 1x Promega buffer, 0.25 mM BSA, 2.5 mM $MgCl_2$, 0.4 µM of 1406 F-primer and 23S R-primer, 0.025 U/µl Promega GoTaq and 2 µl purified DNA (10 ng/ µl). PCR cycle was composed of: initial denaturation at 94^{o}C for 2 min, 26 cycles of 94^{o}C for 35 s, 55^{o}C for 45 s, and 72^{o}C for 2 min, followed by a final extension at 72^{o}C for 2 min. DNA fragments generated from ARISA were analyzed by denaturing capillary electrophoresis using an ABI 3730XL Genetic Analyzer (PE Biosystems, Foster City, CA). Details about this method were described previously (Kent et al., 2007).

Ammonia oxidizer community composition was analyzed using terminal restriction fragment length polymorphism (T-RFLP) analysis of the *amoA* gene encoding the catalytic α-subunit of archaeal ammonia monooxygenase (Liu et al., 1997). Since the number of archaeal *amoA* is about six times higher of bacterial *amoA* (Appendix C7), only archaeal *amoA* communities were analyzed. PCR reagents contained 50 mM Tris (pH 8.3), 250 µg of BSA per ml, 1.5 mM $MgCl_2$, 200 µM of each dNTP, 0.4 µM of each primer (amoA-F, 5'-STAATGGTCTGGCTTAGACG-3', and amoA-R, 5'-GCGGCCATCCATCTGTATGT-3') (Francis et al., 2005; Peralta, 2012), 2.5 U

of Tag polymerase (Promega, Madison, WI), and 5 µl DNA in a final volume of 50 µL. The *amoA* F-primer was labeled with the fluorescent dye HEX, the *amoA* F-primer was labeled with the fluorescent dye NED. PCR cycle was composed of: initial denaturation at 94^{o}C for 5 min, 30 cycles of 94^{o}C for 45 s, 53^{o}C for 1 min, and 72^{o}C for 1 min, then followed by a final extension at 72^{o}C for 15 min. PCR products were purified using the MinElute PCR purification kit (Qiagen, Valencia, CA, USA), and then were digested with RsaI (New England Biolabs Inc. Ipswich, MA). The terminal restriction fragments labeled with fluorescence were analyzed by denaturing capillary electrophoresis using an ABI 3730XL Genetic Analyzer (PE Biosystems, Foster City, CA).

Denitrifier community composition was also analyzed using the T-RFLP analysis. The nitrous oxide reductase gene (*nosZ*) targets the denitrifiers that are involved in the transformation of nitrous oxide to dinitrogen gas (Rich et al., 2003). PCR reaction mixtures contained 50 mM Tris (pH 8.3), 0.25mg per ml BSA, 2.0 mM MgCl2, 0.2 mM dNTPs, 0.2 µM of each primer, 2.5 U of Taq polymerase (Promega, Madison, WI), and 10 µl extracted DNA (10 ng/ µl) in a final volume of 50 µl. The nosZ gene was amplified using nosZ-F-1181 (5′-CGCTGTTCITCGACAGYCAG-3′) and nosZ-R-1880 (5′-ATGTGCAKIGCRTGGCAGAA-3′). The *nosZ* F-primer was labeled with the dye 6-FAM. Reaction cycle was composed of: initial denaturation at 94 ℃ for 3 min, 25 cycles of 94 ℃ for 45 s, 56 ℃ for 1 min, and 72 ℃ for 2 min, then followed by a final extension carried out at 72 ℃ for 7 min. Similarly, the *nosZ* PCR products were purified using a MinElute PCR purification kit, and then were digested in single-enzyme restriction digests containing either AluI or HhaI (New England Biolabs Inc. Ipswich, MA). The length and relative abundance of terminal restriction fragments were determined by denaturing capillary electrophoresis using an ABI 3730xl Genetic Analyzer (Applied Biosystems, Foster City, CA).

5.2.5 Denitrifier gene abundance determination

The *nosZ* gene was amplified using nosZ1527F, 5'- CGC TGTTC(A/C/T) TCG ACA G(C/T)C A-3' and nosZ1622R, 5'- CGC (G/A)A(C/G)GGC AA(G/C) AAG GT(G/C) CG-3' (Throback et al., 2004). PCR reactions contained 1X 5 µl SYBR green master mix (Applied Biosystems Inc., Foster City, CA), 0.4 mM of each primer, 0.5 mg per ml BSA, and 1 µl of DNA of known concentration (10 ng/ µl) in a final volume of 10 µl. Fragments were amplified with an initial denaturation step at 95 ℃ for 5 min, followed by 40 cycles of 95 ℃ for 1 min, 56 ℃ for 1

min and 72 ℃ for 1 min. Triplicates of each sample were analyzed. Standard curves were obtained based on serial dilutions of mixed PCR products of biofilter samples. Reactions were analyzed on a 384-well Applied Biosystems 7900HT Fast Real-Time PCR System (Applied Biosystems Inc., Foster City, CA).

5.2.6 Statistical analyses

Analysis of variance (ANOVA) was used to compare the physical and chemical properties, including total C, organic matter, total N, organic N, NH_3-N, pH values and size distribution, of biofilter media before and after the test. Abundance of *nosZ* genes was also compared using ANOVA. LSD Post hoc test was applied to estimate the difference in ammonia removal efficiency and nitrous oxide generation in the four operation steps. Daily averaged data of ammonia removal efficiency and nitrous oxide data were used as the inputs.

Bacterial and functional gene communities were analyzed using multivariate technologies. ARISA and T-RFLP data were Hellinger-transformed in order to convert the raw density of each peak to a relative intensity (Legendre and Gallagher, 2001). Non-metric multidimensional scaling (NMDS) was applied to visualize the results (Legendre and Legendre, 1998; Mccune and Grace, 2002). The Bray-Curtis distance matrices were taken as NMDS inputs (Legendre and Legendre, 1998), and the centroid and standard deviation of each group were showed on the reported figures (Yannarell et al., 2011). To examine how biofilter operation step, moisture level, sampling location and the replicates affect the bacterial, *amoA* and *nosZ* communities, PerMANOVA tests were carried out (McArdle and Anderson, 2001). Unless noticed, the original media –samples taken before biofilter operation- were included in the statistical test and were recognized as step 0. To statistically compare two sample groups, pairwise analysis of similarity (ANOSIM) based on Bray-Curtis distance matrices was conducted (Clarke and Warwick, 2001). The analysis of multivariate homogeneity of group dispersions (following Marti Anderson's PERMDISP2 procedure) was carried out to assess the homogeneity of microbial communities within a group of samples (Anderson, 2006; Anderson et al., 2006). The Hellinger-transformed data set was used as inputs and the average distance of each sample to its centroids was calculated. It generated a distance between 0 and 1, with longer distance shows lower homogeneity.

Calculations of ANOSIM and NMDS were carried out using PRIMER 6 (Primer-E Ltd., Plymouth, United Kingdom); calculation of ANOVA, post hoc and PerMANOVA significant

levels (function: adonis), and the group dispersion distances (function: betadisper) were performed in the R statistical environment (R Development Core Team, 2009) using functions found in the packages "MASS" and "vegan". The R codes are shown in the Appendix C8.

5.3 Results

5.3.1 Physical and chemical properties of media

The four biofilters were operated continuously for four months. The physical and chemical properties of media changed dramatically over time mainly due to intensive chemical and biological processes (Table 5-2). Total carbon and organic matter, which served as nutrient sources, were consumed and significantly decreased. In contrast, total nitrogen and organic nitrogen concentration significantly increased as a result of ammonia absorption and immobilization. The pH values were significantly decreased most likely caused by microbial activities, especially the nitrification process that releases H^+. (Taghipour et al., 2008). Also, media became relatively smaller after the test (Table 5-3). Microbial activities might be responsible for breaking down big wood chips into smaller pieces.

Table 5-2 Chemical properties of media.

	Total C	Organic matter	Total N	Organic N	NH_3-N	pH
Before test [a]	45.3 ±1.8	85.6 ±6.6	1.3 ±0.2	1.2 ±0.2	0.03 ±0.03	8.1 ±0.5
After test [b]	32.0 ±2.6***	66.2 ±12.5*	2.1 ±0.7*	1.9 ±0.5*	0.2 ±0.2	6.1 ±0.4***

Data analyzed in the Midwest Laboratories, Omaha, NE.
[a] four replicates.
[b] one sample from each layer of four biofilters, eight replicates totally.
Null hypothesis: the variables are the same before and after the test. The variables were tested separately.
Significance level: ***: p <0.001, *: p <0.05.

Table 5-3 Media size distribution, three replicates.

	>1.9cm	0.8-1.9cm	0.2-0.8cm	<0.2cm
before test [a]	15.7 ±1.1	43.3 ±2.5	31.8 ±1.9	9.3 ±1.2
After test [a]	4.0 ±0.7	34.5 ±1.1	46.2 ±1.1	15.4 ±0.6
p-value	***	**	***	**

[a] three replicates.
Null hypothesis: the percentages of each size range were the same before and after the test.
Significance level: ***: p <0.001, **: p <0.01.

5.3.2 Moisture management

To assess how well moisture was managed, moisture contents from both upper and lower layers of the four biofilters were measured weekly and the results are shown in figure 5.6. Since

water was added onto the top surface of media, upper layers were usually wetter than the lower layers. Moisture contents of upper layers were relatively constant during step 2 to 4 in all four biofilters, while moisture contents of lower layers were managed to be different. In step 3, lower layers of BF1 and BF2 (59.7±1.6%) pair were much wetter (p <0.01) than that of the control, BF3 and BF4 (48.8±1.1%) pair. Averaged moisture contents of upper and lower layers of the four biofilters are listed Table 5-4, and were quite close the target moisture contents.

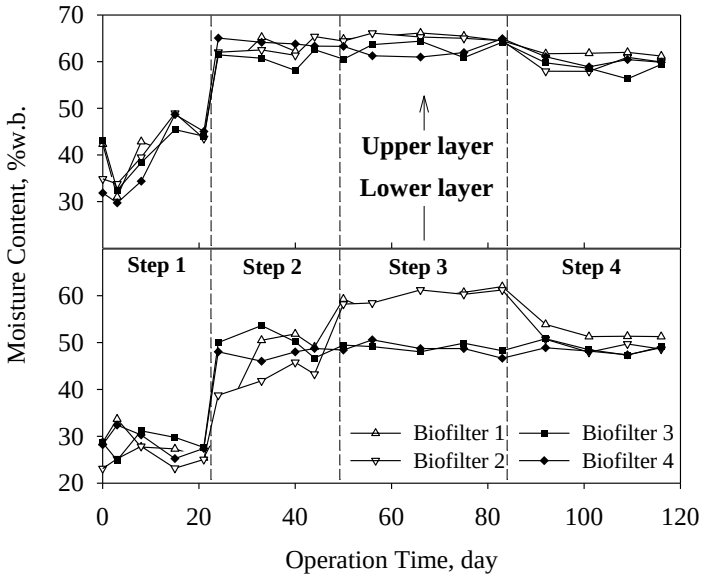

Figure 5.6 Moisture contents of biofilter media in the lower and upper layers.

Table 5-4 Averaged moisture contents.

MC, %	BF1	BF2	Targeted	BF3	BF4	Targeted
Step 1	34.1	32.5	35	34.6	33.3	35
Step 2	53.1	52.6	55	55.4	55.9	55
Step 3	62.4	62.5	63	55.8	55.6	55
Step 4	56.8	54.2	55	53.7	54.2	55

5.3.3 Biofilter performance

Biofilter performance, including ammonia removal efficiency and generated nitrous oxide concentration, were measured continuously. For the treatment biofilters, BF 1 and BF2, ammonia removal efficiencies (RE) jumped from 40% to 70% when media was wetted from 35% to 55%, and then slightly increased (9-11%, Fig. 5.7, Table 5-5) to 80% when media were further wetted to 63%. In contrast, a very small increase (0.10-0.11 ppm, Fig. 5.8, Table 5-5) of produced nitrous oxide concentrations were observed when media was wetted from 35% to 55%; but when

media were further wetted to 63%, generated nitrous oxide concentration rose quickly by 0.62-0.67 ppm within 2 days. When the moisture content was returned to 55% in the step 4, both the ammonia removal efficiencies and nitrous oxide concentrations were restored to previous values as shown in step 2. For the two control biofilters, BF3 and BF4, the nitrous oxide concentrations were quite constant in step 2-4. Table 5-5 shows the Post hoc test of ammonia RE and nitrous oxide concentrations in four steps of each biofilter.

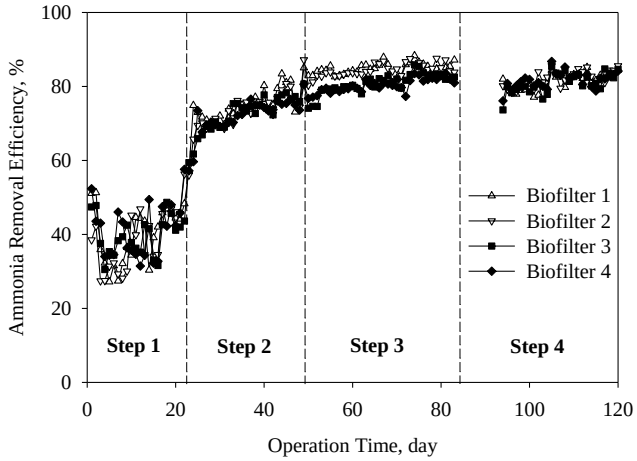

Figure 5.7 Ammonia removal efficiencies of four biofilters.

Note: the media was dried during the days between step 3 and step 4. The ammonia concentrations of inlet and outlet gases were not recorded. The measured data is listed in the appendix C1.

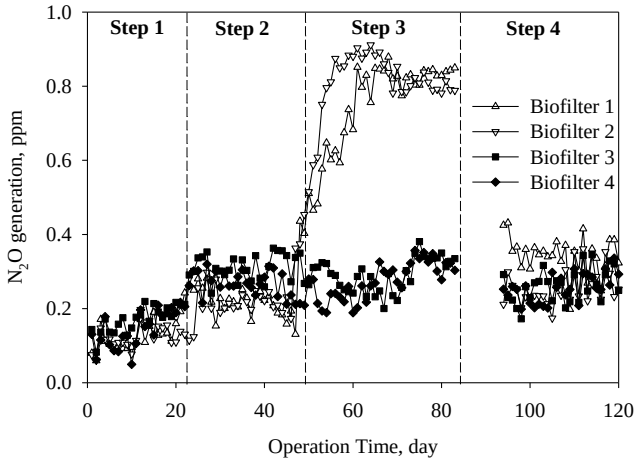

Figure 5.8 Nitrous oxide concentration generated from four biofilters.

Note: the media was dried during the days between step 3 and step 4. The nitrous oxide concentrations of inlet and outlet gases were not recorded. The measured data is listed in the appendix C2.

Table 5-5 LSD Post hoc test of performance of four biofilters.

	Biofilter 1					Biofilter 2			
	Step1	Step2	Step3	Step4		Step1	Step2	Step3	Step4
Step1		0.10*	0.62*	0.22*	Step1		0.11*	0.68*	0.13*
Step2	34.60*		0.52*	0.12*	Step2	34.97*		0.57*	0.02
Step3	44.33*	9.73*		-0.40*	Step3	45.87*	10.90*		-0.54*
Step4	42.51*	7.92*	-1.81		Step4	44.83*	9.86*	-1.04	
	Biofilter 3					Biofilter 4			
	Step1	Step2	Step3	Step4		Step1	Step2	Step3	Step4
Step1		0.15*	0.12*	0.09*	Step1		0.13*	0.13*	0.12*
Step2	32.42*		-0.02	-0.05*	Step2	32.05*		0.01	-0.01
Step3	40.74*	8.32*		-0.03	Step3	39.47*	7.42*		-0.01
Step4	42.04*	9.61*	1.30		Step4	41.89*	9.84*	2.42	

For each biofilter, the lower triangle compares the means of ammonia removal efficiencies (%) among different steps, it equals to: the mean value of Step I (raw) - mean value of Step J (column). The upper triangle shows the mean value differences of produced nitrous oxide concentration (ppm) among different Steps. It equals to: the mean value of Step J (column) - mean value of Step I (raw).
* Significant different at 5% significance level.

5.3.4 Bacterial community structures as determined by ARISA analyses

Bacterial communities showed significant variations over moisture content, operation steps and sampling locations (Table 5-6). As the lower and upper layers showed distinguishable moisture contents during the test (Fig. 5.2), their bacterial communities were analyzed separately (Fig. 5.9). In the lower layers, the bacterial communities of the treatments (BF1 and BF2) varied significantly across the four steps (S_i, i =1, 2, 3, 4) and become less variable (Table 5-7). Similarly, the bacterial communities of the controls (BF1 and BF2) varied significantly from step 1 to step 3 and become homogenized, while the communities in the step 3 and step 4 were close to each other. For the upper layers, bacterial communities of treatments shifted significantly from step 1 to step 3, however, moving from step 3 to step 4 did not lead to statistical difference (ANOSIM, p = 0.053). Pairwise contrasts also indicated that the bacterial community composition of treatments were not different from the controls in the step 3 (ANOSIM, p = 0.077).

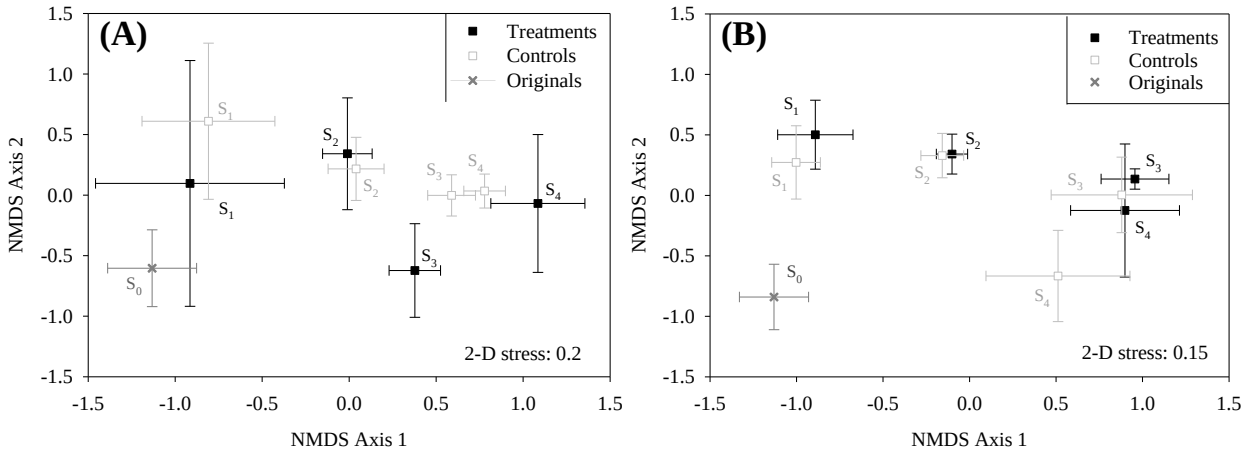

Figure 5.9 Bacterial community composition varies with experimental steps in the lower layers (A) and upper layers (B).

Note: Two-dimensional non-metric multidimensional scaling (NMDS) plots reveal how moisture relates to changes in media bacterial communities. The large symbols represent the centroids of all samples from each step, and the bars show the SD along each NMDS axis. S_0 means samples taken before the test began; S_1, S_2, S_3 and S_4 means the samples taken in the end of step 1, 2, 3, and 4, respectively.

5.3.5 amoA and nosZ community structure as determined by T-RFLP analyses

Biofilter operation divided the *amoA* communities into two major groups. The samples taken in the step 1 were significantly different from those taken in step 2-4 (Fig. 5.10) for both treatments and controls. The *amoA* communities become less diverse from step 1 to step 4 (Table 5-7). Neither moisture level nor biofilter replicates affected the community compositions significantly (Table 5-6). The observation that moisture level did not significantly affect communities seems to conflict with the significant differences (p <0.001) across operation steps, since moisture levels were changed with operation steps. It could be because the two factors, operation step and moisture level, were correlated, and operation step was listed ahead of moisture level in the PerMANOVA test, thus may attribute to a major part of differences.

The *nosZ* communities displayed a similar pattern as the bacterial communities (Fig. 5.11). The communities showed significant variations (p <0.001) over moisture levels and operation steps; sampling location also affected the communities (Table 5-6). In the lower layers, the *nosZ* communities of the treatments were shaped continuously from step 1 to step 4 with a trend of slowly decreasing diversity. In the step 4, the *nosZ* communities in the treatments were similar to the controls (ANOSIM, p =0.174). In the upper layers, due to the less varied moisture content, the *nosZ* community composition were constant in the step 3 and 4 (ANOSIM, p =0.468).

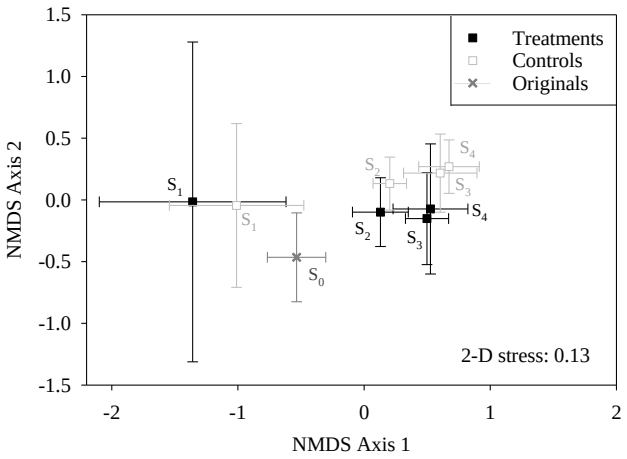

Figure 5.10 amoA gene community composition changes with experimental steps.

Two-dimensional non-metric multidimensional scaling (NMDS) plots reveal how moisture relates to changes in media *amoA* communities in the four biofilters. Note: The large symbols represent the centroids of all samples from each step, and the bars show the SD along each NMDS axis. S_0 means samples taken before the test began; S_1, S_2, S_3 and S_4 means the samples taken in the end of step 1, 2, 3, and 4, respectively.

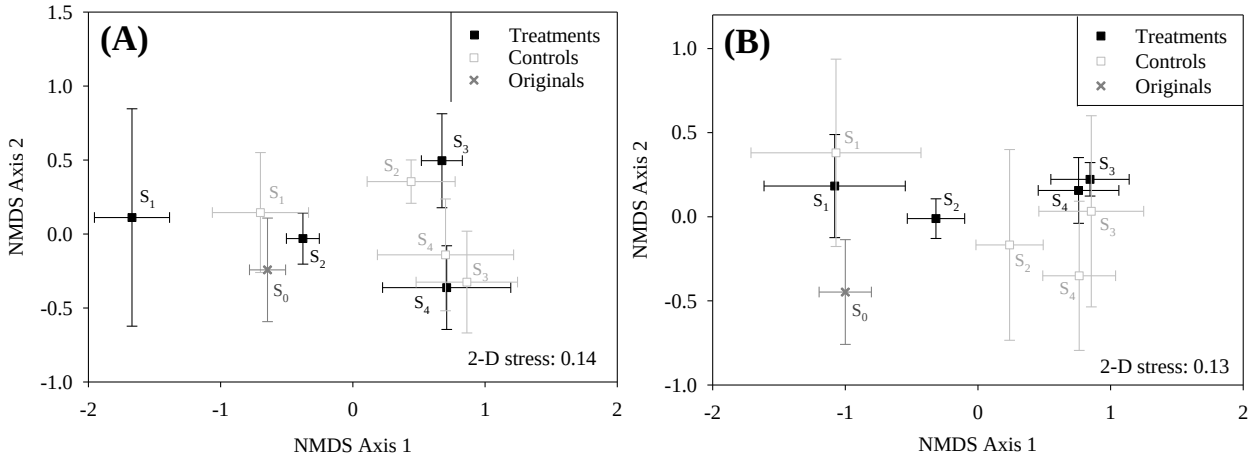

Figure 5.11 nosZ gene community composition varies with experimental steps in the lower layers (A) and upper layers (B).

Note: Two-dimensional non-metric multidimensional scaling (NMDS) plots reveal how moisture relates to changes in media *nosZ* gene communities. The large symbols represent the centroids of all samples from each step, and the bars show the SD along each NMDS axis. S_0 means samples taken before the test began; S_1, S_2, S_3 and S_4 means the samples taken in the end of step 1, 2, 3, and 4, respectively.

Table 5-6 Significance levels of effects on microbial community compositions.

Model terms	Bacteria		*amoA* gene		*nosZ* gene	
	treatments	controls	treatment	controls	treatment	controls
Operation step [a]	0.001***	0.001***	0.001***	0.001***	0.001***	0.001***
Moisture level [b]	0.001***	0.001***	0.510	0.065	0.001***	0.001***
Sampling location [c]	0.001***	0.001***	0.017*	0.052	0.006**	0.016*
Biofilter replicate [d]	0.022*	0.024*	0.052	0.051	0.051	0.015*

[a] include initial samples (step 0) and four operation steps.
[b] include three moisture levels: Low <45%, 45%≤medium≤55%, and high >55%.
[c] include upper and lower layers.
[d] biofilter 1 and 2 are considered as treatment replicates, biofilter 3 and 4 are control replicates.
Null hypothesis: the variables have no effects on the microbial communities.
Significance level determined by permutational MANOVA. Significance levels: *** $p < 0.001$; ** $0.001 \leq p \leq 0.01$; *$0.01 < p < 0.05$.

Table 5-7 Dispersion of microbial communities.

Steps	Bacteria				*amoA* gene		*nosZ* gene			
	Lower layer		Upper layer				Lower layer		Upper layer	
	treatment	control	treatment	control	treatment	control	treatment	control	treatment	control
Step 0 [a]	0.28		0.28		0.17		0.18		0.18	
Step 1	0.40	0.35	0.28	0.30	0.44	0.26	0.25	0.27	0.30	0.26
Step 2	0.29	0.27	0.25	0.23	0.14	0.18	0.16	0.22	0.20	0.20
Step 3	0.33	0.26	0.23	0.26	0.21	0.17	0.17	0.24	0.17	0.26
Step 4	0.31	0.25	0.26	0.27	0.23	0.17	0.17	0.18	0.26	0.26

The numbers shows the mean distance (bray-cutis)-to-centroid of the levels of the grouping factor with the specified family. [a] the initial samples taken before biofilter running.

5.3.6 Abundance of nosZ genes as determined by real-time PCR

The qPCR standard curves are shown in the Fig. 5.12. The amplification efficiencies were calculated to be 1.90 and 1.97 for two tested plates.

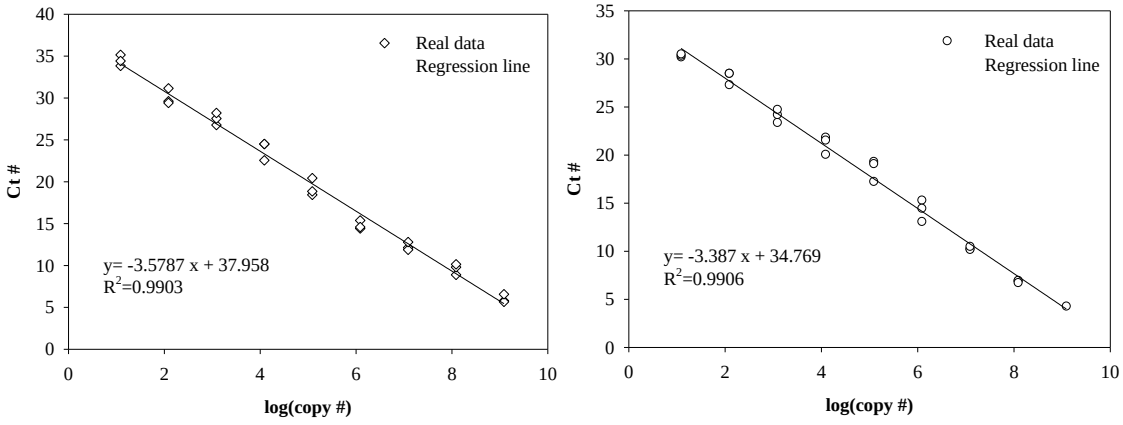

Figure 5.12 Two qPCR standard curves.

Note: Amplification efficiency = -1+10(-1/slope).

Quantities of *nosZ* genes in both treatments and controls varied over biofilter operation steps, moisture levels and sampling locations (Fig. 5.13, Table 5-8). The upper layers contained fewer genes than the lower layers. If only the step 2, 3 and 4 are considered, the quantity of *nosZ* genes in the controls was not significantly affected by operation step, moisture levels or biofilter replicates. For the treatments, the quantities were increased from step 1 to step 2 when moisture increased from 35% to 55%, and then decreased in the step 3 when moisture was further increased to 63%. Its quantity was recovered when moisture content decreased to 55% in the step 4.

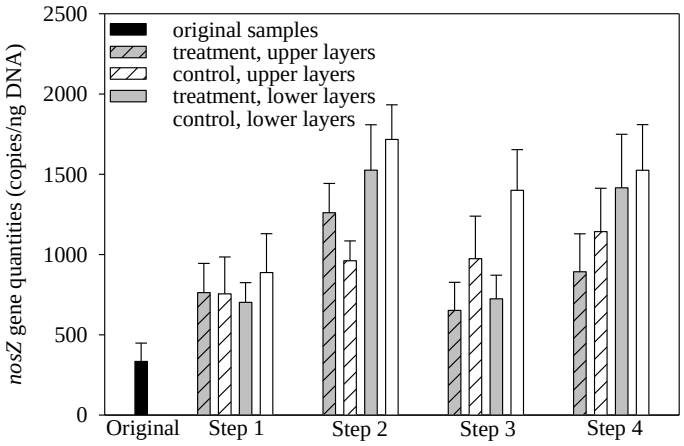

Figure 5.13 Changes in abundance of nosZ genes in the biofilters.

Note: The copy number of genes in each ng DNA was estimated based on the results of real-time PCR. The R^2 of the standard curve was higher than 0.99. The real-time amplification efficiency was 1.94 ±0.05.

Table 5-8 Significance levels of effects on the abundance of *nosZ* gene.

Model terms	*p*-value		
	treatments	controls	Controls [a]
Operation step	0.001***	0.001***	0.163
Moisture level	0.004**	0.024*	0.465
Sampling location	0.001***	0.001***	0.001***
Biofilter replicate	0.934	0.137	0.210

[a] only samples taken in step 2, 3 and 4 are included.
Null hypothesis: the variables have no effects on the microbial community.
Significance level determined by ANOVA.
Null hypothesis: the variables have no effects on the nosZ gene copies.
Significance levels: *** $p < 0.001$; ** $0.001 \leq p \leq 0.01$; *$0.01 < p < 0.05$.

5.4 Discussions

5.4.1 Optimize biofilter operations

This study showed that the performance of biofilters was greatly controlled by the moisture content in the media. With 35% moisture (step 1), the ammonia removal efficiency was low at ~40%; while at 63% moisture (step 4), high concentration of nitrous oxide was produced (Fig. 5.7 and 5.8). When moisture decreased to 55% from 63%, nitrous oxide concentrations dropped as well. These observations strongly suggest that the moisture content is a key to the success of biofiltration and should be optimized. High moisture content was chosen to maximize ammonia removal efficiency in previous practices (Chen et al., 2009; Poulsen and Jensen, 2007). This study showed that ammonia removal efficiencies were not significantly changed with moisture content ranging from 55% and 63% (step 3 and step 4 in the Table 5-5). In contrast, nitrous oxide concentration increased (0.52-0.57 ppm) significantly with moisture increasing from 55% to 63%. Therefore, it is not advisable to run biofilters with extremely high moisture contents. A moisture range of 50-55% can be a good balance to achieve high ammonia removal and low nitrous oxide concentration.

Other factors, such as pH value and particle size distribution, also influence the biofilter performance as well. Biofilter media can become acidified due to release of H^+ during a nitrification process (Rodriguez et al., 2008). Liu *et al*. (Liu et al., 2010) found that N_2O/N_2 ratio increased with decreasing pH within the range of 5 to 8 in a long-term soil liming experiment. It was observed in this study that pH was reduced from 8.1 to 6.1, while N_2O concentrations were stable in the BF 3 and BF4 (Table 5-2 and 5-5). This phenomenon is in line with Cuhel's observation that "the $N_2O/ (N_2O+N_2)$ ratio increased with decreasing pH, while no change in N_2O production" (Cuhel et al., 2010). A lower pH condition can be a problem, as "the major denitrification gaseous products will be N_2O and NO at pH 4.9" (Wijler and Delwiche, 1954) and "eighty percent of N_2O will be generated from denitrification at pH 4.5" (Baggs et al., 2010). Regarding particle size distribution, small media size benefits ammonia removal (Garrido-Fernandez et al., 2000), however, it may form dead zones (Sales et al., 2008) and enhance the barrier of oxygen availability which leads to local anaerobic environments, thus favoring nitrous oxide generation (Braker and Conrad, 2011). In this test, the media size became significantly smaller after four months' operation (Table 5-3); however, how it contributed to ammonia removal and nitrous oxide production was not clear.

5.4.2 Resistance, resilience and redundancy of communities to moisture change

Biofiltration comprises many processes, including absorption, adsorption, nitrification, denitrification, mineralization, and so on (Devinny et al., 1999; Nicolai et al., 2006b). Moisture directly affects absorption of gas phase ammonia into biofilter (Nicolai et al., 2006b); moisture affects nitrification and denitrification by shaping the function of microbes which is related with community abundance and diversity (Szukics et al., 2010; Well et al., 2006). Bacterial, *amoA* and *nosZ* gene communities varied with moisture change, but they displayed different patterns. For bacterial and *nosZ* gene communities, the compositions shifted significantly from step 0 (original samples) to step 1 and became more diverse, showing an obvious acclimatization process. Moving from step 1 to step 2, the communities became less diverse but still significantly different. It might be another acclimatization step, or it may indicate that bacterial and *nosZ* gene communities were not resistant to moisture change from 35% to 55%. Further increasing moisture to 63% and then returned to 55% can be considered as a "moisture disturbance-disturbance relief" process (Allison and Martiny, 2008). The bacterial and *nosZ* gene communities were not resilient to this disturbance given the significant composition differences in the lower layers (Fig. 5.9 and 5.11). The quantities of *nosZ* genes were also altered during this process (Fig. 5.13). As the ammonia removal efficiency and nitrous oxide concentration stayed similar in the step 2 and step 4, it indicates a functional redundancy. For *amoA* gene communities, they become significantly different in composition from step 0 to step 1, showing a similar acclimatization process. When moisture was changed from 35% to 55%, the composition was also altered. However, *amoA* gene communities were not changed in the "moisture disturbance-disturbance relief" process as their composition stayed similar in the step 2, 3 and 4 (Fig. 5.10), suggesting a resistance to moisture changes. Resistance of *amoA* communities supports the observation of relatively constant ammonia removal efficiencies in these three steps.

5.4.3 Stability of biofilters

The present work revealed that biofilters can be managed to provide stable functions to remove ammonia and limit nitrous oxide production with appropriate control of moisture content in biofilter media. Microbial succession, such as the resistance of *amoA* gene communities to moisture ranging from 55% to 63%, is meaningful to stability; however, it is not definitely needed to maintain constant functionality. As shown in the bacterial and *nosZ* gene communities, their diversity and abundance were altered significantly during moisture change; but different

species will carry out the same function when moisture content was back to the right range. Notice that low ammonia removal efficiency in step 1 could be due to the low efficiency of absorbing ammonia gas, which is usually considered the bottleneck step of biofiltration, and highly depends on media moisture content. The high nitrous oxide concentration in step 3 can be caused by the decreasing number of *nosZ* genes (Fig. 5.11). With that extreme high moisture, a much thicker biofilm can be formed which retards the transfer of nutrients and carbon sources to the surface of substrates where denitrifiers stay.

A better understanding of the biofilter stability can be reached. The function of a biofilter can be broken into: (i) absorption/adsorption of ammonia, which is usually known as ammonia removal, and is affected by moisture content, and (ii) transforming dissolved ammonium into other nitrogen forms, such as nitrate and nitrous oxide, where microorganisms play a central role. Ammonia removal function can be high and stable with media moisture ranging of 50-65%. The composition of ammonia oxidizers is resistant to moisture variation, and so is the function of oxidizing ammonia to nitrite. Abundance of *nosZ* communities can be reduced by extremely high moisture; however, redundancy of *nosZ* communities would make it able to recover its function of converting nitrous oxide into nitrogen gas as long as moisture was in an appropriate range. These conclusions help predict the performance of a biofilter undergoing failures. For example, a biofilter without a cover can be totally saturated after a storm and would start producing high concentration of nitrous oxide; however, the failure would not last long if moisture content was reduced immediately.

5.5 Conclusions

It was shown that the moisture content affected biofilter performance in these experiments. Ammonia removal efficiency was greatly improved as media moisture was increased from 35% to 55%; further increasing moisture to 63% only slightly promoted ammonia mitigation. In contrast, little increase of nitrous oxide was observed when moisture was increased from 35% to 55%, but further increasing moisture to 63% quickly peaked nitrous oxide generation. Upon restoring moisture to 55%, high ammonia removal efficiency and low nitrous oxide concentration were re-obtained. The ammonia oxidizer community was changed when moisture increased from 35% to 55%, and then resisted the “moisture disturbance- disturbance relief” process, which was in line with the ammonia removal efficiencies. The bacterial communities and *nosZ* gene communities displayed a functional redundancy to moisture changes. The

quantity of *nosZ* gene was reduced at 63% moisture, and may cause the increasing of nitrous oxide concentration. Taking all results together, this study provides a suitable approach for gas phase biofilter moisture management to obtain reliable function of mitigating ammonia and limiting nitrous oxide generation.

Chapter 6:IMPEDANCE BASED MOISTURE SENSOR DESIGN AND TEST FOR GAS-PHASE BIOFILTER APPLICATIONS

6.1 Introduction

The moisture content of biofilter media can vary to a large degree, affecting biofilter performance. Too little moisture slows microbial activities and reduces ammonia removal (Bohn and Bohn, 1999), while too much water forms anaerobic zones (Maia et al., 2012a) and produces nitrous oxide as shown in the Chapter 4. The need for moisture control thus calling for the development of sensors for continuous moisture content measurement in biofilters. Unlike soils, for which convenient moisture sensors have been developed over years, woodchips and composts are composed of much larger materials (Yang et al., 2011). Moreover, the distribution of moisture content is not even. Therefore, a sensor capable of determining water content of media in a sample volume representing many particles is needed.

Several approaches to solve the moisture sensing problem in biofilter have been tried. A method for measuring moisture content in woodchips with X-radiation was proposed by Nordell and Vikterloef (Nordell and Vikterloef, 2000). Theoretically, determination of moisture content using this method is independent of the media type, media size, and temperature; but it is very expensive (Kullenberg et al., 2010). A less expensive probe, based on time-domain reflectometry (TDR), was shown capable of responding to changes in mean moisture content in a bulk of material and was used in experiments to determine moisture content in woodchips (D'Amico et al., 2010). The tests showed a good response to moisture change but its variation increased significantly when moisture was higher than 30% (wet basis). No test was conducted with moisture content higher than 40%. Given that most biofilters are operated with moisture content of 35-65% (Dorado et al., 2010; Webster, 1996; Yang et al., 2012), further development of this technology will be needed for biofilter applications. Measuring capacitance of solid biomaterials such as grains and seeds by correlating with water content was the most commonly studied method in the past two decades, especially for low moisture content materials (Nelson et al., 1992; Nelson and Trabelsi, 2011; Nystrom and Dahlquist, 2004; Ramasamy and Moghtaderi, 2010). With higher moisture content such as seen in biofilter media, conductivity can become a problem for moisture determination with either parallel-plate or coaxial sample holders where samples are introduced between the electrodes. More recently, relating impedance of materials to

moisture content attracted the attention of researchers (Tiitta and Olkkonen, 2002; Titta et al., 2011; Zelinka et al., 2008). Impedance spectroscopy separating out capacitance and resistance (Barsoukov and Macdonald, 2005) allows signal phase angle and magnitude to be used to distinguish moisture content differences (Titta et al., 2011).

A prototype large-area capacitive parallel-plate moisture sensor with a radio frequency sine-wave voltage input was developed in our group previously (Funk et al., 2007; Robert et al., 2005). Recent tests on this sensor showed that the earlier mathematical model needed to be refined for other materials, and new observations spurred us to consider other factors including conductance of the media. As a result of that, a new moisture sensor based on impedance of woodchips and composts (our preferred media types) was developed.

The objectives of the present study are:

(i) To test the parallel-plate sensor circuit's ability to correlate the impedance of enclosed-sample media, at varying moistures, to an impedance reference;

(ii) To evaluate the effects of temperature and artificial compaction on media impedance. Often, biofilters are built outdoors and it exposed to ambient conditions. Thus, it is necessary to study the possible variances of impedance caused by temperature changes. A biofilter is a dynamic biological system with continuous flow of air, movement of media and water, and evolution of microbial communities. The profile of media, such as composition and media size distribution, is undergoing changes all the time. Compaction of media, caused by gravity force, media movement or biomass accumulation, is one important phenomenon in biofilters.

6.2 Materials and Methodologies

6.2.1 Materials

Two woodchips (shredded woodchip, or SWC; and chipped woodchip, or CWC) and one compost (mushroom compost, or MRC) were selected in this study. Their physical and chemical properties were described in details in a previous study (Yang et al., 2011). Medium (woodchips or compost) was dried in an oven at 49℃ with forced ventilation for 48 hours to about 3% MC and then was sieved using a Penn State Forage Particle Separator (NASCO, product #: C24682N). The sieve apparatus is composed of four trays that stack on top of each other; the top three trays have unique hole sizes (1.9cm, 0.8cm and 0.2cm, respectively) designed to separate samples into four distinct particle size ranges. After sieving, 0.2-0.8 cm and 0.8-1.9 cm media were re-mixed at a 1:1 volume ratio in a 0.5 m^3 chamber and its moisture content was determined

using 105℃ oven drying method. The density and porosity of the three media (after mixing) is shown in Table 6-1. The density of MRC was much higher than the other two materials.

Table 6-1 Density and porosity of three media.

	CWC [a]	SWC	MRC
Density, g/cm^3	246±4	253±3	402±8
Porosity, %	68±2	63±2	61±3

[a] average ± S.D. of triplicates.
SWC: shredded woodchip.
CWC: chipped woodchip.
MRC: mushroom compost.

6.2.2 Impedance measurement

Media impedance was measured using Agilent 4294A Precision Impedance Analyzer (Santa Clara, CA, Fig. 6.1) with a sample holder of 101.8× 27.7 ×76.2 mm (L×W×H) and a radio frequency sine-wave voltage input in range of 100 Hz–100 MHz. Impedance of media was measured at 22℃ (room condition), 27℃ and 32℃. For measurements at 27℃ and 32℃, medium was packed using a sealed plastic Ziploc bag, and then was warmed up to the desired temperature in an oven. Their impedance was measured immediately after moving medium out of the oven. Moisture content of medium was increased step by step from 3% to 65% by adding appropriate volumes of water to medium to achieve the desired moisture contents. Each sample was made up in triplicate.

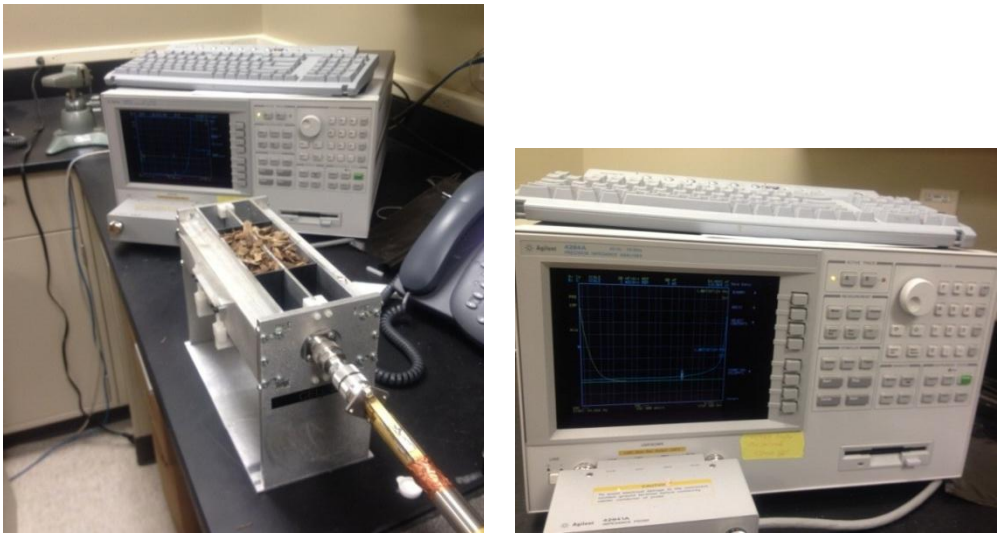

Figure 6.1 Impedance measurement.

6.2.3 Sensor construction

A "voltage divider" circuit followed by a "peak detector" circuit was designed to compare the impedance of media mounted between the sensor plates to a reference, C_{ref} (Fig. 6.2, Fig. 6.3). R_1 is a low-value resistor and R_2 is a high-value resistor in order to reduce bias currents. The impedance of media is recognized as a parallel connection of a resistor and a capacitor. To reduce effects of environmental noise, three plates were used, the upper and lower plates being grounded and the middle plate being energized by a high frequency (100K) sine wave voltage at +/- 1 V p-p. A moisture change between the plates will affect the capacitance and conductivity of medium, which is reflected through the measurement of the output voltage. DC voltages (V_{in} and V_{out}) were recorded using a data acquisition system (Personal Daq/56, Measurement Computing CO., Norton, MA) and were used in Equation 6-1.a. The ratio of V_{in} over V_{out} is reported in this paper as a function of medium impedance, which is correlated to moisture content. The circuit design was simulated and tested using OrCAD Capture CIS 16.3 (Cadence Design System, Inc., San Jose, CA) and the testing results are shown in Fig. 6.4.

$$V_{in}/V_{out}=(| Z_{sensor} | + | Z_{ref} |) / | Z_{sensor} | = 1+ | Z_{ref} | /| Z_{sensor} | \quad (6\text{-}1.a)$$

$$Z_{ref} =1/j\omega C_{ref} \quad (6\text{-}1.b)$$

$$Z_{sensor} = R + jX \quad (6\text{-}1.c)$$

Where, Z is the impedance, and | Z | is the magnitude of impedance. The real part of impedance is the resistance R and the imaginary part is the reactance X. $\omega= 2\pi f$, ω is the angular frequency and f is the frequency of the imposed alternating field.

In order to measure moisture of a representative amount of medium, plate size of 30cm by 30cm was chosen, and the distance between the energized plate and either grounded (outside) plate was 7.5cm. The plates were made of perforated steel (expanded metal sheet) with 2.54 mm holes (80% hollow) on it which allows gas, water, and media to transport in and out of the plates freely. The three plates were separated by a set of three plastic bars between each plate pair (Fig. 6.5).

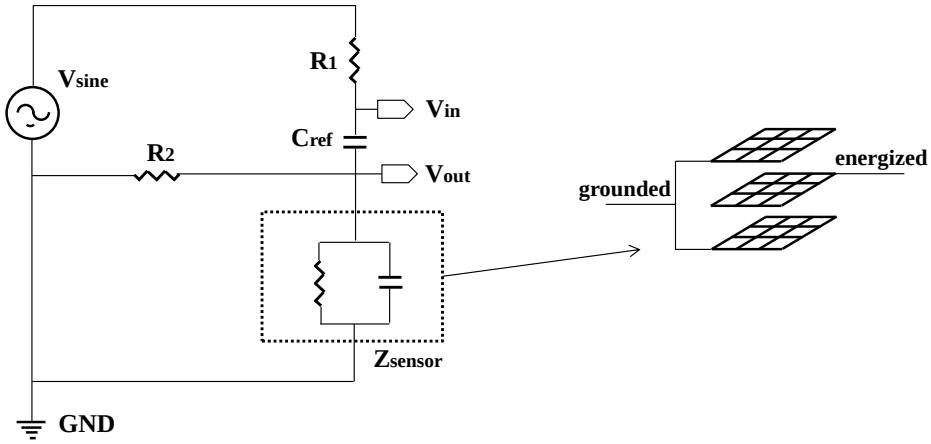

Figure 6.2 Simplified schematic design of the sensor circuit and parallel plates.

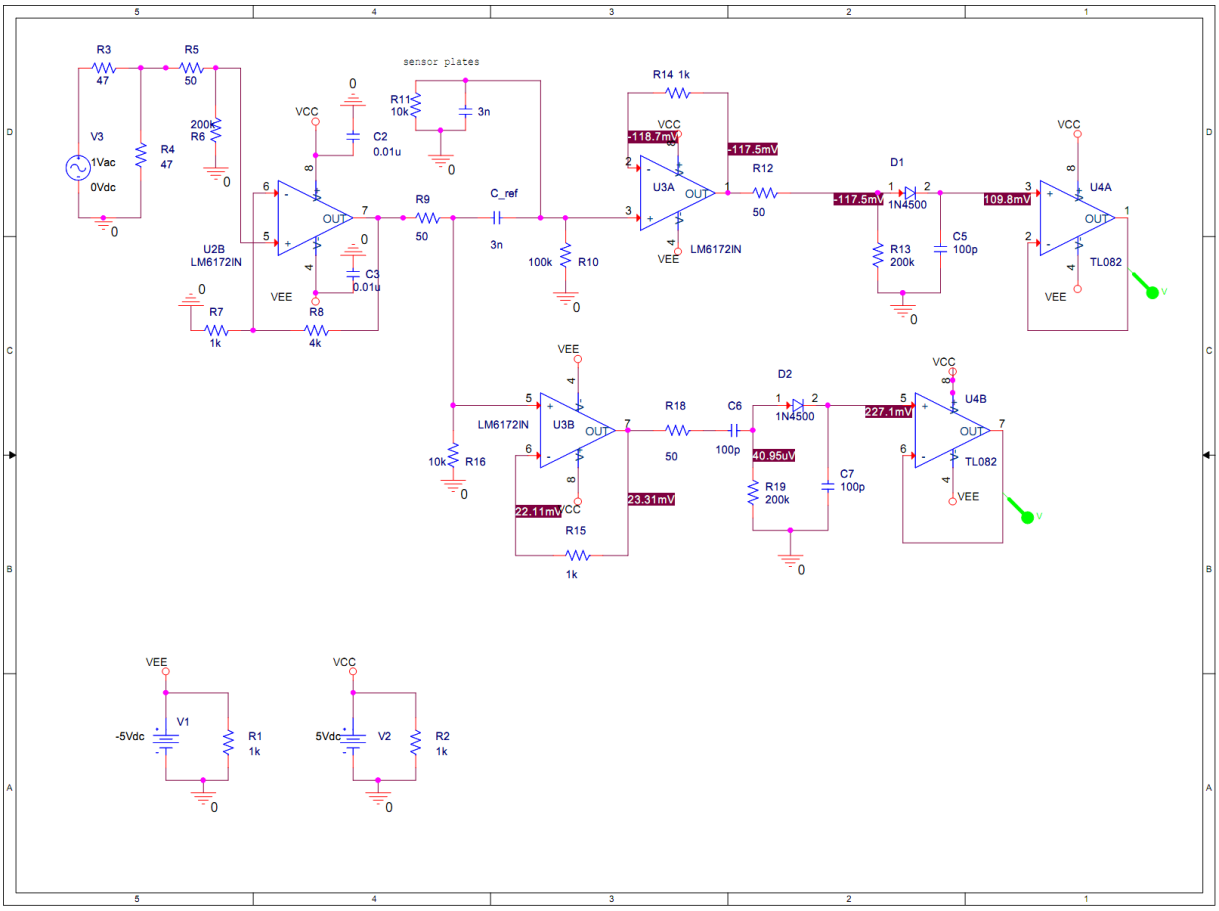

Figure 6.3 Schematic circuit design using SPICE.

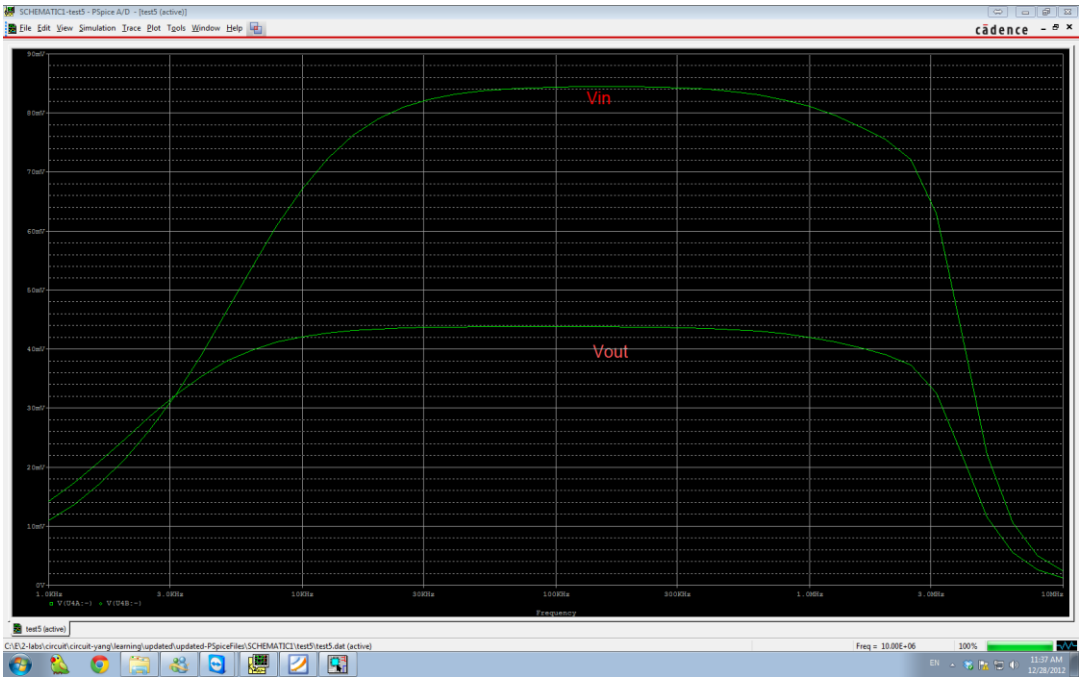

Figure 6.4 The SPICE simulation results with a parallel connection of a resistor (10K Ω) and a capacitor (3n Farad).

Figure 6.5 Built sensor plates.

6.2.4 Sensor test

Each medium was dried to 5%w.b. and then two particle size groups (size: 0.8cm-1.9cm and 0-0.8cm) were mixed at a 1:1 volume ratio. The sensor plates were set in the center of a sealed plastic testing chamber (L×W×H: 50cm×50cm×30cm, Fig. 6.6) filled with media. Medium moisture content was increased step by step by adding water. For each step, the medium was taken out of the testing chamber and mixed with water as evenly as possible on a tray. After mixing, the medium was placed into the testing chamber, along with the sensor plates. Sensor

outputs were recorded every two minutes for 3-4 days using a data acquisition system (Personal Daq/56, Measurement Computing CO., Norton, MA).

Figure 6.6 Sensor test experimental setup.

6.2.5 Compaction test

To test whether compaction of media will affect moisture sensor outputs, a two-plate sensor was tested in a large testing chamber (L×W×H =1.0m×0.6m×0.6m) filled with a chipped woodchip of 55% moisture content. Medium was sieved and two size groups (size: 0.8cm-1.9cm and 0-0.8cm) were tested separately. Two plates (one energized, one grounded, 10cm between each other) were placed on top of 10cm medium, then the plates were buried with 10cm medium, and another 20cm medium was placed onto the top of plates to create a compaction. Due to the varied medium size, small particles tend to transport downwards and fill the voids among big woodchips; also, gravity force compacts the medium between the two plates. Theoretically, more woodchips, more water and less air will be located between the two plates as time goes by. After compacting for four days, a weight equal to 10cm of medium was added on the top of medium to create a second compaction. Sensor readings were recorded continuously using a data acquisition system (Personal Daq/56, Measurement Computing CO., Norton, MA).

To evaluate the intensity of compaction, the medium pressure drop was measured at the beginning and the end of the test. Details about the pressure drop test were described in a previous study (Yang et al., 2011). To check the consistency of moisture content, four media samples (~50 grams each) located between the sensor plates were randomly taken at the beginning and also at the end of the test.

6.2.6 Data treatment and statistical methods

To assess the sensor accuracy, analysis of covariance (ANCOVA) was carried out to compare the sensor output data (measured data $=V_{in}/V_{out}$) to the ideal values (predicted data) obtained from Equation 6-1.a. The impedance obtained from the impedance analyzer was used as the inputs of Equation 6-1.a. Box-Cox power transformation was applied to obtain a normalized data set and the best fit one-dimensional transformation parameter, λ, based on the measured data set. Then, the same λ was used to transform the predicted data set, given the measured data set has more data points than the predicted data set (the details about Box-Cox transformation are shown in the Appendix D1). The linearity of the two transformed data sets was tested using analysis of variance (ANOVA). And finally, ANCOVA, which includes three models, was used to compare the slope and intercept of the two transformed linear lines. To determine if the second compaction cause a significant difference in moisture sensing, a *t*-test was applied. The sensor voltages obtained before and after the second compaction were used as the inputs for *t*-test.

Data analyses were performed in the R statistical environment (R Development Core Team, 2005) using functions (boxcox, bcPower, aov, anova, t.test) found in the packages "car" (Fox and Weisberg, 2010), "Mass" (Venables and Ripley, 2008) and "stats". The R codes are shown in the Appendix D2 and D3.

6.3 Results and Discussion

6.3.1 Impendence measurement results

Magnitude of impedance decreases with increasing moisture content and increasing frequency in all three media (Fig. 6.7). The impedance curves of very dry media (3% MC) are highly linear, while the others were quite flat over a frequency range from 10^2 to10^6 Hz and then converged at frequency of 10^6 -10^8 Hz. As moisture content increased, the difference in impedance narrowed. However, the impedances of media with 50% and 63% moisture are still distinguishable, thus making the sensor applicable to high moisture content determination.

The phase angles were constant (about -90 degree) for very dry (3%) media for all three media (Fig. 6.7). With higher moisture contents, the phase angles were affected by frequency and moisture levels. The phase angle of CWC became narrowed with increasing moisture content, while the trends in the SWC and MRC were slightly complicated. This difference may be due to the nature of materials as similar results were found in the other studies as well (Titta et al.,

2011). A tail, or Warburg element, was observed in phase angle at frequency close to 10^8 Hz. According to a previous study, it can be caused by the diffusion of dissolved ions in the media (Zelinka et al., 2008). In this case, moisture may enhance the diffusion of ions, thus made the Warburg element stronger at higher moisture contents.

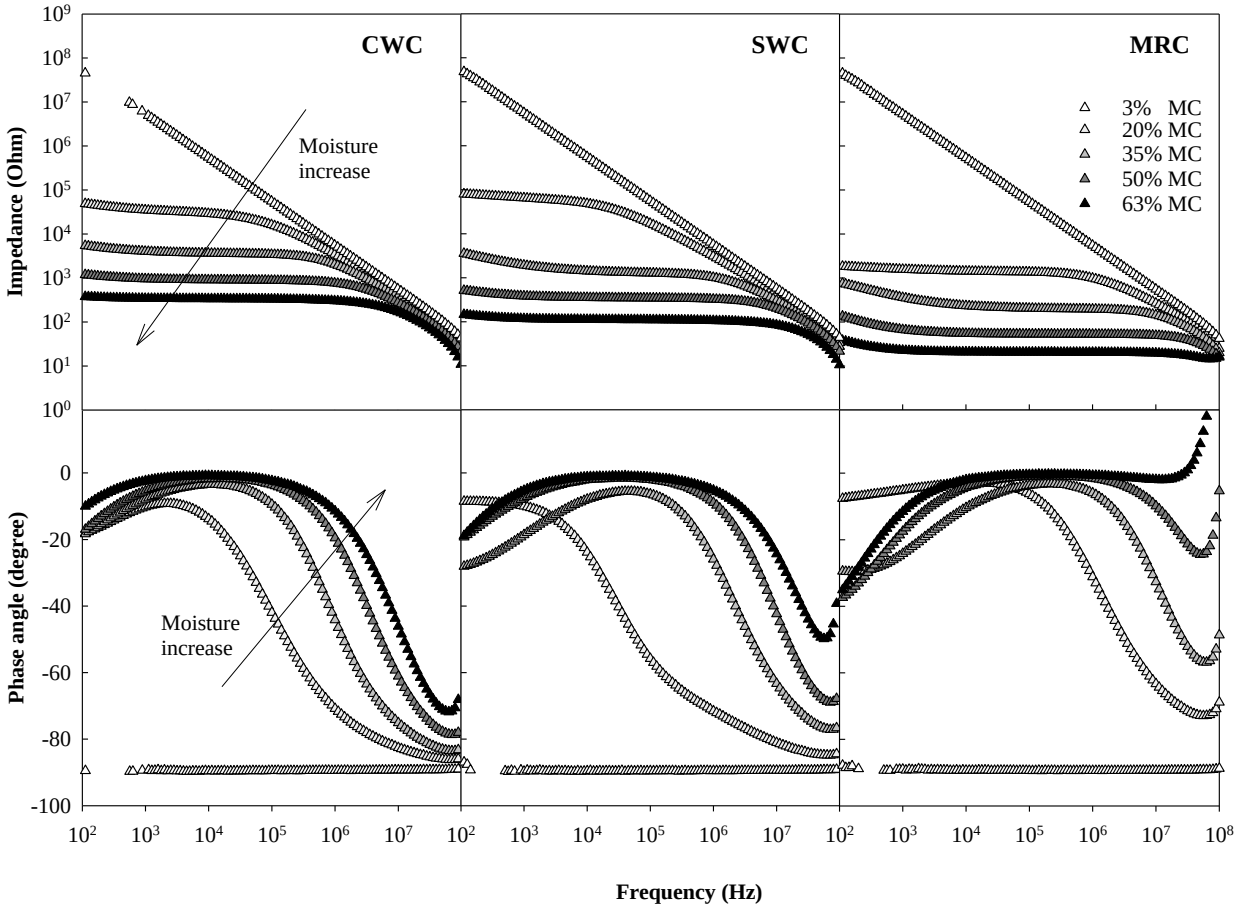

Figure 6.7 Impedance and phase angle of woodchips and compost.

Note: CWC: chipped woodchips; SWC: shredded woodchips, MRC: mushroom compost. Triplicates were conducted for each moisture level, but only one measurement result was shown here. Similar trends were obtained from the other two measurements.

The above observations suggested that the magnitude of impedance is a good indicator of moisture content, and is distinguishable at frequency of 100k Hz. Therefore, the sensor circuit was designed to compare the magnitude of impedance at frequency of 100k Hz. The impedance of the media at 100k Hz is listed in Table 6-2.

Table 6-2 Impedance of media at frequency of 100K Hz, ohm.

Moisture	CWC[a]	SWC	MRC
3%	55682 ±189	56153 ±719	54686 ±24
20%	18751 ±2269	16655 ±493	1872 ±923
35%	3393 ±102	1378 ±92	212 ±10
50%	852 ±28	393 ±42	54 ±1
63%	345 ±31	105 ±5	21 ±1

[a] average ± S.D. of triplicates. Data was extracted from impedance analyzer measurement results.

6.3.2 Parallel-plate sensor measurement results

The sensor reading (V_{in}/V_{out}) increases with moisture content (Fig. 6.8). In Fig. 6.8A, a 30-day real-time measurement of CWC with moisture content ranging from 5% to 65% is shown. Sensor response is flat for very dry media and increases rapidly with moisture increase above 35%. For each moisture content step, a continuous measurement was carried out for 3- 4 days. Often, an increase was observed in the beginning of each measurement and stayed constant afterwards, showing the testing system needs a short period of time to be stabilized for water mixing and media settling. A typical sensor reading with moisture of 50% is shown in the Fig. 6.8.A inset.

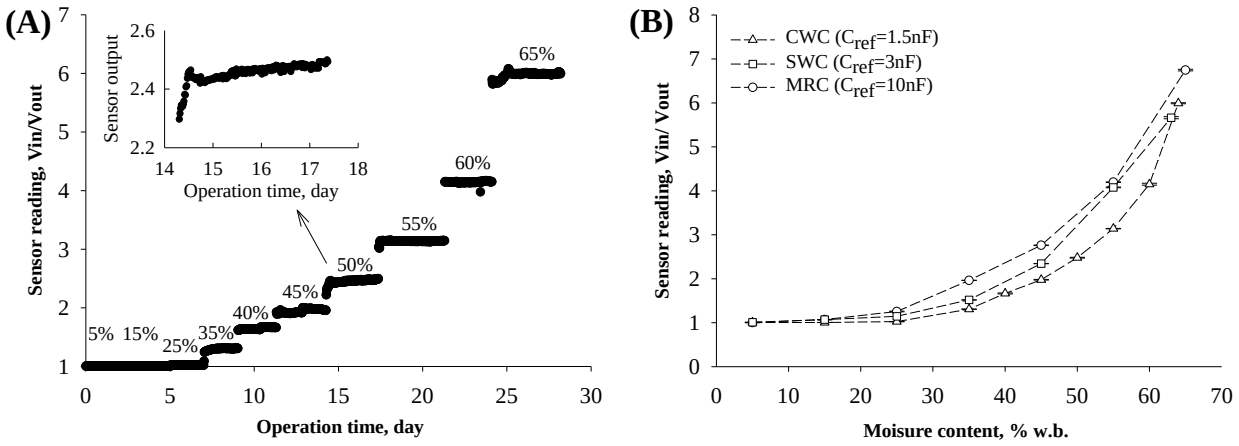

Figure 6.8 Sensor measuring results. Real-time recording of sensor reading at each moisture step (A) and averages and standard deviations of sensor readings at each moisture level (B).

Note: Unit nF = 10^{-9} farad.

The averages and standard deviations of sensor outputs in each moisture content step are shown in Fig. 6.8.B for all three media. In order to optimize the sensor response, a difference reference capacitor was applied for each of the three media, but the three curves display a similar increasing trend. The sensor outputs range from 1 to 7, showing a very usable signal response to moisture content of 25-63%. The slopes of all the curves increase at high moisture range, which

indicates that the sensor method is suited for measuring high moisture content of these organic media.

6.3.3 Model and sensor comparison

To compare the measured sensor output data (Fig. 6.8) to the predicted data (calculated from Equation 6-1.a, using impedance data shown in Table 6-2), Box-Cox transformation was carried out. The measured data and predicted data were transformed into two linear data sets. The statistical tests showed that the slopes of transformed data sets are significant for all three media (Table 6-3).

Table 6-3 Coefficient test of the regressions obtained from the transformed data.

Data group	coefficients	**CWC**: λ= -1.05[d]		**SWC**: λ = -1.31		**MRC**: λ = -0.62	
		Estimate	Pr(>|t|)	Estimate	Pr(>|t|)	Estimate	Pr(>|t|)
Measured data [a]	(Intercept)	-0.213	0.008 **	-0.119	3.67e-2 *	-0.186	0.016 *
	MC [c]	1.537	3.96e-06 ***	1.311	6e-05 ***	2.021	2.15e-05 ***
Predicted data [b]	(Intercept)	-0.116	0.252	-0.115	0.21	-0.182	0.172
	MC	1.269	8.34e-3 **	1.219	6.3e-3 **	2.108	3.62e-3 **

[a]. transformed data based on moisture sensor measured results as shown in the figure 3.
[b]. calculated data based on Equation 6-1.a and impedance data showed in the Table 2.
[c]. MC= moisture content.
[d]. λ is the best fit one-dimensional transformation parameter. Same λ was applied for transformation of both measured data set and predicted dataset.
Null hypothesis: the intercept and the variable MC are not significant.
Significance level: ***: p <0.001, **:0.001< p <0.01, *: p <0.05.

In the ANCOVA model 1, sensor output was modeled as the dependent variable with "MC" as the factor and "Type" as the covariate (Table 6-4). The summary of the results show a significant effect of MC and Type, but no significant interaction. These results suggest that the slope of the regressions between moisture range and sensor output is similar for both measured data and predicted data. A more parsimonious model 2 (Table 6-4) without the interaction was used to test differences in the slope. It shows that MC has a significant effect on the dependent variable (sensor output) while Type is not, which suggests no significant difference in 'intercepts' between the regression lines of measured data and predicted data. A further F test of model 1 and model 2 confirms that removing the interaction will not significantly affect the fit of the model (Table 6-4). In all, the ANCOVA test shows that the sensor outputs are significantly affected by moisture content, but there are no significant differences (slope and intercept) between the regression lines of measured data and predicted data. It means that the real measured sensor data fit the theoretical results.

Table 6-4 *p*-values of ANCOVA Test.

Factor	CWC	SWC	MRC
	*Model 1: Sensor Output ~ MC*Type*		
MC [a]	***	***	***
Type [a]	0.986	0.135	0.391
MC : Type	0.274	0.160	0.237
	Model 2: Sensor Output ~MC +Type		
MC	***	***	***
Type	0.986	0.157	0.403
	F test: model 1 VS. model 2		
F value	0.274	0.160	0.237

[a]. MC= moisture content.
[b]. Type: "measured data" or "predicted data".
Null hypothesis: the variables are not significant.
Significance level: ***: p <0.001.

6.3.4 Temperature effects

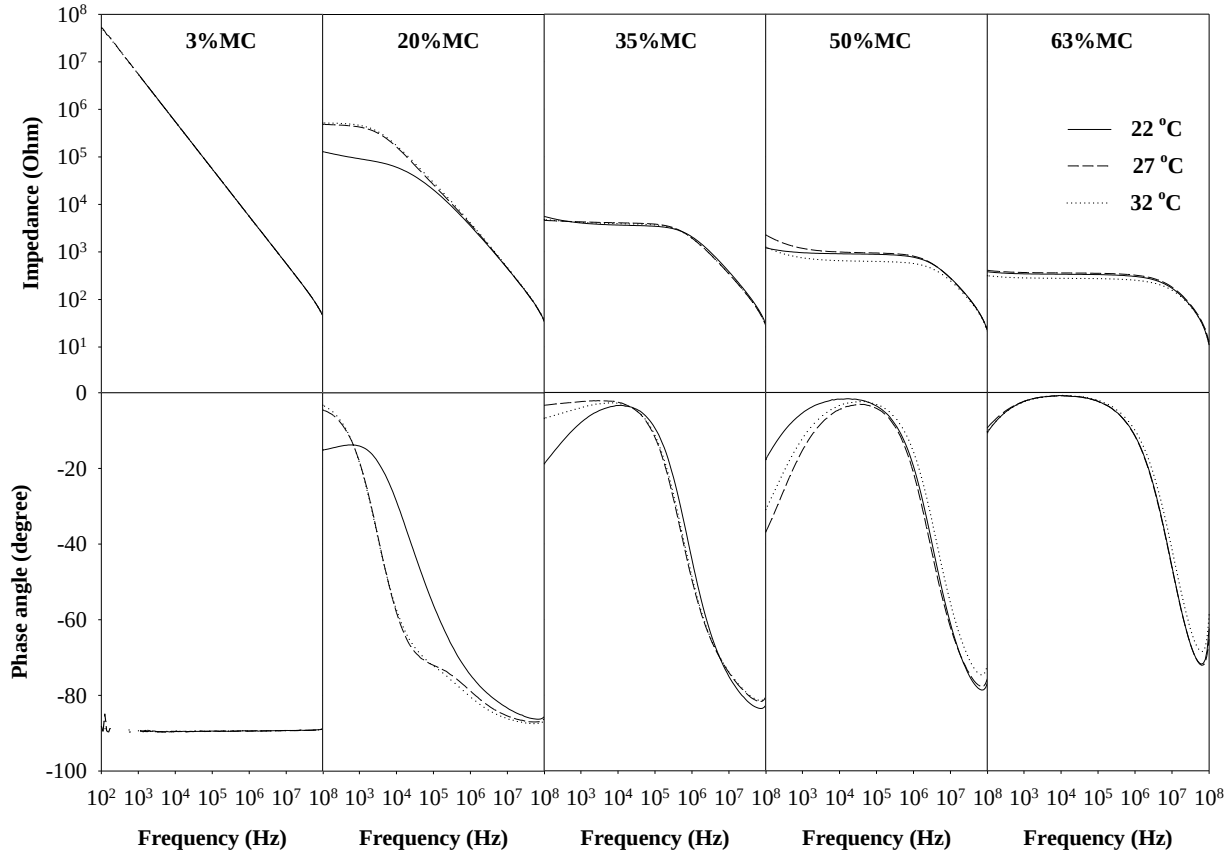

Figure 6.9 Temperature effects on CWC impedance and phase angle.

Note: Triplicates were conducted for each test, but only one measurement result was shown here. Similar trends were obtained from the other two measurements.

As shown in Fig. 6.9, the impedances and phase angles were very close at 22℃, 27℃ and 32℃ with either very low moisture content (3%) or very high moisture content (63%). Impedances

and phase angles varied with moisture content of 20% and 50%; however, the temperature effects were limited and mixed. With 20% moisture content, impedances at 32℃ and 27℃ were very similar and were both higher than that at 22℃ at frequencies ranging from 10^2 to 10^5 Hz. The three curves converge at frequencies above 10^5 Hz. At 35% moisture content, impedances at three temperature levels were very close to each other. With 50% moisture content, impedance at 27℃ was slightly higher than that at 22℃ and 32℃, which is different from the trends displayed with 20% moisture content. Similarly, the curve of phase angles was lower at 22℃ than that at 27℃ and 32℃ with moisture content of 35%, but was higher with moisture content of 50%. At 20% moisture content, an intersection was observed between the three curves.

These results suggest that, except 20% moisture content, the range of temperatures tested had a very limited impact on both impedance and phase angle; and experimental variations may have caused these differences in the tests. Regarding the results obtained with 20% moisture content, since water was added into media step by step, it was highly likely that water distribution in the media was not as homogenized as in the other conditions. Therefore, when a certain amount of media was sampled and put into the testing sample holder, the true moisture content may be varied and caused the differences in impedance and phase angle. In contrast, at the very dry condition or much wetter conditions (e.g. 63%), water distribution was more even and the temperature effects become less important. This explains the differences noticed in the samples with 35% and 50% moisture content as well. A similar conclusion was reached by others, as no influence of sample temperature on moisture content prediction was detected with their radio frequency method with temperature ranging from 1℃ to 63℃ (Paz et al., 2006). Thus, the stability of the moisture sensor in a biofilter with a changing environmental temperature should be acceptable for the applications under consideration.

6.3.5 Compaction effects

The test showed that compaction affects sensor reading (Fig. 6.10A) with constant moisture contents (Table 6-5). Compaction can be caused by the movement of media, water and air. As the medium was compacted in the test, voids were reduced. In other words, medium and water occupied more space between the plates and the volume fraction of air was decreased, leading to a decrease of impedance. For both small and large size media, it took about two days for the sensor output to be stabilized, which was much longer than the results showed in the Fig. 6.8.A. Two reasons can be suggested for the longer stabilization process: a thicker medium bed and a

different sensor plate setup. There was 20 cm medium placed on the top of the sensor plates- a two-plate system- in this test, while a three-plate sensor was applied in the previous study with a layer of 7.5 cm medium set on top of the plates. When an extra weight was added, sensor reading was further increased. The extra weight caused slightly bigger increase in sensor output in the large size medium than in the small size medium. It might be because the large size medium has higher porosity, thus making it easier for the extra weight to affect a second compaction. Student *t*-test shows that the sensor readings on Days 0-4 were slightly lower than those obtained on Days 4-8 (Table 6-5), but it is significant in *t*-test.

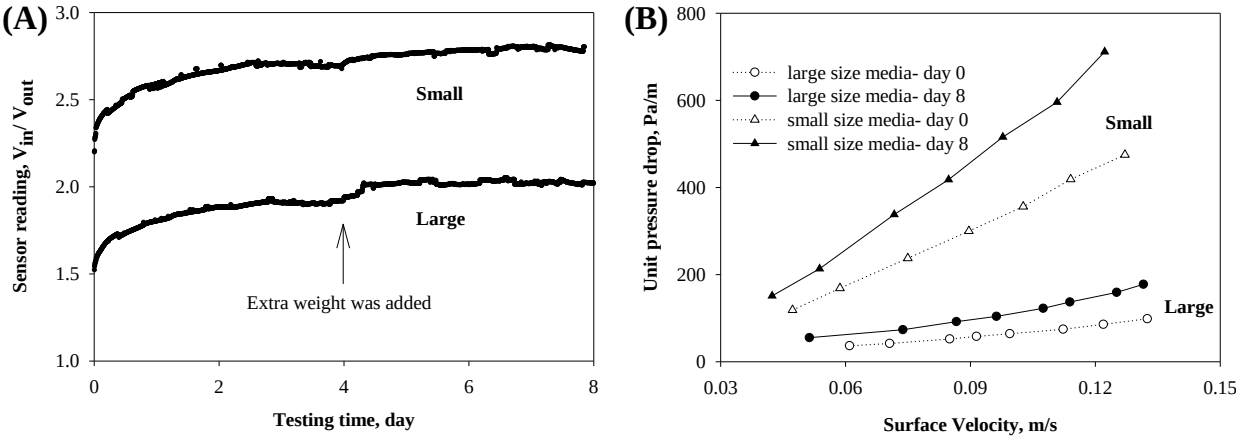

Figure 6.10 Compaction effects on sensor test (A) and medium pressure drop (B) of CWC.

Note: "Small": medium size of 0.2-0.8 cm and "Large": medium size of 0.8-1.9 cm. Extra weight was added on the day 4. Day 0 means the very beginning of the test, and day 8 represents the end of test.

Table 6-5 Results of Student-*t* tests for media moisture content and sensor output.

Factors	*p* value
[a] **Medium MC***: day 0 VS. day 8*	
small size medium	0.602
large size medium	0.783
Sensor reading*: day0-4 VS. day4-8*	
small size medium	***
large size medium	***

[a]. Four replicates.
Null hypothesis: the variables are not significant.
Significance level: ***: p <0.001.

Compaction in a biofilter can be caused by gravity settling, PM loading and biomass accumulation; it is often evaluated by measuring pressure drop (Yang et al., 2011). It was predicted that pressure drop of a biofilter can be doubled at the end of its media change-out cycle,

which usually takes several years (Yang and Allen, 1994). Thus, compaction may cause sensor drift in a long-term use. Taking the large size medium for example, its pressure drop on Day 8 was 50-70% higher than that measured on Day 0 (Fig. 6.10B) and its sensor reading on Day 4-8 was ~10% higher than that displayed on Day 0-4 (Fig. 6.10A). In a much longer test, e.g. a media change-out cycle, compaction effects can be more significant, and re-calibration of the sensor might be needed one or more times during the period of operation.

6.4 Conclusions

A moisture sensor designed for biofilter applications was built and tested. In addition, an impedance analyzer was used to measure media sample impedance and phase angle at various conditions. After data transformation, the sensor measured results fit predictions quite well; suggesting impedance is an appropriate indicator of the moisture content in the organic media considered.

Increasing temperature from 22℃ to 27℃ and further to 32℃ did not affect impedance of woodchips significantly. However, compaction of woodchips for eight days did affect impedance of woodchips significantly. For biofilter applications, it means that small daily or seasonal temperature variations may not affect sensor reading, but that long-term operation and the concomitant compaction of media can cause sensor response changes that may require re-calibration of the sensor to reflect true media moisture content.

Chapter 7:MOISTURE MONITORING AND CONTROL IN GAS-PHASE AMMONIA MITIGATION BIOFILTERS

7.1 Introduction

In the Chapter 5, the accuracy of the developed moisture sensor was tested, and how it responds to moisture change from 5% to 65% was measured in a 50cm×50cm×30cm chamber. The ultimate goal of developing this sensor is to use it for moisture control in biofilter application. Thus, it is necessary to test the potential of this sensor in a long-term biofilter application. This chapter shows the results of a one-month case study, where sensors were incorporated with two gas-phase ammonia mitigation biofilters. The objectives of this chapter are:

(i) To test the feasibility, including stability and sensitivity, of using the developed moisture sensor in biofilter application.

(ii) To develop a moisture control strategy to maintain the media moisture within 45-50% by utilizing the sensor readings as feedbacks.

(ii) To achieve high ammonia removal efficiency and low nitrous oxide concentration with the continuously control of media moisture content.

7.2 Methods and Materials

7.2.1 Sensor-medium calibration

The relationship between sensor readings and medium MC was found by conducting a sensor-media calibration, where the medium MC was increased step by step and the sensor readings were recorded accordingly. Then, a statistical method was applied to model the relationship. A woodchip was selected as the biofilter medium in this study. The woodchip sample was dried to about 5% MC in a 49℃ oven with forced ventilation for 24 hours, and then was sieved using a Penn State Forage Particle Separator (NASCO, product #: C24682N). A same amount of woodchip with size of 0.8cm-1.9cm and woodchip with size of 0-0.8cm were re-mixed as the final material (density: 240 g/L, porosity: 66.2%, C: 46.4%, total N: 1.4%, Org. matt: 84.9%, Org. N: 1.3%, pH: 7.2) for the sensor-media calibration and the biofilter application.

The sensing plates were set in the center of a sealed testing chamber (L×W×H: 50cm×50cm×30cm) filled with the pre-treated woodchip. The moisture content of woodchip was increased step by step from 15% to 63% by adding water. For each step, the woodchip was

wetted as evenly as possible out of the testing chamber on a tray, and then was placed back into the chamber after water addition. A pre-test showed that a stabilization process was needed and can take up to 2-3 days. Thus, the testing unit was stabilized for 3 days and then the sensor readings were recorded continuously every 2 min for 24 hours using a data acquisition system (Personal Daq/56, Measurement Computing CO., Norton, MA).

The means of each 24-hour measuring data and the moisture contents of each step were fitted into a quadratic polynomial equation using SigmaPlot 11.0 (Systat Software, Inc, Chicago, IL). The significance of coefficients was tested. The confidence bands and prediction bands with 95% confidence level were estimated in the R statistical environment (R development Core Team) using functions (confint, and predict) found in the package "stats".

7.2.2 Ammonia mitigation biofilter operation incorporated with moisture sensor

After the sensor-medium calibration, the same moisture sensors were applied in two ammonia mitigation biofilters. The response of the sensors to moisture in the biofilter medium was assumed to be same as found in the sensor-medium calibration test.

7.2.3 Biofilter apparatus

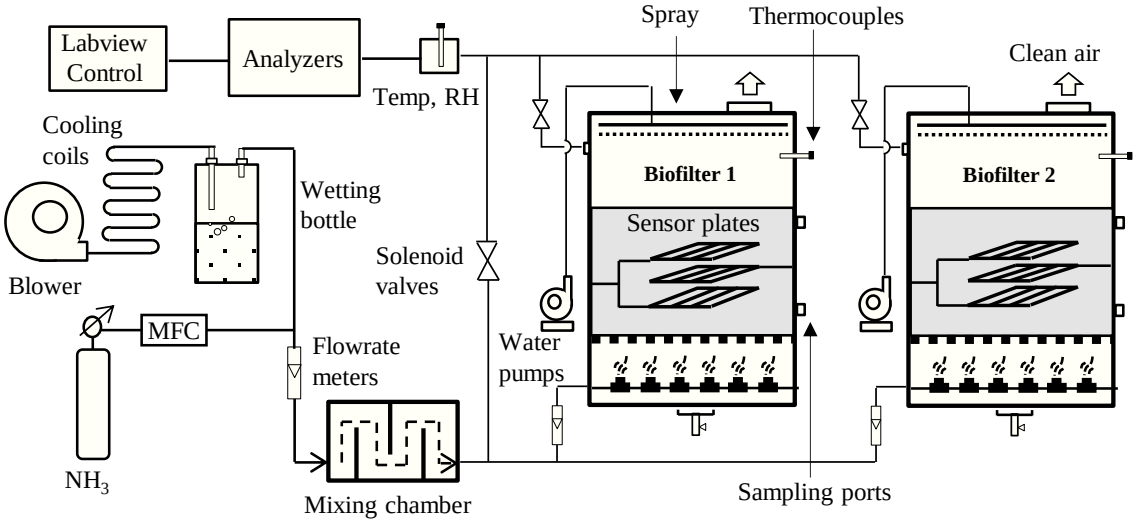

Figure 7.1 Schematic design of biofilter setup incorporated with moisture sensors.

Two bench-scale cylindrical biofilters (ID=45cm, H=50cm) made of transparent plastics were built for this test (Fig. 7.1). Anhydrous ammonia (99.99%, S.J. Smith CO., Urbana, IL) regulated by a mass flow controller (Model 825, Edwards High Vacuum International, Wilmington, MA) was diluted by pre-humidified ambient air to provide 30-36 ppm, 70 liter per minute (lpm)

ammonia to each biofilter. Air from the blower was 2-3℃ warmer than the room condition, so a cooling coil was used to make it closer to room temperature. Air temperature and relative humidity (RH) were measured with a probe (HMP155, Vaisala Inc., Woburn, MA). A layer of 25cm woodchip was supported by a perforated floor; the moisture sensor plates were fixed in the center of biofilter media. Empty bed retention time (EBRT) was 34 s. Water was added at a constant rate via a coiled soaker hose (OD=0.64 cm) located on top of the media. Ammonia and nitrous oxide concentrations were measured by an analyzer (INNOVA1412, California Analytical, Inc., Orange, CA. Calibration of INNOVA is shown in the Appendix E6). The analyzer was calibrated before the experiment started and was checked regularly using certified gases (80 ppm) every two weeks. The ammonia and nitrous oxide concentration, gas temperature and relative humidity, and sensor (Fig. 7.2) outputs were recorded every 20 seconds; the water pump (170DM5, Stenner Pumps & Parts, Indianapolis, IN) and solenoid valves (C2DB1062, and C3LM1075, Parker Hannifin, Cleveland, OH) were controlled by a site-built control and data acquisition system (Labview, National Instruments CO., Austin, TX, and Personal Daq/56, Measurement Computing CO., Norton, MA). No extra nutrients or inoculum cultures were added after a 9-day start-up with 10ppm ammonia.

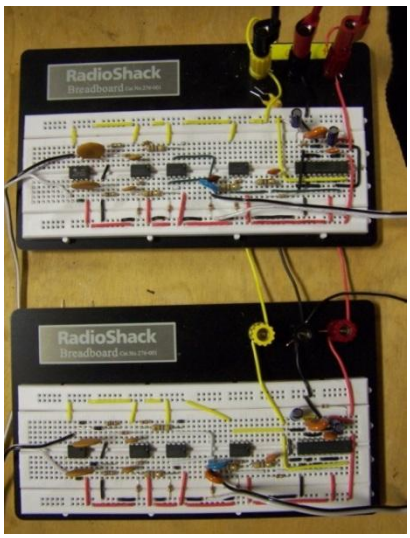

Figure 7.2 Sensor circuits.

7.2.4 Gas, media sampling and sensor output data collection

Each of the three gas sources (inlet gas, Biofilter 1 and Biofilter 2 outlet gases) was analyzed for eight hours daily in a rotation, using one analyzer (INNOVA 1412, LumaSense Technologies,

Santa Clara, CA), by means of the control system via the solenoid valves. Every week, woodchip samples (~30 gram) were taken from the two sampling ports located 5 cm above the bottom of media (lower port) and 5 cm beneath the surface of media (upper port), respectively. On each day, the sensor readings were collected for 20 hours; the collection started 4 hours after water addition under the control of "Approach 1", which will be introduced in the following "water pump control strategy" section.

7.2.5 Water pump control strategy

Three options were made available to control the water pumps: "always on", "always off" and "left to control". If it was needed, the pumps can be turned on or off any time during the experimental period. The "left to control" option provided two approaches for water addition (Fig. 7.3). Approach 1 was set to add water regularly for 30 seconds (water addition of 120 ml) every day. Approach 2 compared the sensor reading (Vin/Vout) to two values (2.4 and 3.0. These two numbers were selected based on the sensor-medium calibration results mentioned in the "Sensor response to moisture change" section). Every three hours, the control system checked the sensor reading for 30 seconds. If the reading was lower than 2.4 (means over dry), a water pump will be turned on automatically to add water for 30 seconds at the most; if the reading was higher than 3.0 (means over wet), both approaches will be terminated until the sensor reading went below 3.0 again.

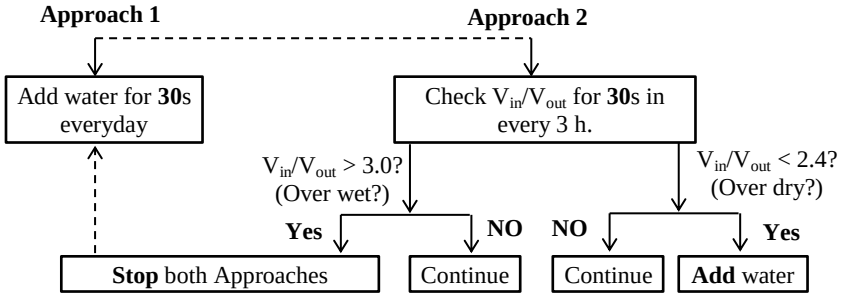

Figure 7.3 Water pumps control strategy. "Continue" means no action was taken.

7.2.6 Water balance calculation

In order to keep moisture content constant, water addition should be close to water loss. In this case:

$$\text{Water addition rate} = \text{water pump working time per day} \times \text{water flowrate} \quad (7\text{-}1)$$

$$\text{Water loss rate} = (\text{outlet abs. humidity} - \text{inlet abs. humidity}) \times \text{air flowrate} \quad (7\text{-}2)$$

The water flowrate was 4 ml per second and the air flowrate was 70 lpm. The abs. humidity was calculated using the measured temperature and relative humidity. Thus, daily moisture content change can be calculated as:

$$\text{(Water addition rate - Water loss rate)/ Medium weight} \times 100\% \quad (7\text{-}3)$$

The moisture contents were quite constant during the experiment period, and so was the medium weight. The medium weight was estimated to be 29.2 kg.

7.3 Results and Discussion

7.3.1 Sensor response to moisture change

For the sensor-medium calibration experiment setup used, the sensor reading (V_{in}/V_{out}) increased with medium moisture content (Fig. 7.4). The reading was relative flat at low moisture levels and then curved upward rapidly. The big increase at moisture higher than 35% may be largely attributed to the reduced impedance of medium. With the tested moisture contents, the sensor displayed a wide range of readings- approcimate 1 to 6- demonstrating a high feasibility of measurement. The general small standard deviations (less than 0.1 at all six moisture levels) showed that sensor reading was stable during the measurement. A quadratic polynomial model (R^2= 0.996, see Table 7-2) was applied to fit the calibration curve. The confidence bands and prediction bands at 95% confidence level were also plotted on the figure. The model coefficients depend on the properties of materials, including particle size distribution, density, porosity, and surface chemisty (Dam et al., 2002). For the tested woodchip medium, the coefficients were all significant and the *p* values were shown in Table 7-2.

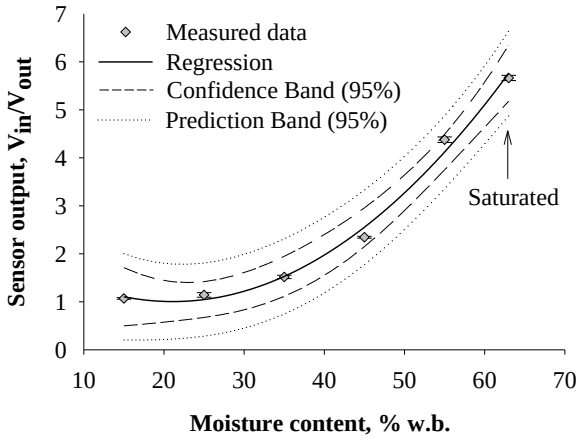

Figure 7.4 Sensor-medium calibration curve with confidence bands and prediction bands at 95% confidence level.

Table 7-1 Statistical parameters of quadratic polynomial regressions.

Material	Regression equation with S.D.	R^2	*p*-values
woodchip	V_{in}/V_{out}= (2.2 ±0.52) - (0.11 ±0.030) ×MC+(0.0027 ±0.00040) × MC^2	0.996	y_0: *p*= 0.0237 a: *p*= 0.0310 b: *p*= 0.0054

Note: MC= moisture content, %.
Null hypothesis: the variables are not significant.

According to the regression equation in Table 7-1, the moisture content of woodchip medium will be 44% and 49% if the sensor reading was 2.4 and 3.0, respectively. Thus, these two values (2.4 and 3.0) were chosen and coded into the biofilter water pump control program as limiting thresholds (Fig. 7.4).

7.3.2 Sensor readings during an one-month operation

The two biofilters were operated continuously for a month as replicates. Biofilter moisture content was managed automatically by taking sensor readings as feedback and relaying the water pump control strategy to adjust the moisture condition. The Fig. 7.5A shows a typical one-day cycle of sensor reading with one-time water addition under the "Approach 1" only (Fig. 7.3). A peak (Δ (V_{in}/V_{out}) > 0.1 within one hour) was generated when water was added, and then the sensor reading decreased slightly as a result of water vapor loss. It indicates that the sensor was sensitive to moisture content changes. Notice that diffusion of water in the medium can take hours after water addition, and the sensor readings can be increased when moisture distribution become more even; thus, the diffusion can partially offset the decrease of sensor reading. This may explain why the curve was relative flat during hour 12- 24.

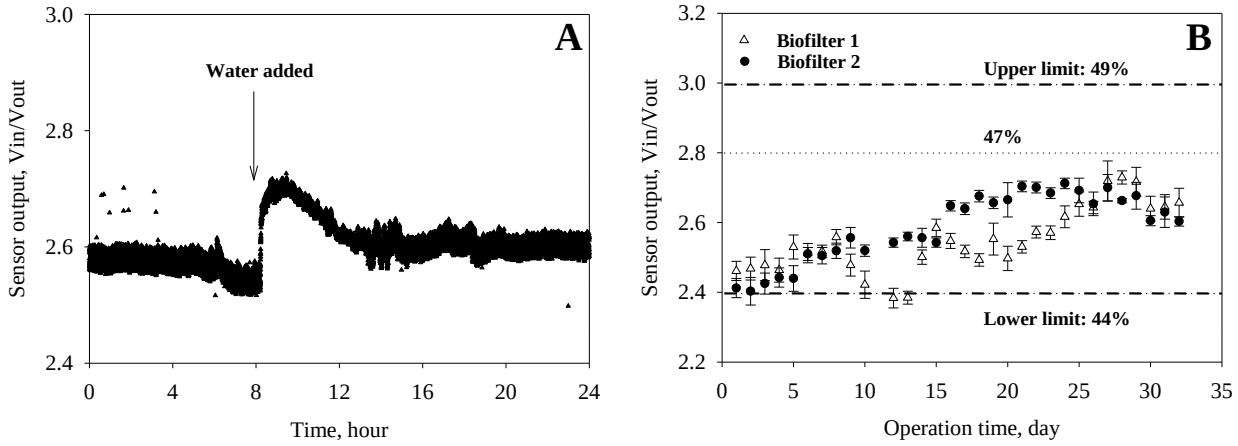

Figure 7.5 Moisture sensor reading. A: a typical one-day observation with one-time water addition and B: one-month observation.

Note: For figure B, each point represents a one-day average and standard deviation. The dashed lines represent 44%, 47% and 49% MC, respectively. The moisture contents were calculated based on regression equation in Table 7-1.

The sensor readings were successfully managed within the designed range of 2.4-2.8, a very narrow range (Fig. 7.5B, the details are shown in the Appendix E5.). Applying the regression equation in Table 7-1 to sensor reading results, the medium moisture contents were estimated to be 44-47%. There were a few days (Biofilter 1: day 12-16; Biofilter 2: day 1-5) that the sensor readings were occasionally below 2.4. At those days, the pumps were automatically turned on under the control of the "Approach 2" so that sensor readings were stepped up to above 2.4 again. For Biofilter 1, its sensor readings increased in the first half of the experimental period and then were generally stable; indicating the amount of water addition was very close to the amount of water vapor loss. For Biofilter 2, its sensor readings decreased during the day 9-12 and then increased as a result of extra water addition during the day 13-16; a second small decrease was observed during the day 16-20 and followed by a second increase in the day 20-29 and a third decrease in the day 29-32. Although there were fluctuations, the control system displayed its ability to maintain the sensor reading within the desired range. Accumulation of salts, such as nitrite and nitrate, may affect the impedance measurement- a phenomenon called Warburg element (Zelinka et al., 2008). However, how the Warburg element influenced the sensor reading was not clear.

7.3.3 Water balance

The daily changes of moisture contents were calculated based on the water addition and water loss rate applying equation 7-3. The relative humidity of inlet and outlet gas was 85-90% and 88-

94%, respectively (the inlet and outlet humidity are shown in the Appendix E1, E2, and E3). The results show that all daily changes were within ± 1% during the test (Fig. 7.6A) and the overall moisture changes of Biofilter 1 and 2 were 1.08% and 0.30%, respectively, which was in line with the sensor readings (Fig. 7.5B). The water addition rates are shown in the Appendix E4.

The medium samples were taken from both upper and lower sampling ports and their moisture content were measured using 105 ℃ oven drying. The moisture contents were quite stable after the first week of operation and the medium in the upper layer showed much higher moisture content comparing to the medium located in the lower layer (Fig. 7.6B). Combining moisture content of both lower layer and upper layer, the overall measured moisture content was 49.0 ± 4.9 and 49.1 ± 5.0 for Biofilter 1 and 2, respectively. These results were 5-10% higher than the sensor estimated values (Fig. 7.5B).

The results obtained from the three methods (sensor reading, balance calculation and oven drying) agreed with each other, although the oven drying method showed slightly higher results. However, the results provided by oven drying method were discrete and less representative given that only a small amount of sample were analyzed. Thus, we believe the sensor accuracy displayed in this study is acceptable for biofilter applications.

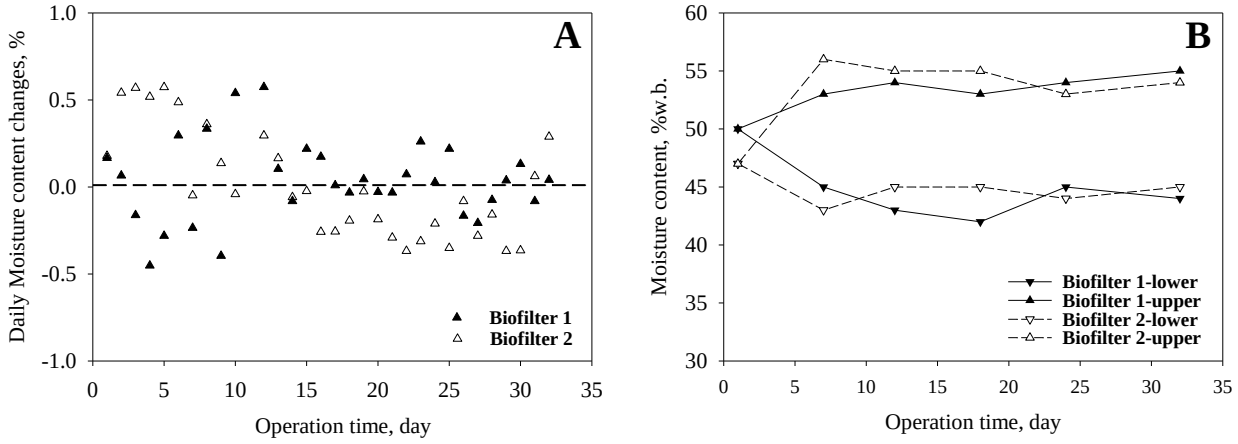

Figure 7.6 Moisture contents in two biofilters. A: calculated daily moisture changes based on humidity difference between inlet and outlet gases; and B: medium moisture contents measured by 105℃ oven drying.

7.3.4 Ammonia removal efficiency and nitrous oxide generation

With proper control of moisture content, both biofilters achieved high and stable performance-high ammonia removal efficiencies and low produced nitrous oxide concentrations. Ammonia removal efficiencies of the two biofilters were 82-92% and increased slightly during the test (Fig.

7.7A). The removal rates were consistent with those reported previously (Jiang et al., 2009a; Pagans et al., 2005; Sakuma et al., 2008). The increases could be caused by the moisture changes (Fig. 7.5B), or could be due to the microbial acclimation (Villaverde et al., 2000). Comparing to a previous study in which 0.6-2.0 ppm nitrous oxide was produced with 60% MC (Maia et al., 2012a; Maia et al., 2012b), the nitrous oxide concentrations observed in this study were much lower (< 0.32 ppm in all days, Fig. 7.7B). On the day 1 and day 2, the nitrous oxide concentrations were nearly negligible - lower than 0.1 ppm - a phenomenon may be caused by the medium adsorption of nitrous oxide (Akdeniz and Janni, 2012).

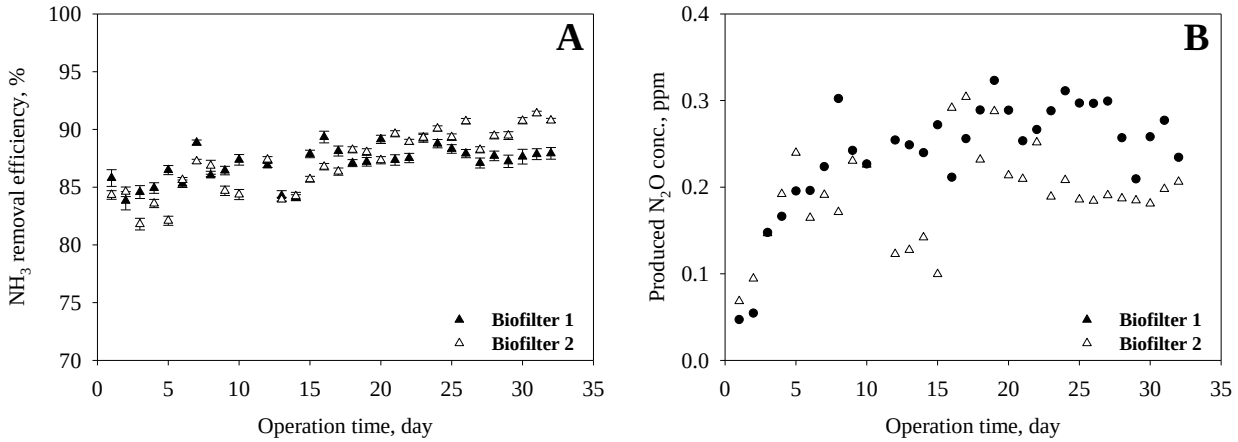

Figure 7.7 Biofilter performance. A: NH_3 removal efficiencies of replicated biofilters in a one-month test and B: the concentration of generated N_2O.

Note: the concentration of N_2O was calculated by subtracting the inlet N_2O concentration from the outlet N_2O concentration.

7.3.5 Biofilter moisture management

The above results showed that the medium moisture content of the two tested biofilters can be controlled well by applying the developed moisture sensor and water addition strategy. Although this test only focused on maintaining moisture within a small range (45-50% MC), this monitoring and control method have the potential to be applied to other cases where a more challenging moisture control – for example, higher than 60% or lower than 40%- is needed.

A gas-phase biofilter is an integrated system. It involves, at least, ammonia adsorption, nitrification and denitrification. Many factors such as temperature, pH, MC and compaction – alone or combined with others- can complicate the system. Moisture content is a key factor that affects ammonia absorption, oxygen and nutrients transport, microbial growth and inhibition, and many others. Maintaining biofilter MC at a well-suited range can maximize ammonia removal

efficiency, minimize nitrous oxide generation or provide a balance between ammonia removal efficiency and nitrous oxide generation. This study presents a feasible and cost effective method to achieve this goal on bench scale biofilters. For pilot or industrial scale biofilters, larger sensing plates or multiple sets of sensors will be needed given the moisture distribution is often heterogeneous. Sensor-media calibration curves are case specific, and might need re-calibration to correct reading drift caused by possible compaction or salt accumulation.

7.4 Conclusions

A moisture sensor and a moisture control strategy were developed and applied in two bench-scale ammonia mitigation biofilters that use woodchip as packing medium. In a one-month test, the sensor was sensitive to biofilter medium moisture changes, and the moisture content was successfully managed within a narrow range of 44-47% according to the sensor measurement. Water balance calculation based on water addition and water loss rates confirmed the stability of moisture content during the test; while the oven drying method showed slightly higher (5-10%) results than the moisture contents measured by the sensors. At the controlled moisture condition, the two biofilters displayed high and stable function- high ammonia removal efficiencies (82-92%) and low produced nitrous oxide concentrations (0-0.32 ppm).

Chapter 8:SUMMARIES AND RECOMMENDATIONS

8.1 Summaries

This study addressed several issues in livestock building gas-phase ammonia emission mitigation biofilters. It includes an engineering survey study of biofilter media (Chapter 3), a baseline test of biofilter performance (Chapter 4), an examination of moisture effects on ammonia removal efficiency and nitrous oxide generation (Chapter 5), and a design and application of moisture sensor (Chapter 6 and 7).

First, to facilitate biofilter media selection, physical and chemical properties of eleven commonly used biofilter media (four wood mulches, three composts, one topsoil, one sludge, one peat, and one activated carbon) were characterized, and their airflow resistance properties were estimated since the pressure drop is a common constraint of biofilter design. It was found that the moisture content (8.3-75%), particle size distribution (>1.9cm, 0.8-1.9cm, 0.2-0.8cm and <0.2cm), compaction (artificial driller compaction) and bed thickness (20-58 cm) can affect the airflow resistance significantly. The correlationships between unit pressure drop and cross area airflow rate was assessed by fitting the results into the *Hukill and Ives* (1955) equation which returns two constants that can be used for comparison. Totally, 91 sets of the equation constant pairs were obtained that can be an initial database for predicting pressure drop of various materials for biofilter designers. Besides that, an empirical modification of the *Hukill and Ives* (1955) equation was conducted by adding three derating factors that were obtained based on the 91 sets of measured results.

Secondly, a baseline test was carried out to examine biofilter ammonia removal efficiency and nitrification kinetics. A mixture of fine shredded hardwood mulch and manure compost at a 1:1 weight ratio was used as the biofilter medium. At high pH conditions, the two bench-scale biofilters reached up to 94% ammonia removal efficiency but then decreased. An N-depleting step was carried out after the first N-enriching step, and it partially recovered the biofilter function but did not last long. The concentrations of NH_4^+-N, NO_2^--N and NO_3^--N in the biofilter medium were measured every two days. A mass balance test showed that the NH_4^+-N and NO_3^--N were the major N-containing compounds in the medium, and NH_4^+-N, NO_2^--N and NO_3^--N accumulated in medium accounted for 50-100% of N captured from the inlet gas. Other N-containing compounds could be organic compounds or gases. A model that considers

nitrification as a two-step reaction was developed to estimate the N transformation rates. It provided two very measurable indicators of biofilter performance, the nitrification rate, k_1 and k_2. It was found that the nitrification transformation constants decreased in both N-enriching steps, indicating the reactions were inhibited. By examining the concentrations of N-containing compounds in the medium, it was very likely that high concentration of free ammonia, or FA, had a strong negative feedback to the biofilter performance. It can inhibit the ammonia oxidizers. Thus, it is very necessary to manage the concentrations of N-containing compounds, especially FA, in biofilter medium.

Thirdly, a four-month test was conducted to study the effects of moisture content on biofilter ammonia removal efficiency and nitrous oxide generation. Four biofilters were built for this study and the moisture contents in the media were manipulated step by step. It was found that ammonia removal efficiency was improved as media moisture content increased from 35% to 55%; but further increasing moisture content to 63% only slightly promote ammonia mitigation. In contrast, little increase of nitrous oxide was observed when moisture content was increased from 35% to 55%, but further increasing moisture content to 63% quickly peaked nitrous oxide generation. Thus, to achieve high ammonia removal efficiency and low nitrous oxide generation, it is important to maintain the moisture content within the appropriate range (approximately, 40−55%MC). The microbial communities in the biofilter media were also analyzed after each moisture content change. The bacterial community was analyzed using ARISA, the ammonia oxidizer and denitrifier communities were analyzed using T-RFLP. Real time qPCR was used to measure the gene copy of denitrifiers. The results showed that ammonia oxidizer community resisted to the "moisture disturbance-disturbance relief (MC: 55%-63%-55%)" process; while the bacterial communities and *nosZ* gene communities showed a functional redundancy to the moisture changes. The relative constant of ammonia oxidizers supports the observation of the flat ammonia removal efficiencies at that moisture range. The qPCR test results showed that the quantity of *nosZ* gene copy was significantly reduced at extremely high (63%) moisture content. This result explained why the concentration of the nitrous oxide was dramatically increased at that condition.

Fourthly, given the importance of moisture management as shown in the above test, a moisture sensor was developed for biofilter applications. The sensor was designed based on impedance measurement. It has a large-format sensing unit and a circuit that returns dc voltage

signals. The dc voltage signal is correlated with the moisture content. In a validation test, the moisture sensor returned 1−7 volt dc signal when the moisture content (woodchips and compost) range was 5−63%. ANCOVA analysis showed that the sensor measured results were in line with the predictions, indicating that impedance is an appropriate predictor of the moisture content. The temperature and compaction effects on moisture measurement were also estimated. The temperature of tested woodchips were heated to 22℃ to 27℃ and further to 32℃ with moisture content of 3−63%, however, the impedance of tested woodchips were not changed dramatically. In the compaction test, a chipped woodchip of 55% moisture was sieved and two size groups (size: 0.8cm−1.9cm and 0−0.8cm) were tested separately. 20cm of woodchip was put on top of the sensor plates to create a compaction force for eight days. The results showed that the sensor readings were increased slightly but significantly in *t*-test, indicating that signal drifting can happen if the sensor was used in a long-term application.

And finally, the moisture sensor, together with a water pump control strategy, was applied in two biofilters for one month. The water pump control strategy aimed to maintain the sensor reading within 2.4 (44% MC) and 3.0 (49% MC). Results showed that the sensor was sensitive to moisture changes, and the moisture content was successfully managed within the desired range of 44–47%. Water balance calculation confirmed the stability of moisture content during the test; while the oven drying method showed slightly higher (5-10%), but acceptable, results than the moisture contents measured by the sensors. At the controlled moisture condition, the two biofilters achieved high ammonia removal efficiencies (82-92%) and low nitrous oxide concentrations (0-0.32 ppm).

8.2 Recommendations

Based on the results of this study, the following recommendations are made for future biofilter designers:

1. Select appropriate material(s) to reduce biofilter pressure drop.

Although woodchips and composts are widely used as biofilter media, their airflow resistance properties are quite varied. Generally speaking, unit pressure drops of composts are much higher than that of woodchips. Besides that, composts are more likely to be compacted and lead to increase of pressure drop comparing to woodchips. The porosity and particle size distribution play an important role in determining airflow resistance. The lower the porosity and smaller the particle size distribution, the higher the unit pressure drop.

To select appropriate materials for biofilter application, the first thing one need to know is the available pressure head and the designed media bed thickness. The designer should take the potential pressure drop increase into consideration. The following equation was developed from this study and it is believed that it can be used to predict the actual pressure drop.

$$\frac{\Delta P}{L} = \frac{aQ^2}{\ln(1+bQ)}[1+c(MC-52.5)]\times[1+d(L-0.2)]\times(1+tT) \quad (8\text{-}1)$$

Where c = 0.005~0.015, d = 0.65~1.70 and t= 0.10~0.25. Constants a and b can be obtained from Table 3-4, if one of the tested materials or mixtures is selected for use in the design.

The designer can calculate both the lowest possible pressure drop and the highest possible pressure drop using the above equation and compare them to the available pressure head (taking into consideration the pressure drops from ductwork, etc.). Then, the designer can select materials that will fit into the range. If mixtures of materials are considered, the pressure drops of the mixtures usually in between the two materials that are used separately.

2. Appropriately manage N-containing compounds in the media to achieve stable ammonia removal efficiency.

High concentration of N-containing compounds can inhibit nitrification and thus degrading biofilter function. A typical biofilter is an N-enriching environment where gas-phase ammonia is continuously absorbed and/or adsorbed into the biofilter. Although N is converted into gases, such as N_2 and N_2O, the concentrations of ammonium, nitrite and nitrate can be increased quickly during biofilter operation. High concentration of free ammonia (FA) and free nitric acid (FNA) can inhibit nitrifiers. To determine if a biofilter is inhibited, one way is to measure the concentration of ammonium, nitrite and nitrate, and then use the following two equations to calculate the kinetic constants, k_1 and k_2. If these two constants are decreasing, the nitrification rates are retarded.

$$C_{\mathrm{NH_4^+}} = \frac{C_{in-}(C_{in}-k_1\mathrm{CH_4^+},0\,)e^{-k_1 t}}{k_1} \quad (8\text{-}2)$$

$$C_{\mathrm{NO_2^-}} = \frac{C_{in}}{k_2}(1-e^{-k_2 t}) + \frac{C_{in}-k_1\mathrm{CH_4^+},0}{k_2-k_1}\,(e^{-k_2 t} - e^{-k_1 t}) \quad (8\text{-}3)$$

Several methods can be used to control the FA and FNA concentrations in biofilter media. Nitrification process produces H^+ and thus decreasing pH value. The pH concentration can be adjusted by adding chemicals, such as limestone, to balance the increase of H^+ and also to decrease the concentrations of FA and FNA. However, very high pH value can degrade ammonia

removal efficiency as well. Alternatively, the biofilter can be "washed" for a very short time to allow leachate to take away accumulated FA and FNA. This process cannot be continued for a long time, e.g. a day, because high moisture content of biofilter media can trigger the generation of nitrous oxide. It may take 1−2 days for microbial activities to be altered and produce nitrous oxide under high moisture condition.

3. Appropriately manage moisture content in media to achieve high ammonia removal and low nitrous oxide generation.

Based on this study, we know that moisture content higher than 55% does not help increase ammonia removal efficiency; in contrast, it will dramatically increase nitrous oxide generation. On the other hand, low moisture content, e.g. lower than 35%, will reduce the ammonia removal efficiency. Therefore, it is important to control biofilter media moisture content within an optimum range.

The moisture sensor developed in this study can help solve this problem. For each biofilter medium, the correlation between the sensor reading and medium moisture content can be quite different, therefore, it is necessary to calibrate the sensor for each selected biofilter medium. For large scale biofilters, the moisture distribution can be varied in both vertical and horizontal directions, thus multiple sensors will be needed. To reduce evaporation, very often, soaker hoses are buried inside of biofilter media. In this case, the sensor plates should be some distance away from the soaker hoses to avoid generating spurious peak signals. If a data logger is used to record the sensor reading, a signal processer will be needed to filter randomly generated peaks.

If no moisture sensor is applied to continuously monitor media moisture content, other grab-sample methods should be considered. The media can be sampled and the moisture content can be measured by oven drying at 105 ℃ for 24 hours. Alternatively, the water holding capacity of a sample can be quickly measured and then the results can be used to calculate media moisture content.

For biofilters using woodchips and compost, controlling moisture content in the range of 40-50% might be a good choice in most cases. In case of over-wet conditions, the easiest way to recover the biofilter performance is stopping adding water onto the media and waiting until the moisture content drops to the normal range. In case of over-dry condition, water should be added step by step to avoid overly wetting the media.

For biofilters with an open top, the moisture content in biofilter media can be changed dramatically by weather events. Our study shows that ammonia oxidizers are resistant to moisture change (55-63% MC); therefore, as long as moisture content is in the normal range, the function of ammonia oxidizer can be sustained. Similarly, the denitrifiers can show a functional redundancy to moisture changes. Therefore, after a moisture disturbance, new denitrifier groups will carry out the same functions. These observations show that both ammonia oxidizers and denitrifiers have a capacity to tolerate moisture changes. However, it is extremely difficult to estimate the tolerance. The microbes follow these observations when moisture was changed from 55% to 63% and then back to 55% as shown in our study, however, we do not know if this response would be sustained at much more dynamic conditions.

REFERENCES

Acuna, M. E., F. Perez, R. Auria, and S. Revah. 1999. Microbiological and kinetic aspects of a biofilter for the removal of toluene from waste gases. *Biotechnology and Bioengineering* 63(2):175-184.

Agrawal, M. P., A. Shukla, and M. Singh. 1985. Nitrification inhibition of added nitrogenous fertilizers by potassium-chloride in soil. *Plant and Soil* 86(1):135-139.

Akdeniz, N., and K. A. Janni. 2012. Full-scale biofilter reduction efficiencies assessed using portable 24-hour sampling units. *Journal of the Air & Waste Management Association* 62(2):170-182.

Akdeniz, N., K. A. Janni, and I. A. Salnikov. 2011. Biofilter performance of pine nuggets and lava rock as media. *Bioresource Technology* 102(8):4974-4980.

Akiyama, H., and H. Tsuruta. 2003. Nitrous oxide, nitric oxide, and nitrogen dioxide fluxes from soils after manure and urea application. *Journal of Environmental Quality* 32(2):423-431.

Allison, S. D., and J. B. H. Martiny. 2008. Resistance, resilience, and redundancy in microbial communities. *Proceedings of the National Academy of Sciences of the United States of America* 105:11512-11519.

Allison, S. D., K. L. McGuire, and K. K. Treseder. 2010. Resistance of microbial and soil properties to warming treatment seven years after boreal fire. *Soil Biology & Biochemistry* 42(10):1872-1878.

Amlinger, F., S. Peyr, and C. Cuhls. 2008. Green house gas emissions from composting and mechanical biological treatment. *Waste Management & Research* 26(1):47-60.

Anderson, M. J. 2006. Distance-based tests for homogeneity of multivariate dispersions. *Biometrics* 62(1):245-253.

Anderson, M. J., K. E. Ellingsen, and B. H. McArdle. 2006. Multivariate dispersion as a measure of beta diversity. *Ecology Letters* 9(6):683-693.

Anthonisen, A. C., R. C. Loehr, T. B. S. Prakasam, and E. G. Srinath. 1976. Inhibition of nitrification by ammonia and nitrous-acid. *Journal Water Pollution Control Federation* 48(5):835-852.

Arogo, J., P. W. Westerman, and A. J. Heber. 2003. A review of ammonia emissions from confined swine feeding operations. *Transactions of the ASAE* 46(3):805-817.

Arogo, J., P. W. Westerman, A. J. Heber, W. P. Robarge, and J. J. Classen. 2001. Ammonia in animal production- a review.

ASAE.2007.Resistance to Airflow of Grains, Seeds, Other Agricultural Products, and Perforated Metal Sheets. ASAE standards, St Joseph, MI, USA: ASABE.

Avrahami, S., and B. J. A. Bohannan. 2007. Response of Nitrosospira sp. strain AF-like ammonia oxidizers to changes in temperature, soil moisture content, and fertilizer concentration (vol 73, pg 1166, 2007). *Applied and Environmental Microbiology* 73(9):3121-3121.

Baggs, E. M., C. L. Smales, and E. J. Bateman. 2010. Changing pH shifts the microbial sourceas well as the magnitude of N2O emission from soil. *Biology and Fertility of Soils* 46(8):793-805.

Baho, D. L., H. Peter, and L. J. Tranvik. 2012. Resistance and resilience of microbial communities - temporal and spatial insurance against perturbations. *Environmental Microbiology* 14(9):2283-2292.

Baquerizo, G., J. P. Maestre, T. Sakuma, M. A. Deshusses, X. Gamisans, D. Gabriel, and J. Lafuente. 2005. A detailed-model of a biofilter for ammonia removal: Model parameters analysis and model validation. *Chemical Engineering Journal* 113(2-3):205-214.

Barsoukov, E., and J. R. Macdonald. 2005. *Impedance spectroscopy theory, experiment, and applications*. Wiley-Interscience, New York, N.Y.

Baxevanou, C., D. Fidaros, T. Bartzanas, and C. Kittas. 2008. Ammonia emission from a livestock building. *Agricultural and biosystems engineering for a sustainable world. International Conference on Agricultural Engineering, Hersonissos, Crete, Greece, 23-25 June, 2008*:P-022.

Bernet, N., P. Dangcong, J. P. Delgenes, and R. Moletta. 2001. Nitrification at low oxygen concentration in biofilm reactor. *Journal of Environmental Engineering-Asce* 127(3):266-271.

Bohn, H. L., and K. H. Bohn. 1999. Moisture in biofilters. *Environmental Progress* 18(3):156-161.

Bradley, R. H. 2011. Recent Developments in the Physical Adsorption of Toxic Organic Vapours by Activated Carbons. *Adsorption Science & Technology* 29(1):1-28.

Brady, N. C., and R. Weil, R. 2000. *Elements of the Nature and Properties of Soils*. Prentice-Hall, Upper Saddle River, NJ.

Braker, G., and R. Conrad. 2011. Diversity, Structure, and Size of N2O-Producing Microbial Communities in Soils-What Matters for Their Functioning? *Advances in Applied Microbiology, Vol 75* 75:33-70.

Burnett, W. E. 1969. Odor transport by particulate matter in high density poultry houses. *Poultry Science* 48(1):182-&.

Cabrol, L., L. Malhautier, F. Poly, X. Le Roux, A. S. Lepeuple, and J. L. Fanlo. 2012a. Resistance and resilience of removal efficiency and bacterial community structure of gas biofilters exposed to repeated shock loads. *Bioresource Technology* 123:548-557.

Cabrol, L., L. Malhautier, F. Poly, A. S. Lepeuple, and J. L. Fanlo. 2012b. Bacterial dynamics in steady-state biofilters: beyond functional stability. *Fems Microbiology Ecology* 79(1):260-271.

Casciotti, K. L., and B. B. Ward. 2001. Dissimilatory nitrite reductase genes from autotrophic ammonia-oxidizing bacteria. *Applied and Environmental Microbiology* 67(5):2213-2221.

Chen, L., and S. J. Hoff. 2009. Mitigating Odors from Agricultural Facilities: A Review of Literature Concerning Biofilters. *Applied Engineering in Agriculture* 25(5):751-766.

Chen, L. D., S. Hoff, L. S. Cai, J. Koziel, and B. Zelle. 2009. Evaluation of Wood Chip-Based Biofilters to Reduce Odor, Hydrogen Sulfide, and Ammonia from Swine Barn Ventilation Air. *Journal of the Air & Waste Management Association* 59(5):520-530.

Chen, Y. X., J. Yin, and K. X. Wang. 2005. Long-term operation of biofilters for biological removal of ammonia. *Chemosphere* 58(8):1023-1030.

Choi, O., and Z. Q. Hu. 2009. Role of Reactive Oxygen Species in Determining Nitrification Inhibition by Metallic/Oxide Nanoparticles. *Journal of Environmental Engineering-Asce* 135(12):1365-1370.

Chou, M. S., and C. H. Wang. 2007. Elimination of ammonia in air stream by a Fern-Chip biofilter. *Environmental Engineering Science* 24(10):1423-1430.

Chung, Y. C. 2007. Evaluation of gas removal and bacterial community diversity in a biofilter developed to treat composting exhaust gases. *Journal of Hazardous Materials* 144(1-2):377-385.

Chung, Y. C., and C. P. Huang. 1998. Biotreatment of ammonia in air by an immobilized Nitrosomonas europaea biofilter. *Environmental Progress* 17(2):70-76.

Ciarlo, E., M. Conti, N. Bartoloni, and G. Rubio. 2007. The effect of moisture on nitrous oxide emissions from soil and the N2O/(N2O+N-2) ratio under laboratory conditions. *Biology and Fertility of Soils* 43(6):675-681.

Clarke, K. R., and R. M. Warwick. 2001. *Change in marine communities: an approach to statistical analysis and interpretation.* PRIMER-R Ltd., Plymouth.

Clemens, J., and C. Cuhls. 2003. Greenhouse gas emissions from mechanical and biological waste treatment of municipal waste. *Environmental Technology* 24(6):745-754.

Colliver, B. B., and T. Stephenson. 2000. Production of nitrogen oxide and dinitrogen oxide by autotrophic nitrifiers. *Biotechnology Advances* 18(3):219-232.

Colon, J., J. Martinez-Blanco, X. Gabarrell, J. Rieradevall, X. Font, A. Artola, and A. Sanchez. 2009. Performance of an industrial biofilter from a composting plant in the removal of ammonia and VOCs after material replacement. *Journal of Chemical Technology and Biotechnology* 84(8):1111-1117.

Company, H. 1996-2000. *DR/2010 Spectrophotometer Procedure Manual*. Iowa.

Cuhel, J., M. Simek, R. J. Laughlin, D. Bru, D. Cheneby, C. J. Watson, and L. Philippot. 2010. Insights into the Effect of Soil pH on N2O and N-2 Emissions and Denitrifier Community Size and Activity. *Applied and Environmental Microbiology* 76(6):1870-1878.

D'Amico, M., F. Fantozzi, M. Dionigi, and A. Moschitta. 2010. A simple time-domain-reflectometry based methodology for wood-chip humidity measurements. In *Environmental Energy and Structural Monitoring Systems (EESMS), IEEE Workshop on*.

Dam, R. L., E. H. Den Berg, S. Heteren, C. Kasse, J. A. M. Kenter, and K. Groen. 2002. Influence of organic matter in soils on radar-wave reflection: Sedimentological implications. *Journal of Sedimentary Research* 72(3):341-352.

De Clippeleir, H., E. Courtens, M. Mosquera, S. E. Vlaeminck, B. F. Smets, N. Boon, and W. Verstraete. 2012. Efficient Total Nitrogen Removal in an Ammonia Gas Biofilter through High-Rate OLAND. *Environmental Science & Technology* 46(16):8826-8833.

de Vries, M., and I. J. M. de Boer. 2010. Comparing environmental impacts for livestock products: A review of life cycle assessments. *Livestock Science* 128(1-3):1-11.

Demmers, T. G. M., C. M. Wathes, P. A. Richards, N. Teer, L. L. Taylor, V. Bland, J. Goodman, D. Armstrong, D. Chennells, S. H. Done, and J. Hartung. 2003. A facility for controlled exposure of pigs to airborne dusts and gases. *Biosystems Engineering* 84(2):217-230.

Devinny, J. S., M. A. Deshusses, and T. S. Webster. 1999. *Biofiltration for Air Pollution Control*. Taylor & Francis Ltd, London.

Dewes, T. 1999. Ammonia emissions during the initial phase of microbial degradation of solid and liquid cattle manure. *Bioresource Technology* 70(3):245-248.

Dorado, A. D., J. Lafuente, D. Gabriel, and X. Gamisans. 2010. The role of water in the performance of biofilters: Parameterization of pressure drop and sorption capacities for common packing materials. *Journal of Hazardous Materials* 180(1-3):693-702.

Dumont, E., Y. Andres, P. Le Cloirec, and F. Gaudin. 2008. Evaluation of a new packing material for H2S removed by biofiltration. *Biochemical Engineering Journal* 42(2):120-127.

EC. 2003. integrated pollution prevention and control (IPPC). Reference document on best available techniques for intensive rearing of poutry and pigs. E. Commission, ed.

Ergas, S. J., and B. C. Gonzalez. 2004. Biofiltration: Past, Present and future directions. *Biocycle* 48(6):35-39.

Faulkner, W. B., and B. W. Shaw. 2008. Review of ammonia emission factors for United States animal agriculture. *Atmospheric Environment* 42(27):6567-6574.

Fisher, M. M., and E. W. Triplett. 1999. Automated approach for ribosomal intergenic spacer analysis of microbial diversity and its application to freshwater bacterial communities. *Applied and Environmental Microbiology* 65(10):4630-4636.

Fox, J., and S. Weisberg. 2010. *An R Companion to Applied Regression.* SAGE Publications, Inc, Thousand Oaks, CA.

Francis, C. A., K. J. Roberts, J. M. Beman, A. E. Santoro, and B. B. Oakley. 2005. Ubiquity and diversity of ammonia-oxidizing archaea in water columns and sediments of the ocean. *Proceedings of the National Academy of Sciences of the United States of America* 102(41):14683-14688.

Funk, T. L., M. J. Roberts, J. M. Appleford, and Y. Chen. 2007. Two novel sensor systems for monitoring moisture content in biofilters treating exhaust ventilation air from livestock production facilities. In *International symposium on air quality and water management for agriculture*. Broomfield, CO.

Gadal-Mawart, A., L. Malhautier, C. Renner, J. Rocher, and J. L. Fanlo. 2012. Treatment of a gaseous mixture by biofilters filled with an inorganic packing material: performance and influence of inoculation on removal efficiency levels. *Journal of Chemical Technology and Biotechnology* 87(6):824-830.

Garrido-Fernandez, J. M., R. Mendez, J. M. Lema, and V. Lazarova. 2000. The circulating floating bed reactor: effect of particle size distribution of the carrier on ammonia conversion. *Water Science and Technology* 41(4-5):393-400.

Gates, R. S. 2008. US Animal Feeding Operations Air Emissions Mitigation State of Science. In *Proceedings from the National Conference on Mitigating Air Emissions from Animal Feeding Operations*. Ames, Iowa.

Gay, S. W., D. R. Schmidt, C. J. Clanton, K. A. Janni, L. D. Jacobson, and S. Weisberg. 2003. Odor, total reduced sulfur, and ammonia emissions from animal housing facilities and manure storage units in Minnesota. *Applied Engineering in Agriculture* 19(3):347-360.

Gentile, M., T. Yan, S. M. Tiquia, M. W. Fields, J. Nyman, J. Zhou, and C. S. Criddle. 2006. Stability in a denitrifying fluidized bed reactor. *Microbial Ecology* 52(2):311-321.

Graham, J. R. 1996. GAC based gas phase biofiltration. In *Conference on Biofiltration*. Tustin, CA: The Reynolds Group.

Griffiths, B. S., P. D. Hallett, H. L. Kuan, A. S. Gregory, C. W. Watts, and A. P. Whitmore. 2008. Functional resilience of soil microbial communities depends on both soil structure and microbial community composition. *Biology and Fertility of Soils* 44(5):745-754.

Hanaki, K., C. Wantawin, and S. Ohgaki. 1990. Nitrification at low-levels of dissolved-oxygen with and without organic loading in a suspended-growth reactor. *Water Research* 24(3):297-302.

Hao, X. Y., C. Chang, H. H. Janzen, B. R. Hill, and T. Ormann. 2005. Potential nitrogen enrichment of soil and surface water by atmospheric ammonia sorption in intensive livestock production areas. *Agriculture Ecosystems & Environment* 110(3-4):185-194.

Hartung, J. 1995. Gas and Particulate-Emissions from Livestock Housing. *Deutsche Tierarztliche Wochenschrift* 102(7):283-288.

Hassan, A. A., and G. Sorial. 2009. Biological treatment of benzene in a controlled trickle bed air biofilter. *Chemosphere* 75(10):1315-1321.

Havlikova, M., C. Kroeze, and M. Huijbregts. 2008. Environmental and health impact by dairy cattle livestock and manure management in the Czech Republic. *SCIENCE OF THE TOTAL ENVIRONMENT* 396(2-3):11.

Hoff, S. J., J. D. Harmon, L. Chen, K. A. Janni, D. R. Schmidt, R. E. Nicolai, and L. D. Jacobson. 2009. PARTIAL BIOFILTRATION OF EXHAUST AIR FROM A HYBRID VENTILATED DEEP-PIT SWINE FINISHER BARN. *Applied Engineering in Agriculture* 25(2):269-280.

Hort, C., S. Gracy, V. Platel, and L. Moynault. 2009. Evaluation of sewage sludge and yard waste compost as a biofilter media for the removal of ammonia and volatile organic sulfur compounds (VOSCs). *Chemical Engineering Journal* 152(1):44-53.

Hristov, A. N. 2011. Technical note: Contribution of ammonia emitted from livestock to atmospheric fine particulate matter (PM(2.5)) in the United States. *Journal of Dairy Science* 94(6):3130-3136.

IPCC. 2007. Climate change 2007: synthesis report-summary for policymakers. IPCC, ed. Geneva, Switzerland.

Ivanova, T. G., G. A. Lazerko, I. N. Ermolenko, and L. N. Drik. 1984. Effect of Moisture on the Absorption of Ammonia by Fibrous Activated Carbon Chemisorbents. *Colloid Journal of the Ussr* 46(4):689-692.

Janni, K. A., D. R. Schmidt, A. G. Goldman, and T. Schaar. 2009. Alternative gas-phase biofilter media characteristics and performance. St. Joseph, MI.

Jiang, X., R. Yan, and J. H. Tay. 2009a. Simultaneous autotrophic biodegradation of H2S and NH3 in a biotrickling filter. *Chemosphere* 75(10):1350-1355.

Jiang, X., R. Yan, and J. H. Tay. 2009b. Simultaneous autotrophic biodegradation of H(2)S and NH(3) in a biotrickling filter. *Chemosphere* 75(10):1350-1355.

Jones, K. D., and C. Banuelos. 2000. Using compost/wood chip material as biofiltration media. *Biocycle* 41(10):50-52.

Juneson, C., O. P. Ward, and A. Singh. 2001. Microbial treatment of a styrene-contaminated air stream in a biofilter with high elimination capacities. *Journal of Industrial Microbiology & Biotechnology* 26(4):196-202.

Kapfenberger, J., S. Kabasci, R. Kummel, and H. Fahlenkamp. 2003. Material moisture determination in biofilters with the aid of conductivity measurement. *Chemie Ingenieur Technik* 75(12):1909-1913.

Kastner, J. R., K. C. Das, and B. Crompton. 2004a. Kinetics of ammonia removal in a pilot-scale biofilter. *Trans. ASABE* 47(5):1867-1878.

Kastner, J. R., K. C. Das, and B. Crompton. 2004b. Kinetics of ammonia removal in a pilot-scale biofilter. *Transactions of the Asae* 47(5):1867-1878.

Kent, A. D., A. C. Yannarell, J. A. Rusak, E. W. Triplett, and K. D. McMahon. 2007. Synchrony in aquatic microbial community dynamics. *Isme Journal* 1(1):38-47.

Kevin, A. J., R. S. David, G. Alexandra, and S. Troy. 2009. Alternative Gas-phase Biofilter Media Characteristics and Performance.

Kim, J. H., E. R. Rene, and H. S. Park. 2007. Performance of an immobilized cell biofilter for ammonia removal from contaminated air stream. *Chemosphere* 68(2):274-280.

Kim, N. J., M. Hirai, and M. Shoda. 2000. Comparison of organic and inorganic packing materials in the removal of ammonia gas in biofilters. *Journal of Hazardous Materials* 72(1):77-90.

Klapkova, E., M. Halecky, M. Fitch, C. R. Soccol, and J. Paca. 2006a. Impact of biocatalyst and moisture content on toluene/xylene mixture biofiltration. *Brazilian Archives of Biology and Technology* 49(2):347-352.

Klapkova, E., M. Halecky, M. Fitch, C. R. Soccol, and J. Paca. 2006b. Impact of biocatalyst and moisture content on toluene/xylene mixture biofiltration. *Brazilian Archives of Biology and Technology* 49(6):1001-1006.

Kong, Z., L. Farhana, R. R. Fulthorpe, and D. G. Allen. 2001. Treatment of volatile organic compounds in a biotrickling filter under thermophilic conditions. *Environmental Science & Technology* 35(21):4347-4352.

Kosteltz, A. M., A. Finkelstein, and G. Sears. 1996. What are the "real opportunities" in biological gas cleaning for North America. In *89th Annua Meeting and Exhibition of the Air and Waste Management Association*. Pittsburgh, PA: The Air and Waste Management Association.

Kristensen, E. F., and P. D. Kofman. 2000. Pressure resistance to air flow during ventilation of different types of wood fuel chip. *Biomass & Bioenergy* 18(3):175-180.

Kristiansen, A., S. Lindholst, A. Feilberg, P. H. Nielsen, J. D. Neufeld, and J. L. Nielsen. 2011a. Butyric Acid- and Dimethyl Disulfide-Assimilating Microorganisms in a Biofilter Treating Air Emissions from a Livestock Facility. *Applied and Environmental Microbiology* 77(24):8595-8604.

Kristiansen, A., K. H. Pedersen, P. H. Nielsen, L. P. Nielsen, J. L. Nielsen, and A. Schrarmm. 2011b. Bacterial community structure of a full-scale biofilter treating pig house exhaust air. *Systematic and Applied Microbiology* 34(5):344-352.

Kullenberg, R., M. Hultnas, V. Fernandez, M. Nylinder, S. Toft, and F. Danielsson. 2010. Dual-Energy X-Ray Absorptiometry Analysis for the Determination of Moisture Content in Biomass. *Journal of Biobased Materials and Bioenergy* 4(4):363-366.

Lee, J., and Y. H. Zhang. 2008. Evaluation of gas emissions from animal building dusts using a cylindrical convective chamber. *Biosystems Engineering* 99(3):403-411.

Legendre, P., and E. D. Gallagher. 2001. Ecologically meaningful transformations for ordination of species data. *Oecologia* 129(2):271-280.

Legendre, P., and L. Legendre. 1998. *Numerical Ecology*. Elsevier Science, Amsterdam.

Leson, G., and A. M. Winer. 1991. Biofiltration - an Innovative Air-Pollution Control Technology for Voc Emissions. *Journal of the Air & Waste Management Association* 41(8):1045-1054.

Li, X., G. Upadhyaya, W. Yuen, J. Brown, E. Morgenroth, and L. Raskin. 2010. Changes in the Structure and Function of Microbial Communities in Drinking Water Treatment Bioreactors upon Addition of Phosphorus. *Applied and Environmental Microbiology* 76(22):7473-7481.

Lim, T. T., Y. M. Jin, J. Q. Ni, and A. J. Heber. 2012. Field evaluation of biofilters in reducing aerial pollutant emissions from a commercial pig finishing building. *Biosystems Engineering* 112(3):192-201.

Liu, B. B., P. T. Morkved, A. Frostegard, and L. R. Bakken. 2010. Denitrification gene pools, transcription and kinetics of NO, N2O and N-2 production as affected by soil pH. *Fems Microbiology Ecology* 72(3):407-417.

Liu, P. K. T., R. L. Gregg, H. K. Sabol, and N. Barkley. 1994. Engineered Biofilter for Removing Organic Contaminants in Air. *Journal of the Air & Waste Management Association* 44(3):299-303.

Liu, Q., M. Li, R. Chen, Z. Y. Li, G. R. Qian, T. C. An, J. M. Fu, and G. Y. Sheng. 2009. Biofiltration treatment of odors from municipal solid waste treatment plants. *Waste Management* 29(7):2051-2058.

Liu, W. T., T. L. Marsh, H. Cheng, and L. J. Forney. 1997. Characterization of microbial diversity by determining terminal restriction fragment length polymorphisms of genes encoding 16S rRNA. *Applied and Environmental Microbiology* 63(11):4516-4522.

Liu, X. T., X. Quan, L. L. Bo, S. Chen, and Y. Z. Zhao. 2004. Simultaneous pentachlorophenol decomposition and granular activated carbon regeneration assisted by microwave irradiation. *Carbon* 42(2):415-422.

Lu, C. S., M. R. Lin, and C. H. Chu. 2002. Effects of pH, moisture, and flow pattern on trickle-bed air biofilter performance for BTEX removal. *Advances in Environmental Research* 6(2):99-106.

Mackie, R. I., P. G. Stroot, and V. H. Varel. 1998. Biochemical identification and biological origin of key odor components in livestock waste. *Journal of Animal Science* 76(5):1331-1342.

Maia, G. D. N., G. B. Day, R. S. Gates, and J. L. Taraba. 2012a. Ammonia biofiltration and nitrous oxide generation during the start-up of gas-phase compost biofilters. *Atmospheric Environment* 46:659-664.

Maia, G. D. N., G. B. Day, R. S. Gates, J. L. Taraba, and M. S. Coyne. 2012b. Moisture effects on greenhouse gases generation in nitrifying gas-phase compost biofilters. *Water Research* 46(9):3023-3031.

Maia, G. D. N., G. T. Sales, G. B. Day, R. S. Gates, and J. L. Taraba. 2012. Characterizing Physical Properties of Gas-Phase Biofilter Media. *Transactions of the Asabe* 55(5):1939-1950.

Manuzon, R. B., L. Y. Zhao, H. M. Keener, and M. J. Darr. 2007. A prototype acid spray scrubber for absorbing ammonia emissions from exhaust fans of animal buildings. *Transactions of the Asabe* 50(4):1395-1407.

Marek, J., J. Paca, B. Koutsky, and A. M. Gerrard. 1999. Determination of local elimination capacities and moisture contents in different biofilters treating toluene and xylene. *Biodegradation* 10(5):307-313.

Matthew, J. R., L. F. Ted, J. M. Appleford, and C. Yong. 2005. Moisture Sensing Methods for Biofilters Treating Exhaust Air from Livestock Buildings.

McArdle, B. H., and M. J. Anderson. 2001. Fitting multivariate models to community data: A comment on distance-based redundancy analysis. *Ecology* 82(1):290-297.

Mccune, B., and J. B. Grace. 2002. *Analysis of Ecological Communities*. MjM software, Oregon, USA.

McLain, J. E. T., and D. A. Martens. 2006. N2O production by heterotrophic N transformations in a semiarid soil. *Applied Soil Ecology* 32(2):253-263.

Medina, V. E., T. Webster, M. Ramaratnam, and J. S. Devinny. 1995. Treatment of Gasoline Residuals by Granular Activated Carbon-Based Biological Filtration. *Journal of Environmental Science and Health Part a-Environmental Science and Engineering & Toxic and Hazardous Substance Control* 30(2):407-422.

Melo, L. D. 2011. Moisture control methodoloty for gas phase compost biofilters. University of Kentucky, Biosystems and Agricultural Engineering

Melse, R. W., and N. W. M. Ogink. 2005. Air scrubbing techniques for ammonia and odor reduction at livestock operations: Review of on-farm research in the Netherlands. *Transactions of the Asae* 48(6):2303-2313.

Melse, R. W., N. W. M. Ogink, and W. H. Rulkens. 2009. Overview of European and Netherlands' regulations on airborne emissions from intensive livestock production with a focus on the application of air scrubbers. *Biosystems Engineering* 104(3):289-298.

Menig, H., H. Krill, and T. Jaeschke. 1997. Kosten und Effizienz biologischer Verfahren im Vergleich zu anderen Abluftreinigungssystemen. In *Biological Waster Gas Cleaning*. Duesseldorf, Germany.

Mertens, J., S. Ruyters, D. Springael, and E. Smolders. 2007. Resistance and resilience of zinc tolerant nitrifying communities is unaffected in long-term zinc contaminated soils. *Soil Biology & Biochemistry* 39(7):1828-1831.

Morkved, P. T., P. Dorsch, and L. R. Bakken. 2007. The N2O product ratio of nitrification and its dependence on long-term changes in soil pH. *Soil Biology & Biochemistry* 39(8):2048-2057.

Nelson, S. O., A. W. Kraszewski, C. V. K. Kandala, and K. C. Lawrence. 1992. High-Frequency and Microwave Single-Kernel Moisture Sensors. *Transactions of the Asae* 35(4):1309-1314.

Nelson, S. O., and S. Trabelsi. 2011. A brief history of grain and seed moisture sensing through dielectric properties. In *9th international conference on electromagnetic wave interaction with water & moist substances*. Kansas City, MO.

Nicolai, R. E., C. J. Clanton, K. A. Janni, and G. L. Malzer. 2005. Ammonia Removal during Biofiltration as Affected by Inlet Air Temperature and Media Moisture Content. *Trans. ASABE* 49(4):1125-1138.

Nicolai, R. E., C. J. Clanton, K. A. Janni, and G. L. Malzer. 2006a. Ammonia removal during biofiltration as affected by inlet air temperature and media moisture content. 49(4):1125-1138.

Nicolai, R. E., C. J. Clanton, K. A. Janni, and G. L. Malzer. 2006b. Ammonia removal during biofiltration as affected by inlet air temperature and media moisture content. *Transactions of the Asabe* 49(4):1125-1138.

Nicolai, R. E., and K. A. Janni. 1997. Development of a low cost biofilter on swine production facilities. St. Joseph, Mich.: ASAE.

Nicolai, R. E., and K. A. Janni. 1998. Biofiltration - adaptation to livestock facilities. In *In Proc. of USC-TRG conference on biofiltration*. Los Angels, CA: Elsvier Publishing.

Nicolai, R. E., and K. A. Janni. 2001a. Biofilter media mixture ratio of wood chips and compost treating swine odors. *Water Science and Technology* 44(9):261-267.

Nicolai, R. E., and K. A. Janni. 2001b. Determining pressure drop through compost-wood chip biofilter media. St. Joseph, MI.

Nordell, A., and K. J. Vikterloef. 2000. Measurements of moisture content in wood fuels with dual energy x-ray. *Varmeforsk Service AB.*

Nystrom, J., and E. Dahlquist. 2004. Methods for determination of moisture content in woodchips for power plants - a review. *Fuel* 83(7-8):773-779.

Oslislo, A., and Z. Lewandowski. 1985. Inhibition of nitrification in the packed-bed reactors by selected organic-compounds. *Water Research* 19(4):423-426.

Pagans, E., X. Font, and A. Sanchez. 2005. Biofiltration for ammonia removal from composting exhaust gases. *Chemical Engineering Journal* 113(2-3):105-110.

Pagans, E., X. Font, and A. Sanchez. 2007. Adsorption, absorption, and biological degradation of ammonia in different biofilter organic media. *Biotechnology and Bioengineering* 97(3):515-525.

Pan, L., S. X. Yang, and J. DeBruyn. 2007. Factor analysis of downwind odours from livestock farms. *Biosystems Engineering* 96(3):387-397.

Park, B. G., W. S. Shin, and J. S. Chung. 2009a. Simultaneous biofiltration of H2S, NH3 and toluene using cork as packing material. *Korean Journal of Chemical Engineering* 26(1):79-85.

Park, H. D., S. Y. Lee, and S. Hwang. 2009b. Redundancy Analysis Demonstration of the Relevance of Temperature to Ammonia-Oxidizing Bacterial Community Compositions in a Full-Scale Nitrifying Bioreactor Treating Saline Wastewater. *Journal of Microbiology and Biotechnology* 19(4):346-350.

Park, S., W. Bae, and B. E. Rittmann. 2010. Operational Boundaries for Nitrite Accumulation in Nitrification Based on Minimum/Maximum Substrate Concentrations That Include Effects of Oxygen Limitation, pH, and Free Ammonia and Free Nitrous Acid Inhibition. *Environmental Science & Technology* 44(1):335-342.

Paz, A., J. Nystrom, and E. Thorin. 2006. Influence of Temperature in Radio Frequency Measurements of Moisture Content in Biofuel.

Peralta, A. 2012. Soil microbial community structure and function along environmental gradients: implications for wetland nitrogen cycling. University of Illinois at Urbana-Champaign, School of Integrative Biology

Petersen, S. O., S. Stamatiadis, and C. Christofides. 2004. Short-term nitrous oxide emissions from pasture soil as influenced by urea level and soil nitrate. *Plant and Soil* 267(1-2):117-127.

Pitcher, H., and K. Ebi. 2004. Health status outcomes for the marker scenarios in the IPCC's special report on emissions scenarios. *Epidemiology* 15(4):S93-S93.

Poulsen, T. G., and A. H. B. Jensen. 2007. Gaseous ammonia uptake in compost biofilters as related to compost water content. *Journal of the Air & Waste Management Association* 57(8):940-946.

Poulsen, T. G., and P. Moldrup. 2007. Comparison of sewage sludge and yard waste compost as biofilter material for ammonia removal. *Compost Science & Utilization* 15(3):151-158.

R Development Core Team. 2009. *R: A language and environment for statistical computing*. R Foundation for Statistical Computing.

Radon, K., A. Peters, G. Praml, V. Ehrenstein, A. Schulze, O. Hehl, and D. Nowak. 2004. Livestock odours and quality of life of neighbouring residents. *Annals of Agricultural and Environmental Medicine* 11(1):59-62.

Ramasamy, S., and B. Moghtaderi. 2010. Dielectric Properties of Typical Australian Wood-Based Biomass Materials at Microwave Frequency. *Energy & Fuels* 24:4534-4548.

Ramirez, M., J. M. Gomez, G. Aroca, and D. Cantero. 2009. Removal of ammonia by immobilized Nitrosomonas europaea in a biotrickling filter packed with polyurethane foam. *Chemosphere* 74(10):1385-1390.

Rappert, S., and R. Muller. 2005. Odor compounds in waste gas emissions from agricultural operations and food industries. *Waste Management* 25(9):887-907.

Rich, J. J., R. S. Heichen, P. J. Bottomley, K. Cromack, and D. D. Myrold. 2003. Community composition and functioning of denitrifying bacteria from adjacent meadow and forest soils. *Applied and Environmental Microbiology* 69(10):5974-5982.

Ro, K. S., L. L. McConnell, M. H. Johnson, P. G. Hunt, and D. Parker. 2008. Livestock air treatment using PVA-coated powdered activated carbon biofilter. *Applied Engineering in Agriculture* 24(6):791-798.

Robert, M. J., T. L. Funk, J. M. Appleford, and Y. Chen. 2005. Moisture sensing methods for biofilters treating exhaust air from livestock buildings. St. Joseph, Mich.

Rodriguez, M. B., A. Godeas, and R. S. Lavado. 2008. Soil Acidity Changes in Bulk Soil and Maize Rhizosphere in Response to Nitrogen Fertilization. *Communications in Soil Science and Plant Analysis* 39(17-18):2597-2607.

Rosenkranz, P., N. Bruggemann, H. Papen, Z. Xu, G. Seufert, and K. Butterbach-Bahl. 2006. N2O, NO and CH4 exchange, and microbial N turnover over a Mediterranean pine forest soil. *Biogeosciences* 3(2):121-133.

Ryu, H. W., K. S. Cho, and T. H. Lee. 2011. Reduction of ammonia and volatile organic compounds from food waste-composting facilities using a novel anti-clogging biofilter system. *Bioresource Technology* 102(7):4654-4660.

Sadaka, S., C. R. Magura, and D. D. Mann. 2002. Vertical and horizontal airflow characteristics of wood/compost mixtures. *Applied Engineering in Agriculture* 18(6):735-741.

Sakano, Y., and L. Kerkhof. 1998. Assessment of changes in microbial community structure during operation of an ammonia biofilter with molecular tools. *Applied and Environmental Microbiology* 64(12):4877-4882.

Sakuma, T., S. Jinsiriwanit, T. Hattori, and M. A. Deshusses. 2008. Removal of ammonia from contaminated air in a biotrickling filter - Denitrifying bioreactor combination system. *Water Research* 42(17):4507-4513.

Sales, G. T., G. B. Day, and R. S. Gates. 2008. Assessment of Different Biofilter Media Particle Sizes for Ammonia Removal Optimization. St. Joseph, MI.

Saliling, W. J. B., P. W. Westerman, and T. M. Losordo. 2007. Wood chips and wheat straw as alternative biofilter media for denitrification reactors treating aquaculture and other wastewaters with high nitrate concentrations. *Aquacultural Engineering* 37(3):222-233.

Schmidt, D., K. A. Janni, and R. E. Nicolai. 2004a. Biofilter Design Information. In *Biosystems and Agricultural Engineering Update*. University of Minnesota Extension.

Schmidt, D., K. A. Janni, and R. E. Nicolai. 2004b. Biofilter design information. BAEU-18: Biosystems and Agricultural Engineering Department, University of Minnesota.

Seedorf, J. 2004. Environmental impact of airborne pollutants from livestock operations. *Stocarstvo* 58(2).

Shah, S. B., T. J. Basden, and D. K. Bhumbla. 2003. Bench-scale biofilter for removing ammonia from poultry house exhaust. *Journal of Environmental Science and Health Part B-Pesticides Food Contaminants and Agricultural Wastes* 38(1):89-101.

Souri, M. K. 2010. Effectiveness of Chloride Compared to 3,4-Dimethylpyrazole Phosphate on Nitrification Inhibition in Soil. *Communications in Soil Science and Plant Analysis* 41(14):1769-1778.

Stein, L. Y., and Y. L. Yung. 2003. Production, isotopic composition, and atmospheric fate of biologically produced nitrous oxide. *Annual Review of Earth and Planetary Sciences* 31:329-356.

Sun, Y. M., X. Quan, J. W. Chen, F. L. Yang, D. M. Xue, Y. H. Liu, and Z. H. Yang. 2002. Toluene vapour degradation and microbial community in biofilter at various moisture content. *Process Biochemistry* 38(1):109-113.

Sunesson, A. L., J. Gullberg, and G. Blomquist. 2001. Airborne chemical compounds on dairy farms. *Journal of Environmental Monitoring* 3(2):210-216.

Swanson, W. J., and R. C. Loehr. 1997. Biofiltration: Fundamentals, design and operations principles, and applications. *Journal of Environmental Engineering-Asce* 123(6):538-546.

Szukics, U., G. C. J. Abell, V. Hodl, B. Mitter, A. Sessitsch, E. Hackl, and S. Zechmeister-Boltenstern. 2010. Nitrifiers and denitrifiers respond rapidly to changed moisture and increasing temperature in a pristine forest soil. *Fems Microbiology Ecology* 72(3):395-406.

Taghipour, H., M. R. Shahmansoury, B. Bina, and H. Movahdian. 2008. Operational parameters in biofiltration of ammonia-contaminated air streams using compost-pieces of hard plastics filter media. *Chemical Engineering Journal* 137(2):198-204.

Taketani, R. G., N. O. Franco, A. S. Rosado, and J. D. van Elsas. 2010. Microbial Community Response to a Simulated Hydrocarbon Spill in Mangrove Sediments. *Journal of Microbiology* 48(1):7-15.

Tallec, G., J. Garnier, and M. Gousailles. 2006. Nitrogen removal in a wastewater treatment plant through biofilters: nitrous oxide emissions during nitrification and denitrification. *Bioprocess and Biosystems Engineering* 29(5-6):323-333.

Thornpson, W. H., P. B. Leege, P. Millner, and M. E. Watson. 2002. Test methods for the examination of composting and compost. U. S. C. C. U. S. a. D. o. Agriculture, ed. Washington, DC: U.S. Government Printing Office.

Throback, I. N., K. Enwall, A. Jarvis, and S. Hallin. 2004. Reassessing PCR primers targeting nirS, nirK and nosZ genes for community surveys of denitrifying bacteria with DGGE. *Fems Microbiology Ecology* 49(3):401-417.

Tiitta, M., and H. Olkkonen. 2002. Electrical impedance spectroscopy device for measurement of moisture gradients in wood. *Review of Scientific Instruments* 73(8):3093-3100.

Titta, M., L. Tomppo, and R. Lappalainen. 2011. Electrical impedance spectroscopy and acoustic emission methods for analyses of forest residuals and wood chips. In *9th international conference on electromagnetic wave interaction with water & moist substances.* Kansas City, MO.

USEPA. 2004a. Emissions from animal feeding operations. Available at: http://www.epa.gov/ttn/chief/ap42/ch09/draft/draftanimalfeed.pdf.

USEPA. 2004b. National emission inventory-ammonia emissions from animal husbandry operations.

USEPA. 2005. Animal Feeding Operations Air Agreements. *http://www.epa.gov/compliance/resources/agreements/caa/cafo-agr.html*.

Valentin-Vargas, A., G. Toro-Labrador, and A. A. Massol-Deya. 2012. Bacterial Community Dynamics in Full-Scale Activated Sludge Bioreactors: Operational and Ecological Factors Driving Community Assembly and Performance. *Plos One* 7(8).

Van Nostrand, J. D., L. Y. Wu, W. M. Wu, Z. J. Huang, T. J. Gentry, Y. Deng, J. Carley, S. Carroll, Z. L. He, B. H. Gu, J. Luo, C. S. Criddle, D. B. Watson, P. M. Jardine, T. L. Marsh, J. M. Tiedje, T. C. Hazen, and J. Z. Zhou. 2011. Dynamics of Microbial Community Composition and Function during In Situ Bioremediation of a Uranium-Contaminated Aquifer (vol 77, pg 3860, 2011). *Applied and Environmental Microbiology* 77(14):5063-5063.

VanLith, C., G. Leson, and R. Michelsen. 1997. Evaluating design options for biofilters. *Journal of the Air & Waste Management Association* 47(1):37-48.

Venables, W. N., and B. D. Ripley. 2008. *Modern applied statistics with S (statistics and computing).* Springer.

Venterea, R. T., P. M. Groffman, L. V. Verchot, A. H. Magill, J. D. Aber, and P. A. Steudler. 2003. Nitrogen oxide gas emissions from temperate forest soils receiving long-term nitrogen inputs. *Global Change Biology* 9(3):346-357.

Villaverde, S., F. Fdz-Polanco, and P. A. Garcia. 2000. Nitrifying biofilm acclimation to free ammonia in submerged biofilters. Start-up influence. *Water Research* 34(2):602-610.

Wallenstein, M. D., D. D. Myrold, M. Firestone, and M. Voytek. 2006. Environmental controls on denitrifying communities and denitrification rates: Insights from molecular methods. *Ecological Applications* 16(6):2143-2152.

Wang, X., X. Wen, C. Criddle, H. Yan, Y. Zhang, and K. Ding. 2010. Bacterial community dynamics in two full-scale wastewater treatment systems with functional stability. *Journal of Applied Microbiology* 109(4):1218-1226.

Webster, T. S. 1996. Control of air emissions from publicly owned treatment works using biological filtration. University of Southern California, Los Angeles, Calif

Well, R., I. Kurganova, V. L. de Gerenyu, and H. Flessa. 2006. Isotopomer signatures of soil-emitted N2O under different moisture conditions - A microcosm study with arable loess soil. *Soil Biology & Biochemistry* 38(9):2923-2933.

Weslien, P., A. K. Klemedtsson, G. Borjesson, and L. Klemedtsson. 2009. Strong pH influence on N2O and CH4 fluxes from forested organic soils. *European Journal of Soil Science* 60(3):311-320.

Wheeler, E. F., K. D. Casey, R. S. Gates, H. Xin, J. L. Zajaczkowski, P. A. Topper, Y. Liang, and A. J. Pescatore. 2006. Ammonia emissions from twelve US broiler chicken houses. *Transactions of the Asabe* 49(5):1495-1512.

Wijler, J., and C. C. Delwiche. 1954. Investigations on the Denitrifying Process in Soil. *Plant and Soil* 5(2):155-169.

Xia, S. Q., J. X. Li, R. C. Wang, J. Y. Li, and Z. Q. Zhang. 2010. Tracking composition and dynamics of nitrification and denitrification microbial community in a biofilm reactor by PCR-DGGE and combining FISH with flow cytometry. *Biochemical Engineering Journal* 49(3):370-378.

Yang, L., X. Wang, T. L. Funk, and R. S. Gates. 2011. Biofilter Media Characterization and Airflow Resistance Test. *Transactions of the Asabe* 54(3):1127-1136.

Yang, L., X. Wang, T. L. Funk, R. S. Gates, and Y. Zhang. 2012. Transport and fate of nitrogen-containing compounds in gas-phase biofilters: a swing test to mitigate ammonia. *Trans. ASABE* 55(5):8.

Yang, Y. H., and E. R. Allen. 1994. BIOFILTRATION CONTROL OF HYDROGEN-SULFIDE .1. DESIGN AND OPERATIONAL PARAMETERS. *Journal of the Air & Waste Management Association* 44(7):863-868.

Yannarell, A. C., R. R. Busby, M. L. Denight, D. L. Gebbart, and S. Taylor. 2011. Soil bacteria and fungi respond on different spatial scales to invasion by the legume *Lespedeza cunneata*. *Frontiers in Microbiology* 2.

Yasuda, T., K. Kuroda, Y. Fukumoto, D. Hanajima, and K. Suzuki. 2009. Evaluation of full-scale biofilter with rockwool mixture treating ammonia gas from livestock manure composting. *Bioresource Technology* 100(4):1568-1572.

Yasuda, T., K. Kuroda, D. Hanajima, Y. Fukumoto, M. Waki, and K. Suzuki. 2010. Characteristics of the Microbial Community Associated with Ammonia Oxidation in a Full-Scale Rockwool Biofilter Treating Malodors from Livestock Manure Composting. *Microbes and Environments* 25(2):111-119.

Yin, J., and W. F. Xu. 2009. Ammonia biofiltration and community analysis of ammonia-oxidizing bacteria in biofilters. *Bioresource Technology* 100(17):3869-3876.

Yudelson, J. M. 1996. The future of the U.S. biofiltration industry. In *Conference on Biofiltration*. Tustin, CA: The Reynolds Group.

Zeisig, H. D., and T. U. Munchen. 1987. Experiences with the use of biofilters to remove odours from piggeries and hen hourses. In *Volatile Emissions from Livestock Farming and Sewage Operations*, 209-216. N. V.C., J. H. Voorburg, and P. L. Hermite, eds. New York: Elsvier Science Publishers.

Zelinka, S. L., D. R. Rammer, and D. S. Stone. 2008. Impedance spectroscopy and circuit modeling of Southern pine above 20% moisture content. *Holzforschung* 62(6):737-744.

Zhu, J. 2000. A review of microbiology in swine manure odor control. *Agriculture Ecosystems & Environment* 78(2):93-106.

Zumft, W. G. 1993. The Biological Role of Nitric-Oxide in Bacteria. *Archives of Microbiology* 160(4):253-264.

APPENDIX A: SUPPLEMENTARY INFORMATION FOR CHAPTER 3

A1- Moisture and compaction effects on airflow resistance- all results.

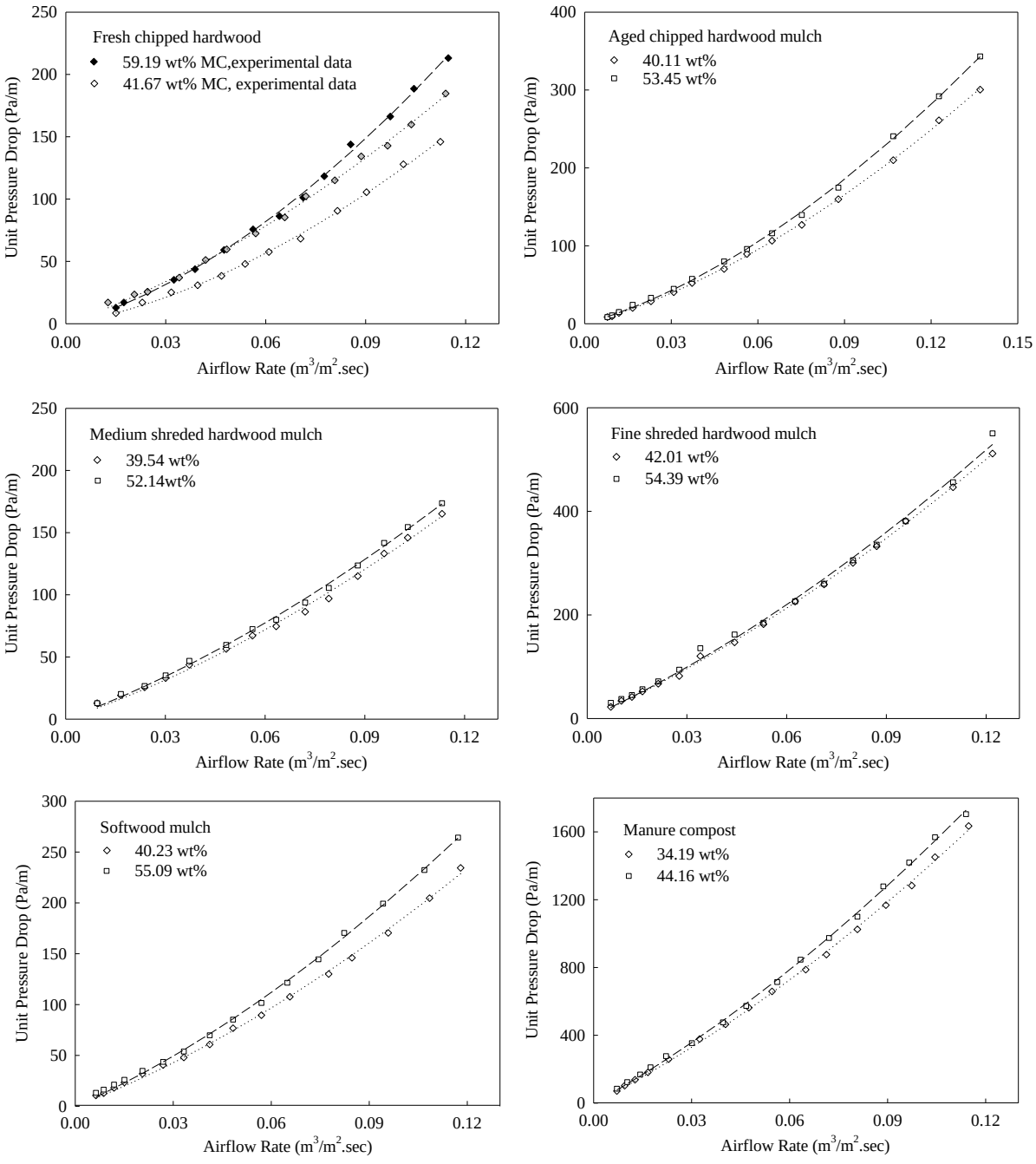

Figure A.1 The effect of moisture, compaction on airflow resistance.

Continue.

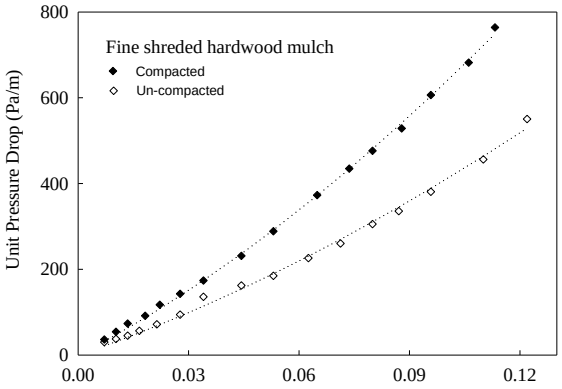
Fine shreded hardwood mulch
Compacted
Un-compacted
Unit Pressure Drop (Pa/m)
800
600
400
200
0
0.00
0.03
0.06
0.09
0.12

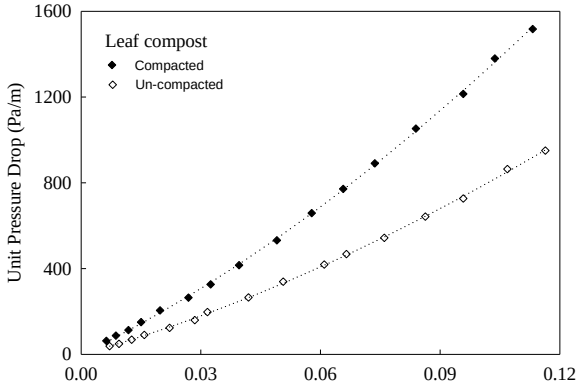
Leaf compost
Compacted
Un-compacted
Unit Pressure Drop (Pa/m)
1600
1200
800
400
0
0.00
0.03
0.06
0.09
0.12

A2- Airflow resistance test results.

Table A-1 Airflow resistance: Fresh chipped hardwood mulch.

airflow rate, m/s	measured pressure drop, Pa	unit pressure drop, Pa/m	measured pressure drop, Pa	unit pressure drop, Pa/m	measured pressure drop, Pa	unit pressure drop, Pa/m	measured pressure drop, Pa	unit pressure drop, Pa/m
Fresh chipped hardwood mulch, 41.7%wb								
	58.4cm		45.7 cm		33.0cm		20.3cm	
0.0150	4.98	8.52						
0.0230	9.96	17.05	4.98	10.89				
0.0317	14.69	25.15	9.96	21.78	4.98	15.08		
0.0396	18.05	30.90	13.70	29.95	7.47	22.62	4.98	24.51
0.0467	22.41	38.36	17.43	38.12	11.21	33.93	6.23	30.63
0.0538	28.01	47.95	19.92	43.57	13.70	41.47	7.47	36.76
0.0610	33.62	57.54	23.66	51.74	16.19	49.02	8.72	42.89
0.0705	39.84	68.20	26.15	57.19	18.68	56.56	9.96	49.02
0.0815	52.91	90.57	39.84	87.14	22.41	67.87	13.70	67.40
0.0903	61.63	105.49	44.82	98.03	27.39	82.95	16.19	79.65
0.1013	74.70	127.87	52.29	114.37	33.62	101.80	18.68	91.90
0.1124	85.28	145.98	59.76	130.71	38.60	116.88	21.17	104.16
Fresh chipped hardwood mulch, 55.0%wb								
	58.4cm		45.7 cm		33.0cm		20.3cm	
0.0127	9.96	17.05						
0.0206	13.70	23.44	11.21	24.51	6.23	18.85		
0.0245	14.94	25.57	11.21	24.51	7.47	22.62		
0.0340	21.58	36.94	18.68	40.85	11.21	33.93	7.47	36.76
0.0420	29.88	51.15	23.66	51.74	16.19	49.02	8.72	42.89
0.0483	34.86	59.67	24.90	54.46	18.68	56.56	9.96	49.02
0.0570	42.33	72.46	32.37	70.80	22.41	67.87	12.45	61.27
0.0657	49.80	85.24	38.60	84.42	26.15	79.18	13.70	67.40
0.0720	59.76	102.29	44.82	98.03	27.39	82.95	14.94	73.52
0.0808	67.23	115.08	49.80	108.92	34.86	105.57	17.43	85.78
0.0887	78.44	134.26	56.03	122.54	38.60	116.88	18.68	91.90
0.0966	83.42	142.79	62.25	136.15	41.09	124.42	19.92	98.03
0.1037	93.38	159.83	68.48	149.77	42.33	128.20	21.17	104.16
0.1140	107.90	184.70	78.44	171.56	49.80	150.82	22.41	110.29
Fresh chipped hardwood mulch, 59.2%wb								
	58.4cm		45.7 cm		33.0cm		20.3cm	
0.0150	7.47	12.79	7.47	16.34	4.98	15.08	2.49	12.25
0.0174	9.96	17.05	9.96	21.78	7.47	22.62	4.36	21.44
0.0245	14.94	25.57	14.94	32.68	9.96	30.16	4.98	24.51
0.0325	20.54	35.16	19.92	43.57	13.70	41.47	7.47	36.76
0.0388	25.52	43.69	26.15	57.19	17.43	52.79	10.58	52.08
0.0475	34.55	59.14	32.37	70.80	22.41	67.87	13.07	64.33
0.0562	44.20	75.65	39.84	87.14	27.39	82.95	14.94	73.52
0.0641	50.42	86.31	44.82	98.03	28.64	86.72	16.19	79.65
0.0713	59.14	101.23	49.80	108.92	34.24	103.69	21.79	107.22
0.0776	69.10	118.28	59.76	130.71	39.84	120.65	21.17	104.16
0.0855	84.04	143.85	70.97	155.22	47.31	143.28	27.39	134.79
0.0974	97.11	166.23	79.68	174.28	53.54	162.13	31.13	153.17
0.1045	110.18	188.60	92.13	201.51	61.01	184.75	33.62	165.43
0.1148	124.50	213.11	7.47	16.34	4.98	15.08	2.49	12.25

Table A-2 Airflow resistance: Aged chipped hardwood mulch.

airflow rate, m/s	measured pressure drop, Pa	unit pressure drop, Pa/m	measured pressure drop, Pa	unit pressure drop, Pa/m	measured pressure drop, Pa	unit pressure drop, Pa/m	measured pressure drop, Pa	unit pressure drop, Pa/m
Aged chipped hardwood mulch, 40.1% wb								
	58.4cm		45.7 cm		33.0cm		20.3cm	
0.0079	4.98	8.52	2.49	5.45				
0.0095	5.60	9.59	4.98	10.89	2.49	7.54	1.00	4.90
0.0119	8.09	13.85	6.23	13.62	3.74	11.31	2.12	10.42
0.0166	11.83	20.25	8.72	19.06	6.23	18.85	3.36	16.54
0.0230	16.81	28.77	12.45	27.23	7.47	22.62	4.98	24.51
0.0309	23.66	40.49	17.43	38.12	11.21	33.93	6.23	30.63
0.0372	30.50	52.21	21.17	46.29	14.94	45.25	7.47	36.76
0.0483	41.09	70.33	28.64	62.63	19.92	60.33	11.21	55.14
0.0562	52.29	89.51	36.11	78.97	23.66	71.64	12.45	61.27
0.0649	62.25	106.56	44.82	98.03	28.64	86.72	14.94	73.52
0.0752	74.08	126.80	54.78	119.82	33.62	101.80	18.68	91.90
0.0879	93.38	159.83	69.72	152.49	44.82	135.74	22.41	110.29
0.1069	122.63	209.92	90.89	198.79	53.54	162.13	29.88	147.05
0.1227	152.51	261.06	109.56	239.63	70.97	214.92	34.86	171.56
0.1370	175.55	300.49	124.50	272.31	78.44	237.54	41.09	202.19
Aged chipped hardwood mulch, 53.4% wb								
	58.4cm		45.7 cm		33.0cm		20.3cm	
0.0079	4.98	8.52	2.49	5.45				
0.0095	6.23	10.66	5.73	12.53	2.49	7.54	1.25	6.13
0.0119	8.72	14.92	7.47	16.34	4.98	15.08	2.49	12.25
0.0166	14.13	24.19	10.46	22.87	8.09	24.51	4.61	22.67
0.0230	19.42	33.25	15.06	32.95	9.96	30.16	5.10	25.12
0.0309	26.15	44.75	21.17	46.29	14.94	45.25	7.47	36.76
0.0372	33.62	57.54	24.90	54.46	17.43	52.79	8.72	42.89
0.0483	46.69	79.92	34.86	76.25	21.17	64.10	11.21	55.14
0.0562	56.03	95.90	39.84	87.14	26.15	79.18	13.70	67.40
0.0649	67.85	116.15	49.80	108.92	31.13	94.26	14.94	73.52
0.0752	81.55	139.59	62.25	136.15	39.84	120.65	19.92	98.03
0.0879	102.09	174.75	78.44	171.56	48.56	147.05	24.65	121.31
0.1069	140.56	240.60	107.07	234.19	64.74	196.06	34.86	171.56
0.1227	170.57	291.96	128.24	280.48	82.17	248.85	41.09	202.19
0.1370	200.45	343.11	149.40	326.77	95.87	290.32	48.56	238.95

Table A-3 Airflow resistance: Softwood mulch.

airflow rate, m/s	measured pressure drop, Pa	unit pressure drop, Pa/m	measured pressure drop, Pa	unit pressure drop, Pa/m	measured pressure drop, Pa	unit pressure drop, Pa/m	measured pressure drop, Pa	unit pressure drop, Pa/m
softwood mulch, 40.2% wb								
	58.4cm		45.7 cm		33.0cm		20.3cm	
0.0063	6.23	10.66	4.98	10.89	3.74	11.31	2.49	12.25
0.0087	7.47	12.79	6.23	13.62	4.61	13.95	3.24	15.93
0.0119	10.58	18.11	8.09	17.70	5.60	16.97	3.74	18.38
0.0150	13.70	23.44	9.96	21.78	7.47	22.62	4.98	24.51
0.0206	18.68	31.97	13.70	29.95	8.72	26.39	6.85	33.70
0.0269	23.66	40.49	17.43	38.12	12.45	37.70	7.47	36.76
0.0333	28.01	47.95	21.17	46.29	14.94	45.25	8.72	42.89
0.0412	35.48	60.74	26.15	57.19	17.43	52.79	9.96	49.02
0.0483	44.82	76.72	32.37	70.80	21.17	64.10	11.21	55.14
0.0570	52.29	89.51	39.84	87.14	23.66	71.64	13.70	67.40
0.0657	62.87	107.62	44.82	98.03	26.15	79.18	14.94	73.52
0.0776	75.95	130.00	53.54	117.09	31.13	94.26	17.43	85.78
0.0847	85.28	145.98	63.50	138.88	38.60	116.88	21.17	104.16
0.0958	99.60	170.49	73.46	160.66	47.31	143.28	23.66	116.41
0.1085	119.52	204.59	87.15	190.62	53.54	162.13	28.64	140.92
0.1180	136.95	234.42	100.85	220.57	57.27	173.44	31.13	153.17
softwood mulch, 55.1% wb								
	58.4cm		45.7 cm		33.0cm		20.3cm	
0.0063	7.72	13.21	5.35	11.71	4.73	14.33	3.49	17.16
0.0087	9.59	16.41	8.09	17.70	5.35	16.21	3.36	16.54
0.0119	12.45	21.31	9.71	21.24	5.10	15.46	3.98	19.61
0.0150	15.19	26.00	10.71	23.42	8.34	25.26	4.73	23.28
0.0206	20.36	34.84	15.56	34.04	10.21	30.92	5.85	28.80
0.0269	25.52	43.69	19.92	43.57	13.07	39.59	7.47	36.76
0.0333	31.44	53.81	24.90	54.46	14.94	45.25	8.84	43.50
0.0412	40.77	69.79	29.88	65.35	19.92	60.33	10.21	50.24
0.0483	49.80	85.24	37.35	81.69	23.66	71.64	13.20	64.95
0.0570	59.32	101.55	44.32	96.94	26.64	80.69	14.94	73.52
0.0649	70.97	121.47	50.05	109.47	27.39	82.95	16.31	80.26
0.0744	84.41	144.49	60.38	132.07	35.98	108.97	19.42	95.58
0.0823	99.60	170.49	72.21	157.94	44.82	135.74	23.66	116.41
0.0942	116.41	199.26	87.15	190.62	54.78	165.90	28.64	140.92
0.1069	135.71	232.29	98.36	215.12	59.76	180.98	31.50	155.01
0.1172	154.38	264.26	113.30	247.80	67.23	203.60	34.86	171.56

Table A-4 Airflow resistance: Medium shredded hardwood mulch.

airflow rate, m/s	measured pressure drop, Pa	unit pressure drop, Pa/m	measured pressure drop, Pa	unit pressure drop, Pa/m	measured pressure drop, Pa	unit pressure drop, Pa/m	measured pressure drop, Pa	unit pressure drop, Pa/m
Medium shredded hardwood mulch, 39.5%wb, un-compacted								
	58.4cm		45.7 cm		33.0cm		20.3cm	
0.0095	7.47	12.79						
0.0166	11.21	19.18	7.47	16.34	4.98	15.08		
0.0238	14.94	25.57	12.45	27.23	9.96	30.16		
0.0301	19.30	33.03	13.70	29.95	9.96	30.16	6.23	30.63
0.0372	25.52	43.69	18.68	40.85	13.70	41.47	8.72	42.89
0.0483	32.99	56.47	23.66	51.74	17.43	52.79	9.96	49.02
0.0562	39.22	67.13	31.13	68.08	22.41	67.87	13.70	67.40
0.0633	43.58	74.59	32.37	70.80	24.90	75.41	14.94	73.52
0.0720	50.42	86.31	37.35	81.69	26.15	79.18	16.19	79.65
0.0792	56.65	96.97	41.09	89.86	31.13	94.26	18.68	91.90
0.0879	67.23	115.08	48.56	106.20	34.86	105.57	21.17	104.16
0.0958	77.81	133.19	56.03	122.54	41.09	124.42	23.66	116.41
0.1029	85.28	145.98	63.50	138.88	47.31	143.28	26.15	128.67
0.1132	96.49	165.16	72.21	157.94	52.29	158.36	31.13	153.17
Medium shredded hardwood mulch, 52.1%wb, un-compacted								
	58.4cm		45.7 cm		33.0cm		20.3cm	
0.0095	7.47	12.79						
0.0166	11.83	20.25	8.72	19.06	4.98	15.08		
0.0238	15.56	26.64	13.70	29.95	9.96	30.16		
0.0301	20.54	35.16	14.94	32.68	11.21	33.93	6.23	30.63
0.0372	27.39	46.88	19.92	43.57	14.94	45.25	9.96	49.02
0.0483	34.86	59.67	26.15	57.19	19.92	60.33	12.45	61.27
0.0562	42.33	72.46	33.62	73.52	24.90	75.41	14.94	73.52
0.0633	46.69	79.92	34.86	76.25	26.15	79.18	16.19	79.65
0.0720	54.78	93.77	39.84	87.14	29.88	90.49	19.92	98.03
0.0792	61.63	105.49	46.07	100.75	34.36	104.06	21.17	104.16
0.0879	72.21	123.60	54.78	119.82	38.60	116.88	23.66	116.41
0.0958	82.79	141.72	62.25	136.15	44.82	135.74	26.15	128.67
0.1029	90.26	154.51	68.48	149.77	51.05	154.59	28.64	140.92
0.1132	101.47	173.69	75.95	166.11	56.03	169.67	34.86	171.56
Medium shredded hardwood mulch, 52.1%wb, compacted								
	58.4cm		45.7 cm		33.0cm		20.3cm	
0.0095	7.47	12.79						
0.0127	12.45	21.31	8.72	19.06				
0.0158	14.44	24.72	11.21	24.51				
0.0198	18.68	31.97	11.21	24.51				
0.0261	23.66	40.49	18.68	40.85	13.70	41.47	8.72	42.89
0.0317	28.01	47.95	21.17	46.29	16.19	49.02	9.96	49.02
0.0388	34.86	59.67	26.15	57.19	19.92	60.33	13.70	67.40
0.0459	41.71	71.39	31.13	68.08	24.90	75.41	14.94	73.52
0.0538	51.05	87.38	39.84	87.14	27.39	82.95	19.92	98.03
0.0633	61.63	105.49	46.07	100.75	36.11	109.34	22.41	110.29
0.0728	74.08	126.80	56.03	122.54	42.33	128.20	27.39	134.79
0.0815	85.28	145.98	65.99	144.32	49.80	150.82	33.62	165.43
0.0895	98.36	168.36	74.70	163.39	57.27	173.44	36.11	177.68
0.0974	112.05	191.80	83.42	182.45	62.25	188.52	39.84	196.06
0.1077	128.24	219.51	95.87	209.68	70.97	214.92	43.58	214.44

Table A-5 Airflow resistance: Fine shredded hardwood mulch.

airflow rate, m/s	measured pressure drop, Pa	unit pressure drop, Pa/m	measured pressure drop, Pa	unit pressure drop, Pa/m	measured pressure drop, Pa	unit pressure drop, Pa/m	measured pressure drop, Pa	unit pressure drop, Pa/m
Fine shredded hardwood mulch, 42.0%wb, un-compacted								
	58.4cm		45.7 cm		33.0cm		20.3cm	
0.0071	13.07	22.38	9.96	21.78	8.72	26.39	6.23	30.63
0.0103	19.92	34.10	13.70	29.95	11.21	33.93	7.47	36.76
0.0135	24.28	41.56	17.43	38.12	13.70	41.47	8.72	42.89
0.0166	30.50	52.21	22.41	49.02	17.43	52.79	9.96	49.02
0.0214	39.22	67.13	28.64	62.63	21.17	64.10	13.70	67.40
0.0277	47.93	82.05	37.35	81.69	26.15	79.18	17.43	85.78
0.0340	70.34	120.41	51.05	111.65	38.60	116.88	23.66	116.41
0.0443	85.91	147.05	62.25	136.15	48.56	147.05	27.39	134.79
0.0530	106.45	182.21	73.46	160.66	54.78	165.90	31.13	153.17
0.0625	131.97	225.90	92.13	201.51	65.99	199.83	38.60	189.94
0.0713	151.27	258.93	102.09	223.29	75.95	230.00	46.07	226.70
0.0800	175.55	300.49	125.75	275.03	93.38	282.78	51.05	251.21
0.0871	194.22	332.45	141.93	310.43	104.58	316.72	56.03	275.71
0.0958	222.86	381.47	156.87	343.11	117.03	354.42	64.74	318.60
0.1100	260.83	446.47	192.98	422.08	138.20	418.52	72.21	355.36
0.1219	298.80	511.47	226.59	495.60	158.12	478.85	78.44	386.00
Fine shredded hardwood mulch, 54.4%wb, un-compacted								
	58.4cm		45.7 cm		33.0cm		20.3cm	
0.0071	16.19	27.70	12.45	27.23	9.96	30.16	7.47	36.76
0.0103	21.79	37.29	14.94	32.68	12.45	37.70	8.72	42.89
0.0135	26.77	45.82	19.92	43.57	14.94	45.25	9.96	49.02
0.0166	34.24	58.61	24.90	54.46	18.68	56.56	11.21	55.14
0.0214	44.20	75.65	32.37	70.80	23.66	71.64	14.94	73.52
0.0277	53.54	91.64	42.33	92.59	31.13	94.26	19.92	98.03
0.0340	79.68	136.39	59.76	130.71	44.82	135.74	27.39	134.79
0.0443	93.38	159.83	69.72	152.49	53.54	162.13	32.37	159.30
0.0530	115.79	198.19	84.66	185.17	61.01	184.75	37.35	183.81
0.0625	142.55	244.01	103.34	226.02	74.70	226.23	46.07	226.70
0.0713	165.59	283.44	114.54	250.52	85.91	260.16	49.80	245.08
0.0800	192.35	329.26	144.42	315.88	100.85	305.41	57.27	281.84
0.0871	211.03	361.22	156.87	343.11	110.81	335.57	61.01	300.22
0.0958	240.29	411.31	176.79	386.68	125.75	380.81	73.46	361.49
0.1100	292.58	500.81	212.90	465.65	150.65	456.22	83.42	410.51
0.1219	354.20	606.30	256.47	560.96	181.77	550.48	99.60	490.16
Fine shredded hardwood mulch,54.4%wb, compacted								
	58.4cm		45.7 cm		33.0cm		20.3cm	
0.0071	21.17	36.23	16.19	35.40	14.94	45.25	9.96	49.02
0.0103	31.75	54.34	24.90	54.46	21.17	64.10	14.94	73.52
0.0135	42.95	73.52	34.86	76.25	24.90	75.41	18.68	91.90
0.0182	53.54	91.64	44.82	98.03	34.86	105.57	24.90	122.54
0.0222	68.48	117.21	52.29	114.37	42.33	128.20	29.88	147.05
0.0277	83.42	142.79	65.99	144.32	52.29	158.36	37.35	183.81
0.0340	101.47	173.69	79.68	174.28	63.50	192.29	42.33	208.32
0.0443	135.08	231.23	109.56	239.63	87.15	263.93	58.52	287.97
0.0530	168.70	288.77	133.22	291.37	105.83	320.49	69.72	343.11
0.0649	217.88	372.95	175.55	383.96	139.44	422.29	92.13	453.40
0.0736	253.98	434.75	202.94	443.86	163.10	493.93	104.58	514.67
0.0800	278.26	476.31	224.10	490.16	175.55	531.63	113.30	557.55
0.0879	308.76	528.52	250.25	547.34	199.20	603.27	129.48	637.20

Continue.

0.0958	354.20	606.30	286.35	626.31	229.08	693.76	146.91	722.98
0.1061	398.40	681.96	312.50	683.50	246.51	746.55	161.85	796.51
0.1132	446.33	764.01	352.34	770.64	273.90	829.50	176.79	870.03

Table A-6 Airflow resistance: Manure compost.

airflow rate, m/s	measured pressure drop, Pa	unit pressure drop, Pa/m	measured pressure drop, Pa	unit pressure drop, Pa/m	measured pressure drop, Pa	unit pressure drop, Pa/m	measured pressure drop, Pa	unit pressure drop, Pa/m
Manure compost, 34.2% wb								
	58.4cm		45.7 cm		33.0cm		20.3cm	
0.0071	41.71	71.39	27.39	59.91	17.43	52.79	9.96	49.02
0.0095	59.76	102.29	43.58	95.31	29.88	90.49	14.94	73.52
0.0127	80.30	137.46	56.03	122.54	39.84	120.65	19.92	98.03
0.0166	105.83	181.15	75.95	166.11	49.80	150.82	27.39	134.79
0.0230	151.27	258.93	104.58	228.74	72.21	218.69	34.86	171.56
0.0325	220.99	378.27	159.36	348.56	107.07	324.26	53.54	263.46
0.0404	271.41	464.58	197.96	432.97	133.22	403.44	67.23	330.86
0.0475	328.68	562.62	240.29	525.56	163.10	493.93	83.42	410.51
0.0546	384.71	658.52	278.88	609.97	192.98	584.42	94.62	465.65
0.0649	460.03	787.45	337.40	737.96	231.57	701.30	114.54	563.68
0.0713	511.70	875.89	378.48	827.82	265.19	803.10	130.73	643.33
0.0808	598.85	1025.07	435.75	953.08	301.29	912.45	153.14	753.62
0.0895	682.26	1167.85	496.76	1086.52	342.38	1036.87	176.79	870.03
0.0974	749.49	1282.93	542.82	1187.27	380.97	1153.76	195.47	961.93
0.1045	847.85	1451.29	616.28	1347.93	422.06	1278.18	211.65	1041.58
0.1148	954.92	1634.57	694.71	1519.49	475.59	1440.31	242.78	1194.76
Manure compost, 44.2% wb								
	58.4cm		45.7 cm		33.0cm		20.3cm	
0.0071	49.80	85.24	31.13	68.08	19.92	60.33	13.70	67.40
0.0103	72.21	123.60	44.82	98.03	28.64	86.72	14.94	73.52
0.0143	98.36	168.36	59.76	130.71	36.11	109.34	21.17	104.16
0.0174	123.26	210.98	74.70	163.39	46.07	139.51	27.39	134.79
0.0222	161.85	277.05	94.62	206.96	59.76	180.98	33.62	165.43
0.0301	206.67	353.77	118.28	258.69	74.70	226.23	46.07	226.70
0.0396	278.26	476.31	173.06	378.51	107.07	324.26	61.01	300.22
0.0467	334.91	573.27	207.92	454.76	129.48	392.13	73.46	361.49
0.0562	417.08	713.93	253.98	555.51	160.61	486.39	90.89	447.27
0.0633	494.27	846.05	292.58	639.93	181.77	550.48	103.34	508.54
0.0720	568.97	973.92	333.66	729.79	210.41	637.20	120.77	594.32
0.0808	642.42	1099.66	388.44	849.61	244.02	739.01	140.69	692.35
0.0887	747.00	1278.67	444.47	972.15	276.39	837.04	159.36	784.25
0.0966	829.17	1419.33	495.51	1083.79	306.27	927.53	174.30	857.78
0.1045	916.32	1568.50	537.84	1176.38	333.66	1010.48	191.73	943.55
0.1140	996.00	1704.90	595.11	1301.64	369.77	1119.82	211.65	1041.58

Table A-7 Airflow resistance: Leaf compost.

airflow rate, m/s	measured pressure drop, Pa	unit pressure drop, Pa/m	measured pressure drop, Pa	unit pressure drop, Pa/m	measured pressure drop, Pa	unit pressure drop, Pa/m	measured pressure drop, Pa	unit pressure drop, Pa/m
Leaf compost, 51.4% wb, un-compacted								
	58.4cm		45.7 cm		33.0cm		20.3cm	
0.0071	22.41	38.36	14.94	32.68	12.45	37.70	4.98	24.51
0.0095	28.64	49.02	21.17	46.29	14.94	45.25	7.47	36.76
0.0127	39.84	68.20	29.88	65.35	19.92	60.33	11.21	55.14
0.0158	52.91	90.57	42.33	92.59	28.64	86.72	13.70	67.40
0.0222	72.21	123.60	57.27	125.26	38.60	116.88	19.92	98.03
0.0285	93.38	159.83	72.21	157.94	49.80	150.82	28.64	140.92
0.0317	115.16	197.13	85.91	187.89	59.76	180.98	32.37	159.30
0.0420	155.00	265.32	118.28	258.69	78.44	237.54	43.58	214.44
0.0507	197.96	338.85	153.14	334.94	102.09	309.18	53.54	263.46
0.0610	244.64	418.76	186.75	408.46	125.75	380.81	64.74	318.60
0.0665	273.28	467.78	211.65	462.93	143.18	433.60	72.21	355.36
0.0760	317.48	543.44	246.51	539.17	165.59	501.47	85.91	422.76
0.0863	375.37	642.53	302.54	661.71	196.71	595.73	103.34	508.54
0.0958	424.55	726.71	323.70	708.01	224.10	678.68	117.03	575.94
0.1069	504.85	864.17	398.40	871.39	258.96	784.25	134.46	661.71
0.1164	555.27	950.48	420.81	920.41	285.11	863.43	150.65	741.36
Leaf compost, 51.4% wb, compacted								
	58.4cm		45.7 cm		33.0cm		20.3cm	
0.0063	36.73	62.87	31.13	68.08	23.66	71.64	16.19	79.65
0.0087	51.05	87.38	42.33	92.59	33.62	101.80	23.66	116.41
0.0119	65.99	112.95	53.54	117.09	43.58	131.97	28.64	140.92
0.0150	87.77	150.24	72.21	157.94	58.52	177.21	39.84	196.06
0.0198	119.52	204.59	99.60	217.85	79.68	241.31	51.05	251.21
0.0269	154.38	264.26	131.97	288.65	100.85	305.41	63.50	312.48
0.0325	190.49	326.06	159.36	348.56	124.50	377.04	83.42	410.51
0.0396	242.78	415.57	206.67	452.03	158.12	478.85	103.34	508.54
0.0491	310.63	531.71	262.70	574.57	204.18	618.35	129.48	637.20
0.0578	384.71	658.52	323.70	708.01	251.49	761.63	161.85	796.51
0.0657	450.69	771.47	380.97	833.27	292.58	886.05	190.49	937.43
0.0736	520.41	890.81	439.49	961.25	323.70	980.31	219.12	1078.35
0.0839	615.03	1052.77	519.17	1135.53	399.65	1210.31	255.23	1256.03
0.0958	709.65	1214.74	591.38	1293.47	451.94	1368.67	291.33	1433.71
0.1037	806.14	1379.90	672.30	1470.47	509.21	1542.11	331.17	1629.77
0.1132	886.44	1517.36	739.53	1617.52	565.23	1711.78	363.54	1789.07

Table A-8 Airflow resistance: Manure compost mixtures.

airflow rate, m/s	measured pressure drop, Pa	unit pressure drop, Pa/m	measured pressure drop, Pa	unit pressure drop, Pa/m	measured pressure drop, Pa	unit pressure drop, Pa/m	measured pressure drop, Pa	unit pressure drop, Pa/m
manure compost and fine shredded hardwood mulch mixture, 54.7%wb								
	58.4cm		45.7 cm		33.0cm		20.3cm	
0.0063	58.52	100.16	34.86	76.25	21.17	64.10	7.47	36.76
0.0150	94.62	161.97	54.78	119.82	36.11	109.34	14.94	73.52
0.0222	130.73	223.77	77.19	168.83	47.31	143.28	22.41	110.29
0.0293	180.53	309.01	120.77	264.14	63.50	192.29	32.37	159.30
0.0372	237.80	407.04	150.65	329.49	85.91	260.16	39.84	196.06
0.0443	283.86	485.90	188.00	411.19	110.81	335.57	51.05	251.21
0.0515	344.87	590.32	225.35	492.88	119.52	361.96	59.76	294.09
0.0594	408.36	699.01	260.21	569.13	156.87	475.08	70.97	349.24
0.0673	470.61	805.56	311.25	680.77	174.30	527.86	79.68	392.13
0.0760	540.33	924.91	341.13	746.13	204.18	618.35	92.13	453.40
0.0839	597.60	1022.94	402.14	879.56	234.06	708.84	105.83	520.79
0.0903	692.22	1184.90	451.94	988.48	262.70	795.56	122.01	600.44
0.0982	761.94	1304.25	486.80	1064.73	285.11	863.43	130.73	643.33
0.1053	841.62	1440.64	551.54	1206.33	303.78	919.99	145.67	716.86
0.1093	864.03	1479.00	566.48	1239.01	326.19	987.86	150.65	741.36
manure compost and medium shredded hardwood mulch mixture, 52.0%wb								
	58.4cm		45.7 cm		33.0cm		20.3cm	
0.0071	28.64	49.02	18.68	40.85	11.21	33.93	6.23	30.63
0.0103	46.07	78.85	26.15	57.19	18.68	56.56	9.96	49.02
0.0135	73.46	125.74	41.09	89.86	24.90	75.41	14.94	73.52
0.0182	93.38	159.83	53.54	117.09	36.11	109.34	22.41	110.29
0.0222	113.30	193.93	73.46	160.66	44.82	135.74	26.15	128.67
0.0317	150.65	257.87	89.64	196.06	58.52	177.21	31.13	153.17
0.0396	195.47	334.59	123.26	269.59	75.95	230.00	38.60	189.94
0.0475	232.82	398.52	149.40	326.77	93.38	282.78	49.80	245.08
0.0554	272.66	466.72	178.04	389.40	113.30	343.11	70.97	349.24
0.0633	322.46	551.96	210.41	460.20	131.97	399.67	80.93	398.25
0.0728	373.50	639.34	247.76	541.90	154.38	467.53	97.11	477.90
0.0792	414.59	709.66	273.90	599.08	173.06	524.09	104.58	514.67
0.0879	473.10	809.83	308.76	675.33	192.98	584.42	117.03	575.94
0.0966	536.60	918.51	349.85	765.19	220.37	667.37	131.97	649.46
0.1045	611.30	1046.38	384.71	841.44	247.76	750.32	144.42	710.73
0.1164	695.96	1191.30	425.79	931.30	275.15	833.27	161.85	796.51

Table A-9 Airflow resistance: Leaf compost mixtures.

airflow rate, m/s	measured pressure drop, Pa	unit pressure drop, Pa/m	measured pressure drop, Pa	unit pressure drop, Pa/m	measured pressure drop, Pa	unit pressure drop, Pa/m	measured pressure drop, Pa	unit pressure drop, Pa/m
Leaf compost and fine shredded hardwood mulch mixture, 53.3%wb								
	58.4cm		45.7 cm		33.0cm		20.3cm	
0.0071	13.70	23.44	9.96	21.78	6.23	18.85	2.49	12.25
0.0103	18.68	31.97	13.70	29.95	8.72	26.39	3.74	18.38
0.0127	24.90	42.62	17.43	38.12	12.45	37.70	6.23	30.63
0.0166	33.62	57.54	23.66	51.74	16.19	49.02	8.72	42.89
0.0222	43.58	74.59	31.13	68.08	21.17	64.10	11.21	55.14
0.0277	56.03	95.90	39.84	87.14	28.64	86.72	17.43	85.78
0.0317	69.72	119.34	54.78	119.82	38.60	116.88	23.66	116.41
0.0396	87.15	149.18	65.99	144.32	48.56	147.05	28.64	140.92
0.0515	115.79	198.19	85.91	187.89	63.50	192.29	37.35	183.81
0.0594	139.44	238.69	99.60	217.85	78.44	237.54	48.56	238.95
0.0681	168.08	287.70	117.03	255.97	93.38	282.78	61.01	300.22
0.0760	191.73	328.19	134.46	294.09	105.83	320.49	74.70	367.62
0.0863	224.10	383.60	161.85	354.00	123.26	373.27	89.64	441.14
0.0950	266.43	456.06	185.51	405.74	138.20	418.52	100.85	496.28
0.1069	323.70	554.09	222.86	487.43	166.83	505.24	119.52	588.19
0.1148	366.03	626.55	251.49	550.07	185.51	561.80	133.22	655.59
Leaf compost and medium shredded hardwood mulch mixture, 55.1%wb								
	58.4cm		45.7 cm		33.0cm		20.3cm	
0.0135	17.43	29.84	8.72	19.06				
0.0190	32.37	55.41	18.68	40.85	11.21	33.93		
0.0269	54.78	93.77	32.37	70.80	21.17	64.10	8.72	42.89
0.0340	72.21	123.60	46.07	100.75	29.88	90.49	14.94	73.52
0.0396	89.64	153.44	57.27	125.26	37.35	113.11	18.68	91.90
0.0491	107.07	183.28	74.70	163.39	49.80	150.82	23.66	116.41
0.0570	133.22	228.03	89.64	196.06	59.76	180.98	29.88	147.05
0.0641	159.36	272.78	104.58	228.74	69.72	211.14	34.86	171.56
0.0705	180.53	309.01	115.79	253.25	79.68	241.31	41.09	202.19
0.0784	204.18	349.50	131.97	288.65	90.89	275.24	43.58	214.44
0.0855	222.86	381.47	136.95	299.54	99.60	301.64	49.80	245.08
0.0934	241.53	413.44	161.85	354.00	108.32	328.03	52.29	257.33
0.1029	276.39	473.11	188.00	411.19	126.99	384.59	61.01	300.22
0.1148	326.19	558.35	221.61	484.71	146.91	444.91	73.46	361.49
0.1219	361.05	618.02	241.53	528.28	163.10	493.93	80.93	398.25

Table A-10 Airflow resistance: Peat, activated sludge, and soil.

airflow rate, m/s	measured pressure drop, Pa	unit pressure drop, Pa/m	measured pressure drop, Pa	unit pressure drop, Pa/m	measured pressure drop, Pa	unit pressure drop, Pa/m	measured pressure drop, Pa	unit pressure drop, Pa/m
				Peat, 48.7%wb				
	58.4cm		45.7 cm		33.0cm		20.3cm	
0.0063	77.19	132.13	63.50	138.88	43.58	131.97		
0.0135	227.84	389.99	165.59	362.17	126.99	384.59		
0.0230	465.63	797.04	352.34	770.64	262.70	795.56		
0.0309	647.40	1108.18	491.78	1075.62	369.77	1119.82		
0.0380	882.71	1510.96	658.61	1440.52	493.02	1493.10		
0.0467	1070.70	1832.76	809.25	1770.01	610.05	1847.52		
0.0538	1195.20	2045.87	921.30	2015.09	659.85	1998.33		
0.0625	1381.95	2365.54	1058.25	2314.63	784.35	2375.38		
				Activated sludge, 75.7%wb				
	58.4cm		45.7 cm		33.0cm		20.3cm	
0.0111			11.21	25.95	8.72	28.59		
0.0174			24.28	56.22	12.45	40.85		
0.0261			39.84	92.26	18.68	61.27		
0.0340			56.03	129.75	29.88	98.03		
0.0412			75.95	175.88	39.84	130.71		
0.0491			102.09	236.43	49.80	163.39		
0.0578			125.75	291.21	59.76	196.06		
0.0657			146.91	340.23	72.21	236.91		
0.0744			174.30	403.66	84.66	277.76		
0.0831			201.69	467.09	97.11	318.60		
0.0910			216.63	501.69	108.32	355.36		
0.1013			237.80	550.71	8.72	28.59		
				Soil, 50.2%wb				
	58.4cm		45.7 cm		33.0cm		20.3cm	
0.0063			22.41	51.90	12.45	40.85	4.98	28.01
0.0135			38.60	89.38	21.17	69.44	9.96	56.02
0.0198			61.01	141.28	34.86	114.37	18.68	105.03
0.0277			89.64	207.60	51.05	167.47	26.15	147.05
0.0356			119.52	276.79	69.72	228.74	34.86	196.06
0.0435			151.89	351.76	89.64	294.09	46.07	259.08
0.0515			186.75	432.49	108.32	355.36	54.78	308.10
0.0602			224.10	518.99	131.97	432.97	67.23	378.12
0.0681			261.45	605.49	154.38	506.50	78.44	441.14
0.0768			303.78	703.52	179.28	588.19	92.13	518.17
0.0847			344.87	798.67	204.18	669.88	104.58	588.19
0.0934			387.20	896.70	230.33	755.66	124.50	700.22

Table A-11 Airflow resistance: Activated carbon.

airflow rate, m/s	measured pressure drop, Pa	unit pressure drop, Pa/m	airflow rate, m/s	measured pressure drop, Pa	unit pressure drop, Pa/m
0.0356	12.45	49.02	0.0063	22.41	88.23
0.0388	14.94	58.82	0.0135	38.60	151.95
0.0475	19.92	78.43	0.0198	61.01	240.18
0.0530	22.41	88.23	0.0277	89.64	352.91
0.0570	24.90	98.03	0.0340	107.07	421.54
0.0633	29.88	117.64	0.0420	138.20	544.07
0.0697	34.86	137.24	0.0499	161.85	637.20
0.0760	39.84	156.85	0.0578	197.96	779.35
0.0815	44.82	176.46	0.0665	235.31	926.40
			0.0744	285.11	1122.46
			0.0831	338.64	1333.23

APPENDIX B: SUPPLEMENTARY INFORMATION FOR CHAPTER 4

B1- Moisture content, NH_4-N, NO_2-N and NO_3-N in the lower layer of Biofilter 1.

Table B-1 Moisture content, NH_4-N, NO_2-N and NO_3-N in the lower layer of Biofilter 1.

Day	date	MC, %	NH_4-N, mg/g-dry media	NO_2-N	NO_3-N	TOTAL
1	9/21/2010	1.55E+01	6.07E-01	1.23E-01	2.17E+00	2.90E+00
3	9/23/2010	1.58E+01	6.44E-01	3.06E-01	2.89E+00	3.84E+00
5	9/25/2010	1.59E+01	1.35E+00	2.00E-01	2.44E+00	3.99E+00
7	9/27/2010	1.90E+01	9.67E-01	1.84E-01	2.89E+00	4.04E+00
9	9/29/2010	3.79E+01	1.37E+00	2.34E-01	3.64E+00	5.25E+00
11	10/1/2010	5.05E+01	2.25E+00	2.59E-01	4.22E+00	6.73E+00
13	10/3/2010	5.72E+01	2.57E+00	3.25E-01	4.80E+00	7.70E+00
15	10/5/2010	5.92E+01	3.27E+00	3.12E-01	4.76E+00	8.33E+00
17	10/7/2010	5.80E+01	3.90E+00	4.39E-01	5.24E+00	9.58E+00
19	10/9/2010	5.96E+01	4.90E+00	4.27E-01	6.61E+00	1.19E+01
21	10/11/2010	5.91E+01	5.53E+00	3.54E-01	6.73E+00	1.26E+01
23	10/13/2010	5.83E+01	5.54E+00	3.74E-01	7.07E+00	1.30E+01
25	10/15/2010	5.71E+01	6.38E+00	4.35E-01	7.12E+00	1.39E+01
27	10/17/2010	5.82E+01	6.84E+00	4.76E-01	7.94E+00	1.53E+01
29	10/19/2010	5.64E+01	6.35E+00	5.59E-01	8.89E+00	1.58E+01
31	10/21/2010	5.95E+01	4.50E+00	5.39E-01	9.06E+00	1.41E+01
33	10/23/2010	6.04E+01	3.68E+00	4.07E-01	8.55E+00	1.26E+01
35	10/25/2010	5.97E+01	3.56E+00	4.08E-01	9.06E+00	1.30E+01
37	10/27/2010	6.10E+01	3.02E+00	3.88E-01	7.89E+00	1.13E+01
39	10/29/2010	6.10E+01	2.57E+00	4.73E-01	7.44E+00	1.05E+01
41	10/31/2010	6.01E+01	2.24E+00	3.65E-01	6.58E+00	9.19E+00
43	11/2/2010	5.80E+01	1.98E+00	3.54E-01	6.45E+00	8.79E+00
45	11/4/2010	5.85E+01	1.90E+00	4.23E-01	5.79E+00	8.11E+00
47	11/6/2010	6.05E+01	1.96E+00	4.43E-01	6.06E+00	8.47E+00
49	11/8/2010	6.00E+01	2.31E+00	2.81E-01	6.19E+00	8.78E+00
51	11/10/2010	5.95E+01	2.55E+00	3.13E-01	6.02E+00	8.89E+00
53	11/12/2010	5.85E+01	3.21E+00	2.72E-01	6.53E+00	1.00E+01
55	11/14/2010	6.04E+01	3.44E+00	3.54E-01	6.66E+00	1.05E+01
57	11/16/2010	6.06E+01	4.28E+00	2.54E-01	7.03E+00	1.16E+01
59	11/18/2010	6.04E+01	4.51E+00	2.12E-01	6.72E+00	1.14E+01
61	11/20/2010	6.05E+01	4.86E+00	2.26E-01	7.50E+00	1.26E+01
63	11/22/2010	5.95E+01	4.87E+00	2.72E-01	7.71E+00	1.29E+01
65	11/24/2010	5.73E+01	4.60E+00	2.45E-01	8.04E+00	1.29E+01
67	11/26/2010	5.82E+01	4.74E+00	2.44E-01	7.48E+00	1.25E+01
69	11/28/2010	5.95E+01	4.81E+00	2.73E-01	8.03E+00	1.31E+01
71	11/30/2010	5.85E+01	4.16E+00	2.78E-01	8.37E+00	1.28E+01
73	12/2/2010	6.05E+01	4.56E+00	2.14E-01	8.41E+00	1.32E+01
75	12/4/2010	5.91E+01	4.22E+00	2.37E-01	8.52E+00	1.30E+01
77	12/6/2010	5.85E+01	4.68E+00	3.56E-01	8.38E+00	1.34E+01
79	12/8/2010	5.88E+01	4.26E+00	2.64E-01	7.95E+00	1.25E+01
81	12/10/2010	5.80E+01	4.16E+00	2.86E-01	8.00E+00	1.24E+01
83	12/12/2010	5.74E+01	4.33E+00	2.70E-01	8.14E+00	1.27E+01

B2- Moisture content, NH_4-N, NO_2-N and NO_3-N in the upper layer of Biofilter 1.

Table B-2 Moisture content, NH_4-N, NO_2-N and NO_3-N in the upper layer of Biofilter 1.

Day	date	MC, %	NH_4-N, mg/g-dry media	NO_2-N	NO_3-N	TOTAL
1	9/21/2010	2.33E+01	5.42E-01	1.07E-01	1.08E+00	1.73E+00
3	9/23/2010	2.41E+01	6.56E-01	3.02E-02	1.79E+00	2.48E+00
5	9/25/2010	2.32E+01	1.60E+00	3.62E-02	2.32E+00	3.96E+00
7	9/27/2010	3.42E+01	1.97E+00	9.76E-02	2.90E+00	4.98E+00
9	9/29/2010	4.73E+01	2.33E+00	2.15E-01	3.40E+00	5.95E+00
11	10/1/2010	5.79E+01	2.69E+00	1.05E-01	3.89E+00	6.69E+00
13	10/3/2010	5.79E+01	2.75E+00	1.07E-01	4.77E+00	7.62E+00
15	10/5/2010	6.11E+01	3.64E+00	1.17E-01	5.28E+00	9.04E+00
17	10/7/2010	6.19E+01	4.25E+00	1.03E-01	5.83E+00	1.02E+01
19	10/9/2010	6.05E+01	5.06E+00	1.57E-01	5.97E+00	1.12E+01
21	10/11/2010	6.06E+01	5.38E+00	1.17E-01	6.86E+00	1.24E+01
23	10/13/2010	6.11E+01	5.25E+00	1.10E-01	6.97E+00	1.23E+01
25	10/15/2010	6.00E+01	6.09E+00	1.87E-01	7.47E+00	1.37E+01
27	10/17/2010	6.12E+01	6.91E+00	2.35E-01	7.98E+00	1.51E+01
29	10/19/2010	6.12E+01	5.73E+00	2.33E-01	7.60E+00	1.36E+01
31	10/21/2010	6.02E+01	4.94E+00	1.88E-01	7.95E+00	1.31E+01
33	10/23/2010	6.11E+01	3.67E+00	2.15E-01	7.79E+00	1.17E+01
35	10/25/2010	6.21E+01	3.77E+00	2.14E-01	8.33E+00	1.23E+01
37	10/27/2010	6.12E+01	2.83E+00	2.13E-01	7.79E+00	1.08E+01
39	10/29/2010	6.07E+01	2.42E+00	2.09E-01	7.22E+00	9.85E+00
41	10/31/2010	6.15E+01	2.58E+00	2.91E-01	6.57E+00	9.44E+00
43	11/2/2010	6.06E+01	2.25E+00	2.20E-01	5.73E+00	8.20E+00
45	11/4/2010	6.06E+01	2.14E+00	1.61E-01	5.70E+00	8.00E+00
47	11/6/2010	6.12E+01	2.11E+00	1.60E-01	5.63E+00	7.91E+00
49	11/8/2010	6.13E+01	2.35E+00	2.20E-01	6.10E+00	8.68E+00
51	11/10/2010	6.05E+01	2.48E+00	2.02E-01	5.79E+00	8.48E+00
53	11/12/2010	6.01E+01	2.90E+00	2.13E-01	6.19E+00	9.30E+00
55	11/14/2010	6.07E+01	3.54E+00	1.49E-01	6.44E+00	1.01E+01
57	11/16/2010	6.12E+01	4.06E+00	7.89E-02	6.97E+00	1.11E+01
59	11/18/2010	6.02E+01	4.40E+00	1.57E-01	6.38E+00	1.09E+01
61	11/20/2010	6.05E+01	4.72E+00	1.66E-01	6.87E+00	1.18E+01
63	11/22/2010	6.12E+01	4.82E+00	1.75E-01	6.92E+00	1.19E+01
65	11/24/2010	6.02E+01	4.48E+00	1.09E-01	6.56E+00	1.11E+01
67	11/26/2010	6.05E+01	5.04E+00	8.96E-02	6.72E+00	1.19E+01
69	11/28/2010	6.16E+01	5.09E+00	1.72E-01	7.57E+00	1.28E+01
71	11/30/2010	6.14E+01	4.80E+00	2.07E-01	7.42E+00	1.24E+01
73	12/2/2010	6.16E+01	4.74E+00	3.39E-01	8.24E+00	1.33E+01
75	12/4/2010	6.16E+01	4.66E+00	3.32E-01	7.35E+00	1.23E+01
77	12/6/2010	6.15E+01	5.19E+00	3.46E-01	8.35E+00	1.39E+01
79	12/8/2010	6.12E+01	4.96E+00	3.14E-01	8.04E+00	1.33E+01
81	12/10/2010	6.12E+01	5.20E+00	3.51E-01	8.24E+00	1.38E+01
83	12/12/2010	6.11E+01	4.93E+00	3.29E-01	7.94E+00	1.32E+01

B3- Moisture content, NH_4-N, NO_2-N and NO_3-N in the lower layer of Biofilter 2.

Table B-3 Moisture content, NH_4-N, NO_2-N and NO_3-N in the lower layer of Biofilter 2.

Day	date	MC, %	NH_4-N, mg/g-dry media	NO_2-N	NO_3-N	TOTAL
2	9/22/2010	1.80E+01	5.24E-01	1.08E-02	1.97E+00	2.50E+00
4	9/24/2010	1.69E+01	8.38E-01	2.58E-02	2.62E+00	3.49E+00
6	9/26/2010	2.23E+01	1.20E+00	9.94E-02	2.84E+00	4.14E+00
8	9/28/2010	6.02E+01	2.35E+00	2.52E-01	3.58E+00	6.18E+00
10	9/30/2010	5.79E+01	2.75E+00	1.91E-01	4.07E+00	7.01E+00
12	10/2/2010	5.76E+01	3.70E+00	3.59E-01	5.00E+00	9.06E+00
14	10/4/2010	5.35E+01	3.37E+00	4.82E-01	6.75E+00	1.06E+01
16	10/6/2010	5.54E+01	4.83E+00	6.99E-01	7.84E+00	1.34E+01
18	10/8/2010	5.50E+01	5.71E+00	6.17E-01	8.16E+00	1.45E+01
20	10/10/2010	5.49E+01	6.17E+00	6.17E-01	8.49E+00	1.53E+01
22	10/12/2010	5.60E+01	6.69E+00	6.14E-01	9.10E+00	1.64E+01
24	10/14/2010	5.75E+01	6.66E+00	5.09E-01	9.75E+00	1.69E+01
26	10/16/2010	5.81E+01	7.20E+00	5.40E-01	1.04E+01	1.81E+01
28	10/18/2010	5.81E+01	7.20E+00	5.18E-01	1.01E+01	1.78E+01
30	10/20/2010	5.85E+01	6.08E+00	5.28E-01	1.06E+01	1.72E+01
32	10/22/2010	5.85E+01	4.83E+00	4.06E-01	1.08E+01	1.61E+01
34	10/24/2010	5.90E+01	4.79E+00	5.04E-01	1.10E+01	1.63E+01
36	10/26/2010	5.96E+01	4.52E+00	4.90E-01	9.79E+00	1.48E+01
38	10/28/2010	5.96E+01	4.35E+00	4.85E-01	9.44E+00	1.43E+01
40	10/30/2010	5.78E+01	3.37E+00	5.03E-01	8.78E+00	1.27E+01
42	11/1/2010	5.74E+01	3.40E+00	5.06E-01	9.64E+00	1.36E+01
44	11/3/2010	5.66E+01	2.65E+00	3.21E-01	8.13E+00	1.11E+01
46	11/5/2010	5.56E+01	2.27E+00	2.29E-01	6.65E+00	9.15E+00
48	11/7/2010	5.76E+01	2.30E+00	2.32E-01	6.76E+00	9.29E+00
50	11/9/2010	5.86E+01	2.59E+00	1.95E-01	7.02E+00	9.81E+00
52	11/11/2010	5.94E+01	2.85E+00	1.88E-01	7.50E+00	1.05E+01
54	11/13/2010	5.90E+01	3.30E+00	2.31E-01	8.13E+00	1.17E+01
56	11/15/2010	5.73E+01	4.28E+00	3.43E-01	8.61E+00	1.32E+01
58	11/17/2010	5.84E+01	4.60E+00	3.58E-01	8.67E+00	1.36E+01
60	11/19/2010	5.88E+01	4.68E+00	2.97E-01	8.78E+00	1.38E+01
62	11/21/2010	5.95E+01	4.82E+00	2.03E-01	9.15E+00	1.42E+01
64	11/23/2010	5.99E+01	4.74E+00	2.97E-01	9.32E+00	1.44E+01
66	11/25/2010	5.89E+01	5.05E+00	3.76E-01	9.70E+00	1.51E+01
68	11/27/2010	6.18E+01	5.33E+00	3.31E-01	9.85E+00	1.55E+01
70	11/29/2010	5.97E+01	5.59E+00	3.37E-01	1.02E+01	1.62E+01
72	12/1/2010	5.83E+01	5.22E+00	3.15E-01	9.90E+00	1.54E+01
74	12/3/2010	5.86E+01	5.61E+00	3.23E-01	9.76E+00	1.57E+01
76	12/5/2010	5.79E+01	5.53E+00	3.64E-01	1.01E+01	1.60E+01
78	12/7/2010	5.73E+01	5.48E+00	3.11E-01	9.59E+00	1.54E+01
80	12/9/2010	5.84E+01	5.81E+00	3.33E-01	9.88E+00	1.60E+01
82	12/11/2010	5.86E+01	5.77E+00	3.07E-01	9.95E+00	1.60E+01

B4- Moisture content, NH_4-N, NO_2-N and NO_3-N in the upper layer of Biofilter 2.

Table B-4 Moisture content, NH_4-N, NO_2-N and NO_3-N in the upper layer of Biofilter 2.

Day	date	MC, %	NH_4-N, mg/g-dry media	NO_2-N	NO_3-N	TOTAL
2	9/22/2010	2.38E+01	8.98E-01	8.98E-03	1.50E+00	2.40E+00
4	9/24/2010	4.20E+01	1.37E+00	3.49E-02	2.05E+00	3.46E+00
6	9/26/2010	4.23E+01	1.82E+00	3.42E-02	2.62E+00	4.48E+00
8	9/28/2010	6.02E+01	2.38E+00	1.32E-01	3.92E+00	6.43E+00
10	9/30/2010	5.86E+01	3.18E+00	1.13E-01	4.24E+00	7.53E+00
12	10/2/2010	6.01E+01	4.19E+00	9.15E-02	4.77E+00	9.05E+00
14	10/4/2010	6.00E+01	4.34E+00	2.43E-01	5.24E+00	9.82E+00
16	10/6/2010	5.90E+01	5.19E+00	3.43E-01	6.19E+00	1.17E+01
18	10/8/2010	5.93E+01	6.18E+00	3.92E-01	7.29E+00	1.39E+01
20	10/10/2010	6.02E+01	7.33E+00	4.74E-01	7.83E+00	1.56E+01
22	10/12/2010	5.96E+01	7.69E+00	5.65E-01	8.48E+00	1.67E+01
24	10/14/2010	6.25E+01	8.65E+00	4.17E-01	9.37E+00	1.84E+01
26	10/16/2010	6.20E+01	9.60E+00	4.71E-01	1.01E+01	2.02E+01
28	10/18/2010	6.20E+01	9.60E+00	4.80E-01	1.06E+01	2.06E+01
30	10/20/2010	5.83E+01	8.37E+00	4.64E-01	1.02E+01	1.90E+01
32	10/22/2010	6.15E+01	7.00E+00	2.67E-01	1.07E+01	1.80E+01
34	10/24/2010	6.17E+01	5.59E+00	3.41E-01	9.73E+00	1.57E+01
36	10/26/2010	6.02E+01	4.36E+00	4.13E-01	9.78E+00	1.45E+01
38	10/28/2010	6.22E+01	4.14E+00	4.20E-01	9.95E+00	1.45E+01
40	10/30/2010	6.20E+01	3.58E+00	4.01E-01	9.66E+00	1.36E+01
42	11/1/2010	5.95E+01	2.37E+00	3.36E-01	8.89E+00	1.16E+01
44	11/3/2010	6.03E+01	2.33E+00	3.54E-01	7.31E+00	9.99E+00
46	11/5/2010	6.22E+01	2.32E+00	3.07E-01	7.41E+00	1.00E+01
48	11/7/2010	6.13E+01	2.57E+00	2.87E-01	7.82E+00	1.07E+01
50	11/9/2010	6.01E+01	2.92E+00	3.45E-01	7.51E+00	1.08E+01
52	11/11/2010	6.10E+01	3.38E+00	2.75E-01	7.67E+00	1.13E+01
54	11/13/2010	6.09E+01	3.48E+00	2.79E-01	8.17E+00	1.19E+01
56	11/15/2010	6.13E+01	4.49E+00	3.18E-01	8.47E+00	1.33E+01
58	11/17/2010	6.01E+01	5.18E+00	3.57E-01	9.06E+00	1.46E+01
60	11/19/2010	6.06E+01	5.99E+00	3.79E-01	8.98E+00	1.54E+01
62	11/21/2010	6.11E+01	5.82E+00	3.61E-01	9.38E+00	1.56E+01
64	11/23/2010	6.20E+01	6.38E+00	4.27E-01	1.03E+01	1.71E+01
66	11/25/2010	6.19E+01	6.08E+00	3.35E-01	1.12E+01	1.76E+01
68	11/27/2010	6.09E+01	5.59E+00	3.60E-01	9.52E+00	1.55E+01
70	11/29/2010	6.16E+01	6.45E+00	3.09E-01	1.04E+01	1.71E+01
72	12/1/2010	6.15E+01	6.58E+00	3.03E-01	1.07E+01	1.76E+01
74	12/3/2010	6.03E+01	6.58E+00	3.52E-01	1.04E+01	1.73E+01
76	12/5/2010	6.03E+01	6.00E+00	3.35E-01	1.00E+01	1.63E+01
78	12/7/2010	6.16E+01	6.64E+00	3.73E-01	1.05E+01	1.75E+01
80	12/9/2010	6.20E+01	6.80E+00	4.13E-01	1.06E+01	1.78E+01
82	12/11/2010	6.12E+01	6.76E+00	3.74E-01	1.04E+01	1.76E+01

APPENDIX C: SUPPLEMENTARY INFORMATION FOR CHAPTER 5

C1- Daily average (Avg.), standard deviation (S.D.) of ammonia concentrations, ppm and removal efficiencies (R.E.) of four biofilters, %.

Table C-1 Measured results of four biofilters.

day	date	Inlet		Biofilter 1			Biofilter 2			Biofilter 3			Biofilter 4		
		S.D.	Avg.	S.D.	Avg.	R.E.	S.D.	Avg.	R.E.	S.D.	Avg.	R.E.	S.D.	Avg.	R.E.
1	7/4	3.2	25.1	0.1	12.3	51.1	0.1	15.5	38.5	0.6	13.2	47.4	0.6	12.0	52.3
2	7/5	2.9	26.7	0.4	13.0	51.3	0.5	15.5	42.2	0.6	14.0	47.8	1.0	15.1	43.6
3	7/6	1.6	20.7	0.4	13.3	35.9	0.4	15.0	27.4	0.4	12.9	37.6	0.3	11.8	43.1
4	7/7	2.4	19.0	0.6	12.9	32.3	0.5	13.8	27.5	0.5	13.2	30.5	0.7	12.5	34.0
5	7/8	2.4	19.0	0.4	13.8	27.2	0.4	13.0	31.4	0.5	12.3	35.3	0.6	12.5	34.4
6	7/9	2.2	19.5	0.4	13.3	31.5	0.5	13.2	32.3	1.3	12.8	34.4	0.6	12.8	34.5
7	7/10	2.0	18.4	0.5	13.4	27.4	0.5	13.0	29.3	0.4	11.4	38.3	0.5	9.9	46.0
8	7/11	1.7	18.2	0.5	12.3	32.1	0.5	13.1	28.2	0.5	11.0	39.3	0.5	10.3	43.4
9	7/12	1.4	16.2	0.4	10.3	36.5	0.4	11.3	30.1	0.3	9.3	42.5	0.5	10.3	36.3
10	7/13	1.4	16.2	0.4	10.6	34.4	0.5	8.9	45.2	0.4	10.1	37.8	0.3	10.4	35.7
11	7/14	1.3	15.3	0.5	8.5	44.6	0.4	9.2	39.9	0.4	9.8	36.3	0.4	10.0	34.6
12	7/15	1.3	17.2	0.4	9.6	44.4	0.5	9.1	46.9	0.4	11.1	35.2	0.4	11.8	31.4
13	7/16	0.9	19.7	0.5	11.1	43.6	0.5	12.9	34.5	0.5	11.3	42.6	0.3	12.9	34.3
14	7/17	0.9	19.3	0.4	13.4	30.3	0.5	11.1	42.4	0.5	11.3	41.5	1.8	9.8	49.4
15	7/18	0.8	12.0	0.5	7.3	39.1	0.5	7.9	34.1	0.4	8.0	33.1	0.4	8.1	32.2
16	7/19	0.8	12.1	0.5	7.0	42.0	0.4	7.9	34.5	0.4	8.3	31.6	0.4	8.1	32.7
17	7/20	1.0	23.7	0.6	12.8	45.9	0.5	12.9	45.6	0.4	13.6	42.6	0.5	12.4	47.5
18	7/21	1.0	23.7	0.5	12.6	46.9	0.7	12.3	48.1	0.6	12.2	48.7	0.6	13.7	42.2
19	7/22	2.7	26.2	0.5	14.0	46.7	0.6	13.9	46.9	0.5	14.2	45.7	0.6	13.6	48.0
20	7/23	0.9	21.3	0.6	11.8	44.5	0.5	11.5	46.1	0.5	12.5	41.1	0.5	12.3	42.4
21	7/24	0.9	21.2	0.5	11.9	44.2	0.5	11.6	45.6	0.4	12.3	42.0	0.4	11.5	45.8
22	7/25	2.1	21.4	0.5	11.1	48.3	0.5	9.4	56.3	0.4	12.1	43.6	0.4	9.1	57.6
23	7/26	0.8	21.5	0.6	9.2	57.1	0.6	9.5	56.0	0.5	8.7	59.4	0.4	9.2	57.2
24	7/27	2.8	22.8	0.5	5.7	74.9	0.3	7.8	65.7	0.5	8.7	61.7	0.4	9.2	59.7
25	7/28	1.1	25.6	0.3	6.9	73.0	0.3	7.8	69.4	0.5	8.7	65.9	0.4	6.8	73.5
26	7/29	1.4	25.0	0.4	7.1	71.7	0.3	7.5	70.1	0.3	8.3	66.9	0.3	8.1	67.7
27	7/30	0.8	25.2	0.4	7.3	70.9	0.4	7.9	68.7	0.3	7.7	69.2	0.6	7.6	69.6
28	7/31	1.2	27.0	0.5	8.3	69.3	0.4	8.2	69.5	0.6	8.5	68.5	0.4	8.0	70.4
29	8/1	0.7	24.8	0.3	7.3	70.5	1.0	7.1	71.4	0.3	7.3	70.4	0.3	7.5	69.6
30	8/2	0.8	26.0	0.4	7.3	72.0	0.2	8.0	69.4	0.7	8.1	68.9	0.2	8.0	69.2
31	8/3	0.8	23.0	0.2	6.9	69.8	0.3	7.2	68.6	0.3	7.1	69.0	0.3	7.1	69.3
32	8/4	0.8	24.9	0.3	6.5	73.9	0.2	6.6	73.4	0.2	7.3	70.6	0.2	7.4	70.3
33	8/5	0.8	24.9	0.4	6.8	72.6	0.3	7.6	69.7	0.2	6.2	75.3	0.2	7.4	70.3

Continue.

34	8/6	0.7	29.5	0.3	7.3	75.3	0.2	7.0	76.2	0.2	7.3	75.4	0.2	8.2	72.1
35	8/7	4.8	29.7	0.3	7.4	75.0	0.3	7.6	74.5	0.2	7.7	74.2	0.2	8.2	72.4
36	8/8	0.5	29.3	0.3	7.8	73.5	0.3	7.1	75.7	0.3	7.8	73.3	0.3	7.6	74.1
37	8/9	0.8	28.4	0.3	6.8	76.0	0.3	7.7	72.7	0.2	7.2	74.5	0.2	6.6	76.6
38	8/10	0.8	28.3	0.3	6.5	77.1	0.4	6.8	76.1	0.3	7.7	72.7	0.2	7.1	75.0
39	8/11	0.8	28.3	0.3	7.1	74.9	0.3	6.8	75.9	0.3	7.1	74.8	0.2	7.1	75.0
40	8/12	1.0	31.0	0.3	6.1	80.2	0.3	7.6	75.4	0.2	6.9	77.7	0.2	8.0	74.3
41	8/13	0.7	29.3	0.3	7.3	74.9	0.3	7.1	75.7	0.2	7.7	73.7	0.2	7.8	73.4
42	8/14	0.8	26.8	0.3	6.7	74.9	0.2	7.4	72.4	0.2	7.4	72.3	0.2	7.1	73.7
43	8/15	0.7	31.1	1.1	6.4	79.4	0.3	7.2	76.8	0.2	7.1	77.0	0.2	7.4	76.1
44	8/16	1.8	30.1	0.4	5.0	83.4	0.3	6.3	79.0	0.2	6.7	77.7	0.2	7.5	75.2
45	8/17	1.0	30.7	0.3	5.8	81.1	0.4	5.9	80.8	0.3	6.7	78.3	0.2	7.6	75.4
46	8/18	2.2	31.7	0.3	5.8	81.7	0.8	6.3	80.0	1.3	7.5	76.4	0.4	7.5	76.5
47	8/19	0.6	28.1	0.3	7.5	73.1	0.3	6.9	75.5	1.9	6.4	77.3	0.3	7.0	75.0
48	8/20	0.6	28.6	0.3	7.0	75.4	0.2	7.3	74.4	0.2	6.9	75.9	0.4	7.6	73.6
49	8/21	18.1	35.7	0.2	5.3	85.0	0.1	4.6	87.2	0.2	6.9	80.6	0.2	6.9	80.6
50	8/22	0.7	27.4	0.3	4.7	82.9	0.2	5.4	80.3	0.1	7.1	74.1	0.3	6.4	76.8
51	8/23	0.6	26.0	0.3	4.4	83.0	0.1	4.9	81.2	0.1	6.6	74.6	0.2	5.9	77.1
52	8/24	0.4	26.6	0.2	4.2	84.1	0.2	4.5	83.0	0.2	6.8	74.6	0.2	6.0	77.5
53	8/25	0.8	28.2	0.2	4.4	84.5	0.2	4.9	82.7	0.2	5.9	79.0	0.3	5.9	79.1
54	8/26	0.7	28.5	0.2	4.5	84.4	0.2	4.7	83.7	0.2	5.9	79.1	0.2	5.8	79.5
55	8/27	0.6	30.1	0.2	4.3	85.6	0.2	4.9	83.9	0.2	6.2	79.3	0.2	6.6	78.2
56	8/28	0.5	29.7	0.2	5.2	82.6	0.2	5.1	82.8	0.2	6.0	79.6	0.2	6.2	79.2
57	8/29	0.5	30.4	0.2	5.2	82.9	0.2	5.2	82.8	0.2	6.4	79.1	0.4	6.5	78.6
58	8/30	0.5	30.8	0.2	5.2	83.3	0.2	5.1	83.3	0.2	6.2	79.9	0.2	6.4	79.2
59	8/31	0.5	30.8	0.2	5.0	83.8	0.2	5.0	83.7	0.2	6.2	79.9	0.4	6.4	79.4
60	9/1	0.5	31.5	0.2	5.0	84.3	0.2	5.1	83.7	0.2	6.2	80.3	0.3	6.2	80.2
61	9/2	0.6	33.7	0.3	5.4	83.9	0.3	5.6	83.5	0.2	6.9	79.4	0.3	6.9	79.5
62	9/3	0.4	30.3	0.1	4.4	85.6	0.2	5.1	83.3	0.2	6.7	78.0	0.2	6.5	78.6
63	9/4	0.4	30.2	0.3	4.3	85.8	0.2	4.8	84.0	0.1	5.6	81.4	0.1	5.5	81.9
64	9/5	0.7	29.5	0.2	4.5	84.7	0.2	4.7	84.0	0.1	5.3	82.0	0.4	5.8	80.3
65	9/6	0.0	28.1	0.2	4.3	84.8	0.2	3.8	86.6	0.2	5.7	79.8	0.3	5.4	80.8
66	9/7	0.7	27.1	0.2	3.9	85.8	0.1	3.8	86.1	0.2	4.9	82.1	0.2	5.5	79.6
67	9/8	0.4	30.2	0.1	3.7	87.9	0.1	4.0	86.8	0.1	5.6	81.6	0.8	5.8	80.8
68	9/9	1.8	28.9	0.2	4.1	85.9	0.2	4.4	84.9	0.1	5.0	82.9	0.1	5.6	80.6
69	9/10	0.8	31.9	0.2	6.1	81.0	0.1	5.1	84.2	0.1	6.1	80.9	0.1	6.3	80.3
70	9/11	0.8	33.1	0.2	5.9	82.1	0.2	5.1	84.7	0.2	6.0	82.0	0.2	6.6	79.9
71	9/12	0.4	26.9	0.2	4.7	82.5	0.4	4.6	82.9	0.2	5.5	79.5	0.2	5.5	79.7
72	9/13	0.8	27.0	0.2	3.8	85.9	0.2	3.6	86.7	0.1	5.0	81.7	0.2	6.1	77.3
73	9/14	0.8	28.0	0.2	3.8	86.4	0.2	3.5	87.5	0.1	4.7	83.2	0.1	5.2	81.6

Continue.

74	9/15	0.8	33.3	0.2	3.9	88.3	0.1	4.8	85.7	0.1	4.7	85.9	0.1	5.5	83.5
75	9/16	0.2	32.6	0.1	4.4	86.5	0.1	4.4	86.4	0.1	4.8	85.3	0.1	5.5	83.1
76	9/17	0.4	33.9	0.1	4.7	86.0	0.1	4.8	85.7	0.2	5.5	83.7	0.1	6.3	81.4
77	9/18	0.1	35.2	0.1	5.1	85.4	0.1	5.4	84.6	0.1	5.9	83.1	0.1	6.4	81.8
78	9/19	0.7	36.3	0.2	5.9	83.7	0.1	5.5	84.9	0.1	6.2	83.0	0.1	6.5	82.2
79	9/20	0.3	34.0	0.3	5.2	84.7	0.1	4.2	87.6	0.1	5.7	83.3	0.1	6.2	81.9
80	9/21	0.2	34.9	0.2	5.4	84.6	0.1	5.2	85.0	0.1	5.9	83.0	0.1	6.0	82.9
81	9/22	0.3	33.0	0.2	4.9	85.1	0.1	4.2	87.1	0.1	6.0	81.9	0.1	5.4	83.5
82	9/23	0.6	32.2	0.1	4.7	85.4	0.1	5.1	84.2	0.1	5.8	82.0	0.1	5.8	82.0
83	9/24	0.2	32.4	0.2	4.2	87.2	0.1	5.2	83.8	0.1	5.7	82.5	0.1	6.2	81.0
							Drying media								
94	10/5	0.3	22.9	0.2	4.1	82.0	0.2	4.6	80.1	0.1	6.0	73.6	0.1	5.5	76.1
95	10/6	0.3	24.6	0.2	4.8	80.4	0.1	5.1	79.3	0.1	4.9	79.9	0.1	4.7	80.8
96	10/7	0.1	24.6	0.2	5.3	78.3	0.1	5.3	78.4	0.1	5.3	78.3	0.2	5.2	79.0
97	10/8	0.2	25.0	0.2	5.5	77.9	0.1	5.4	78.6	0.1	5.2	79.2	0.2	5.0	80.1
98	10/9	0.6	26.0	0.3	5.5	79.0	0.3	5.0	80.9	0.1	5.3	79.8	0.2	4.9	81.3
99	10/10	0.6	26.0	0.2	5.4	79.1	0.1	5.0	80.9	0.1	5.2	80.0	0.2	4.6	82.3
100	10/11	0.6	24.3	0.2	4.9	79.8	0.3	5.0	79.5	0.1	5.2	78.5	0.2	4.4	81.9
101	10/12	0.1	23.9	0.3	5.5	77.1	0.1	5.0	79.2	0.1	4.8	79.8	0.1	4.8	80.1
102	10/13	0.3	24.4	0.2	5.4	77.6	0.1	3.9	83.9	0.1	4.7	80.7	0.1	4.6	81.0
103	10/14	0.2	20.8	0.1	4.0	80.8	0.1	3.9	81.2	0.1	4.9	76.6	0.1	4.2	80.0
104	10/15	4.4	19.5	0.3	4.0	79.7	0.1	3.4	82.5	0.1	4.3	77.8	0.1	4.0	79.2
105	10/16	0.3	23.6	0.2	3.7	84.4	0.1	3.4	85.6	0.1	3.4	85.5	0.1	3.1	86.8
106	10/17	0.4	22.4	0.2	3.9	82.5	0.2	3.7	83.3	0.1	3.7	83.6	0.1	3.7	83.4
107	10/18	0.2	22.7	0.3	3.8	83.1	0.3	4.6	79.5	0.1	3.8	83.3	0.1	3.9	83.0
108	10/19	1.8	24.8	0.3	5.0	79.8	0.2	4.5	81.8	0.9	3.9	84.2	0.1	3.7	85.2
109	10/20	0.5	23.3	0.2	4.1	82.4	0.2	4.1	82.3	0.2	4.3	81.3	0.2	4.2	82.2
110	10/21	0.2	22.5	0.3	3.8	83.2	0.2	3.7	83.4	0.2	3.9	82.6	0.2	3.9	82.9
111	10/22	0.8	24.7	0.2	4.2	82.9	0.2	3.8	84.8	0.2	4.2	83.2	0.2	4.1	83.2
112	10/23	1.5	21.7	0.2	3.9	82.2	0.2	3.5	84.0	0.2	4.3	80.2	0.2	4.2	80.5
113	10/24	2.8	25.7	0.4	3.8	85.2	0.2	3.8	85.2	0.2	4.5	82.5	0.2	4.3	83.1
114	10/25	0.2	23.7	0.2	4.4	81.2	0.3	4.1	82.7	0.1	4.7	80.1	0.1	4.8	79.9
115	10/26	0.6	21.7	0.1	4.0	81.6	0.1	4.1	81.0	0.1	4.2	80.8	0.1	4.6	78.7
116	10/27	0.5	23.3	0.3	4.0	83.0	0.3	4.2	82.1	0.1	4.8	79.4	0.1	4.2	82.2
117	10/28	0.2	22.5	0.2	3.7	83.6	0.1	4.3	81.0	0.1	3.4	84.7	0.1	4.0	82.0
118	10/29	0.6	23.9	0.3	4.0	83.5	0.2	3.7	84.4	0.9	3.9	83.6	0.1	4.1	82.8
119	10/30	0.3	22.2	0.2	3.6	83.6	0.1	3.5	84.4	0.2	3.9	82.3	0.2	3.7	83.3
120	10/31	0.6	24.2	0.2	3.7	84.5	0.2	3.5	85.5	0.2	3.7	84.6	0.2	3.8	84.2
121	11/1	0.3	22.0	0.1	3.5	84.3	0.2	3.4	84.5	0.1	3.4	84.6	0.2	3.9	82.2

C2- Daily average (Avg.) and standard deviation (S.D.) of nitrous oxide concentrations, ppm, from four biofilters.

Table C-2 Results of nitrous oxide from four biofilters.

day	date	Inlet		Biofilter 1			Biofilter 2			Biofilter 3			Biofilter 4		
		S.D.	Avg.	S.D.	Avg.	Diff.	S.D.	Avg.	Diff.	S.D.	Avg.	Diff.	S.D.	Avg.	Diff.
1	7/4	0.03	1.29	0.02	1.37	0.08	0.02	1.37	0.08	0.06	1.43	0.14	0.04	1.42	0.13
2	7/5	0.03	1.41	0.04	1.47	0.06	0.04	1.47	0.06	0.03	1.49	0.08	0.05	1.47	0.06
3	7/6	0.03	1.23	0.03	1.40	0.17	0.03	1.38	0.15	0.02	1.37	0.14	0.03	1.35	0.12
4	7/7	0.03	1.23	0.03	1.34	0.11	0.03	1.35	0.12	0.04	1.40	0.17	0.05	1.41	0.18
5	7/8	0.03	1.35	0.04	1.45	0.10	0.04	1.46	0.12	0.04	1.48	0.14	0.04	1.45	0.10
6	7/9	0.04	1.36	0.04	1.45	0.10	0.04	1.46	0.10	0.06	1.49	0.13	0.04	1.44	0.09
7	7/10	0.03	1.35	0.04	1.45	0.10	0.04	1.46	0.11	0.04	1.51	0.16	0.04	1.44	0.08
8	7/11	0.04	1.36	0.04	1.45	0.09	0.04	1.47	0.11	0.04	1.53	0.18	0.04	1.48	0.13
9	7/12	0.03	1.36	0.04	1.45	0.09	0.04	1.46	0.10	0.04	1.49	0.13	0.04	1.48	0.13
10	7/13	0.03	1.36	0.04	1.45	0.10	0.04	1.44	0.08	0.04	1.51	0.15	0.04	1.41	0.05
11	7/14	0.04	1.33	0.04	1.44	0.11	0.04	1.44	0.11	0.04	1.50	0.18	0.05	1.43	0.11
12	7/15	0.03	1.30	0.04	1.47	0.17	0.04	1.50	0.20	0.04	1.48	0.18	0.04	1.50	0.20
13	7/16	0.02	1.36	0.04	1.47	0.11	0.04	1.53	0.16	0.04	1.58	0.22	0.03	1.52	0.15
14	7/17	0.02	1.35	0.04	1.50	0.15	0.04	1.52	0.17	0.05	1.52	0.17	0.05	1.51	0.16
15	7/18	0.04	1.34	0.04	1.53	0.19	0.04	1.45	0.12	0.05	1.55	0.21	0.05	1.46	0.13
16	7/19	0.04	1.31	0.05	1.44	0.13	0.04	1.46	0.15	0.05	1.50	0.19	0.04	1.52	0.21
17	7/20	0.04	1.32	0.05	1.45	0.13	0.05	1.47	0.15	0.05	1.50	0.18	0.06	1.50	0.18
18	7/21	0.04	1.32	0.04	1.45	0.13	0.04	1.48	0.16	0.05	1.52	0.20	0.05	1.51	0.19
19	7/22	0.05	1.38	0.04	1.50	0.11	0.04	1.49	0.11	0.05	1.56	0.18	0.06	1.59	0.20
20	7/23	0.05	1.37	0.05	1.53	0.16	0.04	1.48	0.11	0.05	1.59	0.22	0.04	1.56	0.19
21	7/24	0.04	1.35	0.05	1.55	0.19	0.04	1.49	0.14	0.05	1.56	0.21	0.04	1.57	0.22
22	7/25	0.04	1.36	0.05	1.60	0.24	0.04	1.49	0.13	0.05	1.57	0.21	0.04	1.56	0.21
23	7/26	0.04	1.38	0.05	1.64	0.26	0.04	1.49	0.11	0.05	1.67	0.29	0.05	1.64	0.26
24	7/27	0.05	1.37	1.97	1.62	0.25	0.04	1.49	0.12	0.05	1.67	0.30	0.05	1.67	0.30
25	7/28	0.04	1.33	0.03	1.61	0.28	0.04	1.58	0.26	0.04	1.66	0.34	0.07	1.63	0.30
26	7/29	0.07	1.43	0.03	1.69	0.26	0.04	1.63	0.20	0.04	1.77	0.34	0.04	1.65	0.22
27	7/30	0.03	1.28	0.03	1.57	0.28	0.04	1.58	0.30	0.10	1.64	0.35	0.10	1.60	0.32
28	7/31	0.04	1.39	0.03	1.61	0.22	0.04	1.59	0.20	0.04	1.64	0.24	0.06	1.67	0.28
29	8/1	0.03	1.31	0.02	1.47	0.15	0.10	1.59	0.28	0.07	1.62	0.31	0.03	1.61	0.30
30	8/2	0.05	1.40	0.03	1.63	0.23	0.03	1.59	0.19	0.04	1.71	0.30	0.03	1.66	0.26
31	8/3	0.03	1.34	0.04	1.54	0.20	0.04	1.54	0.20	0.04	1.63	0.29	0.04	1.64	0.30
32	8/4	0.04	1.35	0.04	1.57	0.23	0.04	1.56	0.21	0.03	1.65	0.30	0.03	1.61	0.26
33	8/5	0.04	1.35	0.05	1.57	0.22	0.04	1.55	0.20	0.04	1.68	0.33	0.03	1.61	0.26
34	8/6	0.03	1.35	0.04	1.55	0.20	0.03	1.55	0.21	0.03	1.61	0.26	0.04	1.63	0.29
35	8/7	0.06	1.20	0.04	1.45	0.25	0.04	1.44	0.24	0.04	1.53	0.33	0.04	1.51	0.30

Continue.

36	8/8	0.03	1.31	0.04	1.54	0.23	0.04	1.53	0.22	0.04	1.61	0.30	0.04	1.58	0.27
37	8/9	0.04	1.36	0.04	1.52	0.17	0.03	1.55	0.20	0.03	1.63	0.27	0.04	1.61	0.26
38	8/10	0.04	1.37	0.04	1.61	0.24	0.04	1.62	0.25	0.04	1.71	0.34	0.04	1.60	0.24
39	8/11	0.04	1.37	0.04	1.61	0.25	0.03	1.60	0.23	0.05	1.65	0.28	0.04	1.63	0.27
40	8/12	0.04	1.40	0.03	1.62	0.22	0.04	1.62	0.22	0.04	1.66	0.26	0.03	1.68	0.28
41	8/13	0.03	1.36	0.04	1.59	0.23	0.04	1.60	0.25	0.04	1.67	0.31	0.04	1.67	0.31
42	8/14	0.03	1.31	0.03	1.52	0.21	0.03	1.51	0.20	0.04	1.67	0.36	0.04	1.62	0.31
43	8/15	0.03	1.37	0.04	1.55	0.19	0.04	1.57	0.21	0.04	1.72	0.36	0.03	1.60	0.23
44	8/16	0.04	1.37	0.04	1.55	0.18	0.04	1.56	0.19	0.04	1.72	0.36	0.03	1.66	0.29
45	8/17	0.04	1.38	0.04	1.54	0.16	0.04	1.61	0.23	0.04	1.72	0.34	0.03	1.59	0.21
46	8/18	0.17	1.34	0.04	1.54	0.19	0.07	1.52	0.17	0.12	1.62	0.27	0.06	1.58	0.24
47	8/19	0.04	1.35	0.03	1.48	0.13	0.03	1.71	0.36	0.15	1.68	0.34	0.04	1.56	0.21
48	8/20	0.03	1.30	0.03	1.74	0.44	0.03	1.68	0.37	0.03	1.65	0.35	0.04	1.52	0.21
49	8/21	0.39	1.34	0.03	1.74	0.40	0.03	1.79	0.45	0.03	1.60	0.27	0.03	1.54	0.21
50	8/22	0.03	1.27	0.04	1.78	0.51	0.03	1.79	0.51	0.03	1.54	0.26	0.03	1.55	0.28
51	8/23	0.03	1.31	0.06	1.77	0.47	0.04	1.90	0.59	0.03	1.62	0.31	0.04	1.59	0.28
52	8/24	0.05	1.29	0.04	1.78	0.48	0.03	1.90	0.61	0.03	1.61	0.31	0.04	1.51	0.21
53	8/25	0.15	1.38	0.05	1.95	0.58	0.04	2.13	0.75	0.03	1.70	0.32	0.04	1.57	0.19
54	8/26	0.03	1.28	0.06	1.93	0.65	0.03	2.08	0.80	0.04	1.60	0.32	0.04	1.47	0.19
55	8/27	0.03	1.33	0.05	1.93	0.60	0.03	2.14	0.81	0.04	1.62	0.29	0.04	1.57	0.24
56	8/28	0.02	1.31	0.05	1.94	0.63	0.04	2.19	0.87	0.04	1.60	0.29	0.03	1.55	0.24
57	8/29	0.03	1.32	0.05	1.92	0.59	0.05	2.17	0.85	0.04	1.59	0.26	0.05	1.56	0.23
58	8/30	0.03	1.31	0.05	1.99	0.67	0.04	2.17	0.85	0.04	1.57	0.25	0.03	1.53	0.22
59	8/31	0.03	1.30	0.05	2.04	0.74	0.04	2.18	0.88	0.03	1.55	0.25	0.04	1.56	0.26
60	9/1	0.03	1.34	0.06	2.02	0.68	0.06	2.22	0.88	0.04	1.58	0.24	0.04	1.53	0.19
61	9/2	0.05	1.32	0.06	2.17	0.85	0.06	2.23	0.90	0.04	1.61	0.29	0.04	1.52	0.20
62	9/3	0.03	1.30	0.02	2.10	0.80	0.03	2.18	0.88	0.04	1.61	0.31	0.04	1.56	0.26
63	9/4	0.03	1.34	0.09	2.17	0.83	0.04	2.23	0.89	0.03	1.57	0.23	0.03	1.56	0.22
64	9/5	0.04	1.31	0.03	2.06	0.76	0.03	2.22	0.91	0.02	1.59	0.29	0.06	1.57	0.26
65	9/6	0.04	1.30	0.03	2.15	0.85	0.03	2.19	0.88	0.03	1.53	0.23	0.05	1.57	0.27
66	9/7	0.03	1.31	0.05	2.15	0.85	0.03	2.20	0.89	0.05	1.55	0.25	0.04	1.63	0.33
67	9/8	0.03	1.31	0.06	2.15	0.84	0.03	2.17	0.86	0.03	1.51	0.20	0.06	1.61	0.30
68	9/9	0.05	1.32	0.06	2.20	0.88	0.03	2.15	0.84	0.02	1.61	0.29	0.03	1.61	0.29
69	9/10	0.03	1.31	0.06	2.13	0.82	0.03	2.09	0.78	0.03	1.55	0.23	0.03	1.62	0.30
70	9/11	0.04	1.32	0.12	2.14	0.83	0.04	2.17	0.85	0.04	1.54	0.22	0.03	1.59	0.27
71	9/12	0.03	1.29	0.06	2.06	0.77	0.24	2.07	0.79	0.04	1.54	0.26	0.03	1.54	0.26
72	9/13	0.04	1.31	0.06	2.13	0.82	0.03	2.09	0.78	0.02	1.61	0.30	0.03	1.61	0.30
73	9/14	0.03	1.29	0.06	2.12	0.83	0.03	2.09	0.80	0.03	1.56	0.27	0.02	1.61	0.32
74	9/15	0.03	1.25	0.04	2.06	0.80	0.03	2.08	0.82	0.02	1.60	0.35	0.02	1.61	0.36
75	9/16	0.02	1.24	0.02	2.04	0.80	0.02	2.04	0.81	0.02	1.62	0.38	0.02	1.57	0.33

Continue.

76	9/17	0.04	1.26	0.11	2.10	0.84	0.03	2.09	0.84	0.03	1.60	0.34	0.02	1.61	0.35
77	9/18	0.02	1.28	0.14	2.12	0.84	0.02	2.09	0.81	0.02	1.61	0.34	0.03	1.60	0.33
78	9/19	0.03	1.30	0.04	2.15	0.84	0.02	2.09	0.79	0.02	1.64	0.34	0.02	1.65	0.35
79	9/20	0.03	1.30	0.04	2.13	0.83	0.03	2.10	0.79	0.02	1.64	0.34	0.02	1.60	0.30
80	9/21	0.04	1.32	0.06	2.15	0.83	0.04	2.10	0.78	0.02	1.67	0.35	0.02	1.60	0.28
81	9/22	0.02	1.29	0.04	2.12	0.84	0.02	2.10	0.81	0.02	1.60	0.31	0.02	1.61	0.32
82	9/23	0.02	1.30	0.03	2.14	0.84	0.03	2.09	0.79	0.02	1.63	0.33	0.02	1.62	0.32
83	9/24	0.02	1.30	0.02	2.15	0.85	0.02	2.09	0.79	0.02	1.64	0.33	0.02	1.60	0.30
							Drying media								
94	10/5	0.02	1.29	0.03	1.72	0.43	0.03	1.50	0.21	0.02	1.58	0.29	0.03	1.55	0.25
95	10/6	0.02	1.27	0.04	1.70	0.43	0.03	1.57	0.30	0.02	1.50	0.23	0.03	1.51	0.24
96	10/7	0.02	1.31	0.03	1.67	0.35	0.03	1.58	0.26	0.02	1.54	0.22	0.03	1.57	0.26
97	10/8	0.03	1.32	0.04	1.69	0.37	0.03	1.57	0.25	0.03	1.52	0.20	0.03	1.57	0.25
98	10/9	0.03	1.40	0.04	1.71	0.31	0.03	1.60	0.20	0.03	1.57	0.17	0.04	1.60	0.20
99	10/10	0.03	1.35	0.03	1.71	0.36	0.02	1.58	0.23	0.03	1.61	0.26	0.02	1.61	0.26
100	10/11	0.04	1.37	0.04	1.68	0.31	0.03	1.60	0.23	0.02	1.60	0.23	0.02	1.58	0.21
101	10/12	0.02	1.34	0.04	1.71	0.36	0.02	1.58	0.24	0.03	1.61	0.27	0.02	1.55	0.20
102	10/13	0.02	1.36	0.03	1.71	0.35	0.02	1.60	0.23	0.02	1.64	0.27	0.02	1.58	0.21
103	10/14	0.02	1.32	0.02	1.68	0.36	0.02	1.56	0.23	0.03	1.64	0.32	0.02	1.53	0.21
104	10/15	0.09	1.35	0.03	1.69	0.34	0.03	1.56	0.21	0.04	1.62	0.27	0.02	1.55	0.20
105	10/16	0.03	1.28	0.03	1.62	0.34	0.03	1.45	0.17	0.02	1.50	0.22	0.02	1.58	0.30
106	10/17	0.03	1.27	0.03	1.65	0.38	0.03	1.53	0.26	0.02	1.55	0.27	0.02	1.53	0.26
107	10/18	0.03	1.32	0.05	1.65	0.33	0.05	1.56	0.24	0.02	1.60	0.27	0.04	1.61	0.28
108	10/19	0.06	1.44	0.04	1.81	0.37	0.06	1.74	0.30	0.22	1.64	0.20	0.03	1.67	0.24
109	10/20	0.03	1.48	0.04	1.67	0.20	0.04	1.70	0.22	0.04	1.69	0.22	0.04	1.73	0.25
110	10/21	0.02	1.31	0.03	1.66	0.35	0.04	1.66	0.35	0.04	1.60	0.29	0.04	1.62	0.31
111	10/22	0.05	1.45	0.04	1.75	0.30	0.04	1.68	0.23	0.05	1.66	0.22	0.04	1.65	0.21
112	10/23	0.11	1.26	0.05	1.67	0.42	0.03	1.62	0.36	0.04	1.60	0.34	0.04	1.55	0.29
113	10/24	0.10	1.44	0.04	1.71	0.27	0.03	1.66	0.22	0.04	1.68	0.25	0.04	1.73	0.29
114	10/25	0.02	1.29	0.03	1.65	0.36	0.02	1.56	0.27	0.02	1.64	0.35	0.02	1.58	0.29
115	10/26	0.17	1.27	0.04	1.61	0.34	0.03	1.56	0.29	0.03	1.54	0.27	0.02	1.53	0.25
116	10/27	0.03	1.48	0.04	1.72	0.25	0.04	1.70	0.22	0.04	1.69	0.22	0.04	1.73	0.25
117	10/28	0.02	1.31	0.03	1.62	0.31	0.04	1.66	0.35	0.04	1.60	0.29	0.04	1.62	0.31
118	10/29	0.02	1.27	0.03	1.65	0.39	0.03	1.56	0.30	0.04	1.59	0.33	0.02	1.53	0.26
119	10/30	0.02	1.24	0.03	1.63	0.39	0.03	1.47	0.23	0.02	1.56	0.32	0.03	1.58	0.34
120	10/31	0.04	1.34	0.04	1.66	0.32	0.03	1.59	0.25	0.04	1.59	0.25	0.04	1.63	0.29
121	11/1	0.03	1.21	0.03	1.58	0.37	0.03	1.50	0.28	0.03	1.47	0.25	0.03	1.56	0.35

C3- FastDNA SPIN Kit for Soil PROTOCOL.

1. Add up to 500 mg of soil to Lysing Matrix E Tube (this step can be done in advance and soils can be stored in the freezer until further processing).

2. Add 978 µl Sodium Phosphate Buffer and 122 µl MT Buffer. (Filter or regular tips)

3. Place tubes in vortex attachment and vortex at high speed for 15 minutes (or follow FastPrep instructions – speed 5.5, time 30sec).

4. Centrifuge Lysing Matrix E Tubes at maximum speed (14,000 x g) for 90 seconds.

5. Transfer supernatant to a clean 1.5 mL tube. Add 250 µl PPS reagent and mix by inverting the tube by hand 10 times.

6. Centrifuge tube at maximum speed (14,000 x g) for 5 minutes to pellet the precipitate. Transfer supernatant to a clean 15 mL centrifuge tube. ***Re-suspend Binding Matrix Suspension before use. Add 0.75 mL of the Binding Matrix Suspension to the supernatant.

7. Invert tube by hand several times for at least 2 minutes. Place tube in rack for at least 3 minutes (can increase to 15 minutes to allow for more time for DNA to bind).

8. Remove and discard at least 0.75 mL of the supernatant being careful to avoid settled Binding Matrix. Suspend Binding Matrix in the remaining amount of supernatant. Transfer remaining amount of the mixture to a SPIN Filter and centrifuge at maximum speed (14,000 x g) for 1 minute.

Suspend binding matrix and transfer to new filter. Discard liquid in Catch Tube.

9. Add 500 µl SEWS-M to the SPIN Filter and centrifuge at maximum speed (14,000 x g) for 1 minute. Decant flow-through and replace SPIN Filter in Catch tube. Centrifuge at 14,000 x g for 2 minutes to “dry” the matrix of residual SEWS-M wash solution.

10. Remove SPIN Filter and place in clean, autoclaved 1.5 mL micro centrifuge tube. Air-dry the SPIN Filter for 5 minutes at room temperature.

11. Add 100 µl DES (DNase/Pyrogen Free Water = Millipore water) that has been heated to 65 ℃. This water can be heated in heat block to enhance DNA elution. Gently stir matrix on filter membrane with VORTEX to resuspend the silica for efficient elution of DNA. Centrifuge at 14,000 x g for 1 minute to transfer eluted DNA to Catch Tube. Freeze DNA at -20 ℃ until further processing.

C4 - CTAB purification of DNA (post-extraction).

Pre-warm working CTAB stock to 65°C in a 1.5 ml tube in the heat block. Meanwhile, proceed to steps 2 and 3.

Transfer 100 l of the extracted DNA into a 1.5 ml tube for each sample.

Label (long-term storage) one autoclaved 1.5 ml tube for each DNA extraction.

Adjust the NaCl concentration of each DNA extract to 0.7 M: add 16.25 µl of 5 M NaCl (autoclaved) to each DNA extract.

Add 12 l of warm working CTAB stock (0.1 vol). Mix thoroughly and incubate at 65°C for 15 minutes. *use filter tips

Add 128 l (one volume) of chloroform:isoamly alcohol (24:1). Mix carefully but thoroughly. Centrifuge at maximum speed (14,000 x g) for 5 minutes.

*Use filter tips; do not collect white interface layer (only transfer top layer for precipitation)

Carefully remove the top layer to a clean; well-labeled 1.5 ml tube (should get about 125 µl). Add 256 l (two volumes) of cold 100% EtOH to precipitate the DNA. After adding/mixing 100% EtOH, increase precipitation of DNA by putting samples in the freezer (-20°C) for at least 15 minutes (increasing time will increase precipitation—overnight is best).

Mix thoroughly and centrifuge at maximum speed for 5 minutes (increase time to increase expected yield). If low yield is expected, increase centrifugation time to ~15 minutes. ***Make sure to orient the tubes in the same direction (e.g. hinge side point out) so you know the location of the DNA (if hinge side facing out, DNA will be along the side of the hinge).

Carefully avoiding the pellet, remove supernatant. Add 125µl 70% EtOH (cold), flick to mix, and centrifuge at maximum speed for 2 minutes. If low yield is expected, increase centrifugation time to ~7 minutes.

Repeat step 9 once.

Remove supernatant. Allow pellet to air dry (approximately 15 minutes – this may take longer and be careful not to dry down samples all the way). Place tubes upside-down, propped against a tube rack and over kimwipe.

Resuspend pellet in 100 µl dH_2O. If low yield is expected, re-suspend DNA in 50 µl dH_2O.

Wash back side of tube (where DNA is supposed to be) with dH_2O using the pipet. If you orient all your tubes hinge side out in the centrifuge, then the DNA should be along the hinge side, so make sure you run water down that side.

C5 -DNA concentrations after CTAB cleaning and purification.

Table C-3 DNA concentrations after CTAB cleaning and purification.

Step 0		Step 1		Step 2		Step 3		Step 4	
ID	DNA conc. ng/ul	ID	DNA conc. ng/ul	ID	DNA conc. ng/ul	ID	DNA conc. ng/ul	ID	DNA conc. ng/ul
S0-1	10.13	S1-1	2.8	S2-1	7.7	S3-1	20.6	S4-1	6.625
S0-2	20.4	S1-2	6.75	S2-2	6.65	S3-2	10.5	S4-2	19.9
S0-3	23.05	S1-3	6.3	S2-3	8.3	S3-3	14.75	S4-3	22.5
S0-4	19.7	S1-4	8.45	S2-4	11.7	S3-4	6.65	S4-4	17.65
S0-5	19.7	S1-5	22.5	S2-5	18.4	S3-5	4.005	S4-5	9.075
S0-6	20.2	S1-6	15.5	S2-6	11.65	S3-6	11	S4-6	20.2
S0-7	17.4	S1-7	14.65	S2-7	8.75	S3-7	15.3	S4-7	8.95
S0-8	11.6	S1-8	20.55	S2-8	9.93	S3-8	4.75	S4-8	5.65
		S1-9	10.7	S2-9	12	S3-9	10.55	S4-9	10.1
		S1-10	15.75	S2-10	14.3	S3-10	12.25	S4-10	27
		S1-11	12.25	S2-11	15.1	S3-11	9.55	S4-11	7.05
		S1-12	28	S2-12	8.45	S3-12	16.35	S4-12	15.3
		S1-13	8.35	S2-13	17.75	S3-13	16.2	S4-13	4.585
		S1-14	7.2	S2-14	8.9	S3-14	12.1	S4-14	3.935
		S1-15	9.85	S2-15	11.15	S3-15	18.35	S4-15	13.55
		S1-16	12	S2-16	15.45	S3-16	23.55	S4-16	8.25
		S1-17	20.45	S2-17	3.35	S3-17	14.15	S4-17	11.55
		S1-18	8.3	S2-18	10.8	S3-18	10.95	S4-18	12.85
		S1-19	11.3	S2-19	6.15	S3-19	12.75	S4-19	7.35
		S1-20	12.95	S2-20	21.9	S3-20	4.05	S4-20	8.85
		S1-21	12.3	S2-21	10.5	S3-21	12.7	S4-21	11.9
		S1-22	10.1	S2-22	15	S3-22	12.1	S4-22	11.25
		S1-23	15.6	S2-23	6.25	S3-23	9.15	S4-23	21.35
		S1-24	15.6	S2-24	11.2	S3-24	22.9	S4-24	11.3
		S1-25	7.55	S2-25	19.6	S3-25	17.6	S4-25	15.9
		S1-26	11.65	S2-26	17.2	S3-26	16	S4-26	20.2
		S1-27	13.45	S2-27	18.1	S3-27	21.2	S4-27	2
		S1-28	21.65	S2-28	11.3	S3-28	8.45	S4-28	14.7
		S1-29	14.8	S2-29	7.55	S3-29	29.8	S4-29	6.6
		S1-30	18	S2-30	2.375	S3-30	26	S4-30	9.6
		S1-31	20.7	S2-31	7.75	S3-31	21.8	S4-31	12.15
		S1-32	15.9	S2-32	12.5	S3-32	21.05	S4-32	8.67

For step 0: 1- 8 were eight replicates.

For steps 1-4:

1- 4: samples taken from the upper layer of Biofilter 1; 5- 8: samples taken from the lower layer of Biofilter 1.
9- 12: samples taken from the upper layer of Biofilter 2; 13-16: samples taken from the lower layer of Biofilter 2.
17-20: samples taken from the upper layer of Biofilter 3; 21-24: samples taken from the lower layer of Biofilter 3.
24-28: samples taken from the upper layer of Biofilter 4; 29-32: samples taken from the lower layer of Biofilter 4.

C6- Biofilter control system (Labview).

The labview control in composed of "setup (top figure)", "result (middle figure)" and "pDAQ (bottom figure)" pages.

In the "setup", the control panel makes decisions for gas sampling and water pumps. Three choices, including "always on", "always off" and "left to control" were made possible for gas sampling. "Left to control" means the five gases will be measured by taking turns. Similarly, three choices, including "always on", "always off" and "left to control" were made possible for each water pump. In this case, "left to control" means the pump will be turned on for a certain period of time in a day during the test. The time can be set in the "result" page.

In the "result" page, the ammonia and nitrous oxide concentrations, relative humidity and temperature of measured gas was displayed. There daily mean value and standard deviation were recorded automatically. Whenever a specific gas was analyzed, a light will be turned on accordingly. The readings of temperatures may have errors and create peaks, such as the green peaks showed on the "result" page. These peaks can be very high or very low, but always only have one reading. A filter was applied to remove these unexpected peak values.

In the "pDAQ" page, the sampling duration was set to 120 msec.

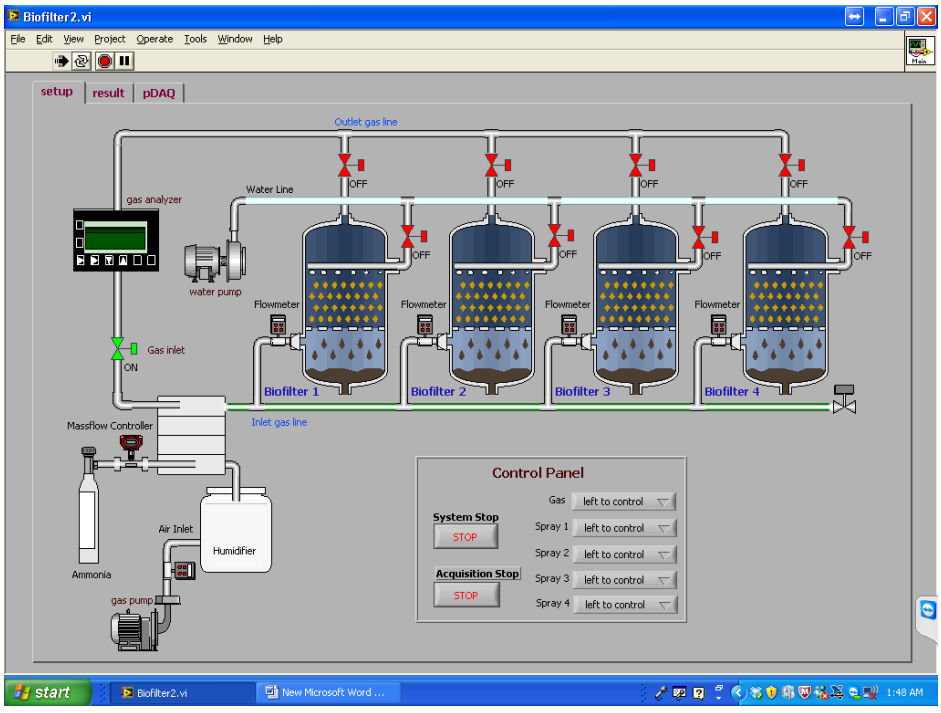

Figure C.1 The front page of Labview control system.

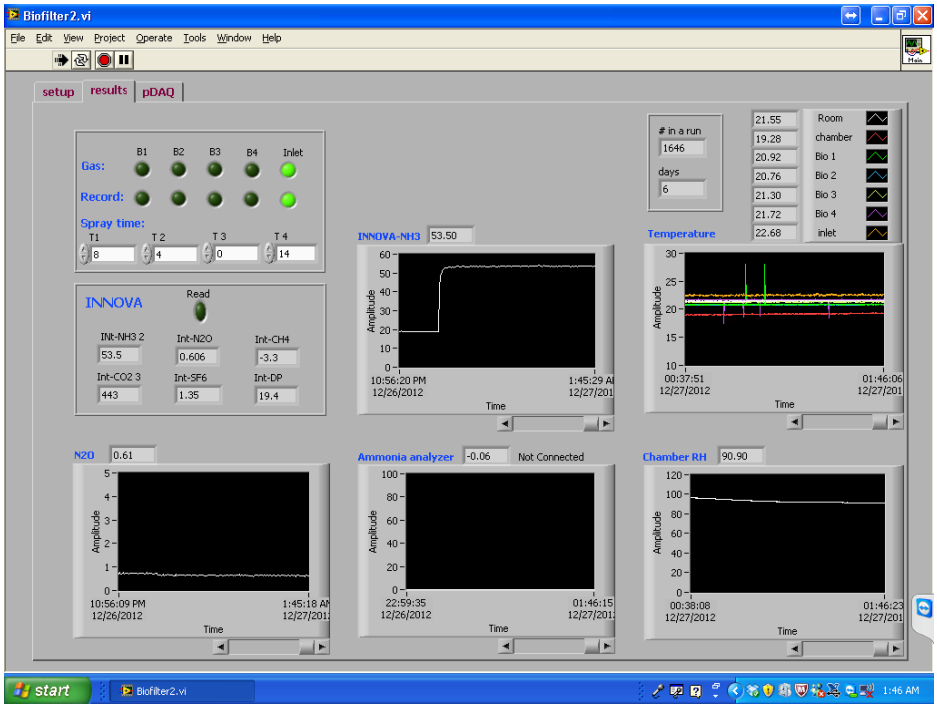

Figure C.2 The result page of Labview control system.

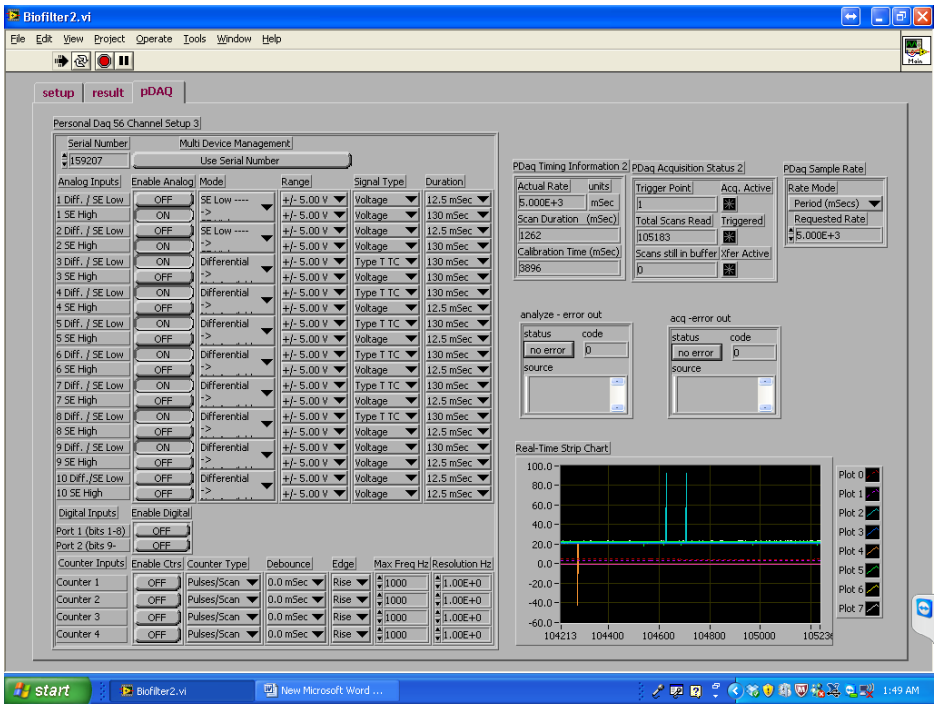

Figure C.3 The control page of Labview control system.

C7- qPCR results of the AOA and AOB.

The average copy # of AOA is about 6 times of the copy # of AOB.

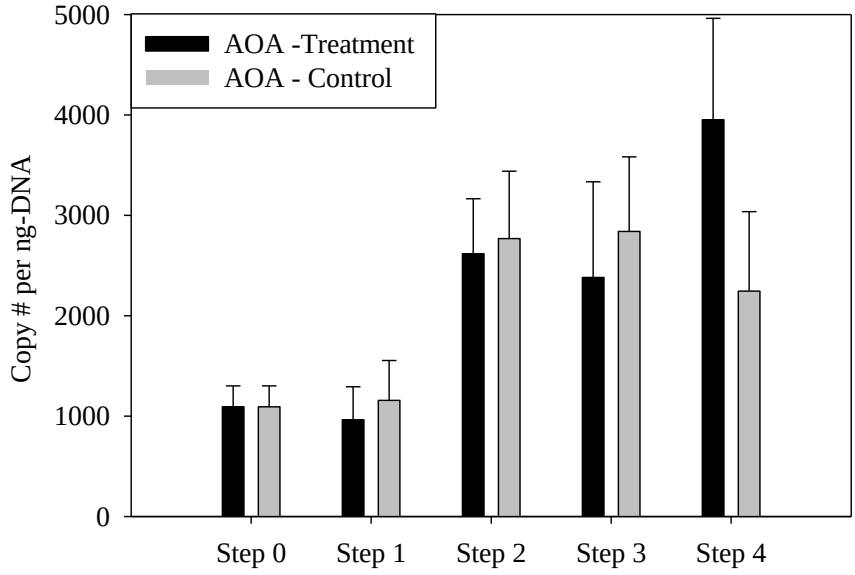

Figure C.4 qPCR results of AOA in the five steps.

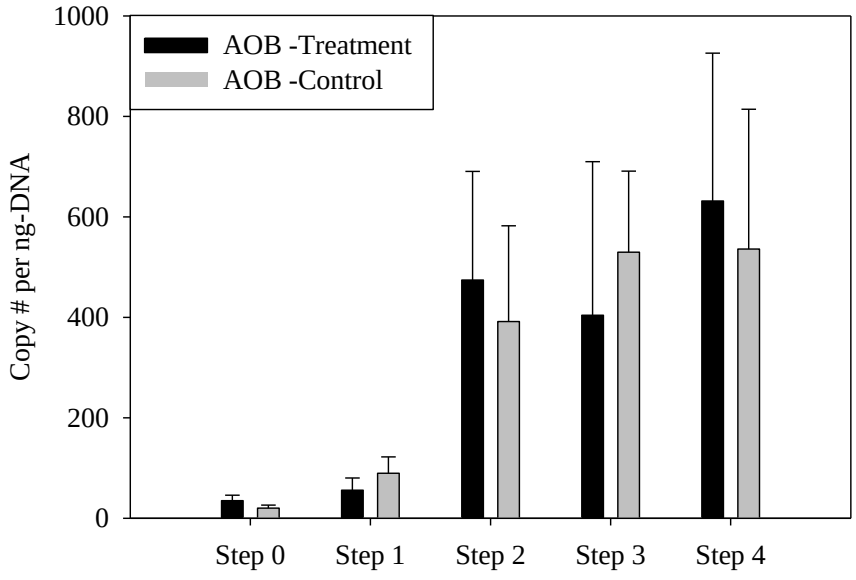

Figure C.5 qPCR results of AOB in the five steps.

C8- R code, use ARISA data treatment as an example.

```
# ARISA data:R table-ARISA
# Raw samples and lower layers samples only.

library(MASS)
library(vegan)
library(plotrix)

# get data table
setwd("C:/Users/## ")
ARISA<-read.csv("R table- arisa.csv",head=T)
head(ARISA[,1:11])

# select data
arisa <- subset(ARISA, ARISA$Group=="Treatment"& ARISA$Layer=="Low")
head(arisa[,1:11])

# Transformation data
df.arisa <- arisa[,-c(1:11)]
df.arisa[1:20,1:11]
df.arisa[is.na(df.arisa)]<-0
df.arisa <- decostand(df.arisa, method="hellinger")

# get factors
df.arisa.fac <- arisa[,1:11]
head(df.arisa.fac[,1:11])

# calculate disperse of samples
dist <- vegdist(df.arisa,method="bray")
mod <- betadisper(dist, df.arisa.fac$Bio12per,type=c("centroid"))
TukeyHSD(mod)
mod


# PERMANOVA

anos<-adonis(df.arisa~Group+Period+MCC+Layer+Biofilter, data=df.arisa.fac,method = "bray")
anos
```

APPENDIX D: SUPPLEMENTARY INFORMATION FOR CHAPTER 6

D1- Box-Cox transformation and ANCOVA flowchart.

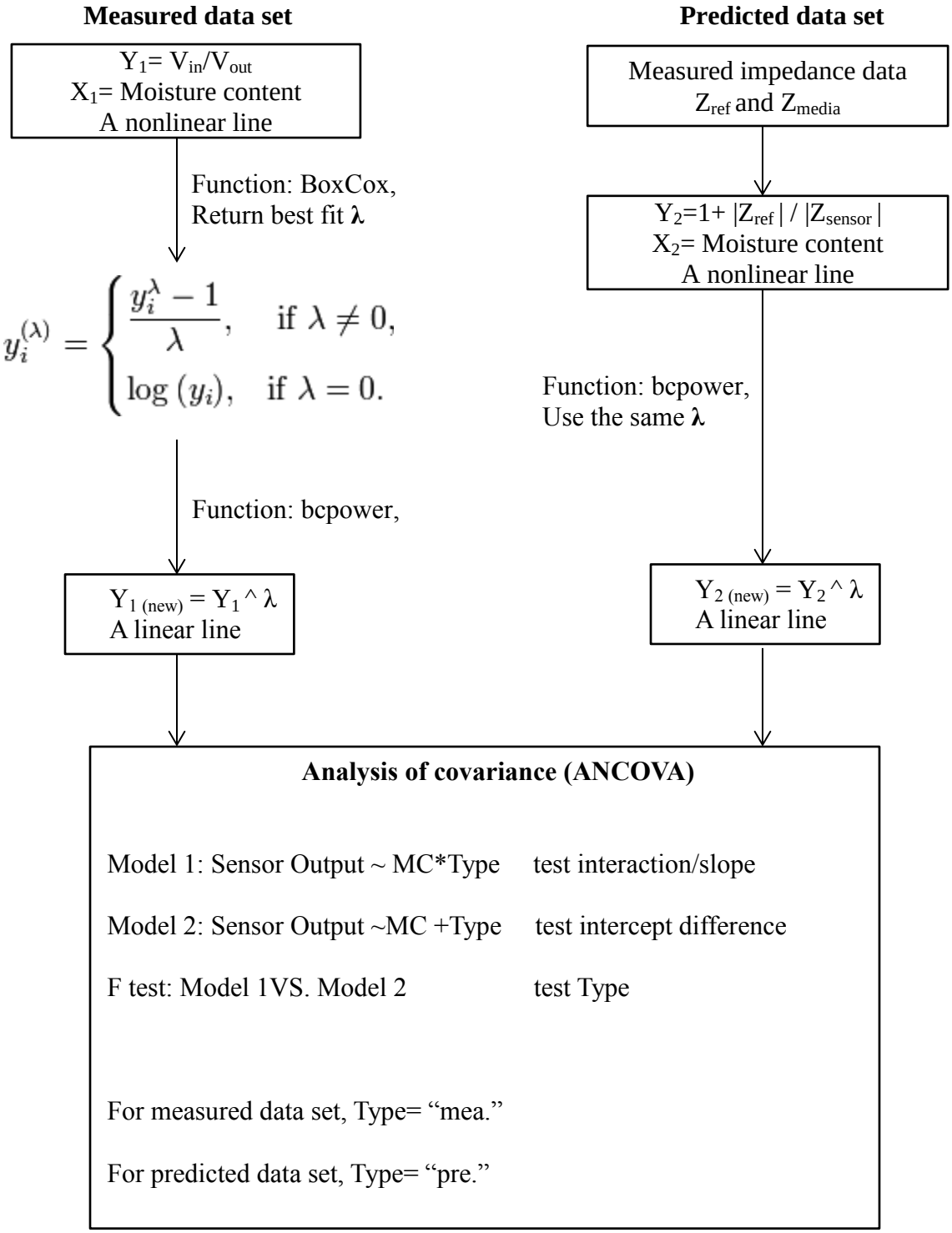

D2- Box-Cox transformation and ANCOVA R code (use SWC as an example).

```
library(ggplot2)
library(MASS)
library(car)
library(HH)
setwd("C:/Users/##")
Data<-read.csv("R table.csv",head=T)
head(Data[,1:12])

#define data
y1<-Data$SWC.M.Y
x1<-Data$SWC.M.X
y2<-Data$SWC.P.Y
x2<-Data$SWC.P.X

#get best lamda
plot(x1,y1)
a<-boxcox(lm(y1~x1),lambda=seq(-2,0,0.01))
best<-a$x[which.max(a$y)]

# transformation data
y1new<-bcPower(y1, best)
fit1<-lm(y1new~x1)
summary(fit1)
y2new<-bcPower(y2, best)
plot(x2,y2new)
fit2<-lm(y2new~x2)
summary(fit2)

#get transformed data
colnames(Data)[1:4]<-rep(c("cwcx","cwcy"),2)
cwc<-rbind(Data[,1:2],Data[,3:4])
cwc$cwcy[1:10]<-y2new
cwc$cwcy[11:20]<-y1new
cwc[,3]<-c(rep("pre",10),rep("mea",10))
colnames(cwc)[3]<-"type"
cwc
y1new
y2new

#test significance
mod1<-aov(cwcy~cwcx*type,cwc)
summary(mod1)
mod2<-aov(cwcy~cwcx+type,cwc)
summary(mod2)
anova(mod1,mod2)
```

D3- Sensor reading and airflow resistance *t*-test R code.

```
# get data
setwd("C:/Users/##")
Data<-read.csv("R table.csv",head=T)
head(Data[,1:8])
attach(Data)

# define data
x1<-largeMC0[1:4]
x2<-largeMC8[1:4]
x3<-smallMC0[1:4]
x4<-smallMC8[1:4]

# t test
t.test(x1,x2)
t.test(x3,x4)
t.test(large0,large8)
t.test(small0,small8)
```

APPENDIX E: SUPPLEMENTARY INFORMATION FOR CHAPTER 7

E1- Biofilter 1 outlet humidity.

Table E-1 Outlet humidity from Biofilter 1.

Day	Date	RH S.D. %	RH avg., %	Temp S.D., ℃	Temp avg., ℃	Abs. humidity, g/m^3
1	7-Mar	0.41	89.02	0.92	23.72	19.15
2	8-Mar	0.79	90.20	0.88	24.35	20.11
3	9-Mar	0.48	90.60	0.91	23.56	19.31
4	10-Mar	0.50	91.77	0.92	24.30	20.40
5	11-Mar	0.78	92.05	0.92	26.31	20.91
6	12-Mar	0.39	92.94	0.87	24.46	20.86
7	13-Mar	0.44	93.27	0.89	25.96	20.77
8	14-Mar	0.32	92.48	0.94	24.28	20.54
9	15-Mar	0.60	92.26	0.89	25.69	22.18
10	16-Mar	0.25	94.14	0.92	25.40	22.27
11	17-Mar					
12	18-Mar	0.35	92.65	0.92	26.44	23.23
13	19-Mar	0.98	90.17	0.89	26.70	22.94
14	20-Mar	0.16	89.73	0.86	26.80	22.95
15	21-Mar	0.69	89.02	0.88	26.46	22.39
16	22-Mar	0.88	89.20	0.96	25.82	21.60
17	23-Mar	0.44	92.60	0.89	25.96	22.54
18	24-Mar	0.31	93.77	0.88	24.40	21.96
19	25-Mar	0.09	93.05	0.55	25.31	21.88
20	26-Mar	1.11	93.94	0.92	23.56	20.03
21	27-Mar	0.60	93.27	0.92	21.69	17.86
22	28-Mar	0.18	88.62	0.90	23.89	19.25
23	29-Mar	0.87	94.35	0.90	22.39	18.80
24	30-Mar	0.19	87.89	1.65	23.57	18.75
25	31-Mar	0.92	90.87	0.88	23.09	18.86
26	1-Apr	0.12	89.55	22.93	24.26	19.87
27	2-Apr	0.36	90.05	0.88	24.96	20.78
28	3-Apr	0.12	89.77	1.65	25.77	21.68
29	4-Apr	0.41	90.01	0.88	25.47	21.38
30	5-Apr	0.18	92.45	0.92	22.53	18.98
31	6-Apr	0.75	97.43	0.90	21.57	19.93
32	7-Apr	0.75	96.43	0.90	21.57	19.53

E2- Biofilter 2 outlet humidity.

Table E-2 Outlet humidity from Biofilter 2.

Day	Date	RH S.D. %	RH avg., %	Temp S.D., ℃	Temp avg., ℃	Abs. humidity, g/m^3
1	7-Mar	0.93	91.33	0.85	23.94	19.90
2	8-Mar	0.17	90.34	0.87	24.84	20.71
3	9-Mar	0.98	93.33	0.88	22.91	19.18
4	10-Mar	0.94	90.23	0.89	22.79	18.41
5	11-Mar	0.67	91.33	0.85	23.36	19.25
6	12-Mar	0.43	92.34	0.87	24.79	21.10
7	13-Mar	0.10	92.33	0.88	25.55	21.02
8	14-Mar	0.79	94.23	0.89	24.57	21.25
9	15-Mar	0.61	93.33	0.85	24.88	21.44
10	16-Mar	0.36	94.34	0.87	25.90	22.95
11	17-Mar					
12	18-Mar	0.49	95.23	0.89	25.19	22.26
13	19-Mar	0.09	95.33	0.88	26.17	23.55
14	20-Mar	0.31	92.64	0.86	26.78	23.67
15	21-Mar	0.49	91.33	0.85	27.19	23.87
16	22-Mar	1.74	92.34	0.87	26.80	23.62
17	23-Mar	0.60	96.33	0.88	26.55	23.30
18	24-Mar	0.21	95.23	0.89	25.32	22.42
19	25-Mar	0.31	95.61	0.88	24.97	22.08
20	26-Mar	1.68	95.18	0.87	24.56	20.48
21	27-Mar	0.48	95.57	0.91	22.88	18.60
22	28-Mar	0.06	100.13	0.92	23.09	20.51
23	29-Mar	0.90	92.64	0.90	24.17	20.44
24	30-Mar	0.43	95.66	0.88	22.71	19.43
25	31-Mar	0.76	94.43	0.90	23.87	20.49
26	1-Apr	0.37	92.80	0.89	23.43	19.63
27	2-Apr	0.34	92.33	0.87	24.73	20.99
28	3-Apr	0.39	93.35	0.88	25.47	21.92
29	4-Apr	0.92	92.35	0.89	25.96	22.54
30	5-Apr	2.17	91.86	0.92	24.29	20.40
31	6-Apr	0.20	98.15	0.88	22.35	19.52
32	7-Apr	0.19	99.94	0.91	21.40	18.82

E3- Inlet humidity.

Table E-3 Inlet humidity results.

Day	Date	RH S.D. %	RH avg., %	Temp S.D., ℃	Temp avg., ℃	Abs. humidity, g/m^3
1	7-Mar	1.11	88.15	0.93	23.24	18.45
2	8-Mar	1.89	91.33	0.91	24.51	19.12
3	9-Mar	1.16	87.76	0.91	22.56	17.67
4	10-Mar	0.64	90.12	0.90	22.35	17.93
5	11-Mar	0.87	91.32	0.92	23.07	18.93
6	12-Mar	1.15	90.45	0.96	24.67	20.53
7	13-Mar	0.45	86.18	0.98	24.08	18.92
8	14-Mar	0.80	90.07	0.93	24.56	20.32
9	15-Mar	0.84	84.42	0.90	25.31	19.87
10	16-Mar	0.58	88.60	0.89	25.32	20.87
11	17-Mar					
12	18-Mar	1.71	91.39	0.90	25.65	21.93
13	19-Mar	0.64	89.69	0.86	26.10	22.06
14	20-Mar	2.43	86.18	0.90	26.39	21.54
15	21-Mar	1.68	90.07	22.97	25.84	21.84
16	22-Mar	1.45	84.42	22.97	26.23	20.92
17	23-Mar	2.11	88.60	0.98	25.76	21.39
18	24-Mar	0.81	92.39	0.90	24.43	20.69
19	25-Mar	0.69	92.88	23.41	24.45	20.83
20	26-Mar	0.58	87.64	33.04	23.64	18.77
21	27-Mar	2.71	90.64	1.12	20.91	16.59
22	28-Mar	1.49	87.40	0.93	23.22	18.28
23	29-Mar	0.52	87.61	0.92	23.27	18.37
24	30-Mar	2.41	92.55	0.93	21.62	17.65
25	31-Mar	2.13	89.23	0.91	22.89	18.31
26	1-Apr	2.59	86.76	0.89	23.29	18.22
27	2-Apr	0.83	86.13	0.92	24.17	19.01
28	3-Apr	1.41	87.61	0.88	25.02	20.29
29	4-Apr	1.49	86.83	0.89	25.20	20.31
30	5-Apr	1.23	85.28	0.89	23.56	18.18
31	6-Apr	3.72	96.44	0.90	21.74	18.52
32	7-Apr	3.55	96.62	0.91	21.67	18.47

E4- Water addition rates.

Table E-4 Measured water addition rates.

Day	Date	Biofilter 1, mg/day	Biofilter 2, mg/day
1	7-Mar	120	200
2	8-Mar	120	320
3	9-Mar	120	320
4	10-Mar	120	200
5	11-Mar	120	200
6	12-Mar	120	200
7	13-Mar	120	200
8	14-Mar	120	200
9	15-Mar	120	200
10	16-Mar	300	200
11	17-Mar		
12	18-Mar	300	120
13	19-Mar	120	200
14	20-Mar	120	200
15	21-Mar	120	200
16	22-Mar	120	200
17	23-Mar	120	120
18	24-Mar	120	120
19	25-Mar	120	120
20	26-Mar	120	120
21	27-Mar	120	120
22	28-Mar	120	120
23	29-Mar	120	120
24	30-Mar	120	120
25	31-Mar	120	120
26	1-Apr	120	120
27	2-Apr	120	120
28	3-Apr	120	120
29	4-Apr	120	120
30	5-Apr	120	120
31	6-Apr	120	120
32	7-Apr	120	120

E5- Sensor readings (V_{in}/V_{out}) and estimated moisture contents.

Table E-5 Recorded sensor readings and estimated moisture content.

Day	Date	Sensor 1 S.D.	Sensor 1 avg.	Sensor 2 S.D.	Sensor 2 avg.	Biofilter 1 MC, %	Biofilter 2 MC, %
1	7-Mar	0.03	2.46	0.03	2.41	44.41	44.01
2	8-Mar	0.03	2.47	0.04	2.40	44.46	43.94
3	9-Mar	0.04	2.48	0.03	2.43	44.54	44.12
4	10-Mar	0.03	2.46	0.03	2.44	44.43	44.26
5	11-Mar	0.06	2.53	0.04	2.44	44.95	44.24
6	12-Mar	0.03	2.51	0.02	2.51	44.81	44.79
7	13-Mar	0.02	2.52	0.02	2.51	44.85	44.75
8	14-Mar	0.02	2.56	0.02	2.52	45.17	44.86
9	15-Mar	0.03	2.48	0.03	2.56	44.54	45.16
10	16-Mar	0.07	2.42	0.02	2.52	44.09	44.87
11	17-Mar						
12	18-Mar	0.03	2.38	0.01	2.54	43.78	45.05
13	19-Mar	0.02	2.38	0.01	2.56	43.79	45.18
14	20-Mar	0.02	2.50	0.03	2.56	44.72	45.15
15	21-Mar	0.03	2.58	0.01	2.54	45.37	45.05
16	22-Mar	0.02	2.55	0.01	2.65	45.08	45.85
17	23-Mar	0.02	2.52	0.02	2.64	44.85	45.79
18	24-Mar	0.02	2.49	0.02	2.68	44.66	46.06
19	25-Mar	0.05	2.55	0.02	2.66	45.13	45.92
20	26-Mar	0.03	2.50	0.15	2.67	44.69	45.98
21	27-Mar	0.02	2.53	0.02	2.70	44.95	46.27
22	28-Mar	0.02	2.57	0.02	2.70	45.28	46.24
23	29-Mar	0.02	2.57	0.02	2.68	45.26	46.12
24	30-Mar	0.03	2.62	0.01	2.71	45.61	46.33
25	31-Mar	0.03	2.65	0.04	2.69	45.89	46.18
26	1-Apr	0.02	2.64	0.03	2.65	45.81	45.89
27	2-Apr	0.06	2.72	0.07	2.70	46.38	46.24
28	3-Apr	0.02	2.73	0.11	2.66	46.45	45.96
29	4-Apr	0.04	2.72	0.10	2.68	46.36	46.07
30	5-Apr	0.08	2.64	0.01	2.61	45.79	45.53
31	6-Apr	0.04	2.65	0.07	2.63	45.83	45.71
32	7-Apr	0.04	2.66	0.01	2.60	45.92	45.51

E6- INNOVA calibration, obtained from INNOVA's manual.

The INNOVA calibration was composed of four steps, including: Step 1–Zero-point calibration for all filters; Step 2- Humidity interference; Step 3- Water vapor span calibration; and Step 4- Span calibration for each filter.

Step 1 - Zero-point calibration for all filters. Pure N_2 gas was supplied to the system for at least 30 minutes, to ensure complete dry zero-air to the INNOVA. The procedure is shown below.

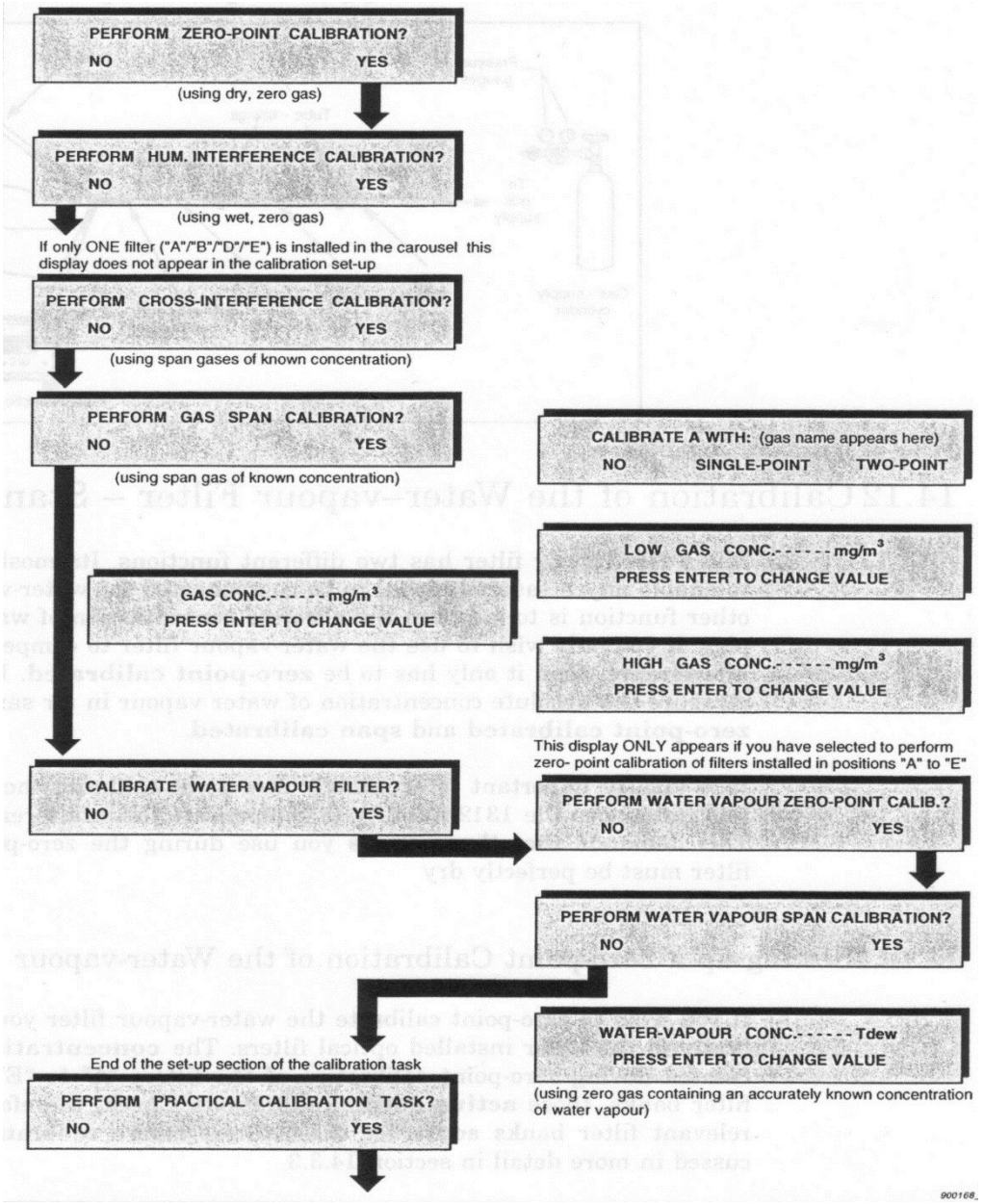

Figure E.1 Calibration step 1.

Step 2 - Humidity interference for all filters

A stable wet N_2 gas was supplied to the INNOVA by water column air bubbling. The dew-point of the air was measured with a hygrometer. The procedure is shown in the following figure.

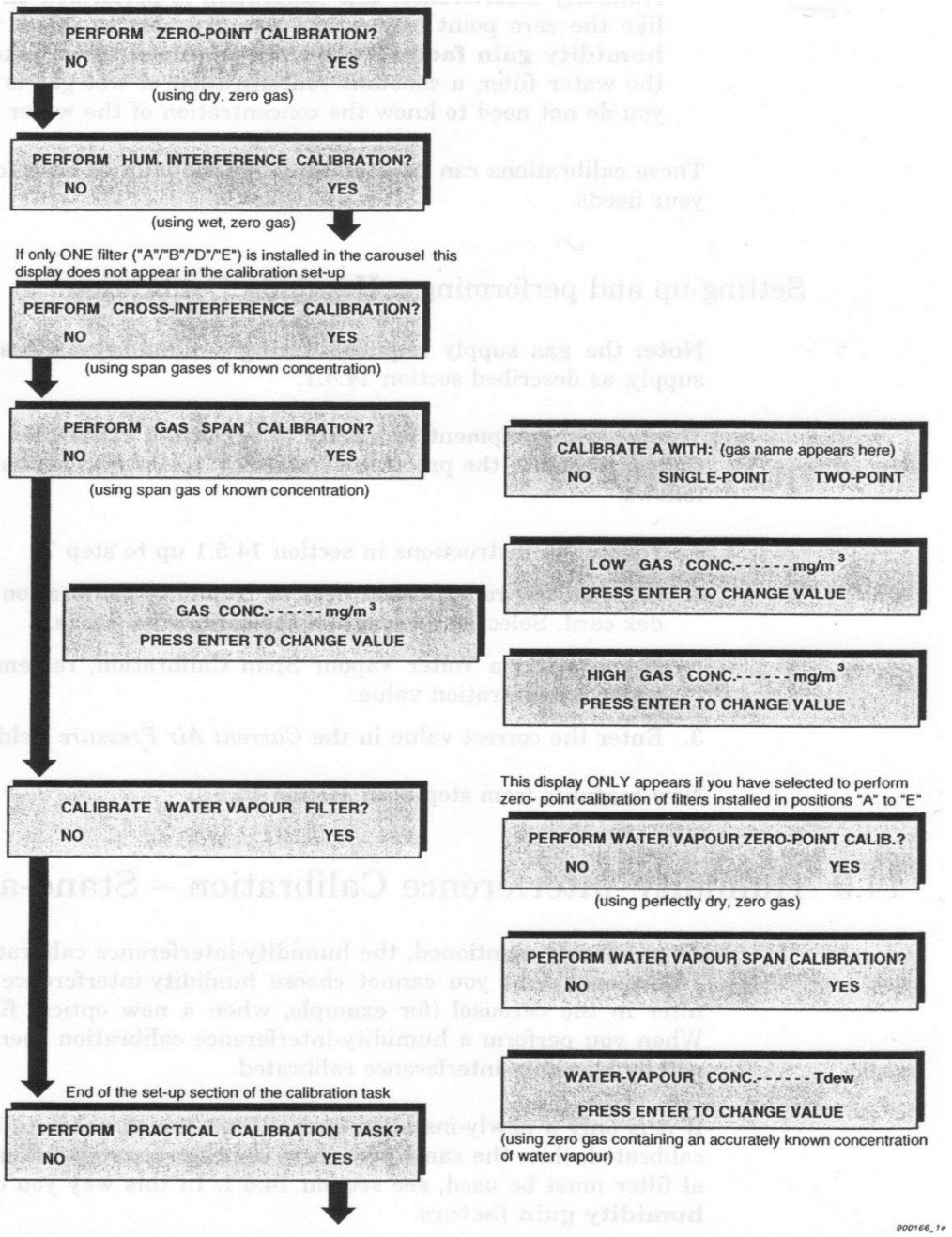

Figure E.2 Calibration step 2.

Step 3 - Water vapor span calibration

The same wet and clean air N_2 gas was supplied to the INNOVA. Its dew-point temperature was inputted to the INNOVA. The procedure is shown in the following figure.

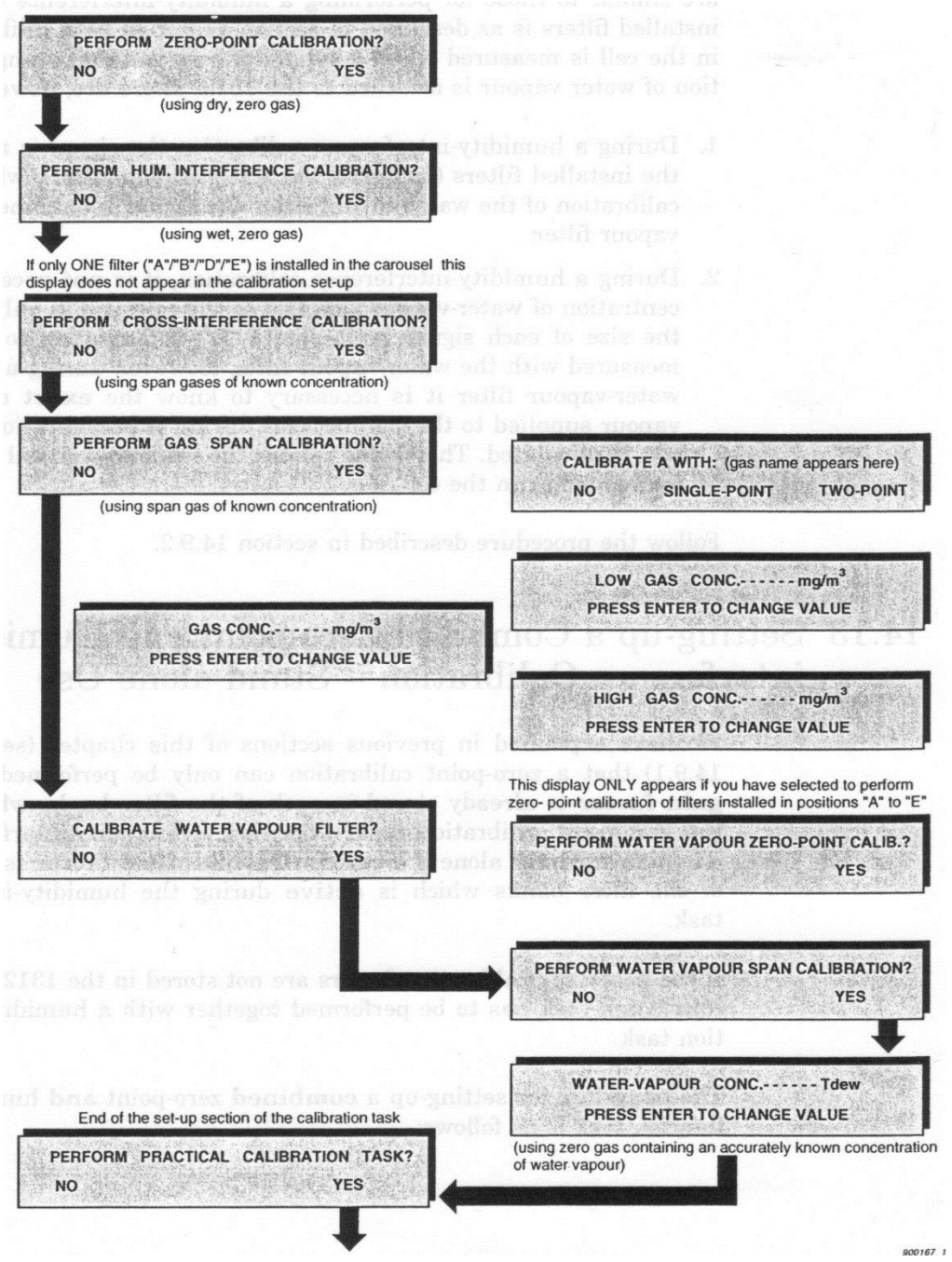

Figure E.3 Calibration step 3.

Step 4 - Span calibration for each filter

Gases including NH_3, N_2O, CO_2, CH_4, and water vapor were calibrated. For nitrous oxide and CO_2 calibration, a nafion tubing was required. The nafion tubing provides a stable and constant supply of humidity that allows CO_2 and N_2O to be rapidly detected by the acoustic sensor. The connection of the tubing and the procedure of calibration are shown as bellow.

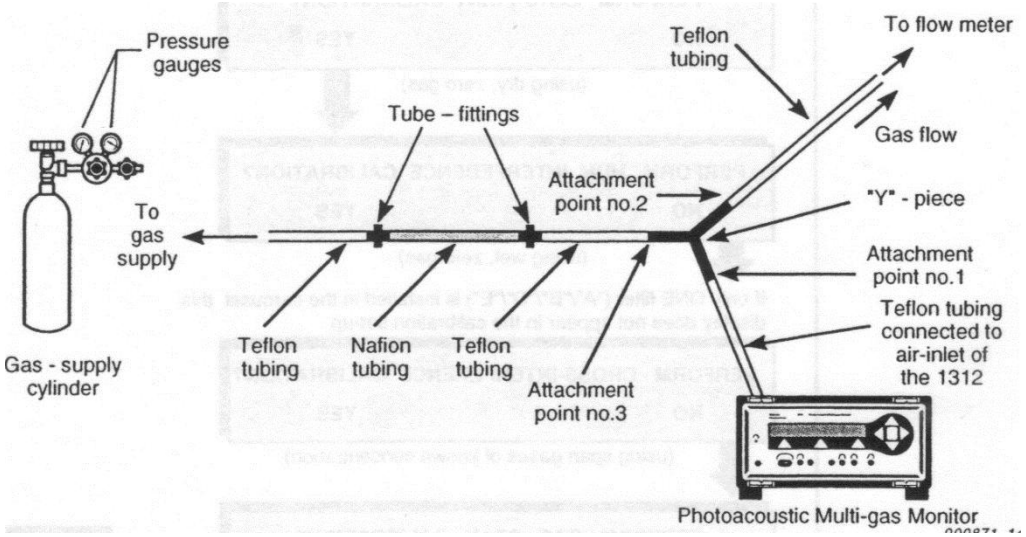

Figure E.4 Span calibration setup.

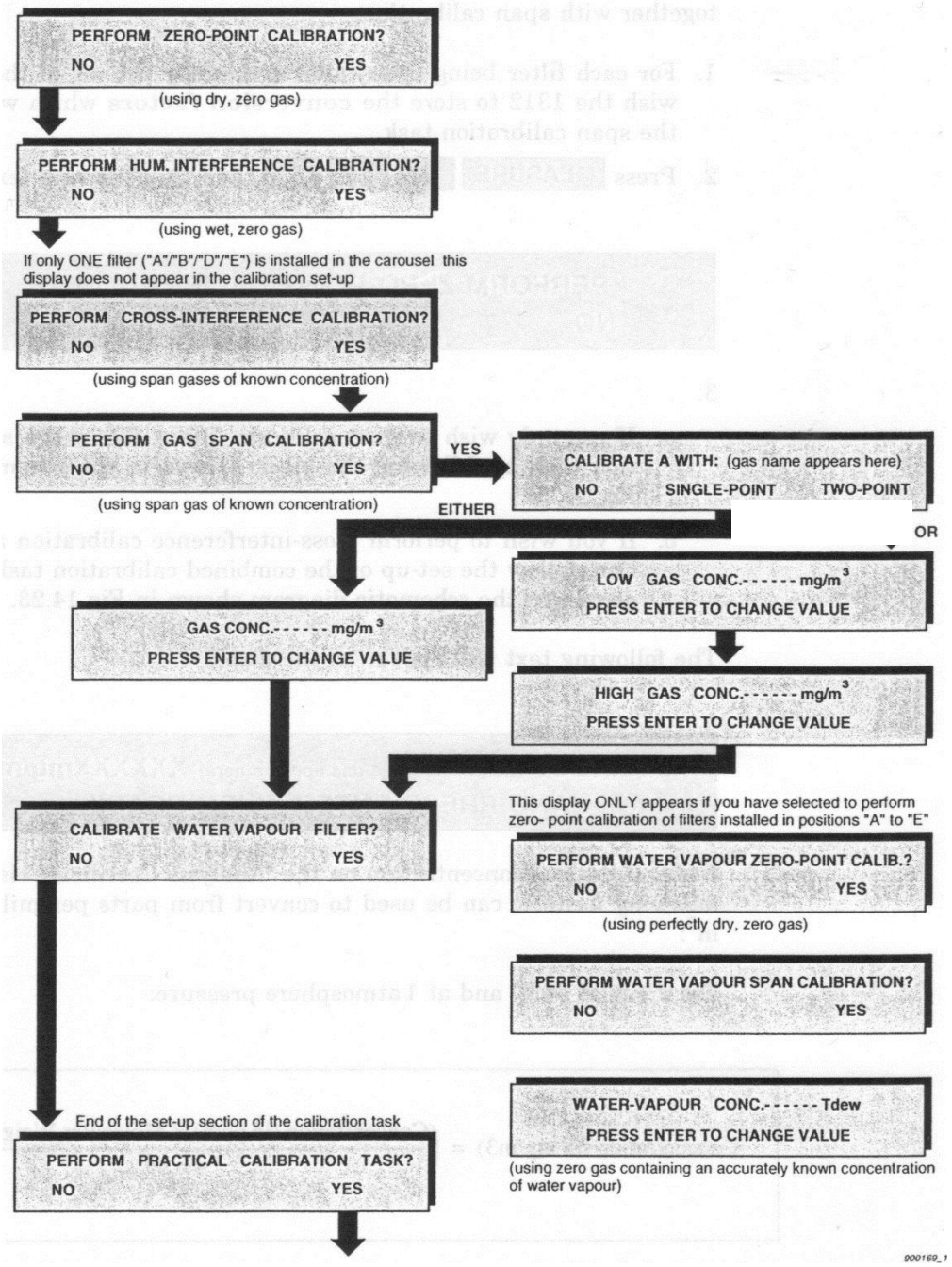

Figure E.5 Span calibration procedure.